Synthesis and Structure–Property Relationships of Polyesters Containing Rigid Aromatic Structures

Hans Eliot Edling

Dissertation submitted to the faculty of the Virginia Polytechnic Institute and State University in partial fulfillment of the requirements for the degree of

Doctor of Philosophy

In

Chemistry

S. Richard Turner, Committee Chair

Timothy E. Long, Committee Member

Richard D. Gandour, Committee Member

Robert B. Moore, Committee Member

February 16th, 2018

Blacksburg, VA

Keywords: -

Synthesis and Structure–Property Relationships of Polyesters Containing Rigid Aromatic Structures

Hans Eliot Edling

ABSTRACT

(Academic)

Polyesters are an attractive class of polymer that can be readily modified with a wide range of different comonomers, during polymerization or with melt blending, to achieve a wide variety of physical properties. This research primarily focuses on polyesters that incorporate rigid aromatic structures that have excellent potential to enhance thermal and mechanical properties. Copolyesters were prepared through melt polycondensation of diesters and diols in the presence of an exchange catalyst. Monomer incorporation was verified with nuclear magnetic resonance (NMR) and molecular weights were obtained by measuring inherent viscosity (η_{inh}). Physical properties were assessed with thermogravimetric analysis (TGA), differential scanning calorimetry (DSC), dynamic mechanical analysis (DMA) and rheology. Mechanical properties were assessed with tensile and impact testing.

Copolyesters of poly(ethylene terephthalate) (PET) were synthesized by substituting dimethyl terephthalate (DMT) with dimethyl 4,4'-biphenyldicarboxylate (4,4'BB) resulting in enhanced glass transition (T_g) temperatures relative to PET while affording melting temperatures (T_m) low enough to allow facile melt processing. Further modification with dimethyl isophthalate (DMI) or dimethyl 3,4'-biphenyldicarboxylate (3,4'BB) slowed crystallization sufficiently to allow biaxial orientation, leading to further studies assessing the permeability of oriented films.

Novel amorphous polyesters were synthesized with 3,4'BB or 4,4'BB in combination with neopentyl glycol (NPG), 1,4-cyclohexandimethanol (CHDM) and ethylene glycol (EG). Use of multiple diols produced clear, amorphous copolyesters with T_gs as high at 129 ℃.

A series of novel high (T_m) copolyesters were synthesized from dimethyl 2,6-naphthalenedicarboxylate (DMN) and 4,4'BB combined with CHDM. Studies were performed with standard DSC and thin film calorimetry to show the convergence of multiples melting endotherms in an effort to determine their origin. Preliminary work was performed on the modification of poly(1,4-cyclohexylenedimethylene terephthalate) (PCT), poly(1,4-cyclohexylenedimethylene 2,6-naphthalate) (PCN) and poly(1,4-cyclohexylenedimethylene 4,4'-bibenzoate) (PCB) with dimethyl *p*-terphenyl-4,4''-dicarboxylate.

Synthesis and Structure–Property Relationships of Polyesters Containing Rigid Aromatic Structures

Hans Eliot Edling

ABSTRACT

(General Audience)

Polyesters have a unique balance of properties that sets them apart from other polymers formed by step growth reactions. The transesterification reaction that forms polyesters occurs continually at reaction temperatures, making it easy to randomly distribute a mixture of different comonomers along the backbone during the polymerization process, or even when blending two different polyesters. Poly(ethylene terephthalate), commonly referred to as PET, is the most important polyester currently in production, and is prized for its transparency, chemical resistance, and recyclability. PET was first made by John Whinfield and James Dickson at Calico Printers' Association of Mansfield, in 1941 and was eventually licensed to DuPont in the 1970s. It has since become a valuable resource for producing synthetic textiles and replacing heavier materials, such as glass and metal, to produce lightweight containers, especially for food storage. Many of the polyesters, such as PET, that we see on a daily basis are actually copolyesters that contain low levels of additional comonomers that have been added to improve some property of the final polymer or to facilitate processing. In research, modification of polyesters with different comonomers broadens our understanding in how the molecular structure of comonomers affects polyester properties. This makes it possible to tune a copolyester's physical properties in a way that can enhance its suitability for a wide range of applications. The research described in this dissertation is focused on exploring how rigid monomer structures containing multiple aromatic

rings might be used to produce polyesters with improved performance relative to current commercial polyesters.

Materials that demonstrate good barrier to gases such as CO_2 and O_2 are important for packaging that can seal in and preserve food and beverages. In our research, we modified PET with bibenzoate structures to produce films that showed improved gas barrier when stretched in a manner that imitates the stretch blow molding process used to produce bottles. These materials showed good promise for packaging capable of preserving food for longer periods of time.

Clear, food safe plastics that do not deform at the boiling temperature of water are important for baby bottles and durable dishwasher safe containers, which are commonly sterilized with boiling water. Until recently, such materials were produced from bisphenol-A polycarbonate (BPA PC), which fell out of favor for food safe applications over concerns that BPA, believed to have endocrine disrupting activity, may leach into food and beverages. Bibenzoate monomers, which increases the application temperature of many polyesters, were combined with different combinations of diol monomers to produce transparent copolyesters that are usable at higher temperatures. These materials demonstrated excellent potential as food safe alternatives to BPA containing materials.

Crystalline plastics that resist distorting at high temperatures are important for applications in the electronics and automotive industry. Semicrystalline polyesters provide less expensive alternatives to the costly liquid crystalline polymers commonly used for high temperature applications. We explored the properties of a number of semicrystalline copolyester compositions capable of exceeding the application temperature of semicrystalline polyesters currently on the market.

Acknowledgements

I am extremely grateful to my research advisor, Dr. S. Richard Turner, for guiding me over the years and urging me to become a better researcher. I continue to be amazed by his enthusiasm for chemistry and his extensive knowledge, which guided me countless times over the years. I would also like to thank my committee members Dr. Richard D. Gandour, Dr. Timothy E. Long and Dr. Robert B. Moore for their invaluable input and guidance on my research projects and presentation skills.

This research would not have been possible without the help of Dr. Long's research group and use of the many instruments they have at their disposal. I especially would like to thank Ryan Mondschein, Katie Valentine, Joseph Dennis, Phillip Scott and Mingtao Chen, all of whom gave up their time to help me with running instruments and performing data analysis. I would like thank Dr. Herve Marand, Dr. Bruce Orler and Matthew Vincent, who provided invaluable help and insights into thermal analysis. I offer special thanks to my collaborators, Dr. David Schiraldi, Dr. Hossein Ghassemi and Dr. Hua Sun, at Case Western Reserve University who provided great help and insightful discussions regarding my research.

I would like to thank all the members of the Turner research group who provided a wonderful learning environment and friendship over the years. I would like to thank past members Zhengmian Chang, Haoyu Liu for providing guidance and friendship in my early years as a graduate student and I would like to thank Jing Huang and Sarah Blosch, who stuck it out with me until the end.

I would like to thank John Echols, Sam Huff, Haleigh Hutcheson and the many members of the VPI Cave Club who became my family away from home and gave me support over the years. I would also like to thank Steffi Muller, who has been a warm and loving partner during my

last year as a graduate student. Lastly, I would like to thank my family; my parents, Francesca and Geoffrey Edling, for encouraging me over my entire life and my brothers, Ivan and Axel, who have been my role models throughout life.

Attributions

Chapter 1: Literature Review on Copolyester Thermoplastics

S. Richard Turner, PhD, Department of Chemistry at Virginia Tech is currently a research professor at Virginia Tech. Dr. Turner supplied a portion of the references and contributed with editorial comments

Chapter 2: Copolyesters Based on Bibenzoic Acids (published in Polymer)

Haoyu Liu, PhD, Department of Chemistry at Virginia Tech, is currently a Senior R&D Scientist/Engineer at Honeywell. Dr. Liu was a co-author on this paper, performed preliminary research on developing melt polymerization, thermal and structural characterization and biaxial orientation.

Hua Sun, PhD, Department of Macromolecular Science and Engineering at Case Western Reserve University. Dr. Sun was a co-author on this paper, performed biaxial orientation, performed barrier measurements and contributed with editorial comments.

David A. Schiraldi, PhD, Department of Macromolecular Science and Engineering at Case Western Reserve University is currently a professor at Case Western Reserve University. Dr. Schiraldi was a co-author on this paper and contributed technical and editorial comments.

Ryan Mondschein, Department of Chemistry at Virginia Tech, is a research scientist at Virginia Tech. Mr. Mondschein was a co-author on this paper, performed preliminary research on melt polymerizations and contributed technical and editorial comments.

Timothy E. Long, PhD, Department of Chemistry at Virginia Tech is currently a professor at Virginia Tech. Dr. Long was a co-author on this paper, contributed technical and ~~with~~ editorial comments.

Charles S. Carfagna Jr., PhD, Macromolecular Materials Discovery Center at Virginia Tech. Dr. Carfagna provided thermogravimetric analysis of polyesters.

ExxonMobil Chemical Company provided materials for polymerization and injection molded dogbones for tensile analysis

S. Richard Turner, PhD, Department of Chemistry at Virginia Tech is currently a research professor at Virginia Tech. Dr. Turner served as the research advisor and was a co-author on this paper and contributed technical and editorial comments.

Chapter 3: Amorphous Copolyester Based on Bibenzoic Acids and Neopentyl Glycol

Ryan Mondschein, Department of Chemistry at Virginia Tech, is a research scientist at Virginia Tech. Mr. Mondschein was a co-author on this paper, performed preliminary research on melt polymerizations and contributed with editorial comments.

Timothy E. Long, PhD, Department of Chemistry at Virginia Tech is currently a professor at Virginia Tech. Dr. Long was a co-author on this paper, assisted in performing rheological measurements and interpreting results and contributed technical and editorial comments.

Charles S. Carfagna Jr., PhD, Macromolecular Materials Discovery Center at Virginia Tech. Dr. Carfagna provided thermogravimetric analysis of polyesters.

ExxonMobil Chemical Company provided materials for polymerization, injection molded dogbones for tensile analysis, injection molded bars for Notched Izod impact testing and performed Notched Izod impact testing.

S. Richard Turner, PhD, Department of Chemistry at Virginia Tech is currently a research professor at Virginia Tech. Dr. Turner served as the research advisor and was a co-author on this paper and contributed technical and editorial comments.

Chapter 4: Synthesis and Crystallization Behavior of Rigid Copolyesters With Biphenyl-4,4'-dicarboxylate and 2,6-Naphthalenedicarboxylate in the Main Chain

Kevin Barr, Department of Chemistry at Virginia Tech, was a research scientist at Virginia Tech. Mr. Barr was a co-author on this paper and performed preliminary research on melt polymerizations and thermal/structural characterization.

Matthew R. Vincent, Department of Chemistry at Virginia Tech, is a research scientist at Virginia Tech. Mr. Vincent was a co-author on this paper, performed calorimetry and contributed with editorial comments.

Hervé Marand, PhD, Department of Chemistry at Virginia Tech is currently a research professor at Virginia Tech. Dr. Marand supervised the thermal analysis portion of this research, was a co-author on this paper and contributed technical and editorial comments.

Solvay Specialty Polymers provided materials for polymerization.

S. Richard Turner, PhD, Department of Chemistry at Virginia Tech is currently a research professor at Virginia Tech. Dr. Turner served as the research advisor, was a co-author on this paper and contributed technical and editorial comments.

Chapter 5: Exploration of Semicrystalline Copolyester Modified with *p*-Terphenyl Units

Solvay Specialty Polymers provided materials for polymerization.

S. Richard Turner, PhD, Department of Chemistry at Virginia Tech is currently a research professor at Virginia Tech. Dr. Turner served as the research advisor, was a co-author on this paper and contributed technical and editorial comments.

Table of Contents

List of Figures

List of Tables

List of Schemes

Chapter 1. Literature Review on Copolyester Thermoplastics

1.1 Introduction to Copolyesters

Polyesters are set apart from other step growth polymers by facile transesterification that occurs continually throughout the polymerization process, making it easy to randomly distribute a mixture of different comonomers along the backbone. This can be done during the initial polymerization process, but also can be achieved by blending different polyesters together in the melt. Many of the homopolyesters, such as poly(ethylene terephthalate) (PET), that we see on a daily basis commonly contain low levels of additional comonomers that have been added to improve some property of the final polymer or to facilitate processing.[1] Modification of homopolyesters with different comonomers assists in establishing structure-property-morphology relationships. This makes it possible to tune a copolyester's physical properties in a way that can enhance glass transition (T_g), melting point (T_m), crystallizability, degradation, gas barrier and chemical resistance.

The term 'glycol modified' refers to copolyesters that have had an additional diol(s) added to modify the polyester properties. Notable instances of glycol modified copolyesters are PCTG (PET modified with more than 50 mol% 1,4-cyclohexanedimethanol (CHDM)) and PETG (PET modified with less than 50 mol% CHDM) (**Figure 1-1a**).[2-3] More recently, copolyesters modified with 2,2,4,4-tetramethyl-1,3-cyclobutanediol (CBDO) have become commercially relevant **(Figure 1-1b).**[4-8] Similarly, 'acid modified' copolyesters contain additional diesters or diacids. The number of available diacids capable of significant property enhancement are limited relative to the diols currently available, however, many have been thoroughly studied.[1, 3, 9-10]

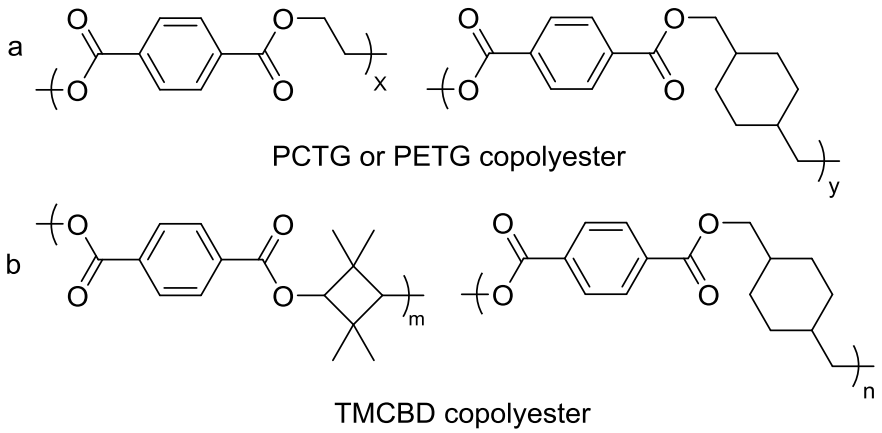

Figure 1-1. Repeat structure of PETG/PCTG copolyester (name depends on diol ratio) (a) and a TMCBD copolyester (b)

1.2 Diester Comonomers

1.2.1 Common Aromatic Acid Modifiers

When trying to understand how different molecular structures are used to tailor or modify polyesters for specific properties, the structure–property–morphology relationship profiles of well-studied diesters such as dimethyl terephthalate (DMT), dimethyl 2,6-naphthalate (DMN), and dimethyl isophthalate (DMI) (**Figure 1-2**) provide fundamental data for establishing fundamental structure–property relationships that can be helpful in predicting polymer properties imparted by prospective new monomers. The linear symmetry and rigid structure of the terephthaloyl unit

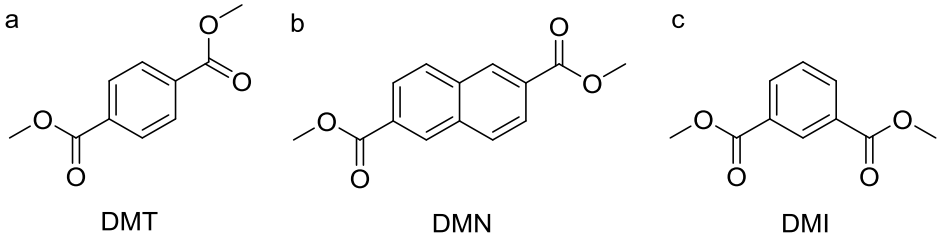

Figure 1-2. Three aromatic diester monomers (dimethyl terephthalate (DMT), dimethyl 2,6-naphthalate (DMN), and dimethyl isophthalate (DMI)) commonly used in commercial polyesters.

(**Figure 1-2a**) favors ordered packing of the chains into crystalline structures, resulting in a semicrystalline polyester. Poly(ethylene terephthalate) (PET) (which combines terephthalic acid and ethylene glycol (EG)) is the most well-known semicrystalline polyester due to its wide utility in commercial applications such as bottling, films and fibers. Poly(butylene terephthalate) (PBT) combines DMT with 1,4-butandiol (BD) and crystallizes much more quickly than PET due to the longer, more flexible butane diol unit (**Figure 1-3**). While it is more expensive, PBT is still widely used because its faster crystallization allows injection molded parts with good dimensional stability to be produced at a much more rapid pace.[10]

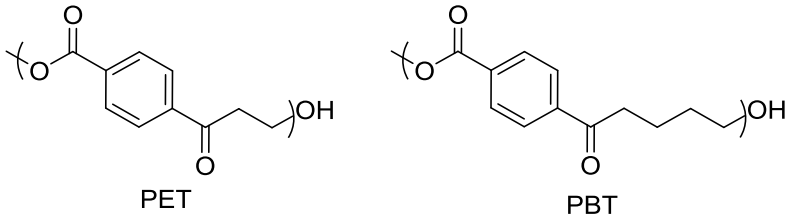

Figure 1-3. Chemical structure of poly(ethylene terephthalate) (a) and poly(butylene terephthalate) (b).

The relationship between symmetry and crystallization is clearly demonstrated when the meta substituted isophthaloyl unit (**Figure 1-2c**) is compared to para substituted terephthaloyl unit (**Figure 1-2a**). The isophthaloyl moiety has a non-linear shape that produces a "kink" in the polymer backbone, making it difficult for polymer chains to stack and decreases and/or slows crystallization. The two fused rings in the naphthalene-2,6-dicarbonyl unit (**Figure 2b**) produce a much more rigid polymer backbone, resulting in a higher T_g, T_m, tensile modulus and tensile strength when compared to PET. Both the isophthaloyl and naphthalene-2,6-dicarbonyl units are nonsymmetrical along the ring-flipping axes, which results in decreased molecular mobility and lower free volume relative to terephthaloyl units (**Figure 1-4**).[11-16] Dynamic mechanical analysis

(DMA) was used to compare the low temperature molecular mobility of polyesters containing isophthalate and 2,6-naphthalate relative to terephthalate units.[17-18] Phenyl ring flips are apparent as sub-T_g relaxations at approximately −60 °C. Tan δ peaks for PEN and PEI have a significantly lower magnitude, further indicating that PET has higher molecular mobility due to its ability to freely undergo phenyl ring flips. Lower gas permeability and higher selectivity are believed to result from more efficient packing in the amorphous regions and from restricted mobility. As a result, there have been attempts to correlate low permeability with lower sub-T_g transitions resulting from higher energy barriers to rotation.[11-12]

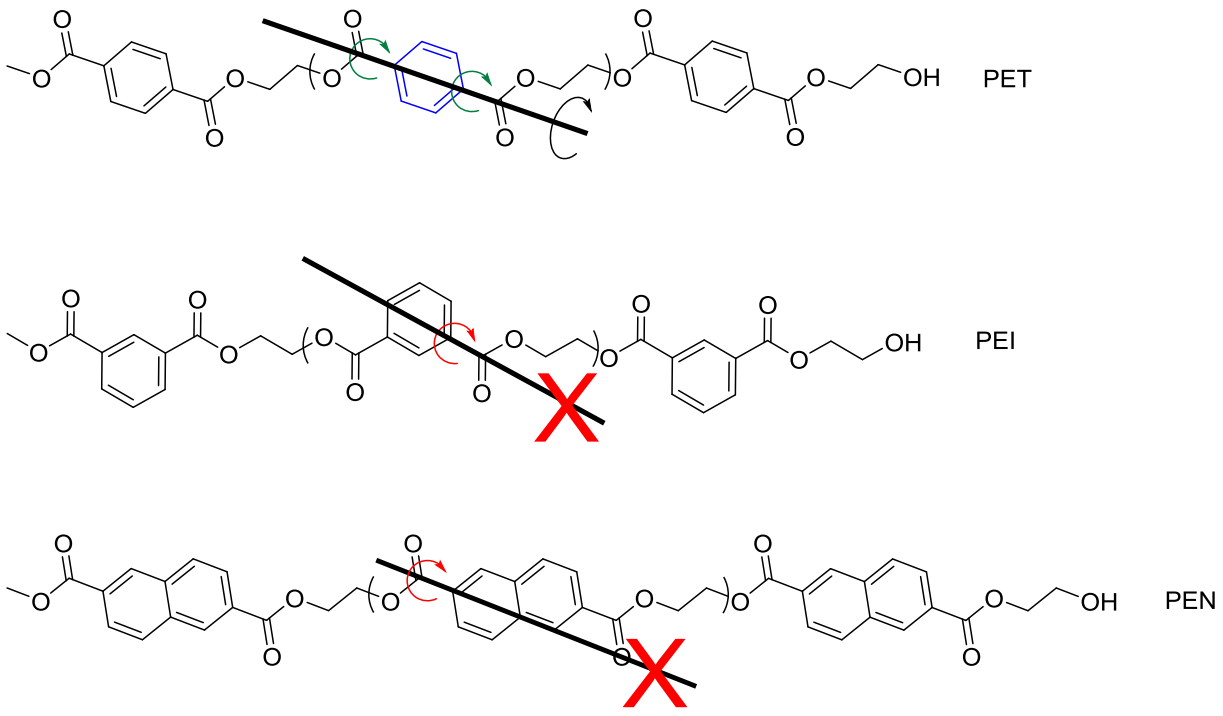

Figure 1-4. Comparison of terephthalate ring flipping to isophthalate and 2,6-naphthalate.

PET is an attractive material for food packing because it has sufficiently high gas barrier to prevent spoilage, is non-toxic and has good organoleptic properties. The commercial value of

PET is derived from its low cost relative to tensile strength, modulus, ductility, T_g and T_m; it can also be readily processed as injection or stretch blow molded parts. To aid in processing, PET is commonly modified with an additional comonomer to help control the rate of crystallization and aid the production of transparent films.[1] Isophthalate is used more than any other comonomer for modifying PET, and is able to effectively slow crystallization by producing a small 'kink' defect in the polyester backbone that disrupts chain packing.[19] The meta substitution of isophthalate has also been shown to improve gas barrier.[15] The PEI homopolyester has low ductility and poor thermal properties relative to PET and PEN (**Table 1-1**), however, a small amount (~5 mol%) of isophthalate in PET effectively suppresses crystallization without significantly impacting the thermal or mechanical properties.[20]

Table 1-1. Thermal and mechanical properties of amorphous PET, PEI and PEN polyesters. Tensile analysis was performed on quenched amorphous samples following ASTM testing method D638.

Property	**PET***	**PEI***	**PEN***
Modulus (MPa)	1580 ± 40	2500 ± 90	1730 ± 30
Yield Stress (MPa)	56 ± 2	64 ± 3	77 ± 1
Breaking Strain (%)	316 ± 4	6 ± 2	130 ± 30
T_g (°C)	81	60	122
T_m (°C)	252	231	265
Permeability (cc.cm/m^2/atm/day)	0.461 ± 0.001	0.090[15]	0.155 0.005

*Data obtained in this study

DMI can also modify semicrystalline polyesters such as poly(1,4-cyclohexylenedimethylene terephthalate) (PCT) to aid in processing. Without modification, polyesters with high melting points, such as PCT (T_m = 290 °C), have to be processed at temperatures where thermal degradation is a concern. As a result, PCT is carefully dried to

minimize degradation and prevent coloring and loss of mechanical properties. The 'kinked' isophthaloyl unit disturbs the crystalline regularity of PCT, reduces the melting temperature, and produces a copolyester that is more susceptible to dying and easier to make into transparent films. More than 35 mol% isophthalate is enough to completely disrupt crystallinity in PCT and produce an amorphous material, and just 5–10 % DMI to PCT is enough to widen the window between the melting and degradation temperatures, making it more straightforward to make PCT films, fibers, and composites.[3, 21] Conveniently, DMI has very little impact on the T_g of PCT, allowing selective suppression of the melting transition temperature without significantly decreasing the T_g of PCT.[20] Adding DMI to PCT has the advantage of preserving the hydrophobic character of PCT and eliminating the need for the extensive pre-drying common in EG containing polyesters.[22]

Dimethyl 2,6-naphthalenedicarboxylate (DMN) is also a useful acid modifier for a range of copolyesters. When compared to PET, poly(ethylene 2,6-naphthalate) (PEN) (**Figure 1-5**) possesses superior properties in many respects including: higher modulus, higher T_g, and lower oxygen and CO_2 permeability.[23] Modifying PET with DMN increases the T_g by 4–5 °C for every 10 mol% added, improves thermal stability and, if more than 15 mol% of DMN is added, crystallization of PET can be disrupted sufficiently to produce clear plastics.[3]

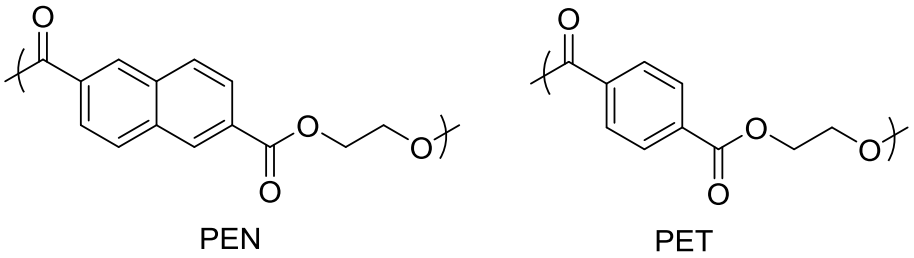

Figure 1-5. Repeat structure of PEN and PET.

1.2.2 Semicrystallinity in Copolyesters

In semicrystalline polyesters, polymer chains are arranged in ordered (crystalline) and disordered (amorphous) morphologies. Polyesters with high melting temperatures are often associated with high performance thermoplastics due to their desirable physical and mechanical properties, while maintaining many of the processing advantages of polyesters. Molecular structures that enhance polymer backbone rigidity have been the subject of numerous studies due to their known relationship to enhanced melting temperatures and T_gs in semicrystalline polyesters.[2, 24-27] Structure–property–morphology relationship studies have shown for quite some times that monomers with high aromatic character are effective in imparting rigidity,[28-30] with monomer symmetry also playing a role.[31-33] As the melting temperature of polyesters approaches 300 °C, thermal degradation becomes a major concern during melt polycondensation. Chain scission resulting in coloration and decreased molecular weight is often observed and well-studied in polyesters is well studied for elevated reactor temperatures.[28-30, 34] High melting temperatures also require high melt processing temperatures in situations where the melted polyester may be exposed to air. Such conditions have been shown to result in crosslinking of PET through formation of a trifunctional 2,3',5-biphenyltricarboxylate moiety (**Figure 1-6**).[35]

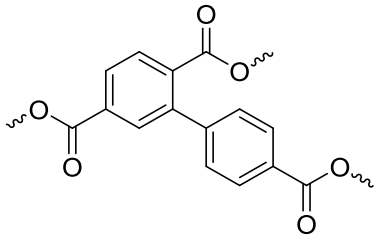

Figure 1-6. Trifunctional 2,4',5-biphenyltricarboxylate moiety responsible for crosslinking of degraded PET samples[35]

Most semicrystalline copolyesters exhibit a decrease in crystallinity with addition of a comonomeric unit. Copolyesters often lose crystallinity altogether to produce a fully amorphous material due to the incompatibility of comonomers within the crystal lattice.[1, 3, 36] However, not all comonomers are completely incompatible, and different levels of cocrystallization have been studied.[37-39] Different homopolyesters are compatible within the crystal lattice when the free energy for cocrystallization is very small. Cocrystallization occurs when two comonomer units have a compatible or similar enough structure to allow them to occupy the same crystal lattice. Many models have been developed over the years to describe the depression of melting temperatures with comonomer content, with the Wendling–Suter model combining many aspects of previous models.[40-44] Isomorphism occurs in rare cases where comonomers are highly compatible, resulting in only one crystalline phase that contains both comonomers over the entire composition range. Isodimorphism occurs when two different crystalline phases are observed over the composition range. In isodimorphism, a homopolyester incorporates low concentrations of minor comonomeric units within its crystalline lattice until the concentration of the minor comonomeric units increases sufficiently to dictate the crystalline phase. In isodimorphism, minor comonomeric units produce minor defects in the crystalline structure that decrease the T_m and rate of crystallization until it reaches a minimum, called a eutectic point, where the crystalline phase changes to that of the minor comonomeric unit and T_m begins to increase again (**Figure 1-7**).[39] One homopolyester may be more accommodating of minor comonomeric units than another and factors affecting isodimorphic behavior are still a rich area of research.[45-49]

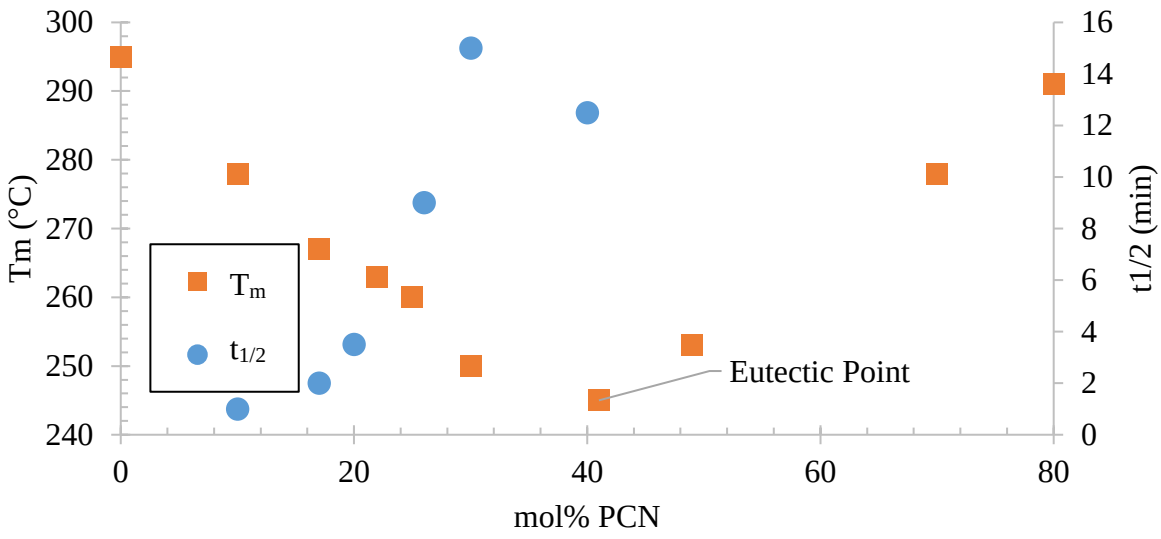

Figure 1-7. Combined figures of copolyester melting temperature and crystallization half-times ($t_{1/2}$).[39] Melting temperature vs composition for PCT/PCN copolyesters shows a eutectic point around 40 mol% PCN (left axes). Crystallization determined via small angle laser light scattering (SALLS) shows a change in crystallization rate at eutectic point, indicating a change in crystalline morphology (right axes).

Lorenzetti et al performed a thorough investigation of cocrystallization in poly(1,3-propylene 2,6-naphthalate) (PPN) and poly(1,3-propylene terephthalate) (PPT) random copolyesters, which exhibit a eutectic point in the melting temperatures (**Figure 1-8**).[37] The appearance of melting temperatures across the composition range with no apparent amorphous window suggests that the structure of PPN and PPT are similar enough to allow some degree of cocrystallization. Wide angle X-ray scattering (WAXS) analysis of copolyester compositions showed a transition from the crystalline phase exhibited by the PPT homopolyester to that exhibited by PPN around 51 mol% PPN, which corresponds with the eutectic point. Defect free energies calculated with Wendling–Suter theory indicate that the PPN crystal lattice is better able to accommodate PPT units. This is was attributed to the larger molar volume of the naphthalate moiety.[37] This contrasts with work done by Jeong and Hoffman who studied cocrystallization of

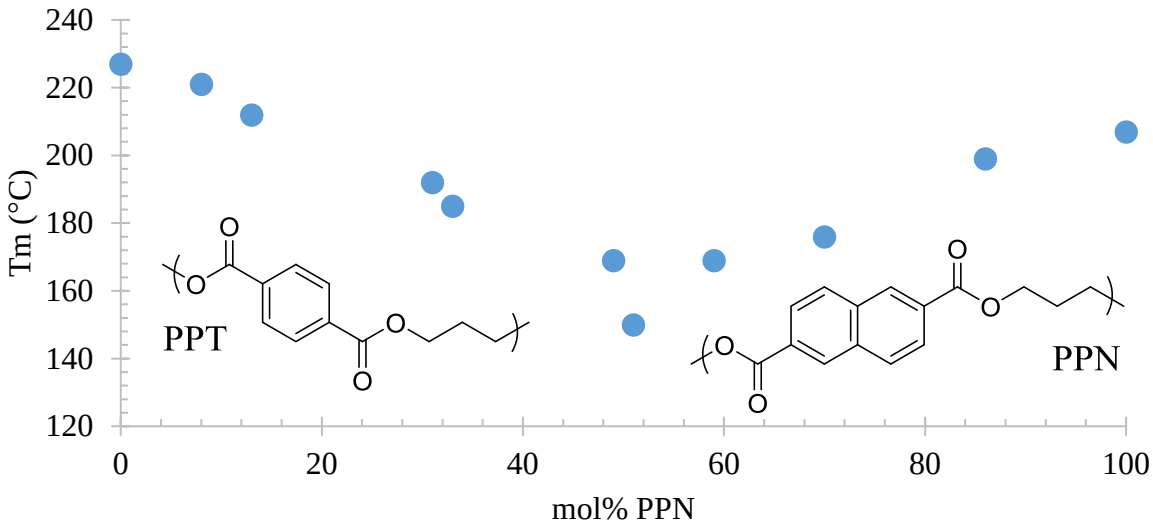

Figure 1-8. Melting temperatures of PPT and PPN copolyesters across the composition range. Adapted with permission from Lorenzelli et al.[37] Copyright 2011 Elsevier

PCT and PCN random copolyesters (**Figure 1-7**).[39, 49] Wendling–Suter calculations by Jeong et al indicated that, unlike with PPN and PPT, the PCT crystal lattice was better at accommodating PCN units into its crystal lattice than the converse. This led them to propose that higher unit cell density might reduce the incorporation of minor copolyester components into the crystal lattice.[49] In most cases, however, homopolyesters with larger unit cell volumes and longer crystallographic repeat lengths are better able to incorporate minor copolyester components within their crystal lattice.[48, 50] Recently, Yu et al. synthesized and characterized four series of linear aliphatic random copolyesters for the purpose of investigating the effect of chain length on isodimorphic behavior, and proposed a new model that expands the Wendling–Suter theory to include the effect of comonomer length.[45] The composition at which the eutectic point is observed is determined by each parent homopolyester's ability to compete with the other and control crystal structure. As such, the eutectic point is often dictated by stiffer, longer monomers with more stabilized

crystalline structures; however, other factors such as cocrystallizability, unit cell volume and unit cell density also play a role.

For copolyesters, eutectic points imply a degree of incompatibility between the crystal lattices of the parent homopolyesters. Isomorphism occurs when the structure of two different homopolyesters are so similar in length, structure and density that only a single crystal lattice is observed over the entire composition range. Studies performed on PCN and poly(hexamethylene 2,6-naphthalate) (PHN) copolyesters showed no eutectic point over the entire composition range (**Figure 1-9**).[38] Wide angle X-ray diffraction shows sharp diffraction peaks over the entire composition range with d-spacings changing linearly with added comonomer content, indicating a continuous variation in composition from PHN to PCN and showing high compatibility between the hexamethylene and the 1,4-cyclohexylenedimethylene units. Isomorphic behavior was not observed for butylene or ethylene diols, indicating that monomer length plays an important role in monomer compatibility.

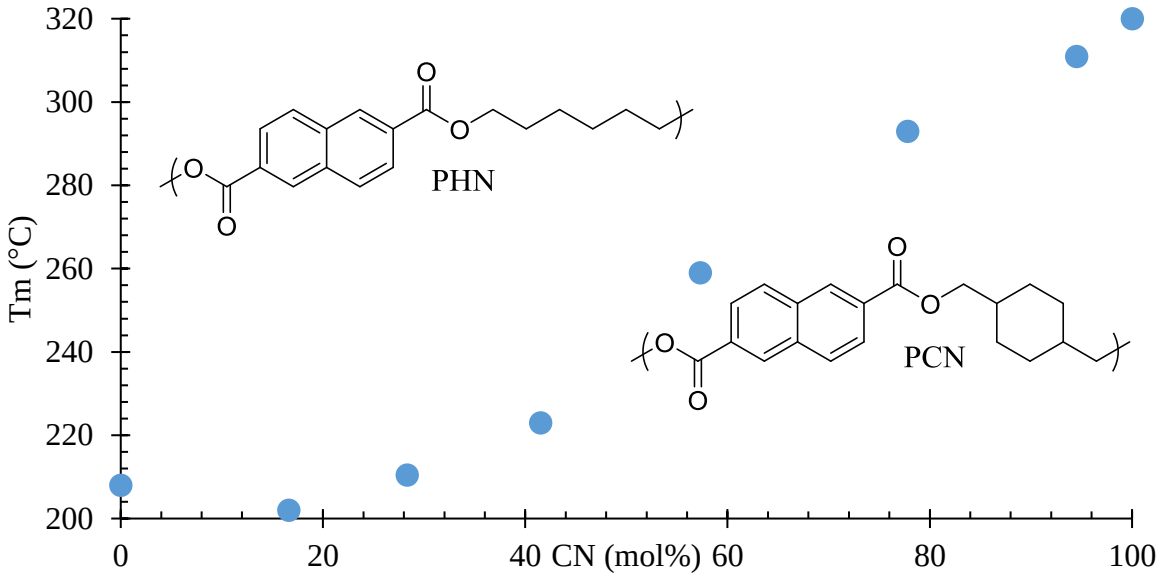

Figure 1-9. Melting temperatures for PHN–PCN copolyesters. Adapted with permission from Jeong et al.[38] Copyright 2003 American Chemical Society

1.2.3 PIDA Copolyesters

Over the years, many different monomers (diacids or diols) have been prepared and studied to modify or enhance polyester properties. One primary goal of acid modification is raising the T_g of PET or PCT, frequently by synthesizing large, rigid diacid monomers. A prime example of this is from Petropoulos,[51] who prepared 3-(4-carboxyphenyl)-1,1,3-trimethyl-5-indane carboxylic acid (PIDA) via dimerization and subsequent oxidation of α,p-dimethylstyrene as shown (**Figure 1-10**). Later, Petropoulos went on to synthesize polyesters by contacting PIDA with glycerin, fatty

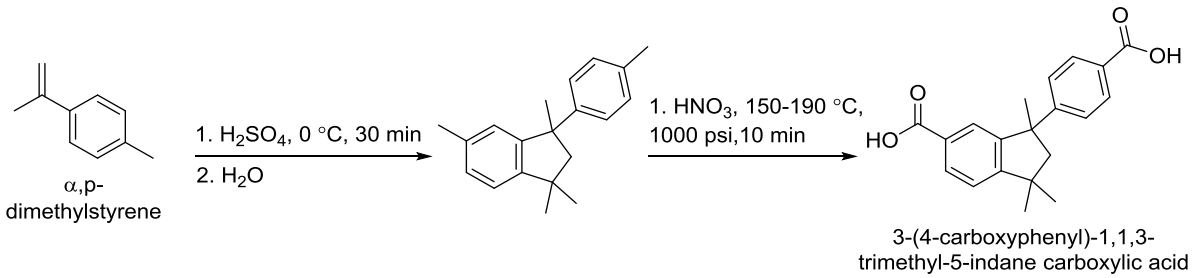

Figure 1-10. Dimerization and subsequent oxidation of α,p-dimethylstyrene into 3-(4-carboxyphenyl)-1,1,3-trimethyl-5-indane carboxylic acid (PIDA) as described by Petropoupos[51]

acids, and ethylene glycol.[52] This patent reports a softening temperature (ball and ring method) of 165 °C for the PIDA–EG polyester. Later, Meyer used an antimony trioxide catalyst to facilitate esterification of PIDA with EG to form a homopolyester.[53] Molecular weights (M_n) as high as 37,500 g/mol were achieved, measured by using vapor pressure osmometry in tetrahydrofuran, and glass transition temperatures (T_g) ranged from 153–154 °C. Meyer was also able to draw fibers, which induced crystallization (T_m of 160 °C measured by polarizing microscope), with tensile strength comparable to PET. Deeken et al. showed the value of PIDA as an acid modifier

to improve the processability of PET without detracting from the physical or thermal properties (**Table 1-2**).[54] They claimed PIDA to be superior to dimethyl isophthalate (DMI), a comonomer

Table 1-2. Thermal properties of PET-based copolyesters containing PIDA

mol% PIDA	Melting (°C)	T_g (°C)
0	265	80
5	215	92
10	231	Not measured
15	220	100
20	Amorphous	Not measured
30	Amorphous	Not measured
100	Amorphous	154

commonly used to reduce crystallinity and improve processability of PET, as an acid modifier for polyesters. DMI, aside from disrupting crystallinity, does not improve the physical properties of PET, but in fact decreases the T_g, which is usually undesirable. PIDA not only disrupts crystallinity much like DMI, but it also increases the T_g and improves the dye receptivity of PET sufficiently to accept disperse dyes without the assistance of dye carriers. Deeken et al. synthesized PET-based copolyesters with up to 10 mol% PIDA while maintaining sufficient crystallinity to draw fibers, and oriented films with up to 15 mol% PIDA, having a T_g of 100 °C, good clarity and high tensile strength. Above 20 mol% PIDA, copolyesters were amorphous, with good clarity making it useful for high T_g injection molded parts, films and coatings. Semicrystalline films and fibers also exhibited high retractability (>10 %) when not annealed, making PIDA modified PET potentially useful for heat-shrink applications. Much more recently Shaikh et al.[55] contacted the dimethyl ester of PIDA with 1,4-cyclohexanedimethanol (CHDM) and tricyclodecane dimethanol (TCD) (**Figure 1-11**) to produce polyesters with high T_gs (163 and 175 °C respectively). They also used PIDA along with dimethyl 1,4-cyclohexanedicarboxylate (DMCD), dimethyl 2,6-naphthalate (DMN),

DMT, tetramethyl cyclobutane diol (TMCBD), TCD and CHDM to produce a range of copolyester compositions, with T_gs in the range of 120–157 °C.

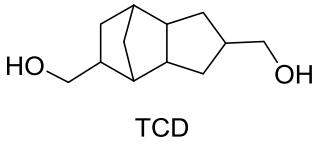

TCD

Figure 1-11. Molecular structure of tricyclodecane dimethanol (TCD)

1.2.4 FDCA Monomers

Terephthalic acid (TA) is an essential monomer produced from petroleum feedstocks that produces many high performance and commodity polymers such as PET. The production of bio-based PET has been the subject of much research; however, an industrially feasible process to produce renewable PET is still unavailable. This has increased interest in 2,5-furandicarboxylic acid (FDCA) (**Figure 1-12**), which has a structure reminiscent of TA, as a potentially suitable bio-based replacement for TA.[16, 56-64] Glucose, fructose, and cellulose have been used to successfully synthesize 5-hydroxymethylfurfural (HMF).[60] To increase the industrial potential of FDCA, scientists have been developing improved synthesis routes for HMF, which is a common precursor to FDCA.

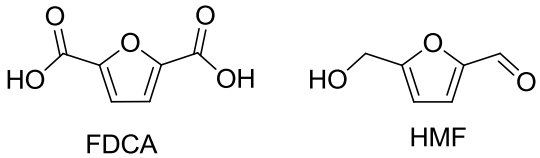

Figure 1-12. Structures of HMF and FDCA

Román-Leshkov et al.[62] explored the conversion of fructose into HMF by using an acid catalyst in a two-phase system with promising yields (90% fructose conversion with 80% HMF selectivity). The dehydration reaction occurs in the aqueous phase, which contains fructose and an acid catalyst. An organic phase consisting of methylisobutylketone and 2-butanol extracts the HMF formed in the aqueous phase. A two-phase system resulted in high selectivity by removing HMF and operates effectively at fructose concentrations as high at 50 weight%. Zhao et al.[63] explored the catalytic conversion of glucose and fructose into HMF with a range of different catalysts. High yields up to 83% were achieved at moderate temperatures for fructose by using 1-ethyl-3-methylimidazolium chloride ([EMIM]Cl), H_2SO_4, and a range of metal chlorides (**Figure 1-13**). They had less luck achieving impressive conversions for glucose to HMF, only reaching

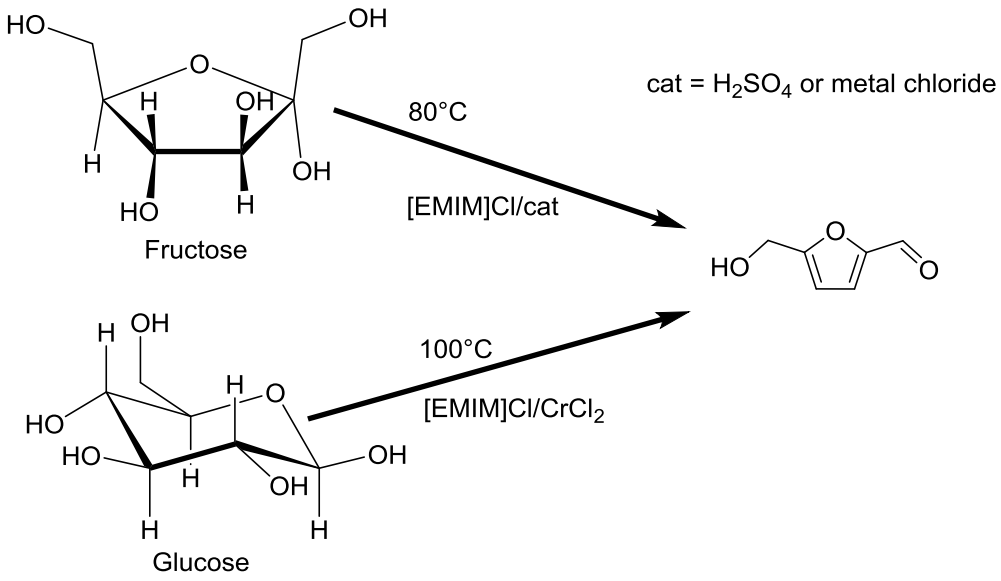

Figure 1-13. Synthesis of HMF from fructose and glucose[63]

70% yield through the use of [EMIM]Cl and $CrCl_2$. Recently, Gupta et al.[60] made impressive progress with hydrotalcite-supported gold nanoparticle catalysts for converting HMF into FDCA with greater than 99% HMF conversion and 99% FDCA selectivity. Heating the reaction at 368 K

under oxygen resulted in greater than 99% selectivity while heating under normal atmosphere produced 81% selectivity. Additionally, they did not detect gold leaching from the catalyst support, which retained 90% selectivity after three uses.

Because FDCA is highly pursued as a renewable substitute for TA, assessing the industrial potential of polymers produced from FDCA for various high performance applications is essential. Despite some similarities, FDCA produces properties distinctly different from TA. FDCA has a lower thermal stability than TA due to its diene character and reduced aromaticity. This requires FDCA based polymers to have milder processing conditions.[61] The acid groups on FDCA are not at an 180˚ angle as in TA, but are closer to 130˚, decreasing polymer chain linearity and introducing a 'kink' much like DMI. This, in addition to being a heterocyclic compound with a distinctly different dipole moment than TA, can have a profound effect on crystallinity.

Much of the recent research performed on FDCA based polymers explores their ability to replace high volume polymers such at PET and PBT. Therefore, studies on production and property analysis of furan-based analogues PEF and poly(propylene-2,5-furanoate) (PPF) have been extensive. Gandini and co-workers[56-58] initially studied the synthesis of the dimethyl ester of FDCA (DMFDCA) via esterification of FDCA and characterized the resulting polymers from melt transesterification polymerizations with EG, isosorbide (ISB) or bis(1,4-hydroxymethyl) benzene. Zhu et al.[64] more thoroughly investigated the mechanical properties of poly(butylene-2,5-furanoate) synthesized via melt transesterification (**Table 1-3**). The color of the samples ranged

Table 1-3. Characterization and thermal properties of FDCA-based polyesters[64]

Polyester	Young's Modulus (MPa)	Elongation to break (%)	Stress at Break (MPa)	M_w (g/mol)
PBT	1000 ± 100	270 ± 70	38 ± 3	47,700
PBF	970 ± 60	1100 ± 20	29± 2	49,000

from light yellow to brown. When compared to a PBT sample at a similar molecular weight, PBF had an almost identical Young's modulus, but a considerably lower stress at break. However, PBF exhibited much higher elongation to break, which is a strong indicator for higher toughness.

Recently Knoop et al.[61] set out to test the industrial potential of FDCA to replace TA by synthesizing PEF, PPF and PBF via melt transesterification and solid-state post condensation (SSPC). The primary focus of this study was to determine the potential of PEF to replace PET. Much like the studies done by Gomes et al.[58] and Zhu et al.,[64] when used to replace TA, FDCA yielded polymers with comparable T_g and T_m values (~50 ˚C lower than the TA counterparts) shown in **Table 1-4**. Knoop et al.[61] managed to eliminate the discoloration usually associated with high molecular weight PEF produced with melt transesterification by using solid state polymerization (SSP) to achieve high molecular weights while avoiding decomposition in the melt. A rotating drum approach, achieved with a rotary evaporator and vacuum pump, was used to perform SSP on PEF. Good polydispersity (Đ≈ 1.95) and high molar masses (M_n ≈83,000 g/mol) were achieved with little to no discoloration. The PEF molecular weight was higher than the commercial PET, which had a molecular weight ~ 33,000 g/mol.[61] Tensile testing showed the Young's modulus of PEF (2450 MPa) to be comparable to PET (2000 MPa). However, compression molded PEF was more brittle compared to PET; PEF only elongated 3 %, much

Table 1-4. Comparison of transition temperatures for polymers containing FDCA and TA diacids

Polyester	T_g (°C)	T_m (°C)	Polyester	T_g (°C)	T_m (°C)
PET	75[a]	260[a]	PEF	77[a], 80[c]	214[a], 215[c]
PPT	48[a]	227[a]	PPF	40[a], 50[c]	171[a], 174[c]
PBT	43[a], 40[b]	220[a], 224[b]	PBF	36[a], 39[b]	177[a], 172[b]

[a] DSC values obtained from Knoop et al.[61]
[b] DSC values obtained from Zhu et al.[64]
[c] DSC values obtained from Gomes et al.[58]

lower than the amorphous PET with a 250% elongation or the semicrystalline PET with a 90% elongation. The low elongation may make it difficult to implement PEF for bottling applications, however, this may be addressed with modifiers, adding comonomers or though different processing conditions. DMA was used to determine the modulus of PEF from 0–220 ˚C to evaluate the application temperatures of PEF. Amorphous PEF underwent a significant drop in storage modulus at the T_g (77 ˚C) and quickly failed before cold crystallization could occur, making hot fill applications seem impractical.

Work by Burgess et al.[65] investigating gas transport through PEF membranes found CO_2 permeability to be 19x lower than PET, signaling good potential in packaging applications where good barrier is desirable. DMA of PET and PEF showed a significant reduction in the β-transitions of PEF relative to PET, which is believed to correlate with lower membrane diffusivity. The lower β-relaxation intensity is believed to result from a higher barrier to furan ring flipping due its non-linear axes of rotation.[16]

1.2.5 Polyesters Containing Succinate and Adipate

Aliphatic polyesters play an important role in the history of synthetic polymers, the most important being those made from succinic acid (SA) and adipic acid (AA) or their dimethyl ester variants dimethyl succinate (DMSu) and dimethyl adipate (DMAd), respectively (**Figure 1-14**). Aliphatic polyesters containing adipate and succinate were first studied by Carothers[66] in the 1930s, but were abandoned for more promising polyesters such as PET due to their low T_ms and the inability to achieve high molecular weights (below 5,000 g/mol), which resulted in weak and brittle materials. Solid state polymerization (SSP) could not be used to increase molecular weight, as with PET, due to the low melting temperature of polyesters made with SA and AA.[67] SSP must be conducted below the T_m of the polymer to prevent melting and above the T_g to allow impurities

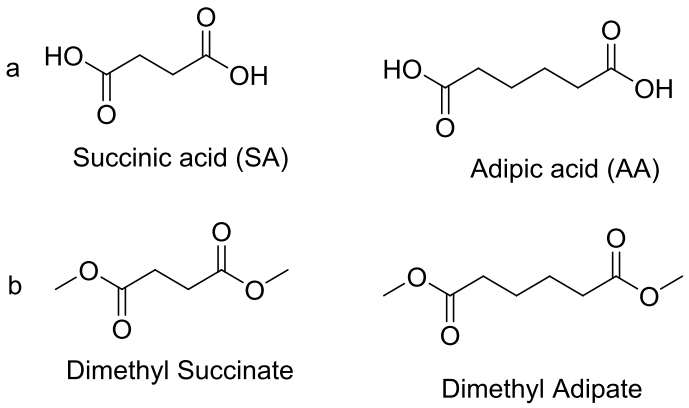

Figure 1-14. Chemical structure of the diacids (a) succinic acid and adipic acid, and the diesters (b) dimethyl succinate and dimethyl adipate

(e.g. methanol or water) to diffuse out of the solid material, however, the low T_m of the polymer makes diffusion so slow as to render it impractical.[68] Improvements in catalyst use, reaction conditions, and more appropriate monomer ratios were used to produce aliphatic polyesters from SA and AA having sufficiently high molecular weights to yield usable materials.[67, 69-70] Takiyama et al. were able to produce aliphatic polyesters with M_ns as high as 200,000 g/mol[71-73] and interest became sufficiently high to fund a pilot plant in 1991, a semi-commercial plant in 1993 and a commercial plant test module in 1993.[74] Indeed, interest in poly(butylene succinate) (PBSu), poly(butylene adipate) (PBAd) and copolyesters thereof (PBSA) (**Figure 1-15)** have continued to increase due to their potential as biodegradable commodity materials. Showa Highpolymer Co., Ltd. developed and markets PBSu and PBSA polyesters as BIONOLLE® for use in agricultural products (compost bags and mulching film), filaments, trash bags, as well as molded parts and bottles.[75-76] The value of aliphatic polyesters comes from their relatively low cost and their ability to combine good biocompatibility and biodegradability with thermal and tensile properties similar to polypropylene (PP) and low density polyethylene (LDPE).[67, 74] Further modifications to improve

biodegradability and barrier to water, alcohol, and CO_2 are expected to increase utilization of polyesters containing SA and AA.

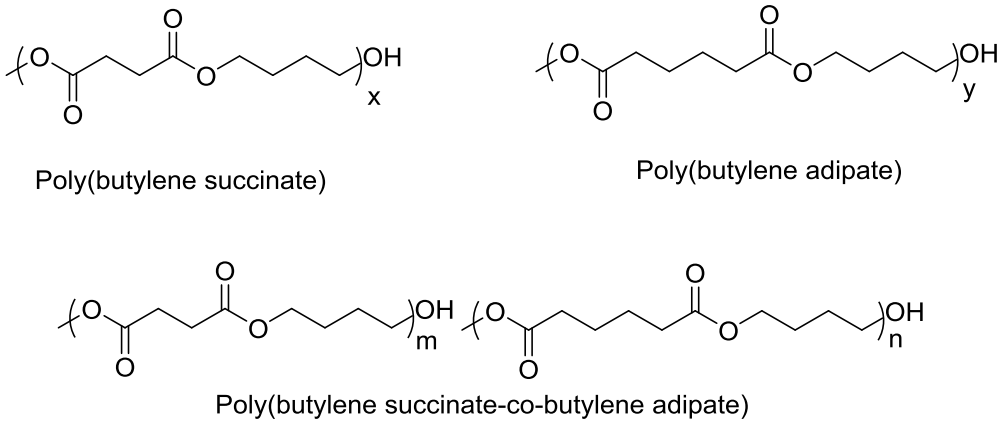

Figure 1-15. Chemical structure of poly(butylene succinate) (PBSu), poly(butylene adipate) (PBAd) and poly(butylene succinate-co-butylene adipate) (PBSA)

SA is commercially manufactured via hydrogenation of maleic anhydride, maleic acid or fumaric acid into succinic anhydride, which is then hydrated to form SA, or though the oxidation of 1,4-butanediol (**Figure 1-16**).[77] However, fermentation of renewable feedstocks (e.g. glucose) has also been demonstrated as an effective synthesis route.[70] AA is commercially manufactured via the hydrogenation of benzene or phenol into cyclohexane or cyclohexanol, which is then oxidized to produce a mixture of cyclohexanol and cyclohexanone that is further oxidized with nitric acid to form AA.[78] Alternative methods to synthesize AA, from butadiene and carbon monoxide, have also been extensively investigated but have not been pursued for the purpose of large scale manufacturing.[78]

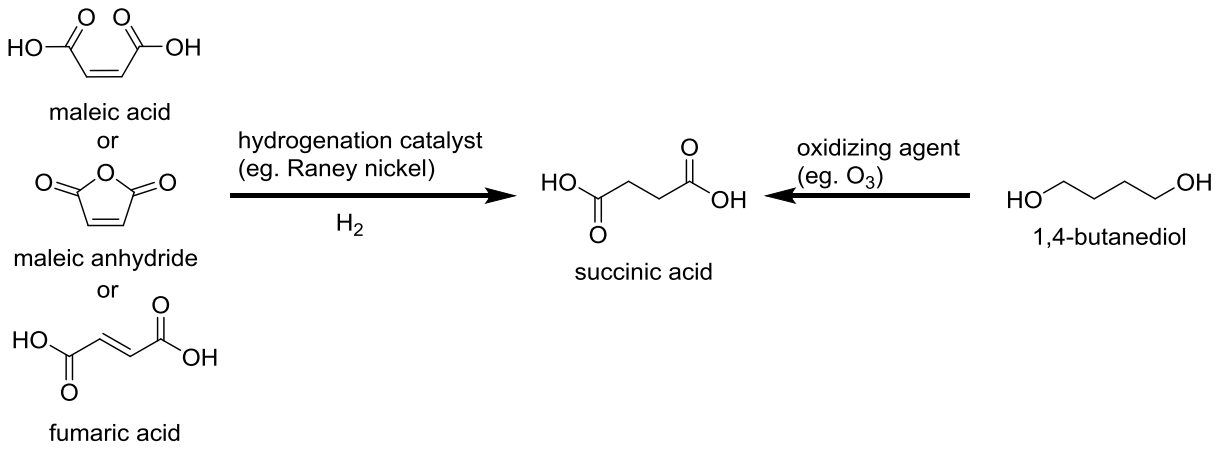

Figure 1-16. Manufacture of succinic is achieved through oxidation of maleic acid, maleic anhydride and fumaric acid or through the oxidation of 1,4-butanediol

SA and AA are effective acid modifiers for tuning specific properties of copolyesters. In a patent filed by Eastman Chemical Company, PET was modified with DMN and SA to produce a copolyester with superior barrier and tensile properties while still maintaining processability comparable to PET homopolymer.[79] DMN imparts better barrier and higher tensile to PET; however, this is at the cost of increasing the melting temperature and melt viscosity, making it more difficult to process. Adding a small amount of SA significantly improves the melt processability of the terpolyester by decreasing the T_m and melt viscosity.

While hydrolysable ester bonds make aliphatic polyesters susceptible to microbial attack, the rate of degradation is highly dependent on the chemical structure, branching, morphology, molecular weight, crystallinity and hydrophobicity.[76, 80] As such, it is possible for researchers to try to improve biodegradability by targeting specific physical properties. Research by Ahn et al.[76] investigated the thermal properties and degradation behavior of PBSu, PBAd and PBSA polyesters with M_ns greater than 100,000 g/mol and narrow Đs (1.8–1.9) (**Figure 1-17**).

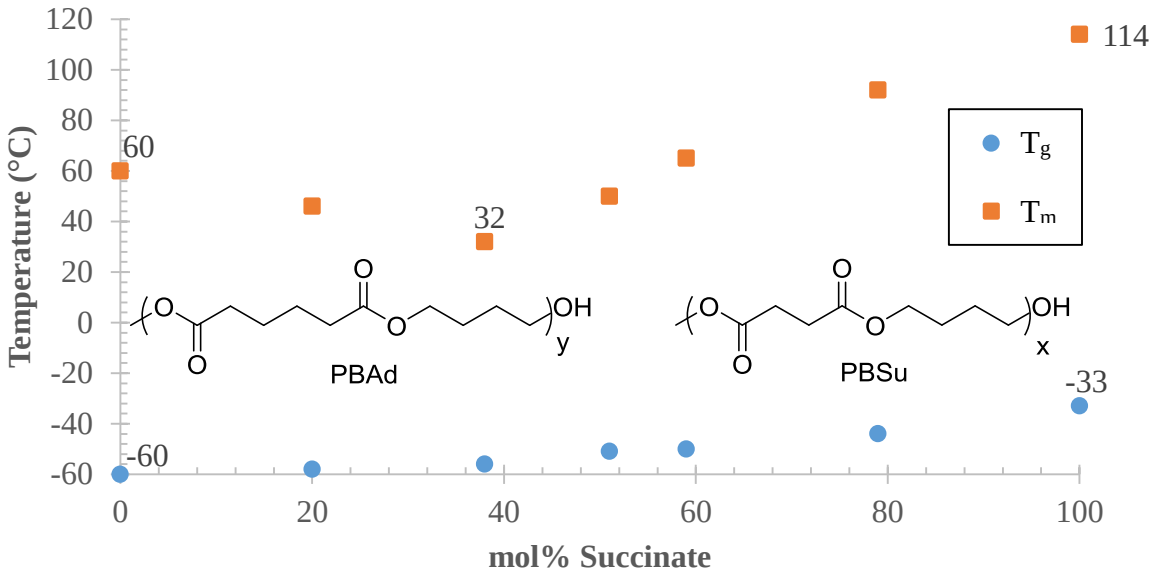

Figure 1-17. Glass transition and melting temperature of PBSu and PBAd copolyesters. Adapted with permission from Ahn et al.[76] Copyright 2001 Wiley.

Because there are fewer carbons separating the carbonyl groups in PBSu, it exhibits transitions at much higher temperatures than PBAd. The shorter distance between carbonyl groups in succinic acid give PBSu a more ridged structure that leads to higher temperature transitions. If the PBAd and PBSu homopolymers are combined to form PBSA copolyesters, the T_m decreases, reaching a minimum at 40 mol% succinate and 60 mol% adipate. Ahn et al.[76] observed an increase in biodegradation with increasing adipate content (along with a decrease in T_m and crystallinity); however, hydrolytic degradation decreased with higher concentrations of the more hydrophobic adipate. Tserki et al.[80] also synthesized a range of PBSA copolyesters and observed thermal behavior comparable to that observed by Ahn et al.[76] Using X-ray diffraction and DSC, Tserki et al.[80] also observed higher levels of crystallinity in PBSu over PBAd and observed a minimum in copolymer crystallinity at 40 mol% succinate. Compositions with higher crystallinity exhibited higher tensile strength and less vulnerability to enzymatic attack during biodegradation.

Chrissafis et al.[68] synthesized a range of succinate homopolyesters with ethylene (PESu), propylene (PPSu), and butylene (PBSu) glycol at different molecular weights to study how molecular weight and chemical structure affects thermal decomposition. Higher rates of chain scission were observed as lower thermal degradation temperatures (T_d) when SA was paired with diols containing longer carbon chains ($T_{d,PESu} > T_{d,PPSu} > T_{d,PBSu}$). TGA revealed degradation temperatures under nitrogen as the peak of the first derivative. Degradation temperatures, measured at the peak of the first derivative ($T_{d,\ peak}$), for PBSu, PPSu, and PESu were 399, 408, and 413 °C respectively, and were consistent with those observed for PET, PPT and PBT.

Zorba et al.[67] built off of work by Chrissafis et al.[68] by studying polyesters synthesized by contacting dimethyl adipate with ethylene (PEAd), propylene (PPAd), and butylene (PBAd) diols. In this example, however, the opposite degradation trend was observed ($T_{d,PBAd} > T_{d,PPAd} > T_{d,PEAd}$) from what was reported earlier by Chrissafis et al.[68] during their study of succinate based polyesters and lower T_ds were observed when AA was paired with diols containing fewer carbons. The $T_{d,\ peak}$s for PBAd, PPAd, and PEAd were 412, 385, and 379 °C respectively. Zorba et al.[67] performed a more detailed analysis of the degradation mechanisms of the three polyesters and concluded that PEAd degrades almost entirely by a single mechanism, while PBAd and PPAd degrade by two different mechanisms, each having different energies.

1.2.6 Copolyesters Based on Bibenzoic Acids

Some of the earliest polyesters containing bibenzoate moieties were synthesized over 60 years ago;[81] however, it wasn't until the 1990s that Dow Chemical Company and Monsanto claimed bibenzoate based copolyester synthesized with dimethyl esters.[81-83] Dow synthesized copolyesters via melt polymerization of 4,4'BB and 3,4'BB diesters (**Figure 1-18**) with a range of

linear aliphatic diols containing 2–12 carbons.[83] Compositions containing ≥ 50 mol% 4,4'BB were semicrystalline and exhibited mechanical and thermal properties sufficient for tire cord, hose reinforcement and conveyor belt applications as well as excellent solvent resistance and low flammability. A recently published study[84] thoroughly explores the thermal, rheological, mechanical and barrier properties of these materials. DOW also claimed a range of copolyester composition suppressing the crystallization of 4,4'BB-EG with 3,4'BB and isophthalate comonomers to produce melt processable copolyesters. The T_m of 4,4'BB-EG homopolyester is very high (343 °C), producing a brittle polyester that is impossible to synthesize by using typical melt polymerization techniques without significant degradation.[83] While the properties of 4,4'BB-EG makes it unusable as a homopolyester, its properties suggest a high potential as a comonomer for the enhancement of more common polyesters such as PET. Monsanto synthesized a range of copolyesters from PET modified with 7–63 mol% 4,4'BB resulting in T_gs of 83–111°C and T_ms of 229–278 °C, however, very little characterization was reported for these materials.[82]

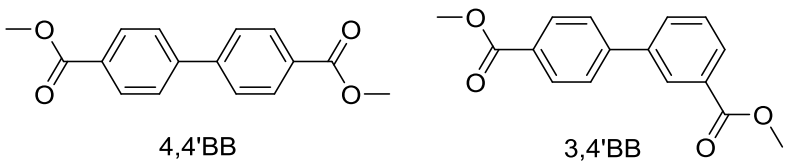

Figure 1-18. Molecular structure of 3,4'BB and 4,4'BB based dimethyl esters

Even though polyesters based on DMN, DMT and DMI have been very successful in producing materials for a wide range of applications, there is still a need to produce newer and better materials. Until recently, many of the food packages and containers requiring high temperature plastics were made from bisphenol-A polycarbonate (BPA PC) (**Figure 1-19**). The excellent mechanical and thermal properties (T_g = 145 °C) made BPA PC ideal for impact resistant dishwasher safe containers and hot fill applications where high temperature liquids such as

pasteurized beer, baby food and juice are packaged without cooling. However, BPA PC is no longer used in most food containers and packages due to concern over BPAs endocrine disrupting activity and the potential for it to leech out of the material.[6, 85-87] A number of different materials have taken the place of BPA PC in a number of applications. Eastman's Tritan™ copolyester has been especially successful in the wake of BPA PC, but there is still strong demand for a suitable BPA PC replacement.[4, 6, 8, 88-89]

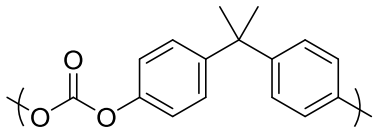

Figure 1-19. Repeat structure of BPA PC.

Both 4,4'BB and 3,4'BB have great potential for commodity applications requiring high temperatures and good mechanical properties. Copolyesters of 4,4'BB have excellent potential to produce materials with high T_gs and 3,4'BB has good potential to produce tough, optically clear materials with good thermal properties. Due to similarities in geometry, many parallels can be drawn between the 4,4'BB and terephthalate moieties, where the para substituted linkages produce a crystalline material, and the isophthalate and 3,4'BB moieties, where meta linkages produce a 'kink' in the polymer backbones that disrupts crystallinity and lowers the T_g relative to the para linkages.[14, 90-92] 3,4'BB based polyesters have higher permeabilities than isophthalate based polyesters when combined with EG, but is a lower permeability material than 4,4'BB and PET, (likely from restricted mobility).[11-12] Surprisingly, oriented 4,4'BB based polyesters have lower permeabilities than PET, which is not well understood and has made it the focus of several studies.[11-12, 14, 91, 93-95] Recent renewed interest in 4,4'BB and 3,4'BB based copolyesters is due, in part, to the development of new monomer synthesis routes. Work by Schiraldi et al.[96-98]

demonstrated how to synthesize and target different substitutions of dimethyl biphenyl from the selective coupling of toluene with palladium triflate and triflic acid (**Figure 1-20a**). More recent work by Dakka et al.[99-100] tested the coupling of toluene in the presence of hydrogen with a range of hydroalkylation catalysts, including supported palladium (**Figure 1-20b).** In both cases, oxidation and esterification were carried out with well-known techniques to obtain the final diesters. Research into new methods of synthesis makes previously unexplored monomers more attractive for the development of structure– property–morphology relationships.

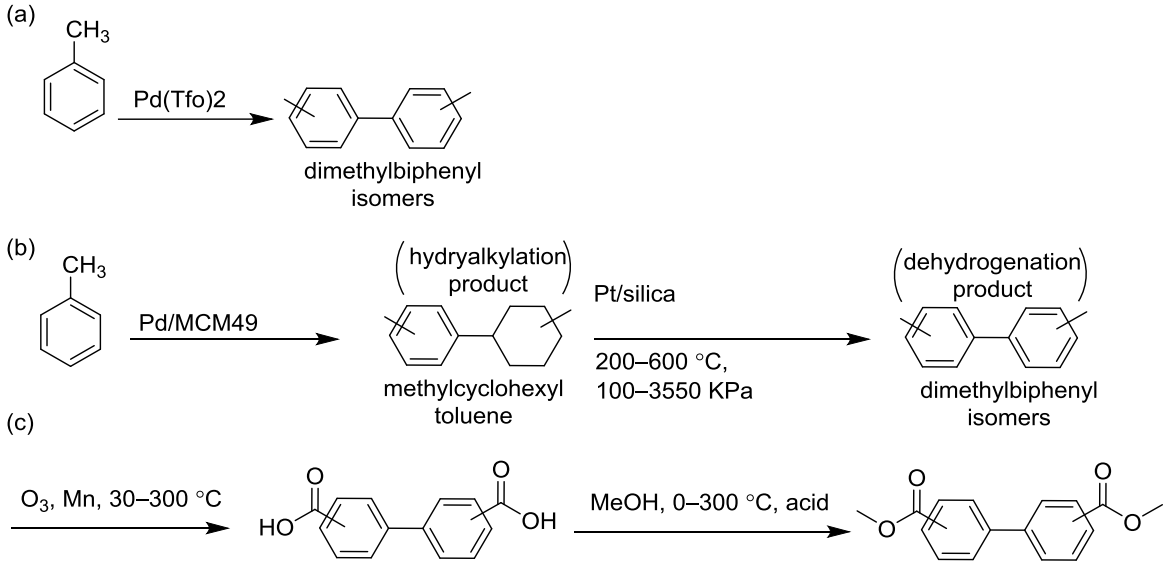

Figure 1-20. Synthesis of dimethyl biphenyl by using palladium triflate (a) or a hydroalkylation catalyst (b) follow by oxidation to produce the diacid and diester (c)

1.3 Diol Modification of Polyesters

1.3.1 PET Modified with CHDM

Ethylene glycol (EG) is the most important diol used in the production of polyesters (e.g. PET). EG has been produced commercially since WWI and is currently produced at low cost from the direct oxidation of ethylene with oxygen, which produces ethylene oxide, followed by thermal hydrolysis at 200 °C without catalyst.[101] PET has experienced wide commercial success as a commodity plastic, but because it deforms at temperatures lower than the boiling temperature of water, PET cannot be used in applications that would bring it into contact with boiling liquids. While this is one of the major drawbacks of PET, there are many other applications that require properties beyond the capabilities of PET. One difficulty in using EG is that it can dimerize to form diethylene glycol (DEG) (**Figure 1-21**) in the main chain during polymerization, primarily during the preheating and low vacuum stage of polycondensation.[102-104] As a result, it is common for commercial PET to contain 2–4 mol% ethyleneoxyethylene units. It is necessary to minimize the formation of DEG since it has been shown to decrease the melting temperature of PET by 5 °C for each mol% increase, disrupts crystallization (DEG > 40 mol% is completely amorphous) and

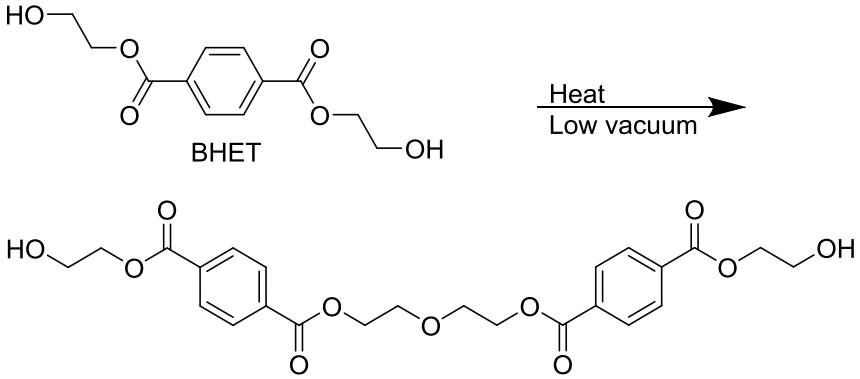

Figure 1-21. Formation of DEG in PET from bis-hydroxyethyl terephthalate (BHET) oligomer.

reduces the glass transition of the final polymer.[105] In an effort to increase the melting point and improve the thermal stability and heat distortion characteristics of PET, Kibler replaced the short, linear EG with a much larger and more structurally rigid CHDM.[2] Poly(1,4-cycloheylenedimethylene terephthalate) (PCT) (**Figure 1-22**) was first produced by the Eastman Kodak Company as Kodel fiber and was commercially successful until it was discontinued in the 1980s.[36] PCT has both a higher T_m (290 vs 260 °C) and T_g (88 vs. 80 °C) relative to PET. CHDM is added to PET as a comonomer that modifies the crystallization characteristics, thereby increasing transparency and widening the processing window for injection blow molded parts.[3] One of the most prized properties of PCT is the heat distortion temperature (HDT), which is high enough (~260 °C) for use in connectors for electronics or automotive applications where it might be exposed to high temperatures. This gives PCT a commercial advantage over significantly more expensive high performance liquid crystalline polymers (LCP) that might otherwise be used.[106] PCT also has the advantage of crystallizing rapidly at temperatures higher than PET, allowing more rapid injection molding of parts. Similar flow characteristics to PET and PBT also allow PCT to be used in the same injection molding equipment with very little alteration. Even though PCT has low moisture uptake relative to PET, its high melting point requires it be processed at temperatures higher than what are typically used for polyesters.[107] As a result, careful drying is

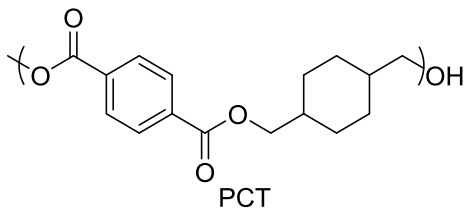

Figure 1-22. Repeat structure of poly(1,4-cyclohexylenedimethylene terephthalate)

required to prevent hydrolytic degradation that can decrease molecular weight during processing and negatively impact the physical properties of injection molded parts. While PCT has higher thermal stability than PET, CHDM has been shown to undergo degradation to form carboxylic acid pendant groups capable of crosslinking.[108] In order to improve processing, it is common to modify PCT with DMI to decrease the melting point and widen the processing window.[109]

CHDM is commercially produced through the hydrogenation of DMT at 250 °C and 5000 PSI in the presence of a copper–chromite–oxide reduction catalyst (**Figure 1-23**).[110] The method used in commercial synthesis of CHDM results in a thermally stable isomer ratio of 30:70 cis/trans that remains constant throughout polymerization (does not isomerize) (**Figure 1-24**). The isomer ratio has a significant impact on the polymer properties and there are a many studies looking at how to produce different isomer ratios and how different isomer ratios affect the physical and thermal properties of CHDM containing polyesters.[21, 111-115] Cyclohexane is known to occupy chair and boat conformations, with chair occupying the lower energy state. When the CHDM trans isomer (**Figure 1-24a**) is in the chair formation, the alcohol substituents are either both equatorial (lower energy) or both are axial (higher energy). In contrast, when the CHDM cis isomer is in the chair conformation, one of the alcohol substituents is axial and the other is equatorial. The cis isomer is able to occupy a boat conformation where both alcohols are in the equatorial position, as

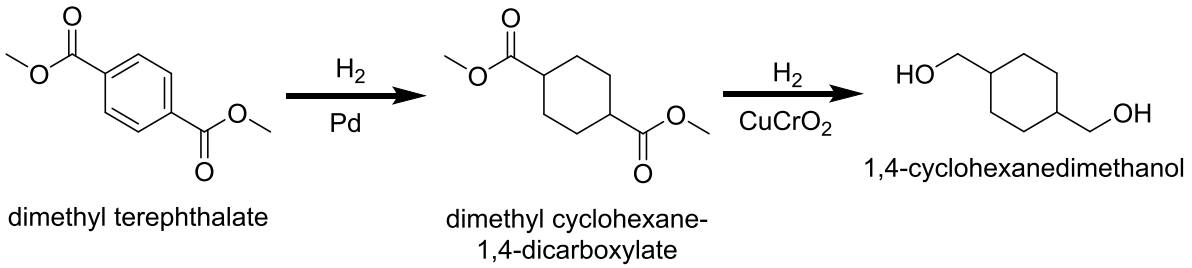

Figure 1-23. Synthesis of 1,4-cyclohexanedimethanol

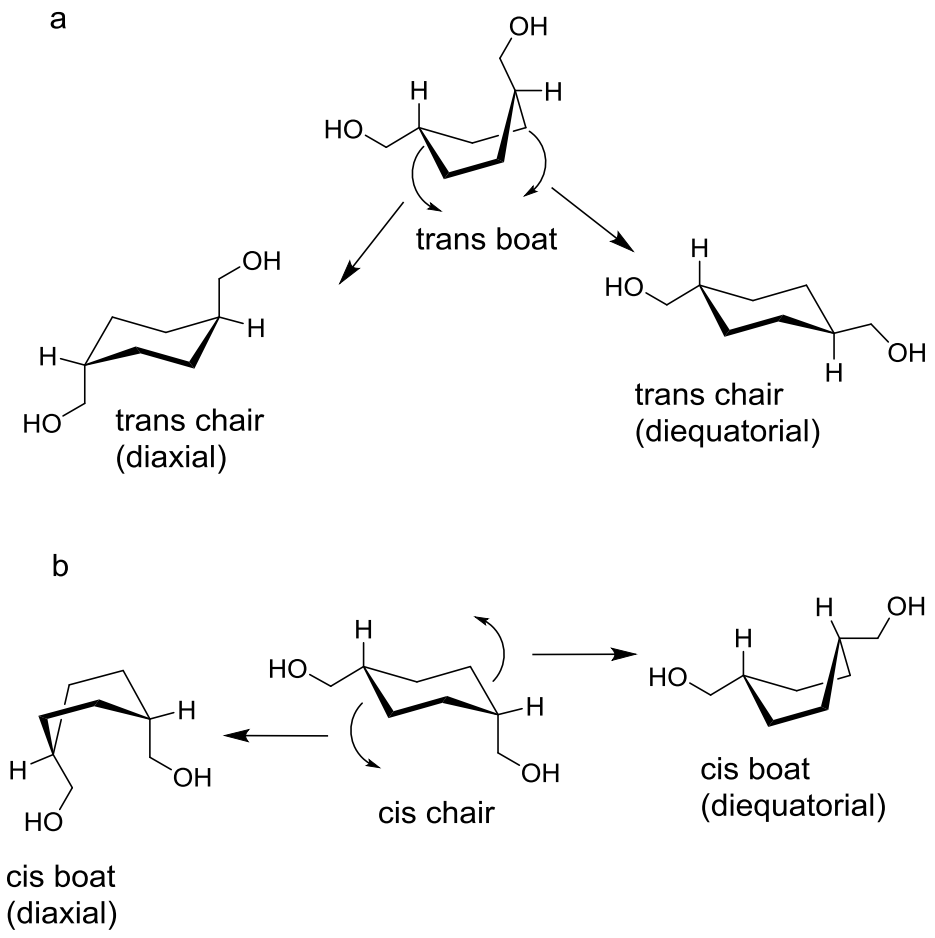

Figure 1-24. Chair and boat conformers of the trans (a) and cis (b) isomers

a result, the cis isomer is much more likely to occupy the boat conformation than the trans isomer.[21, 111, 116] The presence of both boat and chair conformers in the polymer backbone noticeably impacts chain packing, sub-T_g motions and gas transport.[11] In general, PCT has higher oxygen permeability due to the greater degree of free volume created by CHDM relative to EG and is in fact less dense than PET (1.195 g/cc vs 1.334 g/cc).[3] However, the permeability of PCT varies greatly with isomer ratio, with cis having lower permeability.[3]

The melting point of PCT is seen to increase linearly from all cis to all trans with no sign of a eutectic point (**Figure 1-25**).[21, 111] X-ray diffraction studies show a gradual shifting of the crystal lattice as the isomer ratio changes indicating that one isomer form can fit into the lattice of the other, resulting in the gradual melting point change.[117] The lower melting point observed for cis isomers is attributed to how structure symmetry affects packing through the introduction of

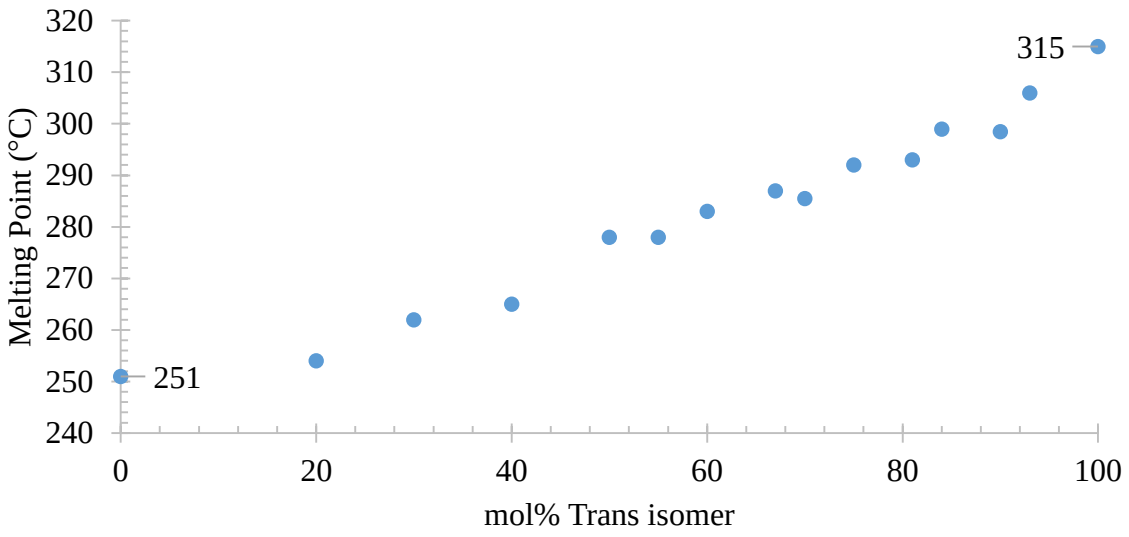

Figure 1-25. Dependence of PCT melting point on cis/trans isomer ratio. Adapted with permission from Kibler et al. [111] Copyright 2001 Wiley.

kinks.[118] Despite having a lower T_m, there is very little observed difference in level of crystallinity or crystallization rate as the isomer ratio changes from cis to trans.[20] Density of the PCT increases as the concentration the cis isomer increases,[119] which has a denser unit cell than the trans isomer.[117]

Mechanical properties are significantly impacted by the presence of CHDM monomers in the polymer backbone. PCT is known to have impact properties superior to PET under notched Izod testing.[3] A great number of studies have attempted to link improved impact properties with

secondary relaxations, especially with cyclohexylene structures, which have been shown to greatly enhance sub-T_g transitions in DMA around −60 °C.[103, 116, 120-122] It is interesting to note that 1,3-cyclohexanedimethanol, similarly prepared from the hydrogenation of DMI, does not exhibit the same enhanced mechanical properties, including impact properties, as CHDM.[2, 123-124]

Terephthalate copolyesters containing EG and CHDM exhibit a eutectic point, with an amorphous window between 20 and 40 mol% CHDM where no melting is observed under normal DSC conditions.[36] Substituting ~40 mol% of CHDM in PCT (PCTG) slows down crystallization sufficiently to produce a polymer that is essentially amorphous. These polymers have high impact and excellent clarity relative to PET and PMMA and are favored for thin walled medical components due to their biocompatibility, ability to resist gamma ray sterilization and ductility.[125] In contrast PETG has about 70 mol% EG and is trade named under Eastman as Spectar®, and commonly used as heavy gauge sheeting in store displays. Increasing EG content increases modulus and tensile strength but decreases impact strength.

1.3.2 Polyesters Modified with TMCBD

When substituted in high enough concentration, almost any comonomer (diol or diacid) has the potential to produce an aliphatic copolyester. CHDM, DMI and DMN have been shown to be commercially valuable for this very purpose; however, aliphatic molecules that are both rigid and thermally stable have been difficult to produce. 2,2,4,4-Tetramethyl-1,3-cyclobutane diol (TMCDB) is an alicyclic diol with a rigid structure that is used to enhance the thermal properties of polyesters. Early work by Eastman Kodak Company[126-129] demonstrated the potential of tetraalkylcyclobutanediols in high temperature polyesters. Work by Kelsey[5, 130] and Crawford[4, 7-8, 88] showed that amorphous copolyesters with superior mechanical properties could be prepared

from terephthalate, TMCDB and one additional diol. The TMCBD monomer can be prepared in high yields (up to 98 %) through the pyrolysis of isobutyric acid into dimethylketene, which cyclizes into a cyclic diketone that can then be hydrogenated into cis/trans isomers of TMBCD with a range of catalysts (**Figure 1-26**).[128-129, 131] Polymerization of polyesters prepared with a range of different isomers[5, 126] have demonstrated a change in properties depending on the cis/trans (**Figure 1-27**) isomer ratio. However, even though methods have been developed and reported in the literature for the separation of the different monomers, TMCBD is typically used as a mixture for cis/trans isomers due to the cumbersome nature of separation.[127] Terephthalate polyesters made with TMCBD were shown early on to have high melting temperatures for all trans TMCBD (>350 °C) relative to all cis TMCBD (170–210 °C) when measured on the hot stage of a microsope[126] and to have high T_gs (184 °C for 60 % trans).[132]

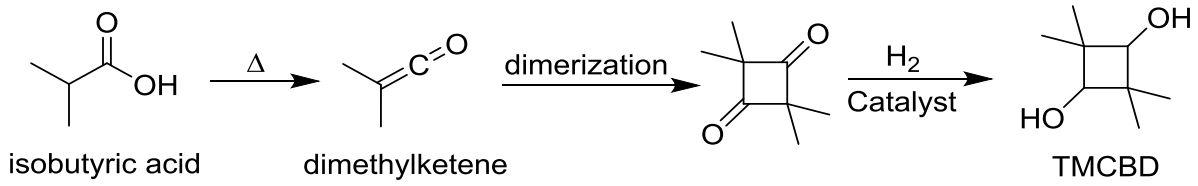

Figure 1-26. Synthesis of TMCBD from isobutyric acid.

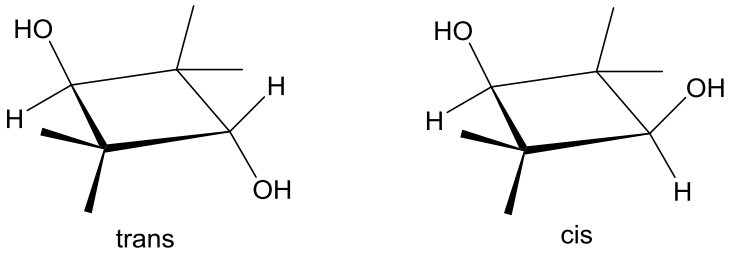

Figure 1-27. Trans and cis isomers of TMCBD

The compact structure of TMCBD situates the secondary alcohols close enough to the adjacent methyl groups which results in steric hindrance of the alcohol functional groups during polymerization. As a result, TMCBD is much slower to polymerize than other primary diols, such as CHDM and EG. Development of TMBCD polyesters utilizing melt polycondensation has involved the testing of several catalysts since typical transesterification catalysts (e.g. titanium catalysts) proved far less effective.[133] Alternative catalysts that have been shown to be effective for the polymerization of TMCBD polyesters include lead catalysts (which lead to a gray color) and tin catalysts, which have shown to be effective for transesterification with DMT at or above 240 °C.[5]

The melt stability of TMCBD is sufficiently high for applications such as extrusion blow molding and melt blending,[130] and the rigid character of the monomers makes it ideal for integration as a comonomer in amorphous and semicrystalline copolyesters for the purpose of enhancing thermal properties and UV resistance.[133-134] Much like with CHDM, TMBCD has been used as a glycol modifier in a number of copolyesters with DMT. Unlike CHDM, however, the low reactivity of TMBCD at low temperatures, due to the steric hindrance of the methyl groups, allow for the polymerization of segmented copolyesters. Quisenberry was able to produce segmented copolyesters with 15 mol% EG[133] and more recently Zhang et al.[135] polymerized oligomers of TMBCD and DMT with DEG and DMAp to produce segmented copolyesters (containing rigid and soft segments) with enhanced properties relative to the random copolyester.

Much like with CHDM, polyester morphology is influenced by the ratio of diols incorporated into the polymer backbone. In semicrystalline copolyester compositions where a linear diol (e.g. 1,3-propanediol) is replaced with up to 40 mol% TMBCD, shifting the isomer ratio of TMCBD to a higher trans content has been shown to potentially promote crystallinity,

however, TMCBD content above 40 mol% tend to produce amorphous and translucent copolyesters (**Figure 1-28**).[5, 130] In the case of PPT, amorphous compositions (from 50–80 mol%

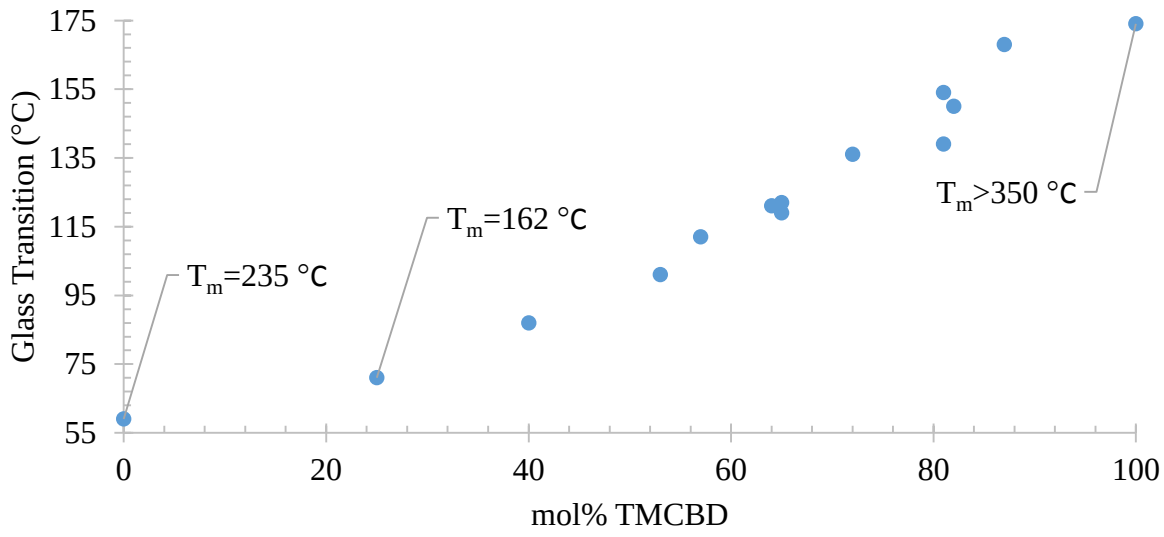

Figure 1-28. Glass transition of PPT copolyesters with increasing TMCBD substitution[5]

TMCBD) have excellent thermal properties (T_gs above 100 °C) relative to the homopolyesters. Cycloaliphatic polyesters typically exhibit T_ms and T_gs that are above linear aliphatic polyesters and below aromatic polyesters. Improved thermal properties relative to linear aliphatic chains is commonly attributed to an increase in restricted mobility brought on by the more rigid cycloaliphatic ring having lower conformation freedom. Conformational studies by Sulatha et al. [134, 136] compared polyester chain properties of all trans terephthalate polyesters of either CHDM or TMBCD utilizing RIS Metropolis Monte-Carlo (RMMC) simulations. RMMC calculations for TMCBD chains dimensions predicted a higher persistence length (L_p) and characteristic ratio (C_n) than those of CHDM, indicating that TMCBD produces a more rigid polymer chain. Even though both monomers have an identical molecular weights, there is a shorter distance between the oxygen atoms in TMBCD and intramolecular repulsive interactions are not

as well separated as in CHDM, resulting in a higher Van Der Waals energy in polyesters containing TMBCD. A reduced degree of freedom in TMBCD containing copolyesters would be expected to have a significant impact on the glass transition temperature. Replacing nearly all (78%) of the diol in PBT with TMBCD increases the T_g to 145 °C, almost 100 °C higher than the original polyester. This addition of TMBCD shows an enhancement of the T_g similar to that of an aromatic monomer.[5]

Recent work done by Iyer[137] used DMA to compare how the TMCBD monomer affects sub-T_g transitions of polyesters relative to CHDM, which is known the enhance the sub-T_g transitions in polyesters, such as PET, at approximately -60 °C. When substituted for CHDM, TMCBD is observed to suppress the sub-T_g transitions, indicating that TMCBD has fewer molecular motions. Increases in low temperature mobility from CHDM correlates linearly with a higher in diffusivity when EG in PET is replaced with CHDM. As a result, permeability of PET (14.3 cc-mil/100in^2 ·day·atm) increases when CHDM is added up to PCT (52.6 cc-mil/100in^2 ·day·atm).[137] However, replacing a portion of PCT with TMCBD significantly decreases the polymer diffusivity, but permeability increases above that of PCT (permeability of PCT with 35 mol% TMCBD is 137.0 cc-mil/100in^2 ·day·atm). This trend indicates that fractional free volume plays a far more significant role in oxygen transport in TMCBD polyesters. This conclusion is also reinforced by recent work done by Dennis et al[138] who used positron annihilation lifetime spectroscopy (PALS) to observe an increase in hole-free volume with increasing TMCBD content.

In 2007, the Eastman Chemical Company commercialized a range of copolyesters for commercialization based on PCT modified with TMBCD under the name Tritan™. Eastman claims their copolyesters meet the high temperature (HDT >95 °C at 264 psi stress) and high

impact requirements needed to for kitchenware, appliances, medical components, water bottles and more.[139-140]

1.3.3 Isohexide Monomers

The incorporation of renewable monomers into existing polymers has the potential of creating unique structures with beneficial properties that could garner interest in renewable materials. The compounds isosorbide (ISB), isoidide (IID) and isomannide (IMN) (**Figure 1-29**) are renewable, rigid and non-toxic compounds that only differ in the configuration of OH at the 2 and 5 positions. ISB is the only one of the three produced industrially and is readily available on the open market for production of pharmaceuticals. Widespread implementation of ISB into polymers has been significantly delayed due to higher manufacturing costs relative to petroleum-based monomers and insufficient purity. The presence of isomers and degradation products in ISB lowers the molecular weight and causes coloration.[141] Noordover et al.[142] were able to obtain colorless polymers by using 98.5+ % purity ISB when copolymerized with succinic acid.

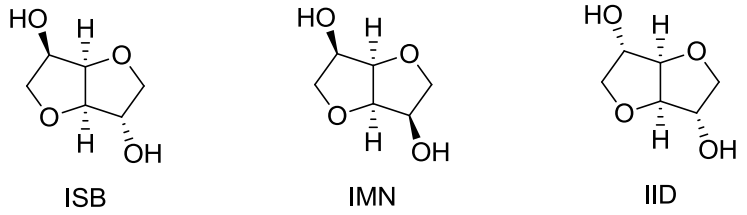

Figure 1-29. Structures of isosorbide, isomannide and isoidide

ISB is synthesized from starch extracted from polysaccharides. An enzymatic process degrades the starch into glucose, followed by hydrogenation from glucose to sorbitol (a reaction performed on an industrial scale) and then dehydration into ISB (**Figure 1-30**). The enzymatic degradation of starch also produces mannose, which is converted into IMN. Nature does not

produce precursors to IID abundantly, thus increasing the cost to produce relative to IMN or ISB.[141, 143] Referred to as isohexides, these compounds are not as reactive as primary alcohols such as EG, which makes it more difficult to synthesize high molecular weight polymers. The configuration of the diols at the 2 and 5 positions also have a significant effect on reactivity.[141-146] In the endo configuration (**Figure 1-31a**), the alcohol is sterically hindered and participates in intramolecular interactions that significantly decrease the reactivity of the molecule. IID has a more preferred configuration of the three isohexides with both alcohols in the exo position (**Figure 1-31b**), but low availability prevents commercial utilization. The all endo configuration of IMN is the least reactive structure of the three, which discourages in-depth study.[141] ISB is more reactive than IMN and more abundant than IID, making it the preferred molecule for commercialization. Roquette Freres has commercialized and sells purified isosorbide suitable for polymerization under the name Polysorb® and produced copolyesters containing ISB.[147-150]

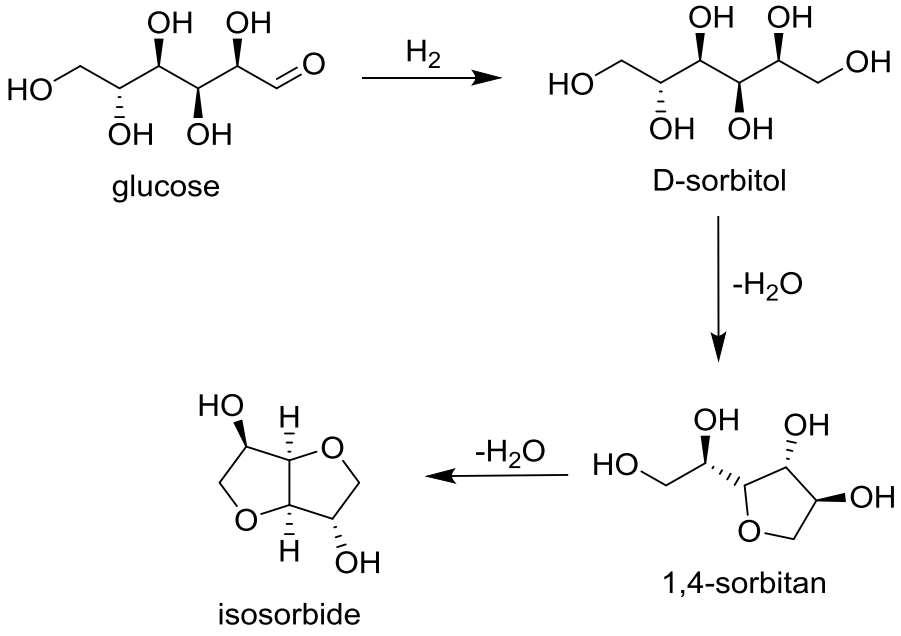

Figure 1-30. Synthesis of ISB from glucose

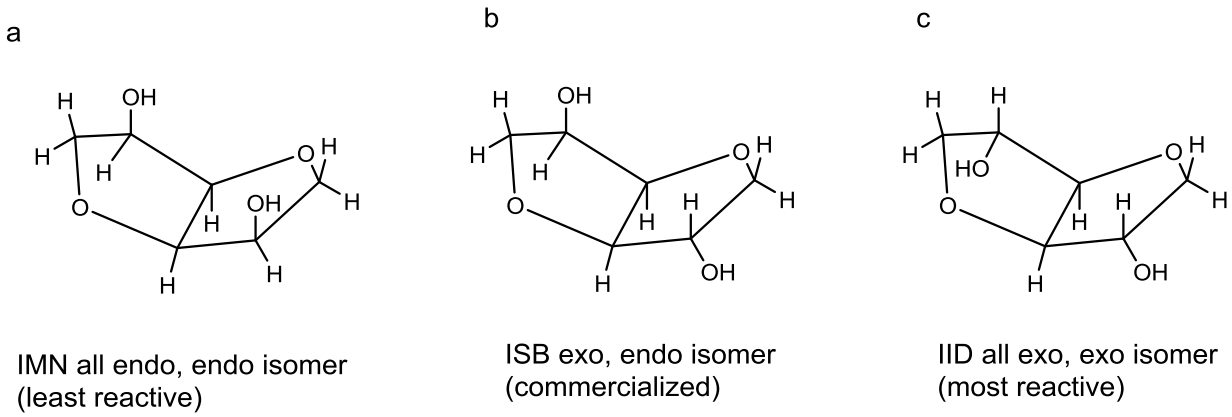

Figure 1-31. Depiction of endo (a) and exo (b) isohexide isomers

The rigid structures of isohexides increase the T_g when added to other polymers, which broadens the application window of existing materials. Many researchers have studied the effect of substituting ISB into various polyesters; the most notable examples are PET and PCT copolyesters.[143-146, 151] While the T_g increasing property does make ISB more attractive to manufacturers, low reactivity and high volatility of ISB makes it difficult to incorporate into other polymers. ISB also has relatively low thermal stability compared to many petroleum-based monomers. This makes it difficult to produce high ISB content polymers via melt transesterification without discoloration.[141, 143-144]

Feng et al.[143] attempted to improve integration of ISB into PET by synthesizing AB monomers from TA and ISB; thereby decreasing the volatility of ISB. They synthesized modified PET with T_gs as high as 150 ˚C with the goal of improving PETs hot fill properties. Yoon et al.[146] showed adding EG can increase ISB incorporation into the backbone. EG undergoes transesterification more readily, enabling incorporation of ISB, and is easier to remove during polycondensation, thereby facilitating the production of higher molecular weight polymers. EG, ISB and CHDM were used to produce terpolyesters with M_ns as high as 25,000 g/mol and T_gs as

high as 143 ˚C. Quintana at al.[144] produced ISB modified PET polymers and studied the effect on crystallizability. They showed that ISB disrupts crystallinity to a greater degree than CHDM and is more effective at increasing T_g than CHDM (**Figure 1-32**). This indicates that ISB has the potential as a renewable alternative to CHDM.

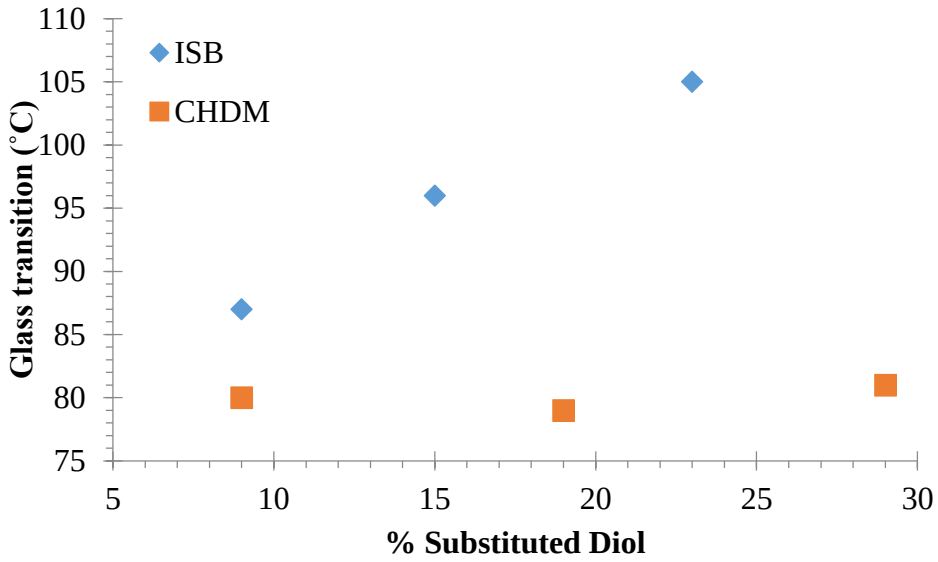

Figure 1-32. T_g as a function of substituted diol for ISB or CHDM in PET[144]

ISB has the advantage of being fully aliphatic, which makes it UV stable. Most aliphatic molecules are too flexible to achieve a high T_gs, making ISB particularly well suited for UV stable coatings. Noordover et al.[142] assessed the suitability of polyesters made from ISB and succinic acid to serve as ISB based powder coatings crosslinked with isocyanates. Since powder coatings are typically low molecular weight, the low reactivity of ISB is far less of a concern. The coatings had sufficiently high T_gs for application purposes (43 ˚C), exhibited good impact resistance under the ASTM D 2794 standard testing method (1 kg, 100 cm), and had Konig hardness levels above 200 s (glass is 235 s).

1.3.4 Polyesters Modified With NPG

While cycloaliphatic diols are known to have increased rigidity that enhances thermal properties relative to linear aliphatic diols, neopentyl glycol (NPG) also has higher rigidity due to the presence of two methyl groups attached at the β-position relative to the oxygen. NPG is manufactured at relatively low cost through a mixed aldol condensation reaction between formaldehyde and isobutyraldehyde in the presence of base (**Figure 1-33**). The resulting hydroxypivaldehyde is then hydrogenated in the presence of a hydrogenation catalyst at 80 °C or higher, producing NPG in yields greater than 90 %.[152] In 2015, global capacity for the production of NPG was as high 800,000 tonnes per year with a projected production of 890,000 tonnes by 2019.[153]

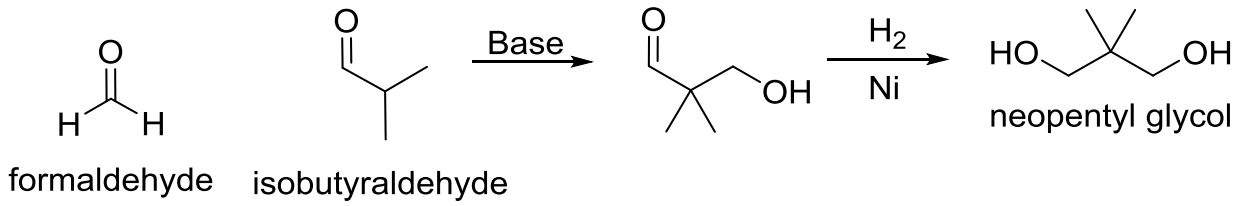

Figure 1-33. Synthesis of NPG from the aldolization of formaldehyde and isobutyraldehyde followed by hydrogenation with a hydrogenation catalyst[152]

NPG incorporation lowers polyester crystallinity (heat of fusion in DSC) and suppresses the melting point. Polyesters containing NPG exhibit unusually high resistance to thermal degradation relative to other polyesters. The polyester of DMT and NPG (PNT) exhibits a $T_{d,5\%}$ as high as 418 °C when measured with TGA under nitrogen, which is 44 °C above that observed for PPT.[154] The thermal stability of NPG is attributed to lateral methyl groups attached to the β-carbon preventing Norrish II scission (**Figure 1-34**), a major degradation pathway that results in the decomposition of diols in polyesters.[155-156] The high thermal stability of NPG polyesters has led to research exploring their feasibility in flame retardant materials.[157] In addition to high thermal

stability, NPG is UV stable,[155] which has led to commercialization by BASF and Eastman Chemical Company as powder coating intermediates used in outdoor applications with high weatherability.

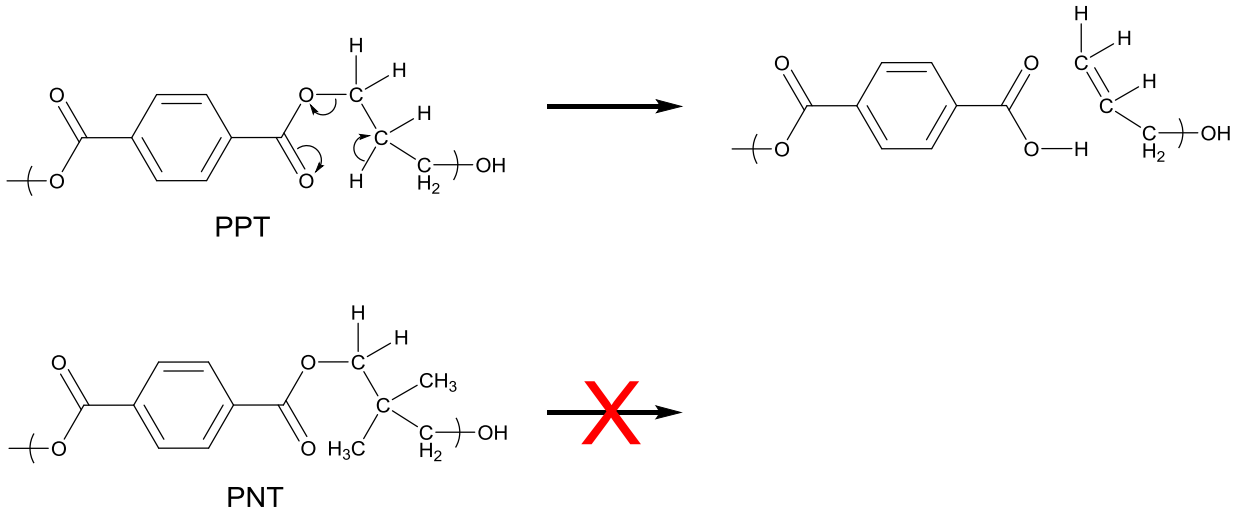

Figure 1-34. Norrish II scission of poly(propylene terephthalate) vs no scission in poly(neopentyl terephthalate)

A range of PCT/PNT copolyester compositions were claimed as higher performance amorphous materials by Eastman Chemical Company to be used as medical devices with improved resistance to hydrolysis and alcoholysis.[158] **Figure 1-35** shows a decrease in the T_g when CHDM in PCT is replaced with either NPG or EG, however NPG consistently produces copolymers with slightly higher glass transitions temperatures than EG.

When polyesters are exposed to increasing shear rates in the melt, they can undergo shear thinning where they exhibit a reversible decrease in shear viscosity. This non-Newtonian behavior is important in the processing and injection molding of part, since low viscosity materials are easier to process. Amorphous copolyesters containing NPG and CHDM exhibited improved shear thinning when compared to PETG copolyesters, indicating improved processing capabilities[158]. At the same time, researchers observed that due to the improved hydrolytic stability and hydrophobic

nature of NPG relative to EG, little to no drying was required before melt processing. This greatly increases ease of processing as EG containing polyester require careful drying before processing, otherwise they experience significant drops in molecular weight due to hydrolytic degradaion.

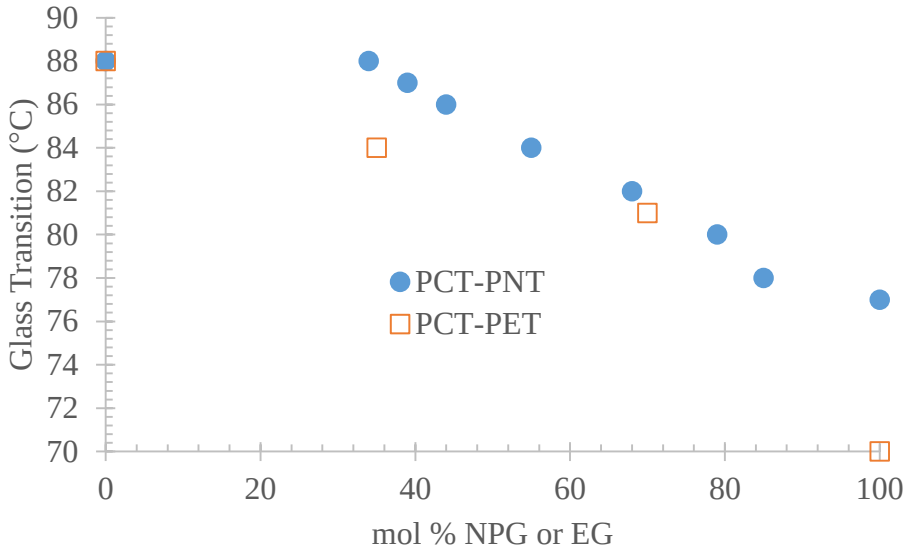

Figure 1-35. Decreasing glass transition temperature with substitution of NPG or EG for CHDM[3, 158]

Comparing PPT polyesters with NPG is a useful comparison, as it allows researchers to observe how the two additional methyl groups impact the properties of the polymers while normalizing all other structural characteristics. Work by Soccio et al. showed how the additional methyl groups in NPG affect crystallinity.[154] Below 10 mol%, NPG was shown to suppress the melting point and slow crystallization sufficiently to produce quenched amorphous films, however, overall crystallinity was not significantly impacted until the NPG content was raised above 10 mol%. In addition, WAXS analysis showed a different diffraction profile for NPG containing segments having lower overall crystallinity, indicating that the two methyl groups on NPG make crystalline order more difficult to achieve. In addition to decreasing crystallizability, the two

methyl groups on NPG are also believed to restrict rotations and molecular movement, resulting in the observed increase in T_g.

Much like with TMBCD, NPG undergoes transesterification slowly. Higher temperatures are needed for NPG to polymerize, however, once reacted the polyesters formed are particularly stable. Moad et al. took advantage of the low reactivity of NPG to prepare reaction resistent poly(neopentyl isophthalate) (PNI) oligomer segments and combine them with PET by reactive extrusion followed by solid state polymerization to form block copolyesters with melting temperatures similar to PET.[159] Due to the decreased reactivity of NPG, the non-reactive PNI segments were carefully prepared to have a majority of isophthalate end groups, whereas the end groups in PET were primarlity EG. While steric effects are commonly cited as the reason behind the slow reactivity of NPG, this has yet to be rigorously proven.

1.4 All Aliphatic Polyesters

While many cycloaliphatic diacids have been studied in the past,[160] the most practiced examples are cyclohexane-based diacids and diesters, such as dimethyl cyclohexane-1,4-dicarboxylate (DMCD) and cyclohexane-1,4-dicarboxylic acid (CHDA) (**Figure 1-36)**, have been proposed as alternatives to aromatic polyesters since the early 1990s for applications where resistance to UV light, good impact and resistance to humidity are desirable, such as in coatings.[161] Previously used materials contained phthalic anhydride and isophthalic acid, used in polyurethane

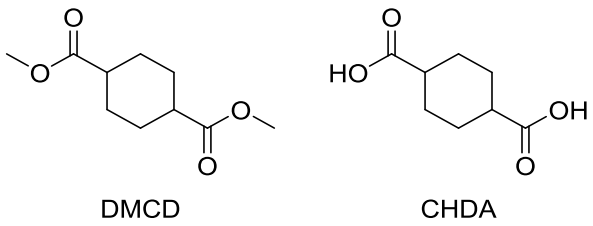

Figure 1-36. Chemical structure of cyclohexane-1,4-dicarboxylate (DMCD)

(PU) coatings, which contain phenyl rings that readily absorb UV light and undergo Norrish I scission, among other degradation mechanisms **(Figure 1-37)**.[155, 162] Photo oxidation can occur in cycloaliphatic moieties, but is much less important than in aromatic polyesters such as PET, and can be readily countered with stabilizers.[163] The restricted mobility of cyclohexane structures generally produces more rigid and higher temperature materials than those produced by linear aliphatic materials, but posses more flexibility than aromatic structures due to their ability to undergo conformational changes.[164-165] It is proposed that these conformational changes allow cyclohexane structures to absorb energy during impacts, producing a tougher material.[166]

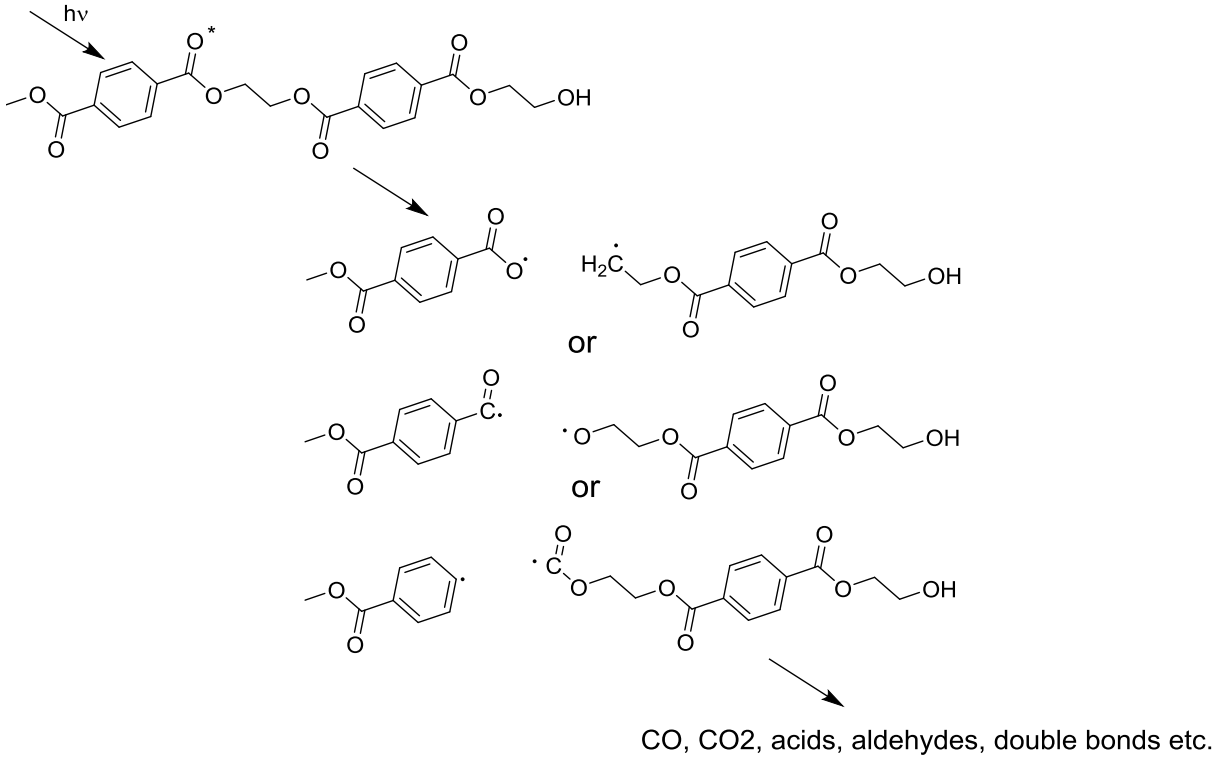

Figure 1-37. Norrish I scission in polyesters.[154]

Poly(1,4-cyclohexylenedimethylene 1,4-cyclohexanedicarboxylate) (PCCD) is one of the most well-known polyesters synthesized entirely from cyclohexane containing moieties (**Figure 1-38**). PCCDs have been known since the 1950s,[2, 111, 167] however, difficulties with polymerization prevented commercially implementation until sometime later.[163] A typical polymerization of PET or PBT polyesters use an excess of diol, which facilitates transesterification and is fairly simple to remove due to the high volatility relative to the aromatic diesters/diacids used. Larger diols, such as CHDM are more difficult to remove, making the build of molecular weight more difficult. In the case of PCCD, CHDM has a boiling point much closer to DMCD, which means it is possible to co-distill both diester and diacid during polymerization, making it more difficult to achieve high molecular weights and reducing yield. A significant amount of work by Brunelle et al.[161, 163, 168] was done to optimize polymerization conditions and improve the reliability of PCCD polymerizations. One technique that improved the ability to obtain high molecular weights was to add an additional, more volatile diol (such as EG) that is removed during the polycondensation step. This technique eliminates the need to carefully control the monomer ratios[167-171] and leaves

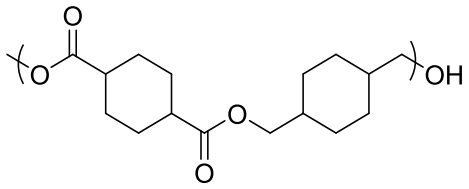

Figure 1-38. Chemical structure of poly(1,4-cyclohexylenedimethylene 1,4-cyclohexanedicarboxylate) (PCCD)

only a few mol% of the additional volatile monomer within the final product.

Much like with CHDM and TMBCD, the cis/trans isomer ratio of DMCD (**Figure 1-39**) has a significant impact on the physical properties of the final polymer, and much research has

been done on the effect each monomer has on the physical and thermal properties.[161, 163, 167-170, 172-174] The glass transition temperature of PCCD can range from 40–70 °C, with higher trans content producing a higher temperature. Below 24 mol% trans DMCD (66 mol% CHDM), PCCD polyesters are amorphous. From 24–97 mol% trans, semicrystalline PCCD compositions have a T_m of 220–235 °C with crystallization temperatures upon cooling (T_c) of 152–175 °C.[168] The structure of the trans isomer, much like with CHDM, has a higher symmetry than the cis isomer, which is believed to contribute to chain packing and crystallization. The cis conformation, on the other hand, produces kinks in the polyester backbone that disrupt the formation of stable crystals. Most research efforts have focused on producing PCCD with high trans content for its suitability

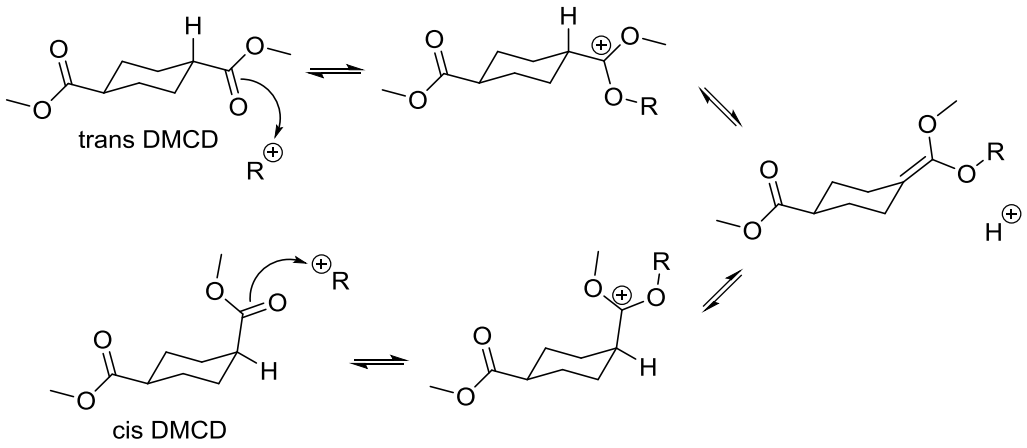

Figure 1-39. Proposed isomerization mechanism for DMCD[173]

for higher temperature applications and faster crystallization, which improves processability.[163] Producing PCCS polyesters with high trans content is especially difficult due to the presence of acid catalysts resulting in isomerization of DMCD at higher temperatures towards its thermodynamic equilibrium around 66 mol% trans isomer (**Figure 1-39**).[173] When synthesized by typical polycondensation procedures, PCCD isomerizes towards its thermodynamic equilibrium,

producing a polyester with a T_m of 225 °C and a T_c of 130–152 °C (compared to PBT with a T_m equal to 226 °C and a T_c of 182 °C). Isomerization is even more difficult to control in polymerizations performed with CHDA as opposed to DMCD, since isomerization is catalyzed by the presence of acids.[168] To increase the rate of crystallization, higher trans content is preferred. DMCD isomerization was prevented by using low catalyst levels, reducing time spent at higher reaction temperatures and using sacrificial diols such as EG. This produced high molecular weight PCCD polyesters with 99 mol% tans and T_c = 193 °C.[163] Solid state polymerization is often used as a way to increase molecular weight without going up to temperatures that would allow significant isomerization.[163, 169] PCCD crystallizes slowly relative to common commercial polyesters such as PET and PBT. The melting temperature of PCCD is relatively close to PBT, however, substituting DMCD for DMT slows crystallization. Interestingly, substitution of DMT with DMCD in PBT produces a linear decrease in both T_m and T_g, indicating isomorphic crystalline behavior.[175]

Cycloaliphatic polyesters containing multiple cyclohexane rings are of great interest for their potential to produce high glass transition temperatures and are excellent impact materials. An early example was synthesized through hydrogenations of bisphenol-A to produce 2,2-bis(4-hydroxycyclohexyl)propane (BHCP) (**Figure 1-40**).[176] BHCP was polymerized with a number of

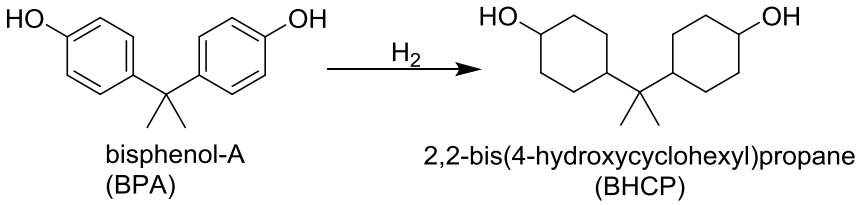

Figure 1-40. Hydrogenation of BPA into BHCP.

diacids including adipic, isophthalic and terephthalic acid, however, the inherent viscosity (η_{inh}) values high enough for impact testing could only be achieved with adipic acid (0.59 dL/g). The glass transition temperatures of the copolyesters produced with BHCP (**Table 1-5**) are as high as 135 °C. The mechanical properties of the polyesters made with adipic acid were compared with Lexan 121 polycarbonate (PC) (**Figure 1-41).**[176] While PC has a much higher flexural modulus and tensile strength, the BHCP–adipate polyester superior impact strength and elongation to break. More recently, Dennis et al. synthesized a series of polyesters from dimethyl decahydro-2,6-naphthalenedicarboxylate (CHDN), through the hydrogenation of dimethyl 2,6-napthalate,[177]

Table 1-5. Thermal properties of BHCP polyesters[176]

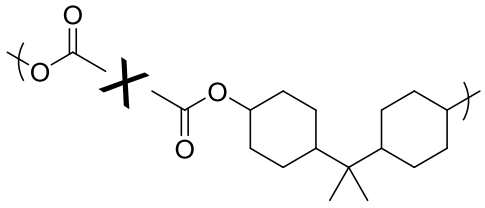	**T_g (°C)**	**T_m (°C)**
$-(CH_2)_4-$	75	180
$-(CH_2)_2-$	113	200
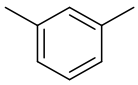	127	267
	135	250

combined with 1,4-butanediol (BD), CHDM (65–96 % trans) and 1,3-cyclohexanedimethanol (1,3-CHDM). The thermal properties of CHDN show improved T_gs. relative to PCCD polyesters (**Table 1-6**), with T_gs approaching 93 °C.[138, 168] Large β-relaxations were observed for CHDN containing polyesters, which has been correlated with impact strength.[166, 178]

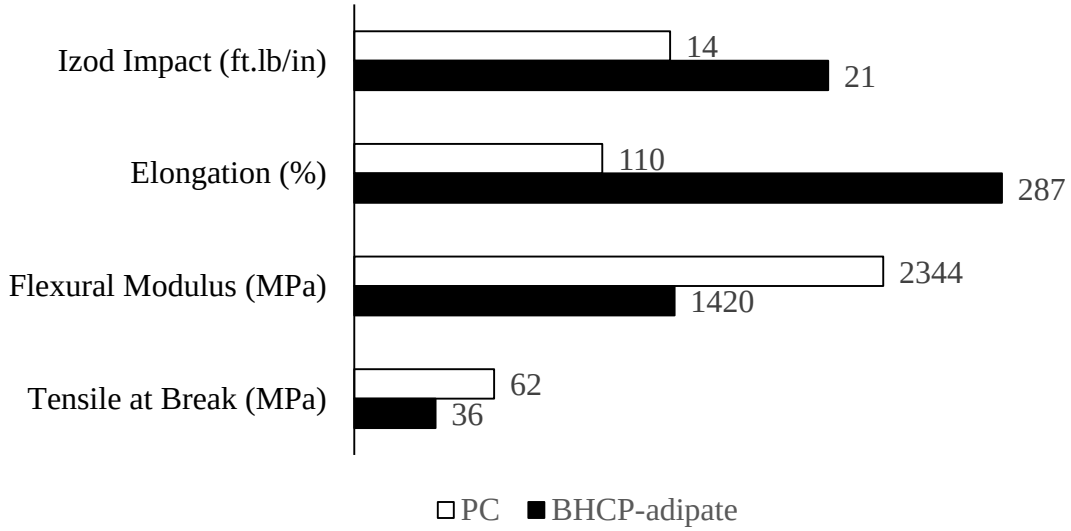

Figure 1-41. Comparison of BHCP–adipate polyester vs. Lexan 121 polycarbonate[176]

Table 1-6. Comparison of T_gs for DMCD-CHDM (PCCD) and CHDN-CHDM polyesters with varying content of different cis/trans isomers[109, 133]

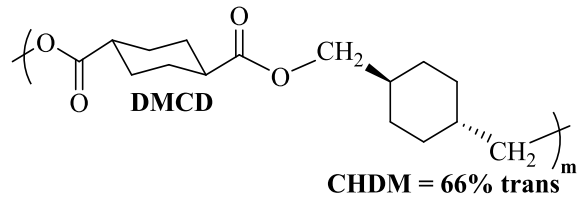

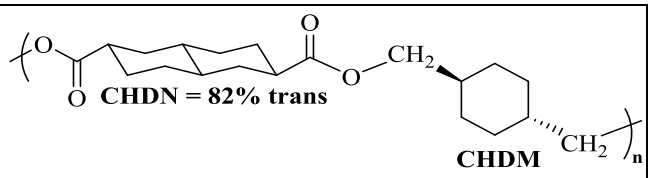

T_g (°C)	mol% trans DMCD	T_g (°C)	mol% trans CHDM
41	24	89	65
56	66	93	96

1.5 Summary

A large variety of copolyesters have been synthesized containing combinations of diols or diesters that are linear aliphatic, cycloaliphatic and aromatic for the purpose of establishing structure–property–morphology relationships. These relationships are needed to effectively target or enhance polyester properties including enhanced glass transition temperatures, high melting temperatures, high modulus, improved photooxidative, thermooxidative and hydrolytic stability, high clarity, etc. Many of the properties pursued for engineering plastics (e.g. high T_g, high modulus) are the result of higher rigidity in the polyester backbone. Large aromatic diacid structures are known for their ability to impart high rigidity, however, many of the readily available aromatic structures are also known for imparting high melting temperatures that preclude conventional melt polycondensation techniques. To overcome many of the processing difficulties associated with high T_ms, comonomers are often added to suppress or eliminate crystallinity while simultaneously trying to preserve the polyester's desirable properties. Additional comonomers may be a diacid or diol chosen for a specific added benefit such as improved thermal stability, gas barrier or enhanced impact properties. Unique properties are continually being discovered for both new and old monomers, making a broad investigation of different comonomers necessary in order to gain better insight into structure–property–morphology relationships.

1.6 References

1. Schiraldi, D. A., New poly(ethylene terephthalate) copolymers. In *Modern Polyesters: Chemistry and Technology of Polyesters and Copolyesters*, Scheirs, J.; Long, T., Eds. John Wiley & Sons: West Sussex, England, 2003; pp 245–262.

2. Kibler, C. J.; Smith, J. G. Linear polyesters and polyester-amides from 1,4-cyclohexanedimethanol. (Eastman Kodak Company). U.S. Patent 2,901,466, 1959.

3. Turner, S. R.; Seymour, R. W.; Dombroski, J. R., Amorphous and crystalline polyesters based in 1,4-cyclohexanedimethanol. In *Modern Polyesters: Chemistry and Technology of Polyesters and Copolyesters*, Scheirs, J.; Long, T., Eds. John Wiley & Sons: West Sussex, England, 2003; pp 267–292.

4. Crawford, E. D.; Pecorini, T. J.; Mcwilliams, D. S.; Porter, D. S.; Connell, G. W.; Germroth, T. C.; Barton, B. F.; Shackelford, D. B. Polyester compositions containing cyclobutanediol having a certain combination of inherent viscosity and moderate glass transition temperature and articles made therefrom. (Eastman Chemical Company). WO 2007053549, 2007.

5. Kelsey, D. R.; Scardino, B. M.; Grebowicz, J. S.; Chuah, H. H., High impact, amorphous terephthalate copolyesters of rigid 2,2,4,4-tetramethyl-1,3-cyclobutanediol with flexible diols. *Macromolecules* **2000,** *33* (16), 5810–5818.

6. Nelson, A. M.; Long, T. E., A perspective on emerging polymer technologies for bisphenol-A replacement. *Polym. Int.* **2012,** *61* (10), 1485–1491.

7. Crawford, E.; Pecorini, T.; Porter, D.; Connell, G.; Keegan, M. Bottles comprising polyester compositions which comprise cyclobutanediol. (Crawford Emmett D, Pecorini Thomas J, Porter David S, Connell Gary W, Keegan Michael J, Less). U.S. Patent 20,060,286,326, 2006.

8. Crawford, E.; Porter, D.; Connell, G. Tough amorphous polyester compositions. (Crawford Emmett D, Porter David S, Connell Gary W). U.S. Patent 20,070,010,650, 2007.

9. Callander, D. D., Properties and applications of poly(ethylene 2,6-naphthalate), its copolyesters and blends. In *Modern Polyesters: Chemistry and Technology of Polyesters and Copolyesters*, Schiers, J.; Long, T., Eds. John Wiley & Sons: West Sussex, England, 2003; pp 323–333.

10. Gallucci, R. R.; Patel, B. R., Poly(butylene terephthalate). In *Modern Polyesters: Chemistry and Technology of Polyesters and Copolyesters*, Scheirs, J.; Long, T., Eds. John Wiley & Sons: West Sussex, England, 2003; pp 293–321.

11. Light, R. R.; Seymour, R. W., Effect of sub-Tg relaxations on the gas transport properties of polyesters. *Polym. Eng. Sci.* **1982,** *22* (14), 857–864.

12. Aitken, C. L.; Koros, W. J.; Paul, D. R., Effect of structural symmetry on gas transport properties of polysulfones. *Macromolecules* **1992,** *25* (13), 3424–3434.

13. Polyakova, A.; Liu, R. Y. F.; Schiraldi, D. A.; Hiltner, A.; Baer, E., Oxygen-barrier properties of copolymers based on ethylene terephthalate. *Journal of Polymer Science Part B: Polymer Physics* **2001,** *39* (16), 1889-1899.

14. Polyakova, A.; Liu, R. Y. F.; Schiraldi, D. A.; Hiltner, A.; Baer, E., Oxygen-barrier properties of copolymers based on ethylene terephthalate. *J. Polym. Sci., Part B Polym. Phys.* **2001,** *39* (16), 1889–1899.

15. Liu, R. Y. F.; Hu, Y. S.; Hibbs, M. R.; Collard, D. M.; Schiraldi, D. A.; Hiltner, A.; Baer, E., Improving oxygen barrier properties of poly(ethylene terephthalate) by incorporating isophthalate. I. Effect of orientation. *J. Appl. Polym. Sci.* **2005,** *98* (4), 1615–1628.

16. Burgess, S. K.; Leisen, J. E.; Kraftschik, B. E.; Mubarak, C. R.; Kriegel, R. M.; Koros, W. J., Chain mobility, thermal, and mechanical properties of poly(ethylene furanoate) compared to poly(ethylene terephthalate). *Macromolecules* **2014,** *47* (4), 1383–1391.

17. Mackintosh, A. R.; Liggat, J. J., Dynamic mechanical analysis of poly(trimethylene terephthalate)—A comparison with poly(ethylene terephthalate) and poly(ethylene naphthalate). *J. Appl. Polym. Sci.* **2004,** *92* (5), 2791–2796.

18. Kawaguchi, T., Dynamic mechanical properties of polyethylene terephthalate. *J. Polym. Sci.* **1958,** *32* (125), 417–424.

19. Li, B.; Yu, J.; Lee, S.; Ree, M., Poly(ethylene terephthalate co ethylene isophthalate)—relationship between physical properties and chemical structures. *Eur. Polym. J.* **1999,** *35* (9), 1607–1610.

20. Schulken, R. M.; Boy, R. E.; Cox, R. H., Differential thermal analysis of linear polyesters. *J. Polym. Sci., C* **1964,** *6* (1), 17–25.

21. Martin, E. V.; Kibler, C. J., Polyester of 1,4-cyclohexanedimethanol. In *Man-Made Fiber Science and Technology*, Mark, H. F.; Atlas, S. M.; Cernia, E., Eds. Wiley-Interscience: New York, 1968; Vol. 3, pp 83-134.

22. Dickerson, J. P.; Brink, A. E.; Oshinski, A. J.; Seo, K. S. Copolyesters based on 1,4-cyclohexanedimethanol having improved stability. (Eastman Chemical Company). U.S. Patent 5,656,715, 1997.

23. Callander, D. D., *Modern Polyesters: Chemistry and Technology of Polyesters and Copolyesters*. John Wiley and Sons: West Sussex, Endland, 2003.

24. Meurisse, P.; Noel, C.; Monnerie, L.; Fayolle, B., Polymers with mesogenic elements and flexible spacers in the main chain: Aromatic-aliphatic polyesters. *Br. Polym. J.* **1981,** *13* (2), 55–63.

25. Wilfong, R. E., Linear polyesters. *J. Polym. Sci., Part A: Polym. Chem.* **1961,** *54* (160), 385–410.

26. Keller, A., The morphology of crystalline polymers. *Makromol. Chem.* **1959,** *34* (1), 1–28.

27. Cabpenter, A. S., Recent developments in synthetic fibres. *J. Soc. Dyers Colour* **1949,** *65* (10), 469–478.

28. Amari, T.; Nishimura, K.; Minou, K.; Kawabata, A.; Ozaki, Y., End-group characterization of homo- and copolyesters of cyclohexane-1,4-dimethanol. *J. Polym. Sci. Part A: Polym. Chem.* **2001,** *39* (5), 665–674.

29. Laubriet, C.; LeCorre, B.; Choi, K. Y., Two-phase model for continuous final stage melt polycondensation of poly(ethylene terephthalate). 1. Steady-state analysis. *Ind. Eng. Chem. Res.* **1991,** *30* (1), 2–12.

30. Ravindkanath, K.; Mashelkar, R. A., Modeling of polyethylene terephthalate reactors: 7. MWD considerations. *Polym. Eng. Sci.* **1984,** *24* (1), 30–41.

31. Daubeny, R. P.; Bunn, C. W., The crystal structure of polyethylene terephthalate. *Proc. R. Soc. London, Ser. A* **1954,** *226* (1167), 531–542.

32. Izard, E. F., The effect of chemical composition on selected physical properties of linear polymers. *J. Polym. Sci., Part A: Polym. Chem.* **1952,** *8* (5), 503–518.

33. Izard, E. F., Effect of chemical structure on physical properties of isomeric polyesters. *J. Polym. Sci., Part A: Polym. Chem.* **1952,** *9* (1), 35–39.

34. Bhatia, A.; Gupta, R. K.; Bhattacharya, S. N.; Choi, H. J., An investigation of melt rheology and thermal stability of poly(lactic acid)/ poly(butylene succinate) nanocomposites. *J. Appl. Polym. Sci.* **2009,** *114* (5), 2837–2847.

35. Nealy, D. L.; Jane Adams, L., Oxidative crosslinking in poly(ethylene terephthalate) at elevated temperatures. *J. Polym. Sci. Part A: Polym. Chem.* **1971,** *9* (7), 2063–2070.

36. Turner, S. R., Development of amorphous copolyesters based on 1,4-cyclohexanedimethanol. *J. Polym. Sci: Part A: Polym. Chem.* **2004,** *42* (23), 5847–5852.

37. Lorenzetti, C.; Finelli, L.; Lotti, N.; Vannini, M.; Gazzano, M.; Berti, C.; Munari, A., Synthesis and characterization of poly(propylene terephthalate/2,6-naphthalate) random copolyesters. *Polymer* **2005,** *46* (12), 4041–4051.

38. Jeong, Y. G.; Jo, W. H.; Lee, S. C., Synthesis and crystallization behavior of poly(m-methylene 2,6-naphthalate-co-1,4-cyclohexylenedimethylene 2,6-naphthalate) copolymers. *Macromolecules* **2003,** *36* (11), 4051–4059.

39. Hoffman, D. C.; Pecorini, T. J., Copolyesters of poly(1,4-cyclohexanedimethylene terephthalate) with isophthalic acid and 2,6-naphthalene dicarboxylic acid. *Am. Chem. Soc., Div. Polym. Chem., Polym. Prepr.* **1999,** *40* (1), 572–573.

40. Wendling, J.; Suter, U. W., A new model describing the cocrystallization behavior of random copolymers. *Macromolecules* **1998,** *31* (8), 2516–2520.

41. Sanchez, I. C.; Eby, R. K., Thermodynamics and crystallization of random copolymers. *Macromolecules* **1975,** *8* (5), 638–641.

42. Helfand, E.; Lauritzen, J. I., Theory of copolymer crystallization. *Macromolecules* **1973,** *6* (4), 631–638.

43. Baur, V. H., Einfluß der sequenzlängenverteilung auf das schmelz-ende von copolymeren. *Makromol. Chem.* **1966,** *98* (1), 297–301.

44. Flory, P. J., Theory of crystallization in copolymers. *Trans. Faraday Soc.* **1955,** *51* (0), 848–857.

45. Yu, Y.; Wei, Z.; Zhou, C.; Zheng, L.; Leng, X.; Li, Y., Miscibility and competition of cocrystallization behavior of poly(hexamethylene dicarboxylate)s aliphatic copolyesters: Effect of chain length of aliphatic diacids. *Eur. Polym. J.* **2017,** *92* (Supplement C), 71–85.

46. Konstantopoulou, M.; Terzopoulou, Z.; Nerantzaki, M.; Tsagkalias, J.; Achilias, D. S.; Bikiaris, D. N.; Exarhopoulos, S.; Papageorgiou, D. G.; Papageorgiou, G. Z., Poly(ethylene furanoate-co-ethylene terephthalate) biobased copolymers: Synthesis, thermal properties and cocrystallization behavior. *Eur. Polym. J.* **2017,** *89* (Supplement C), 349–366.

47. Hong, M.; Tang, X.; Newell, B. S.; Chen, E. Y. X., "Nonstrained" γ-butyrolactone-based copolyesters: copolymerization characteristics and composition-dependent (thermal, eutectic, cocrystallization, and degradation) properties. *Macromolecules* **2017,** *50* (21), 8469–8479.

48. Jeong, Y. G.; Lee, J. H.; Lee, S. C., Structures and cocrystallization behavior of copolyesters based on poly(octamethylene terephthalate) and poly(octamethylene 2,6-naphthalate). *Polymer* **2009,** *50* (6), 1559–1565.

49. Jeong, Y. G.; Jo, W. H.; Lee, S. C., Synthesis and isodimorphic cocrystallization behavior of poly(1,4-cyclohexylenedimethylene terephthalate-co-1,4-cyclohexylenedimethylene 2,6-naphthalate) copolymers. *j. Polym. Sci. Part B: Polym. Phys.* **2004,** *42* (1), 177–187.

50. Kamiya, N.; Sakurai, M.; Inoue, Y.; Chujo, R., Isomorphic behavior of random copolymers: thermodynamic analysis of cocrystallization of poly(3-hydroxybutyrate-co-3-hydroxyvalerate). *Macromolecules* **1991,** *24* (13), 3888–3892.

51. Petropoulos, J. C. Unsaturated polyester resin composition containing indan carboxylic acids and process of preparing the same. (American Cyanamid Company). U.S. Patent 2,830,966, 1958.

52. Petropoulos, J. C. Novel alkyd resins prepared from indandicarboxylic acids and the process of preparing the same. (American Cyanamid Company). U.S. Patent 2,873,262, 1959.

53. Meyer, D. H. Polymeric macropolyesters of phenylindane dicarboxylic acids. (Standard Oil Company). U.S. Patent 3,565,865, 1971.

54. Deeken, W. O.; Keck, M. H.; Wiener, M. V. Terephthalic acid-phenyl indane dicarboxylic acid copolyester resin. (The Goodyear Tire & Rubber Company). U.S. Patent 3,535,286, 1970.

55. Shaikh, A. A.; Kannan, G.; Ganapathi, M. Copolymers containing indan moieties and blends thereof. (General Electric Company). U.S. Patent 20,060,004,151, 2006.

56. Gandini, A.; Coelho, D.; Gomes, M.; Reis, B.; Silvestre, A., Materials from renewable resources based on furan monomers and furan chemistry: work in progress. *J. Mater. Chem.* **2009,** *19* (45), 8656–8664.

57. Gandini, A.; Silvestre, A. J. D.; Neto, C. P.; Sousa, A. F.; Gomes, M., The furan counterpart of poly(ethylene terephthalate): An alternative material based on renewable resources. *J. Polym. Sci., Part A: Polym. Chem.* **2009,** *47* (1), 295–298.

58. Gomes, M.; Gandini, A.; Silvestre, A. J. D.; Reis, B., Synthesis and characterization of poly(2,5-furan dicarboxylate)s based on a variety of diols. *J. Polym. Sci., Part A: Polym. Chem.* **2011,** *49* (17), 3759–3768.

59. Gubbels, E.; Jasinska-Walc, L.; Koning, C. E., Synthesis and characterization of novel renewable polyesters based on 2,5-furandicarboxylic acid and 2,3-butanediol. *J. Polym. Sci., Part A: Polym. Chem.* **2013,** *51* (4), 890–898.

60. Gupta, N. K.; Nishimura, S.; Takagaki, A.; Ebitani, K., Hydrotalcite-supported gold-nanoparticle-catalyzed highly efficient base-free aqueous oxidation of 5-hydroxymethylfurfural into 2,5-furandicarboxylic acid under atmospheric oxygen pressure. *Green Chem.* **2011,** *13* (4), 824–827.

61. Knoop, R. J. I.; Vogelzang, W.; van Haveren, J.; van Es, D. S., High molecular weight poly(ethylene-2,5-furanoate); critical aspects in synthesis and mechanical property determination. *J. Polym. Sci., Part A: Polym. Chem.* **2013,** *51* (19), 4191–4199.

62. Román-Leshkov, Y.; Chheda, J. N.; Dumesic, J. A., Phase modifiers promote efficient production of hydroxymethylfurfural from fructose. *Science* **2006,** *312* (5782), 1933–1937.

63. Zhao, H.; Holladay, J. E.; Brown, H.; Zhang, Z. C., Metal chlorides in ionic liquid solvents convert sugars to 5-hydroxymethylfurfural. *Science* **2007,** *316* (5831), 1597–1600.

64. Zhu, J.; Cai, J.; Xie, W.; Chen, P.-H.; Gazzano, M.; Scandola, M.; Gross, R. A., Poly(butylene 2,5-furan dicarboxylate), a biobased alternative to PBT: synthesis, physical properties, and crystal structure. *Macromolecules* **2013,** *46* (3), 796–804.

65. Burgess, S. K.; Kriegel, R. M.; Koros, W. J., Carbon dioxide sorption and transport in amorphous poly(ethylene furanoate). *Macromolecules* **2015,** *48* (7), 2184–2193.

66. Carothers, W. H. Alkylene ester of polybasic acids. (Du Pont). U.S. Patent 2,012,267, 1935.

67. Zorba, T.; Chrissafis, K.; Paraskevopoulos, K. M.; Bikiaris, D. N., Synthesis, characterization and thermal degradation mechanism of three poly(alkylene adipate)s: Comparative study. *Polym. Degrad. Stab* **2007,** *92* (2), 222–230.

68. Chrissafis, K.; Paraskevopoulos, K. M.; Bikiaris, D. N., Effect of molecular weight on thermal degradation mechanism of the biodegradable polyester poly(ethylene succinate). *Thermochim. Acta* **2006,** *440* (2), 166–175.

69. Bikiaris, D. N.; Achilias, D. S., Synthesis of poly(alkylene succinate) biodegradable polyesters I. Mathematical modelling of the esterification reaction. *Polymer* **2006,** *47* (13), 4851–4860.

70. Xu, J.; Guo, B.-H., Poly(butylene succinate) and its copolymers: Research, development and industrialization. *Biotechnol. J.* **2010,** *5* (11), 1149–1163.

71. Takiyama, E.; Fujimaki, T.; Seki, S.; Hokari, T.; Hatano, Y. Method for manufacturing biodegradable high molecular aliphatic polyester. (Showa Highpolymer Co., Ltd.). U.S. Patent 5,310,782, 1994.

72. Takiyama, E.; Niikura, I.; Hatano, Y. Method for producing saturated polyester. (Showa Highpolymer Co., Ltd.). U.S. Patent 5,306,787, 1994.

73. Takiyama, E.; Hatano, Y.; Fujimaki, T.; Seki, S.; Hokari, T.; Hosogane, T.; Harigai, N. Method of producing a high molecular weight aliphatic polyester and film thereof. (Showa Highpolymer Co., Ltd.). U.S. Patent 5,436,056, 1995.

74. Fujimaki, T., Processability and properties of aliphatic polyesters, 'BIONOLLE', synthesized by polycondensation reaction. *Polym. Degrad. Stab.* **1998,** *59* (1–3), 209–214.

75. Showa Denko Europe GmbH | Shaping ideas. http://www.showa-denko.com/news/bionolle-the-pioneer-in-biodegradable/ (accessed January 12, 2017).

76. Ahn, B. D.; Kim, S. H.; Kim, Y. H.; Yang, J. S., Synthesis and characterization of the biodegradable copolymers from succinic acid and adipic acid with 1,4-butanediol. *J. Appl. Polym. Sci.* **2001,** *82* (11), 2808–2826.

77. Cornils, B.; Lappe, P.; Staff, Dicarboxylic Acids, Aliphatic. In *Ullmann's Encyclopedia of Industrial Chemistry*, Wiley-VCH Verlag GmbH & Co. KGaA: 2000.

78. Musser, M. T., Adipic Acid. In *Ullmann's Encyclopedia of Industrial Chemistry*, Wiley-VCH Verlag GmbH & Co. KGaA: 2000.

79. Minnick, L. A. PET copolyesters containing succinic and naphthalenedicarboxylic acid moieties having improved barrier properties. (Eastman Chemical Company). U.S. Patent 5,506,014, 1996.

80. Tserki, V.; Matzinos, P.; Pavlidou, E.; Vachliotis, D.; Panayiotou, C., Biodegradable aliphatic polyesters. part I. properties and biodegradation of poly(butylene succinate-co-butylene adipate). *Polym. Degrad. Stab* **2006,** *91* (2), 367–376.

81. Izard, E. F., Effect of chemical structure on physical properties of isomeric polyesters. *J. Polym. Sci.* **1952,** *9* (1), 35–39.

82. Asrar, J.; Weinkauff, D. J.; Bhombal, A. H. Hydroxy ethyl bibenzoate. (Monsanto Company). U.S. Patent 5,374,707, 1994.

83. Mang, M. N.; Brewbaker, J. L. Thermoplastic polyesters containing biphenylene linkages. (The Dow Chemical Company). U.S. Patent 5,138,022, 1992.

84. Mondschein, R. J.; Dennis, J. M.; Liu, H.; Ramakrishnan, R. K.; Nazarenko, S.; Turner, S. R.; Long, T. E., Synthesis and characterization of amorphous bibenzoate (co)polyesters: permeability and rheological performance. *Macromolecules* **2017,** *50* (19), 7603–7610.

85. Gore, A. C.; Chappell, V. A.; Fenton, S. E.; Flaws, J. A.; Nadal, A.; Prins, G. S.; Toppari, J.; Zoeller, R. T., Executive summary to EDC-2: the endocrine society's second scientific statement on endocrine-disrupting chemicals. *Endocr. Rev.* **2015,** *36* (6), 593–602.

86. Scott, C. E.; Morris, J. C.; Bradley, J. R. Clear blends of polycarbonates and polyesters. (Eastman Chemical Company). U.S. Patent 6,037,424, 2000.

87. Scott, C. E.; Morris, J. C.; Bradley, J. R. Clear polycarbonate and polyester blends. (Eastman Chemical Company). U.S. Patent 6,043,322, 2000.

88. Crawford, E. D.; Porter, D. S.; Connell, G. W. Polyester compositions wich comprise cyclobutanediol having certain cis/trans ratios. (Eastman Chemical Company). Eur. Pat. 2156934 2011.

89. Barton, B. F.; Shackelford, D. B. Process for the preparation of copolyesters based on 2,2,4,4-tetramethyl-1,3-cyclobutanediol and 1,4-cyclohexanedimethanol. (Eastman Chemical Company). WO 2008140705, 2008.

90. Ma, H.; Hibbs, M.; Collard, D. M.; Kumar, S.; Schiraldi, D. A., Fiber spinning, structure, and properties of poly(ethylene terephthalate-co-4,4‘-bibenzoate) copolyesters. *Macromolecules* **2002,** *35* (13), 5123–5130.

91. Polyakova, A.; Connor, D. M.; Collard, D. M.; Schiraldi, D. A.; Hiltner, A.; Baer, E., Oxygen-barrier properties of polyethylene terephthalate modified with a small amount of aromatic comonomer. *J. Polym. Sci. Part B Polym. Phys* **2001,** *39* (16), 1900–1910.

92. Asrar, J., Synthesis and properties of 4,4′-biphenyldicarboxylic acid and 2,6-naphthalenedicarboxylic acid. *J. Polym. Sci., Part A: Polym. Chem.* **1999,** *37* (16), 3139–3146.

93. Edling, H. E.; Liu, H.; Sun, H.; Mondschein, R. J.; Schiraldi, D. A.; Long, T. E.; Turner, S. R., Copolyesters based on bibenzoic acids. *Polymer* **2018,** *135*, 120–130.

94. Liu, R. Y. F.; Schiraldi, D. A.; Hiltner, A.; Baer, E., Oxygen-barrier properties of cold-drawn polyesters. *J. Polym. Sci., Part B: Polym. Phys.* **2002,** *40* (9), 862–877.

95. Hu, Y. S.; Liu, R. Y. F.; Rogunova, M.; Schiraldi, D. A.; Nazarenko, S.; Hiltner, A.; Baer, E., Oxygen-barrier properties of cold-crystallized and melt-crystallized poly(ethylene terephthalate-co-4,4′-bibenzoate). *Journal of Polymer Science Part B: Polymer Physics* **2002,** *40* (22), 2489–2503.

96. Sherman, S. C.; Iretskii, A. V.; White, M. G.; Gumienny, C.; Tolbert, L. M.; Schiraldi, D. A., Isomerization of substituted biphenyls by superacid. A remarkable confluence of experiment and theory. *J. Org. Chem.* **2002,** *67* (7), 2034–2041.

97. Schiraldi, D. A.; Iretski, A. V.; Sherman, S. C.; Tolbert, L. M.; White, M. G. Acid catalyzed isomerization of substituted diaryls. (Arteva North America S.A.R.L.). U.S. Patent 6,433,236, 2002.

98. Schiraldi, D. A.; Sherman, S. C.; Sood, D. S.; White, M. G. Catalytic system and method for coupling of aromatic compounds. (Arteva North America S.A.R.L.). U.S. Patent 6,103,919, 2000.

99. Dakka, J. M.; DeCaul, L. C.; Tang, W. (Methylcyclohexyl)toluene isomer mixtures,their production and their use in the manufacture of plasticizers. (Exxonmobil Chemical Patents Inc.). WO 2014159100, 2014.

100. Dakka, J. M.; Bai, C.; Tanke, J. J.; De Martin, G. J.; Van Nostrand, M. T.; Salciccioli, M.; Kheir, A. A.; Sangar, N. Methyl-substituted biphenyl compounds, their production and their use in the manufacture of plasticizers. (Exxonmobil Chemical Patents Inc.). U.S. Patent 20,140,275,607 2014.

101. Rebsdat, S.; Mayer, D., Ethylene Glycol. In *Ullmann's Encyclopedia of Industrial Chemistry*, Wiley-VCH Verlag GmbH & Co. KGaA: 2000.

102. Renwen, H.; Feng, Y.; Tinzheng, H.; Shiming, G., The kinetics of formation of diethylene glycol in preparation of polyethylene terephthalate and its control in reactor design and operation. *Makromol. Chem.* **1983,** *119* (1), 159–172.

103. Chen, J. W.; Chen, L. W., The kinetics of diethylene glycol formation from bis-hydroxyethyl terephthalate with antimony catalyst in the preparation of PET. *J. Polym. Sci., Polym. Chem.* **1999,** *37* (12), 1797–1803.

104. Chen, J. W.; Chen, L. W., The kinetics of diethylene glycol formation in the preparation of polyethylene terephthalate. *J. Polym. Sci., Part A: Polym. Chem.* **1998,** *36* (17), 3073–3080.

105. Lee, S. W.; Lee, B.; Ree, M., Poly(ethylene-co-ethyleneoxyethylene terephthalate)s: synthesis and non-isothermal crystallization behavior. *Macromol. Chem. Phys.* **2000,** *201* (4), 453–463.

106. East, A. J., Polyesters, Thermoplastic. In *Kirk-Othmer Encyclopedia of Chemical Technology*, John Wiley & Sons, Inc.: 2000.

107. Auerbach, A. B.; Sell, J. W., Evaluation of poly(1,4-cyclohexylene dimethylene terephthalate) blends for improved processability. *Poly. Eng. Sci.* **1990,** *30* (17), 1041–1050.

108. Grossetête, T.; Rivaton, A.; Gardette, J. L.; Hoyle, C. E.; Ziemer, M.; Fagerburg, D. R.; Clauberg, H., Photochemical degradation of poly(ethylene terephthalate)-modified copolymer. *Polymer* **2000,** *41* (10), 3541-3554.

109. Hoffman, D. C.; Pecorini, T. J., Copolyesters of poly(1,4-cyclohexanedimethylene terephthalate) with isophthalic acid and 2,6-naphthalene dicarboxylic acid. *Polym. Prep.* **1999,** *40* (1), 572–573.

110. Hasek, R. H.; Knowles, M. B. Preparation of trans-1,4-cyclohexanedimethanol. (Eastman Kodak Company). U.S. Patent 2,917,549, 1959.

111. Kibler, C. J.; Bell, A.; Smith, J. G., Polyesters of 1,4-cyclohexanedimethanol. *J. Polym. Sci. Part A: Polym. Chem.* **1964,** *2* (5), 2115–2125.

112. Riande, E.; Gusman, J.; de la Campa, J. G.; de Abajo, J., Configurational properties of polyesters with cyclohexane rings incorporated in the main chain. *Macromolecules* **1985,** *18* (8), 1583–1587.

113. Vanhaecht, B.; Teerenstra, M. N.; Suwier, D. R.; Willem, R.; Biesemans, M.; Koning, C. E., Controlled stereochemistry of polyamides derived from cis/trans-1,4-cyclohexanedicarboxylic acid. *J. Polym. Sci. Part A: Polym. Chem.* **2001,** *39* (6), 833–840.

114. Vanhaecht, B.; Rimez, B.; Willem, R.; Biesemans, M.; Koning, C. E., Influence of stereochemistry on the thermal properties of partially cycloaliphatic polyamides. *J. Polym. Sci. Part A: Polym. Chem.* **2002,** *40* (12), 1962–1971.

115. Jayakannan, M.; Anilkumar, P., Mechanistic aspects of ester–carbonate exchange in polycarbonate/cycloaliphatic polyester with model reactions. *J. Polym. Sci. Part A: Polym. Chem.* **2004,** *42* (16), 3996–4008.

116. Chen, L. P.; Yee, A. F.; Goetz, J. M.; Schaefer, J., Molecular structure effects on the secondary relaxation and impact strength of a series of polyester copolymer glasses. *Macromolecules* **1998,** *31* (16), 5371–5382.

117. Boye, C. A., X-Ray diffraction studies of poly(1,4-cyclohexylenedimethylene terephthalate). *J. Polym. Sci.* **1961,** *55* (161), 275–284.

118. Ridgway, J. S., Polyamides from 1,4-cyclohexanebis(ethylamine) and aliphatic dicarboxylic acids. *J. Appl. Polym. Sci.* **1974,** *18* (5), 1517–1528.

119. Martin, E. V.; Kibler, C. J., Polyesters of 1,4-cyclohexanedimethanol. In *Man-Made Fiber Science and Technology*, Mark, H. F.; Atlas, S. M.; Cernia, E., Eds. Wiley-Interscience: New York, 1968; Vol. 3, pp 83–134.

120. Dennis, J. M.; Enokida, J. S.; Long, T. E., Synthesis and characterization of decahydronaphthalene-containing polyesters. *Macromolecules* **2015,** *48* (24), 8733–8737.

121. Yee, A. F.; Smith, S. A., Molecular structure effects on the dynamic mechanical spectra of polycarbonates. *Macromolecules* **1981,** *14* (1), 54–64.

122. Liu, J.; Yee, A. F., Enhancing plastic yielding in polyestercarbonate glasses by 1,4-cyclohexylene linkage addition. *Macromolecules* **1998,** *31* (22), 7865–7870.

123. Eckart, M. D.; Goodson, R. L. Thermoplastic article having high-relief surface. (Eastman Chemical Company). WO 1999010173, 1999.

124. Jackson, W. J.; Watkins, J. J. High molecular weight polyesters. (Eastman Chemical Compay). U.S. Patent 4,578,453, 1986.

125. Yang, H.; Moskala, E.; Jones, M., Physical performance of copolyesters for medical applications. *J. Appl. Med. Polym.* **1999,** *3* (2), 50–54.

126. Elam, E. U.; Martin, J. C.; Gilkey, R. Linear polyesters and polyester-amides from 2, 2, 4, 4-tetraalkyl-1, 3-cyclobutanediols. (Eastman Kodak Company). U.S. Patent 3,313,777, 1967.

127. Martin, J. C.; Elam, E. U. Separation of cis and trans isomers of tetraalkyl - 1,3 - cyclobutanediols and novel compound obtained thereby. (Eastman Kodak Company). U.S. Patent 3,227,764, 1966.

128. Elam, E. U.; Hasek, R. H. Preparation of tetraalkylcyclo-butanediols. (Eastman Kodak Company). U.S. Patent 3,190,928, 1965.

129. Elam, E. U.; Hasek, R. H. Preparation of 2, 2, 4, 4-tetraalkylcyclobutane-1, 3-diols. (Eastman Kodak Company). U.S. Patent 2,936,324, 1960.

130. Kelsey, D. R. Copolyester composition. (Shell Oil Company). U.S. Patent 5,705,575, 1998.

131. Rylander, P. N. Production of 3-hydroxy-2, 2, 4, 4-tetraalkyl-cyclobutanones. (Englehard Ind Inc). U.S. Patent 3,329,722, 1967.

132. Jackson, W. J.; Gray, T. F.; Caldwell, J. R., Polyester hot-melt adhesives. I. Factors affecting adhesion to epoxy resin coatings. *J. Appl. Polym. Sci.* **1970,** *14* (3), 685–698.

133. Quisenberry, K. R. Segmented copolyester of 2, 2, 4, 4-tetramethyl-1, 3-cyclobutylene terephthalate andethylene terephthalate. (Du Pont). U.S. Patent 3,249,652, 1966.

134. Sulatha, M. S.; Purushotham, S.; Natarajan, U., RMMC simulations of the chain properties of polyester homopolymers from 1,4-cyclohexanedimethanol and 2,2,4,4-tetramethyl-1,3-cyclobutanediol. *Polymer* **2002,** *43* (23), 6295–6305.

135. Zhang, M.; Moore, R. B.; Long, T. E., Melt transesterification and characterization of segmented block copolyesters containing 2,2,4,4-tetramethyl-1,3-cyclobutanediol. *J. Polym. Sci. Part A: Polym. Chem.* **2012,** *50* (18), 3710–3718.

136. Sulatha, M. S.; Natarajan, U., RIS models and unperturbed chain properties of polyesters containing 1,3-cyclobutylene and 1,4-cyclohexylene linkages. *Macromol. Theory Simul.* **2003,** *12* (1), 61–71.

137. Iyer, K. A., Chain mobility, secondary relaxation, and oxygen transport in terephthalate copolyesters with rigid and flexible cyclic diols. *Polymer* **2017,** *129* (Supplement C), 117–126.

138. Dennis, J. M.; Fazekas, N. A.; Mondschein, R. J.; Ramakrishnan, R.; Nazarenko, S.; Long, T. E., Influence of cyclobutane segments in cycloaliphatic decahydronaphthalene-containing copolyesters. *High Perform. Polym.* **2017,** *29* (6), 750–756.

139. Eastman Tritan Copolyester | Applications. http://www.eastman.com/Brands/Eastman_Tritan/Pages/Applications.aspx (accessed December 11, 2017).

140. Coover, H. W.; Sjearer, N. H.; Wicker, T. Polyester molding composition. (Eastman Kodak Company). U.S. Patent T 875,010, 1970.

141. Fenouillot, F.; Rousseau, A.; Colomines, G.; Saint-Loup, R.; Pascault, J. P., Polymers from renewable 1,4:3,6-dianhydrohexitols (isosorbide, isomannide and isoidide): A review. *Prog. Polym. Sci.* **2010,** *35* (5), 578–622.

142. Noordover, B. A. J.; van Staalduinen, V. G.; Duchateau, R.; Koning, C. E.; van, B.; Mak, M.; Heise, A.; Frissen, A. E.; van Haveren, J., Co- and terpolyesters based on isosorbide and succinic acid for coating applications: synthesis and characterization. *Biomacromolecules* **2006,** *7* (12), 3406–3416.

143. Feng, X.; East, A. J.; Hammond, W. B.; Zhang, Y.; Jaffe, M., Overview of advances in sugar-based polymers. *Polym. Adv. Technol.* **2011,** *22* (1), 139–150.

144. Quintana, R.; de Ilarduya, A. m.; Alla, A.; Muñoz-Guerra, S., Polyterephthalates made from ethylene glycol, 1,4-cyclohexanedimethanol, and isosorbide. *J. Polym. Sci., Part A: Polym. Chem.* **2011,** *49* (10), 2252–2260.

145. Wu, J.; Eduard, P.; Jasinska-Walc, L.; Rozanski, A.; Noordover, B. A. J.; van Es, D. S.; Koning, C. E., Fully isohexide-based polyesters: synthesis, characterization, and structure–properties relations. *Macromolecules* **2012,** *46* (2), 384–394.

146. Yoon, W. J.; Hwang, S. Y.; Koo, J. M.; Lee, Y. J.; Lee, S. U.; Im, S. S., Synthesis and characteristics of a biobased high-Tg terpolyester of isosorbide, ethylene glycol, and 1,4-

cyclohexane dimethanol: effect of ethylene glycol as a chain linker on polymerization. *Macromolecules* **2013,** *46* (18), 7219–7231.

147. Adelman, D. J.; Charbonneau, L. F.; Ung, S. Process for making poly(ethylene-co-isosorbide) terephthalate polymer. (E. I. Du Pont De Nemours & Company). U.S. Patent 6,656,577, 2003.

148. Fleche, G.; Fuertes, P.; Tamion, R.; WYART, H. Method for purifying a composition containing at least an internal dehydration product for a hydrogenated sugar. (Roquette Freres). WO 2001094352, 2001.

149. Go beyond PET towards PEIT with our plant-based Polysorb® isosorbide. https://www.roquette.com/industries/performance-materials/polyesters/ (accessed January 06, 2018).

150. Polysorb® - Isosorbide. https://www.roquette.com/industries-polysorb-isosorbide (accessed January 06, 2018).

151. Germroth, T. C.; Turner, S. R.; Treece, L. C. Method for making isosorbide containing polyesters. (Eastman Chemical Company). U.S. Patent 6,914,120, 2005.

152. Weissermel, K.; Arpe, H.-J., Alcohols. In *Industrial Organic Chemistry*, Third ed.; VCH Publishers, Inc.: New York, 1997; pp 191–212.

153. Samanta, C. Neopentyl glycol (NPG): a unique multi-purpose chemical https://www.researchgate.net/publication/320243264_NEOPENTYL_GLYCOL_NPG_A_UNIQUE_MULTI-PURPOSE_CHEMICAL (accessed January 6, 2018).

154. Soccio, M.; Lotti, N.; Finelli, L.; Gazzano, M.; Munari, A., Neopenthyl glycol containing poly(propylene terephthalate)s: structure–properties relationships. *J. Polym. Sci. Part B: Polym. Phys.* **2008,** *46* (2), 170–181.

155. Maetens, D., Weathering degradation mechanism in polyester powder coatings. *Prog. Org. Coat.* **2007,** *58* (2), 172–179.

156. Plage, B.; Schulten, H. R., Thermal degradation and mass-spectrometric fragmentation processes of polyesters studied by time/temperature-resolved pyrolysis-field ionization mass spectrometry. *Macromolecules* **1990,** *23* (10), 2642–2648.

157. Jing, X.-K.; Ge, X.-G.; Xiang, X.; Wang, C.; Sun, Z.; Chen, L.; Wang, Y.-Z., A novel phosphorus-containing copolyester with low melting temperature and high flame retardancy. *Polym. Int.* **2009,** *58* (10), 1202–1208.

158. Turner, S. R.; Milburn, J. T.; Seymour, R. W.; Kab Sik Seo Amorphous copolyesters. (Eastman Chemical Company). U.S. Patent 7,026,027, 2006.

159. Moad, G.; Groth, A.; O'Shea, M. S.; Rosalie, J.; Tozer, R. D.; Peeters, G., Controlled synthesis of block polyesters by reactive extrusion. *Macromol. Symp.* **2003,** *202* (1), 37–46.

160. Liu, Y.; Turner, S. R., Synthesis and properties of cyclic diester based aliphatic copolyesters. *J. Polym. Sci. Part A: Polym. Chem.* **2010,** *48* (10), 2162-2169.

161. Berti, C.; Celli, A.; Marchese, P.; Marianucci, E.; Barbiroli, G.; Di Credico, F., Influence of molecular structure and stereochemistry of the 1,4-cyclohexylene ring on thermal and mechanical behavior of poly(butylene 1,4-cyclohexanedicarboxylate). *Macromol. Chem. Phys.* **2008,** *209* (13), 1333–1344.

162. Dobashi, Y.; Yuyama, T.; Ohkatsu, Y., Interaction of ultraviolet absorbers. *Polym. Degrad. Stab.* **2007,** *92* (7), 1227–1233.

163. Brunelle, D. J.; Jang, T., Optimization of poly(1,4-cyclohexylidene cyclohexane-1,4-dicarboxylate) (PCCD) preparation for increased crystallinity. *Polymer* **2006,** *47* (11), 4094–4104.

164. Awasthi, S.; Agarwal, D., The effect of difunctional acids on the performance properties of polyurethane coatings. *J. Coat. Technol. Res.* **2009,** *6* (3), 329–335.

165. Awasthi, S.; Agarwal, D., Influence of cycloaliphatic compounds in the properties of polyurethane coatings. *J. Coat. Technol. Res.* **2007,** *4* (1), 67–73.

166. Lee, S.-S.; Yee, A. F., Temperature-dependent transition of deformation mode in poly(1,4-cyclohexylenedimethylene terephthalate)/poly(ethylene terephthalate) copolymers. *Macromolecules* **2003,** *36* (18), 6791–6796.

167. Caldwel, J. R.; Gilkey, R. Fiber-forming polyesters from trans-1, 4-cyclohexanedicarboxylic compounds and 1, 1-cyclohexane dimethanol. (Eastman Kodak Company). U.S. Patent 2,891,930, 1959.

168. Berti, C.; Binassi, E.; Celli, A.; Colonna, M.; Fiorini, M.; Marchese, P.; Marianucci, E.; Gazzano, M.; Di Credico, F.; Brunelle, D. J., Poly(1,4-cyclohexylenedimethylene 1,4-cyclohexanedicarboxylate): Influence of stereochemistry of 1,4-cyclohexylene units on the thermal properties. *J. Polym. Sci., Part B: Polym. Phys.* **2008,** *46* (6), 619–630.

169. Patel, B. R.; Smith, G. F. Crystalline polyester resins and process for their preparation. (General Electric Company). U.S. Patent 6,455,664, 2002.

170. Patel, B. R.; Smith, G. F.; Banach, T. E. Crystalline polyester resins and process for their preparation. (General Electric Company). U.S. Patent 5,986,040, 1999.

171. Jackson, W. J.; Darnell, W. R. Process for preparing poly-1,4-cyclohexanedicarboxylate polyesters having high trans isomer content. (Eastman Kodak Company). U.S. Patent 4,327,206, 1982.

172. Ni, H.; Daum, J. L.; Thiltgen, P. R.; Soucek, M. D.; Simonsick Jr, W. J.; Zhong, W.; Skaja, A. D., Cycloaliphatic polyester-based high-solids polyurethane coatings: II. The effect of difunctional acid. *Prog. Org. Coat.* **2002,** *45* (1), 49–58.

173. Kricheldorf, H. R.; Schwarz, G., New polymer syntheses, 17. Cis/trans isomerism of 1,4-cyclohexanedicarboxylic acid in crystalline, liquid-crystalline and amorphous polyesters. *Makromol. Chem.* **1987,** *188* (6), 1281–1294.

174. Brunelle, D. J.; Jang, T. Method for preparing poly(1,4-cyclohexanedicarboxylates). (General Electric Company). U.S. Patent 6,084,055, 2000.

175. Sandhya, T. E.; Ramesh, C.; Sivaram, S., Copolyesters based on poly(butylene terephthalate)s containing cyclohexyl and cyclopentyl ring: effect of molecular structure on thermal and crystallization behavior. *Macromolecules* **2007,** *40* (19), 6906–6915.

176. Gaughan, R. G.; Hill, H. W.; Inda, J. E., Preparation and properties of the polyester made from 2.2-bis(4-hydroxycyclohexyl)propane and adipic acid. *J. Polym. Sci. Part A: Polym. Chem.* **1986,** *24* (3), 419-426.

177. Storms, P. W.; Farrar, G. L., Hydrogenation of naphthalene esters to tetralin esters. *J. Chem. Eng. Data* **1969,** *14* (4), 489–490.

178. Wada, Y.; Kasahara, T., Relation between impact strength and dynamic mechanical properties of plastics. *J. Appl. Polym. Sci.* **1967,** *11* (9), 1661–1665.

Chapter 2. Copolyesters Based on Bibenzoic Acids

(published as: Edling, H. E.; Liu, H.; Sun, H.; Mondschein, R. J.; Schiraldi, D. A.; Long, T. E.; Turner, S. R. *Polymer* **2018,** *135,* 120-130.)

2.1 Authors

H. Eliot Edling[1], Haoyu Liu[1], Hua Sun[2], Ryan J. Mondschein[1], David A. Schiraldi[2], Timothy E. Long[1] and S. Richard Turner[*,1]

[1]Macromolecules Innovation Institute, Department of Chemistry, Virginia Tech, Blacksburg, Virginia 24061, USA

[2]Department of Macromolecular Science and Engineering, Case Western Reserve University, 10900 Euclid Avenue, Cleveland, Ohio 44106

2.2 Abstract

Novel copolyester thermoplastics based on 4,4'-bibenzoate and 3,4'-bibenzoate moieties with ethylene glycol were synthesized via melt polycondensations. Crystallization behavior was modified by the additional incorporation of terephthalate or isophthalate units into the backbones. Copolyester compositions were verified by ^{1}H NMR spectroscopy and molecular weights were assessed by measuring inherent viscosity (ηinh). Thermogravimetric analysis (TGA) showed single-step weight losses in the range of 360–400 °C. Differential scanning calorimetry (DSC) was used to determine melting points and glass transition temperatures over a wide range of copolyester compositions. Observation of thermal data was used to identify amorphous windows in composition ranges containing 3,4′BB and 4,4′BB moieties. Dynamic mechanical analysis (DMA) provided information about thermal transitions and sub-T g relaxations. Mechanical data were obtained with tensile testing to expand structure–property–morphology relationships. Permeability

analysis helped to understand how monomer symmetry affects oxygen diffusivity and solubility in selected amorphous film and biaxially oriented copolyester samples.

2.3 Introduction

The well-defined structure-property relationships with polyesters based upon dimethyl terephthalate (DMT) and dimethyl isophthalate (DMI) (**Figure 2-1**) provide a point of reference

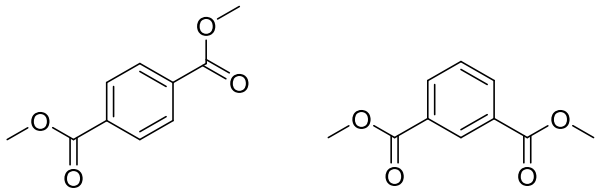

Figure 2-1. Two aromatic diester monomers (dimethyl terephthalate (DMT) and dimethyl isophthalate (DMI)) commonly used in commercial polyesters.

for understanding how structural changes in the polyester backbone influences properties. The linear symmetry and rigid structure of the terephthaloyl unit makes ordered packing of the chains favorable, resulting in a semicrystalline polyester. Poly(ethylene terephthalate), (PET) is the best-known semicrystalline polyester due to its overall properties, which enable utility in bottling, films and fiber applications and low cost. Poly(butylene terephthalate) (PBT) crystallizes much faster than PET as a result of higher chain flexibility from the longer butane diol units, which allows injection molded parts with good dimensional stability to be produced at a much more rapid pace[1]. The term 'acid modified' refers to copolyesters altered with additional diesters or diacids, and while many comonomers have been thoroughly studied, few available aromatic diacids are capable of significant property enhancement.[1-4] The relationship between symmetry and crystallization is clearly demonstrated when the *meta* substituted isophthaloyl unit is compared to *para* substituted terephthaloyl unit. The non-linear shape of the isophthaloyl unit produces a "kink" in the chain

that disrupts crystallization. Because isophthaloyl units are nonsymmetrical along the ring-flipping axes, rotation is impeded by the presence of atoms from other chains. This decreased mobility results in a lower free volume relative to terephthaloyl.[5-10] Lower permeability and higher selectivity is believed to result from more efficient packing in the amorphous regions and from restricted mobility. Over the years, many attempts have been made to correlate low diffusivities with low intensity sub-T_g transitions (resulting from higher energy barriers to rotation) and low solubilities with lower observed glass transition temperatures (T_gs) (resulting from higher excess hole free volumes).[5-6, 8, 11-12]

PET has great commercial value because it can be manufactured at reasonably low cost, is readily processed and stretch blow molded, is non-toxic, has good organoleptic properties, has excellent oxygen and carbon dioxide barriers, has a good tensile strength and modulus, and has a reasonably high T_g and melting temperature (T_m). However, unmodified PET is impractical for many applications. The homopolyester of dimethyl isophthalate (DMI) and ethylene glycol (EG), abbreviated PEI, has poor mechanical and thermal properties when compared to PET (**Table 2-1**). However isophthalate can be integrated into PET at low concentrations (lower than 5 mol%) to disrupt thermal crystallization, which helps to produce clear films and injection molded bottle preforms, and facilitates dying by producing a kink that disrupts chain packing.[13] DMI is used more than any other diacid to modify the properties of PET[3] and is especially useful in decreasing the permeability of PET.[9] Its addition is especially advantageous because small additions (less than 5 mol%) suppresses crystallization with little impact on T_g, making production of transparent films easier.[14]

Table 2-1. Comparison of the thermal and mechanical properties of the PET and PEI homopolyesters. Tensile analysis followed ASTM testing method D638. Dogbones were punched from 0.55 mm compression molded films with a D638-V punch.

	T_g (°C)	T_m (°C) [9, 15 9, 15 9, 15 9, 15 9, 15 9, 15 9, 15]	Modulus (MPa)	Yield Stress (MPa)	Elongation at break (%)	Permeability (cc.cm/m^2/atm/day)[9]
PET	81	252	2076 ± 187	68 ± 1	305 ± 55	0.424
PEI	60	231	2495 ± 94	64 ± 3	6 ± 2	0.090

Polyesters that incorporate biphenyl structures have been known for many years[16] and patents were issued to the Dow Chemical Company and Monsanto in the early 1990s describing a number of copolyesters made with dimethyl biphenyl-3,4′-dicarboxylate (3,4′BB) and dimethyl biphenyl-4,4′-dicarboxylate (4,4′BB) (**Figure 2-2**).[17-18] In their patent, Dow described polyesters

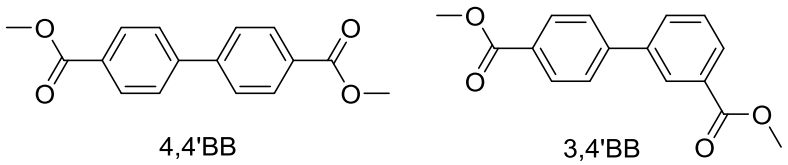

Figure 2-2. Chemical structure of 4,4′BB and 3,4′BB monomers

made with 4,4′BB and 3,4′BB diesters and at least one aliphatic diol containing 2–12 carbon atoms. When synthesized with EG, copolyesters containing more than 50 mol% 4,4′BB were semicrystalline and exhibited high tensile moduli. An example composition with 75 mol% 4,4′BB had a T_g and T_m of 122 °C and 293 °C respectively, and had a high tensile modulus around 4.0 GPa. Compositions with more than 50 mol% 3,4′BB were tough, transparent and had glass transitions ranging from 104–111 °C. Copolyesters containing 3,4′BB and 4,4′BB isomers showed good promise as fibers for tire cord, reinforcement in hoses or conveyor belts, or in composites;[19] they also produce films with good solvent and chemical resistance, low flammability, and good

insulating properties. The homopolymer produced from 4,4′BB and EG has a very high T_m (343 °C) and is highly crystalline, opaque, and brittle.[20] Dow modified the 4,4′BB-EG homopolyester with 3,4′BB and DMT to lower the T_m below 300 °C, making it readily melt processable without the concern of degradation. In their patent, Monsanto described several compositions made by utilizing DMT and 4,4′BB with EG, producing a range of copolyesters with T_gs ranging from 78–111 °C and T_ms ranging from 217–278 °C.[18] However, the patent detailed very little analysis related to mechanical properties or permeability.

Polyesters produced with 4,4′BB or 3,4′BB have shown great potential for thermoplastics with a range of desirable properties including high T_ms and/or high T_gs. Even though polyesters produced with terephthalic and isophthalic acids have been hugely successful in filling many different needs, there is a continual drive to develop new polymers that can perform beyond the capabilities of current polymers. Bisphenol-A polycarbonate (BPA PC), a polymer frequently utilized for its excellent impact and thermal properties (T_g ~ 145 °C), fell out of favor as food safe polymer that will hold its shape when filled with hot liquids (e.g. baby food, pasteurized beer and fruit juice) during hot fill packaging, due to concerns over the endocrine-disrupting activity of BPA contained in polycarbonate and its potential to be release into food and beverages.[21-24] This concern produced a high demand for engineering polymers with high T_gs and without the toxicity concerns of BPA PC. Eastman's Tritan™ copolyester has replaced BPA PC as a food safe engineering polymer in many applications.[22, 25-27]

Modification of PET with 3,4′BB and 4,4′BB has excellent potential to increase the T_g, modulus, strength and barrier properties sufficiently to meet new applications. The different effects 3,4′BB and 4,4′BB exert on polymer properties are comparable to how terephthalate and isophthalate affect polymer properties. Indeed, the high symmetry of 4,4′BB produces highly

crystalline polyesters with very high T_gs, whereas the "kinked" shape of 3,4′BB disrupts crystallization and produces lower T_g materials.[8, 19, 28] While 3,4′BB polymers exhibit lower permeabilities in unoriented films relative to 4,4′BB and PET, oriented films containing 4,4′BB have achieved much lower permeabilities than oriented PET, due to the high extensibility of the rigid 4,4′BB unit.[8, 29-32]

Despite demonstrating excellent potential for property enhancement, the property profiles for many polyester and copolyester compositions containing 3,4′BB and 4,4′BB remain unstudied. Even so, recent studies have disclosed new routes for preparing 3,4′BB and 4,4′BB.[18, 33-41] Impressive work by Schiraldi et al. demonstrated an effective means to selectively couple toluene to produce dimethylbiphenyl isomers with palladium and triflic acid catalysts.[39-41] Alternatively, Dekka et al produced 3,4′BB and 4,4′BB monomers by coupling toluene with hydrogen in the presence of a hydroalkylation catalyst, such as a supported palladium catalyst, to form methylcyclohexyl toluenes, followed by dehydrogenation to dimethylbiphenyl isomers. The potential availability of 3,4'BB and 4,4′BB prompts us to more thoroughly study the structure–property–morphology relationships of copolyesters modified with 3,4′BB and 4,4′BB. While homopolyesters made from 4,4′BB tend to have very high melting temperatures and brittleness associated with high crystallinity, the much higher T_m and T_g of 4,4′BB homopolyesters suggests properly-designed polyesters and copolyesters containing 4,4′BB and 3,4′BB could enhance thermal and mechanical properties relative to known polyester compositions. Copolyesters incorporating significant amounts of 3,4′BB appear attractive for obtaining new tough, highly amorphous materials with good thermal properties[8, 17-18] and a recent study by Mondschein et al thoroughly examines the thermal, mechanical and barrier properties of copolyesters containing 3,4′BB, 4,4′BB and EG.[42]

Past research strongly suggests excellent potential for bibenzoate monomers to increase the gas barrier of PET in cold drawn films.[30] Our initial research showed biaxially oriented films produced from PET, containing low levels of 4,4'-bibenzoate, exhibited increased barrier relative to biaxially oriented PET; however, higher levels of the linear 4,4'-bibenzoate units, which are predicted to lead to even better barrier performance, lead to copolyesters with enhanced crystallization rates. This precludes successful biaxial orientation, which is performed above the T_g, of these copolyesters into transparent films. It is hypothesized that incorporation of kinked comonomer diacids (isophthalate and/or 3,4'-bibenoate units) can lead to copolyester compositions with mitigated crystallization characteristics so that the copolyester films can be biaxially oriented and that the new copolyester compositions will exhibit superior barrier properties. In the collaborative study reported here, meta substituted comonomers, 3,4'-bibenzoate and isophthalate, were incorporated to control the crystallization of PET copolyesters containing 4,4'-bibenzoate and allow biaxial orientation of compression molded films containing up to 55 mol% 4,4'-bibenzoate. The second part of this study, to be published in the near future, will provide in depth analysis for sucessfully biaxially oriented films.

2.4 Experimental

2.4.1 Materials

Dimethyl terephthalate (DMT, ≥99%) and dimethyl isophthalate (DMI, 99%) were purchased from Sigma Aldrich. Dimethyl 4,4′-biphenyldicarboxylate (4,4′BB) and dimethyl 3,4′-biphenyldicarboxylate (3,4′BB) were supplied by ExxonMobil Chemical Company. All diesters were dried in a vacuum oven overnight at 35 °C and stored in a dry box before use. Ethylene glycol (EG, ≥99%) was obtained from Sigma Aldrich and used as received. Dichloroacetic acid (≥99%) was obtained from Alpha Aesar. Titanium (IV) butoxide (97%) was purchased from Sigma

Aldrich. 1-Butanol (99.9%) was purchased from Fisher Scientific and dried over magnesium sulfate. A titanium catalyst solution (ca. 0.02 g/mL) was prepared by placing 0.2 g titanium (IV) butoxide into 10 mL volumetric flask and diluting to the calibration line with 1-butanol. The titanium solution was then transferred to a sealed container and purged with nitrogen for 10 min. Trifluoroacetic acid-d (TFA-*d*, 99.5 atom % D) was obtained from Sigma Aldrich. Chloroform-*d* ($CDCl_3$, 99.8% atom D +0.05% V/V TMS) was obtained from Cambridge Isotope Laboratories, Inc.

2.4.2 Characterization Methods

^{1}H NMR spectroscopy analysis was performed with a Varian Unity 400 MHz spectrometer collecting at least 32 scans at 23 °C. Polymer samples (ca. 50 mg) were dissolved in a binary mixture of TFA-*d*:CDCl3 (5/95). Inherent viscosity (η_{inh}) was measured following a procedure adapted from ASTM method D4603 with a Cannon Type B glass capillary viscometer and dichloroacetic acid. Thermogravimetric analysis was performed with a TA Instruments Q500 starting at 25 °C and proceeding to 600 °C with a 10 °C/min heating rate under nitrogen. Differential scanning calorimetry employed a TA Instruments Q2000 to analyze 5-8 mg samples in a Tzero^{TM} pan under nitrogen with 10 °C/min heating and cooling rates. Dynamic mechanical analysis (DMA) was performed with a TA Instruments Q800 Dynamic Mechanical Analyzer on oscillatory tension mode at 1 Hz, 15 μm amplitude and 0.01 N static force with a temperature ramp of 3 °C/min. Test samples were cut from compression molded 0.25 mm thick films as 5 mm wide strips. Tensile analysis of T-X-4,4′BB-EG and T-X-3,4′BB-EG copolyesters was performed on dogbones cut from 0.55 mm thick compression molded films with a D638-V dogbone punch, with dimensions specified in the ASTM D638 procedure. Tensile analyses were performed with an Instron 5500R on punched dogbone samples with a crosshead motion rate of 10mm/min and an

initial grip separation of 25.4 ± 2.0 mm. Tensile analysis of T-X-4,4′BB-EG and T-X-3,4′BB-EG copolyesters was performed on 2 mm thick, injection molded D638-V dogbones, with dimensions specified in the ASTM D638 procedure. An Epsilon 3442 miniature extensometer obtained tensile modulus data of injected molded dogbones with a MTS Model No. 4204 and a 1kN load cell at a crosshead motion rate of 5 mm/min that increased to 10 mm/min after 5 % strain. Dogbone specimens were injection molded by Exxon Mobil with a Boy XS injection-molding machine with a 45 F mold temperature, a 275 – 290 °C barrel temperature, a 1000 Psi holding pressure and a 60 second cycle time. Dogbones were used as received. Before injection molding, copolyester samples were ground up with a Cumberland 6508 Beside The Press Granulator equipped with a 4.76 mm screen. A Systech Illinois 8001 Oxygen Permeation Analyzer measured oxygen flux for both compression molded and biaxially stretched PET copolyesters films modified with 4,4′BB and 3,4′BB at 23 °C and 0% relative humidity with an oxygen flow of 20 mL/min and a nitrogen flow of 10 mL/min. A MOCON® OX-TRAN 2/21 (Minneapolis, MN) measured oxygen flux *J(t)* for compression molded films made from T-X-I-55-4,4′BB-EG, T-X-I-50-4,4′BB-EG, T-X-3,4′BB-55-4,4′BB-EG and T-X-3,4′BB-50-4,4′BB-EG copolyesters at 23 °C, 0% relative humidity and 1 atm pressure. Specimens were cut from the center of compressed films, placed in a test cell and conditioned until a steady baseline was reached, at which point oxygen was introduced to the test cell[43]. As the oxygen concentration reached a constant distribution, the flux reached steady state value J_0. A Mitutoyo digimatic micrometer measured test film thickness in nine discreet locations, from which the average thickness was calculated. Oxygen permeabilities $P(O_2)$ were calculated based on steady state flux J_0, average thickness l, and the permeant gas pressure drop across the specimen Δp (**Equation 2-1**).

Eq. 2-1

$$P = J_0 \frac{l}{\Delta p}$$

Amorphous, compressed films were cut into 85 cm × 85 cm squares and bialxially stretched in a Brückner Karo IV bialxial stretcher at 25 °C above the $T_{g.}$ The specimen was drawn in both directions simultaneously with an engineering strain rate of 150% s^{-1}; the draw ratio was 3 × 3.

2.4.3 Polymerization

Polymerization of poly(DMT-*co*-4,4′BB)-EG (12-30 g scale). All copolyesters were synthesized in a similar manner. Reactions were performed in a dry round bottom flask equipped with distillation arm, nitrogen inlet and an overhead stirrer. To synthesize the composition T-60-4,4′BB-EG, EG (12.40 g, 0.20 mol), DMT (11.65 g, 0.06 mol) and 4,4′BB (10.65 g, 0.04 mol) were charged into a 100 mL round bottom flask along with the titanium butoxide catalyst solution (40 ppm Ti by mass to the theoretical yield of polymer). Oxygen and moisture were removed from the flask by applying vacuum and purging with nitrogen three times. For the transesterification step, the stirring rate was set to 200 rpm and the flask was submerged into a 180 °C metal bath for 1 h, the temperature was then increased to 200 °C for 1 h, then 220 °C for 2 h and finally increased to 280 °C over 20 min. Once a temperature of 280 °C was reached, vacuum was applied and the polycondensation step was then carried out with a 30–40 rpm stirring rate under reduced pressure (≤ 0.3 mmHg) for 1 h. The flask was then removed from the metal bath and allowed to cool to room temperature. All polyesters were isolated by first breaking the flask and then removing the polyester from the stir rod with a hammer, chisel and end nippers. Isolated polymers were rinsed with DI water and dried overnight in a vacuum oven at 10–20 °C above the glass transition of the polymer.

Polymerization of poly(DMT-*co*-3,4′BB)-EG (20–30 g scale). All compositions were synthesized with the same procedure, conditions and molar ratios as above except for the following conditions: transesterification at 175 °C for 1 h, 200 °C for 1 h, 220 °C for 2 h.

Polymerization of poly(DMT-*co*-4,4′BB-*co*-DMI)-EG (75 g scale). All compositions were synthesized with the same procedure as above. To synthesize the composition T-20-I-55-4,4′BB-EG, EG (37.11 g, 0.60 mol), DMT (14.52 g, 0.07 mol), DMI (11.62 g, 0.06 mol) and 4,4′BB (44.46 g, 0.16 mol) were charged into a 250 mL round bottom flask along with catalyst solution (40 ppm Ti by mass to the theoretical yield). Transesterification was carried out at 180 °C for 1 h, 210 °C for 1 h, 220 °C for 2 h, 280 °C for 1 h. Once the transesterification step had completed, vacuum was applied and the polycondensation step was then carried out with a 30-40 rpm stirring rate under reduced pressure (≤ 0.3 mmHg) for 1 h**.**

Polymerization of poly(DMT-*co*-4,4′BB-*co*-3,4′BB)-EG. All compositions were synthesized with the same procedure, molar ratios and conditions as followed for poly(DMT-*co*-4,4′BB-*co*-DMI)-EG compositions.

2.4.4 Compression Molding Copolyesters

Polymers pieces and or particles were melt pressed into films with a PHI Q-230H hydraulic press heated to 280 °C. Samples (4–5 g) were sandwiched between two aluminum plates, each with a layer of Kapton® film coated with Rexco Partall® Powder Glossy Liquid mold release agent to prevent adhesion. Aluminum shims inserted between the aluminum plates controlled thickness. To press 0.25 mm films, the polyester particles were placed inside the press on top of a Kapton® layered aluminum plate until the sample started to melt (1–3 min), at which point a shim and the second layer of Kapton® and aluminum were added. The plates were then moved to the

center of the press, which was lightly closed until complete melting of the sample (ca. 2 min). Three press-release cycles (30 seconds each) were completed at 5 tons of force, followed by pressing once at 10 tons of force. After pressing, samples were immediately transferred to a ice water bath to quench the samples. Films were subsequently removed from the Kapton® and dried in a 40 °C vacuum oven overnight. T-X-I-55-4,4′BB-EG, T-X-I-50-4,4′BB-EG, T-X-3,4′BB-55-4,4′BB-EG and T-X-3,4′BB-50-4,4′BB-EG copolyesters were compression molded with a 0.3 mm shim for permeability studies and DMA, and a 0.6 mm shim for tensile.

2.5 Results and Discussion

2.5.1 Synthesis and Structural Characterization.

T-X-4,4′BB-EG and T-X-3,4′BB-EG Copolyesters. A range of copolyesters were originally synthesized based on PET with either 4,4′BB or 3,4′BB comonomers incorporated into the backbone along with EG (**Scheme 2-1**). The copolyesters in **Scheme 2-1** follow the naming

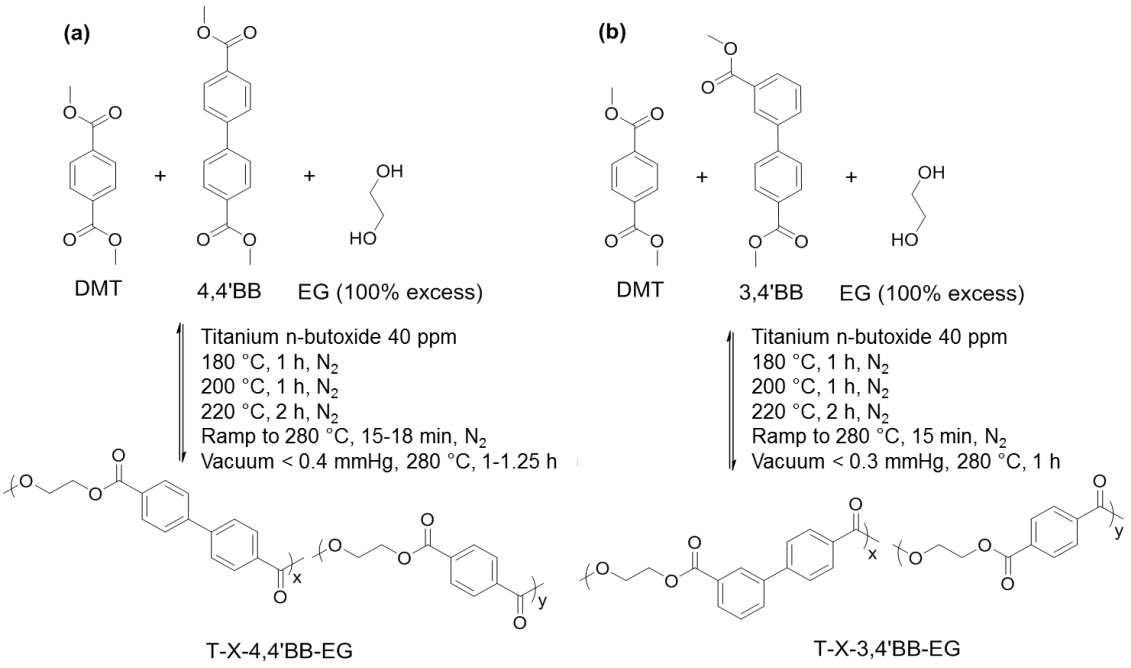

Scheme 2-1. Polymerization of T-X-4,4′BB-EG and T-X-3,4′BB-EG copolyesters

convention: T-X-4,4′BB-EG and T-X-3,4′BB-EG, where X represents how much DMT (T) has been substituted with either 4,4′BB or 3,3’BB. The concentration of titanium alkoxide catalyst

chosen for this system of (co)polyesters was 40 ppm by mass of the theoretical yield to minimize the formation for DEG, while still achieving relatively high molecular weights **(Supplemental 2-1).** ^{1}H NMR spectroscopy confirmed (co)polyester incorporation of DMT and 4,4′BB through unique proton shifts of each diester (**Supplemental 2-2)**. In the example shown in **Figure 2-3**, protons from terephthalate (A) and 4,4′BB (B) overlap, however, two pairs of protons (C) are separate from the other two 4,4′BB protons. As such, the equation shown in **Figure 2-3** can be

used to calculate the relative concentrations of each comonomer. Studies using quantitative ^{13}C NMR spectroscopy showed complete randomization of the DMT and 4,4′BB monomers during melt polymerization **(Supplemental 2-3). T-X-I-55-4,4′BB-EG, T-X-I-50-4,4′BB-EG, T-X-**

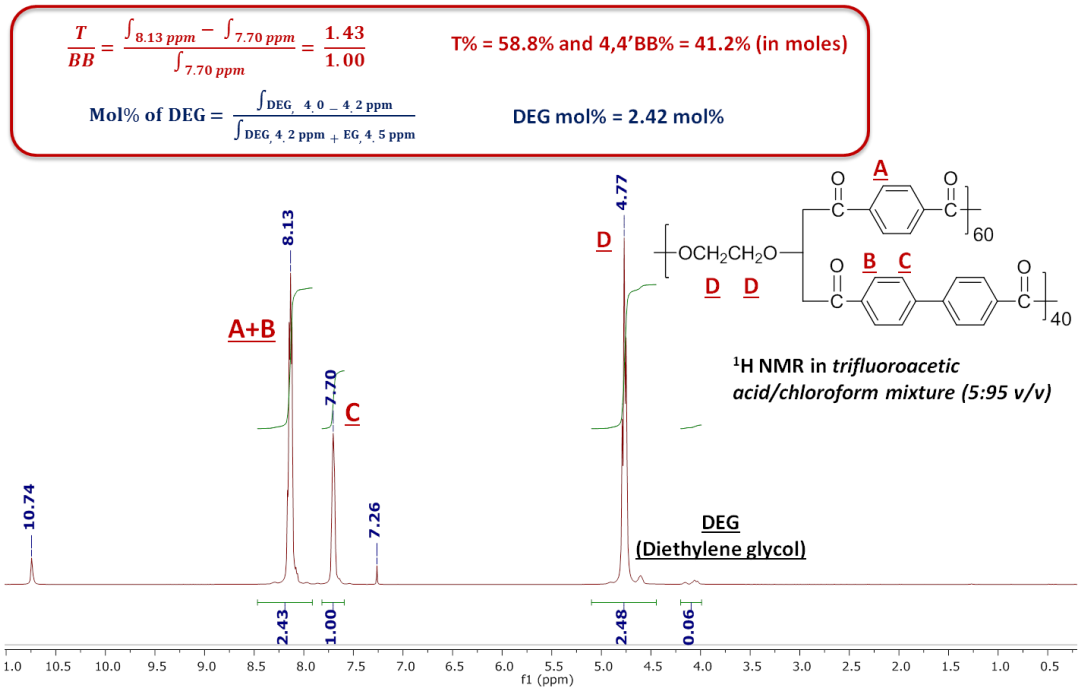

Figure 2-3. ^{1}H NMR of T-40-4,4′BB-EG copolyester. Relative diacid incorporation ratios were calculated with peak A+B and C

3,4′BB-55-4,4′BB-EG and T-X-3,4′BB-50-4,4′BB-EG Copolyesters. Rapid crystallization induced by 4,4′BB made it impossible to quench clear films from T-X-4,4′BB-EG compositions with more than 50–55 mol% 4,4′BB. The high crystallinity in T-55-4,4′BB-EG and T-50-4,4′BB-EG compositions still proved problematic for biaxial orientation due to tearing around small, hazy crystalline regions in the quenched films. Copolyester compositions with high 4,4′BB content (T-55-4,4′BB-EG and T-50-4,4′BB-EG) modified with 3,4′BB and DMI to improve processing while maximizing 4,4′BB content were next studied. A range of compositions were synthesized to further investigate the influence of rigidity, symmetry and monomer length on the thermal, gas barrier and mechanical properties of (co)polyesters (**Scheme 2-2**). The copolyesters in **Scheme 2-2** follow the naming convention T-X-I-55-4,4′BB-EG, T-X-I-50-4,4′BB-EG, T-X-3,4′BB-55-4,4′BB-EG and T-X-3,4′BB-50-4,4′BB-EG where X represents how much DMT has been substituted with either 3,4′BB or DMI (T). ^{1}H NMR analysis confirmed (co)polyester incorporation of DMT, DMI, 3,4′BB and 4,4′BB by using unique proton shifts of each diester. Integrations and calculations were done in a manner similar to the example shown in **Figure 2-3**. All compositions were synthesized within 2 mol% of their targeted molar ratios (**Table 2-2**), indicating that good diester balance was maintained during the polymerization process, and DEG content was kept below 3 mol%. Due to the low solubility of the copolyesters in most common solvents, size exclusion chromatography (SEC) was not possible. In lieu of SEC molecular weight determination, η_{inh} was measured with a 0.5 g/mL (co)polyester and dichloroacetic acid solution at 25 °C[19]. The relationship between the viscosity-average molecular weight (M_v) and η_{inh} has not been determined for bibenzoate containing polyesters; however, the Mark–Houwink–Sakurada parameters for PET in dichloroacetic acid were used in **Equation 2-2** to estimate the M_v. By using this equation, the estimated M_v for synthesized copolyesters with η_{inh} values of 0.8–1.0 is 26,600–34,800 g/mol.

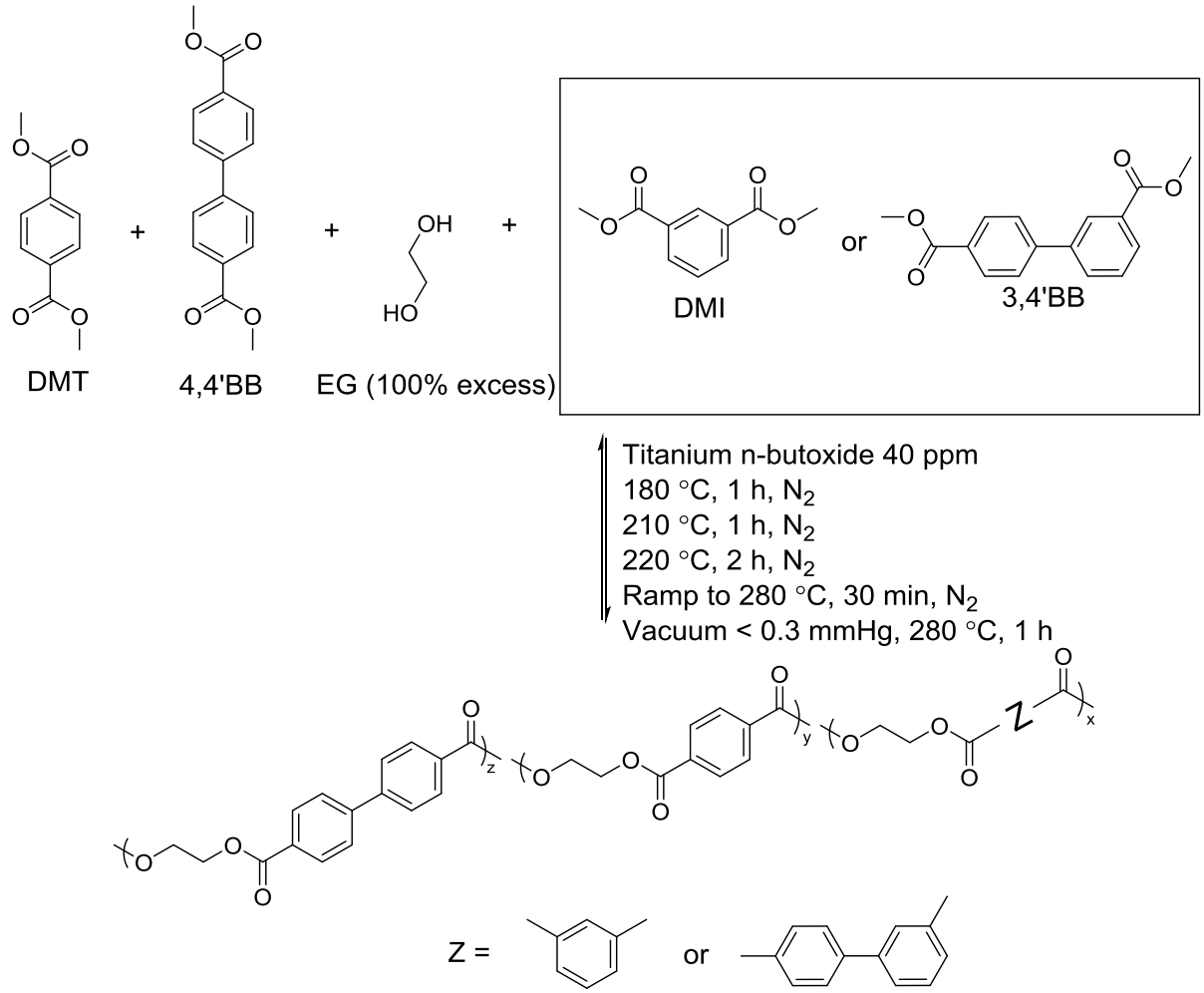

Scheme 2-2. Polymerization of T-X-I-55-4,4′BB-EG, T-X-I-50-4,4′BB-EG, T-X-3,4′BB-55-4,4′BB-EG and T-X-3,4′BB-50-4,4′BB-EG copolyesters where terephthalate has been replaced with 2.5-30 mol% of isophthalate or 3,4′BB

Table 2-2. Compositional and thermal analysis of synthesized T-X-I-55-4,4′BB-EG, T-X-I-50-4,4′BB-EG, T-X-3,4′BB-55-4,4′BB-EG and T-X-3,4′BB-50-4,4′BB-EG copolyesters. η_{inh} measured with 0.5 g/mL (co)polyester and dichloroacetic acid solution at 25 °C.

Composition (From ^{1}H NMR)						
mol% 4,4'BB	mol% I	mol% 3,4'BB	DEG mol%	Tg (°C)	Tm (°C)	η_{inh} (dL/g)
51	0	0	2.5	104	248	0.8
55	0	0	2.8	105	262	0.81
51	0	5	2.4	105	232	0.82
51	0	10	2.1	107	227	0.96
50	0	21	2.1	111	215	1.16
51	0	30	3.1	109	217	7.4
56	0	6	2.5	110	243	1.1
55	0	11	2.4	111	238	0.86
56	0	20	2.5	113	230	0.78
55	0	30	5.8	110	216	1.03
51	5	0	2.4	103	230	0.96
51	10	0	2.4	102	225	0.97
51	19	0	2.3	99	214	1.16
53	27	0	2.5	95	220	0.86
55	5	0	-	104	244	0.8
56	9	0	2.7	102	241	0.94
56	19	0	2.6	100	231	1.18
58	27	0	4.9	95	222	1.33

Eq. 2-2 $$[\eta_{inh}] = 1.7 \times 10^{-4}(M_v)^{0.83}$$

2.5.2 Thermal Properties

T-X-4,4′BB-EG and T-X-3,4′BB-EG copolyesters. TGA analysis of copolyesters showed a single-step weight loss beginning between 360–400 °C. Increasing level of 3,4′BB substituted for terephthalate resulted in slightly higher degradation temperatures, however, the same was not observed for 4,4′BB (**Supplemental 2-4**). **Table 2-3** lists the transition temperatures as obtained by DSC for all T-X-4, 4'BB-EG and T-X-3, 4'BB-EG copolyesters. **Figure 2-4** and

Table 2-3. Compositional and thermal analysis of synthesized T-X-4,4′BB-EG and T-X-3,4′BB-EG copolyesters.

Feed	**Composition (^{1}H NMR)**	**mol% DEG (^{1}H NMR)**	T_g (°C)	T_m (°C)
PET (Lab)		2.1	81	252
T-5-4,4′BB-EG	T-5-4,4′BB-EG	2.5	83	238
T-10-4,4′BB-EG	T-10-4,4′BB-EG	2.0	85	226
T-15-4,4′BB-EG	T-15-4,4′BB-EG	2.6	86	225
T-20-4,4′BB-EG	T-21-4,4′BB-EG	2.0	89	n.d.
T-35-4,4′BB-EG	T-35-4,4′BB-EG	2.4	98	n.d.
T-40-4,4′BB-EG	T-41-4,4′BB-EG	2.2	100	216
T-45-4,4′BB-EG	T-46-4,4′BB-EG	2.7	102	220
T-50-4,4′BB-EG	T-51-4,4′BB-EG	2.5	104	248
T-55-4,4′BB-EG	T-57-4,4′BB-EG	2.8	105	262
T-60-4,4′BB-EG	T-61-4,4′BB-EG	2.7	107	273
T-75-4,4′BB-EG	T-76-4,4′BB-EG	4.4	119	295
T-90-4,4′BB-EG	T-90-4,4′BB-EG	5.3	124	317
T-5-3,4′BB-EG	T-5-3,4′BB-EG	2.6	82	238
T-10-3,4′BB-EG	T-10-3,4′BB-EG	2.0	84	225
T-20-3,4′BB-EG	T-20-3,4′BB-EG	2.7	85	n.d.
T-40-3,4′BB-EG	T-41-3,4′BB-EG	3.1	89	n.d.
T-60-3,4′BB-EG	T-59-3,4′BB-EG	3.0	95	n.d.
T-80-3,4′BB-EG	T-80-3,4′BB-EG	2.2	99	n.d.
100-3,4′BB-EG		2.9	104	n.d.

Figure 2-5 illustrate how substituting DMT with either 3,4′BB or 4,4′BB impacts the T_g and T_m. Substitution of terephthalate with 4,4′BB did not go above 90 mol% due to high melting temperatures, which made it difficult to produce high molecular weight polymers without significant degradation. Meurisse et al.[20] reported a liquid crystalline homopolyester for 4,4′BB-EG with a high T_m of 314 °C and an isotropic phase transition at 350 °C. Initial incorporation of

4,4′BB into PET resulted in a decreased melting temperature up until 20 mol%, where the copolyester becomes amorphous. Once the composition reaches 45 mol% 4,4′BB,it begins to once again exhibit crystallinity. At 55 mol% 4,4′BB, the T_m was similar to PET, but with a faster crystallization and a higher T_g. Incorporation of 3,4′BB has a much more significant impact on crystallinity, with no observed melting after 10 mol% 3,4′BB.

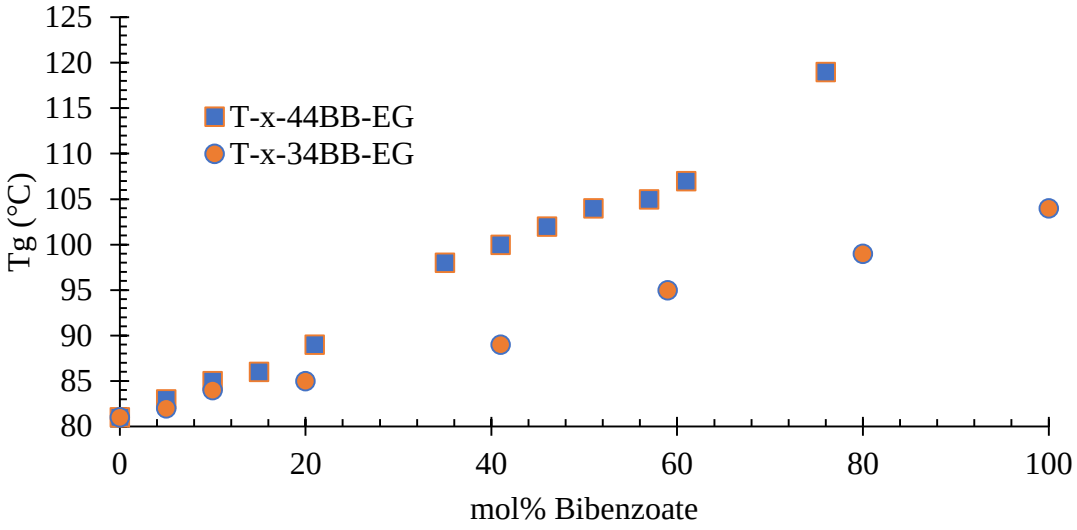

Figure 2-4. Plot of Tg vs mol% of T-X-4,4′BB-EG and T-X-3,4′BB-EG copolyesters

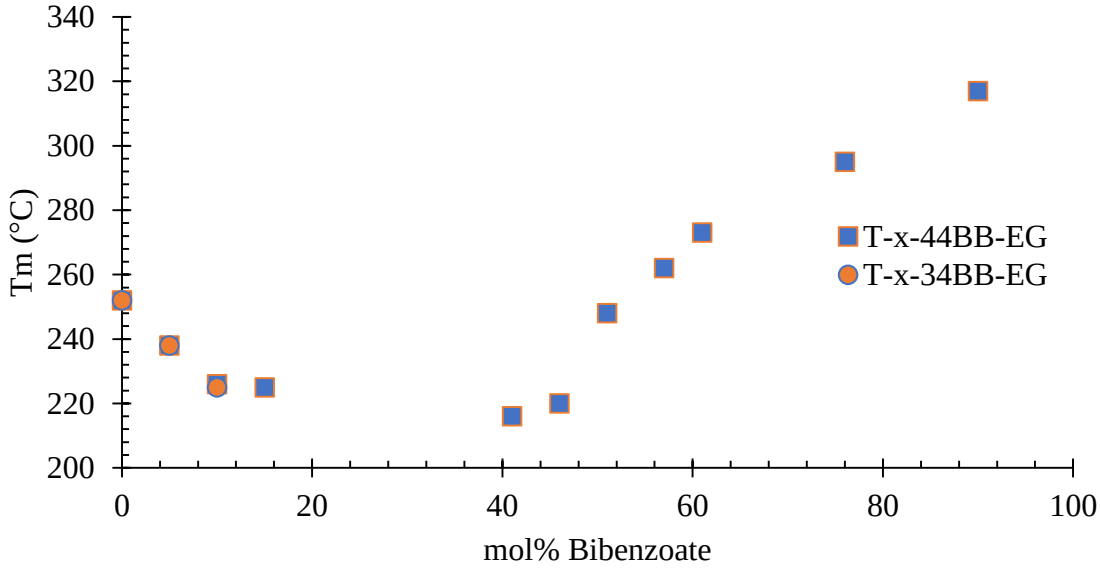

Figure 2-5. Plot of Tm vs mol% of T-X-4,4′BB-EG and T-X-3,4′BB-EG copolyesters

T-X-I-55-4,4′BB-EG, T-X-I-50-4,4′BB-EG, T-X-3,4′BB-55-4,4′BB-EG and T-X-3,4′BB-50-4,4′BB-EG copolyesters. Table 2-2 lists the transition temperatures as obtained by DSC for all T-X-I-55-4,4′BB-EG, T-X-I-50-4,4′BB-EG, T-X-3,4′BB-55-4,4′BB-EG and T-X-3,4′BB-50-4,4′BB-EG copolyesters. The effect each biphenyl monomer has on the thermal properties of each copolyester can be seen in **Figure 2-6** and **Figure 2-7**, which depict how the T_g and T_m are affected when DMI or 3,4′BB replaces DMT in the feed with substitution up to 30 mol%.

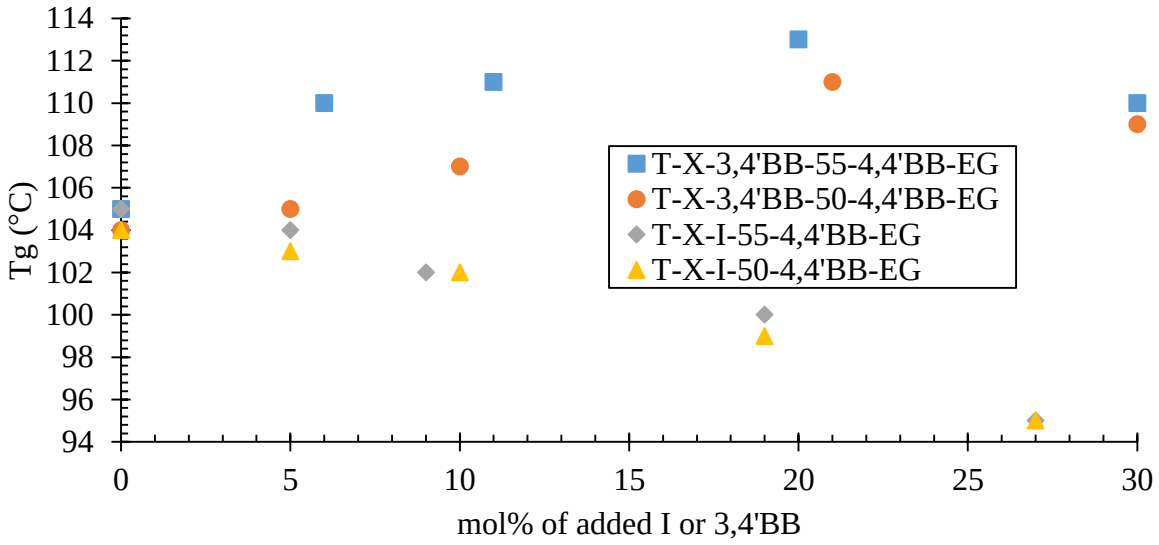

Figure 2-6. Plot of Tg vs mol% of T-X-I-55-4,4′BB-EG, T-X-I-50-4,4′BB-EG, T-X-3,4′BB-55-4,4′BB-EG and T-X-3,4′BB-50-4,4′BB-EG copolyesters.

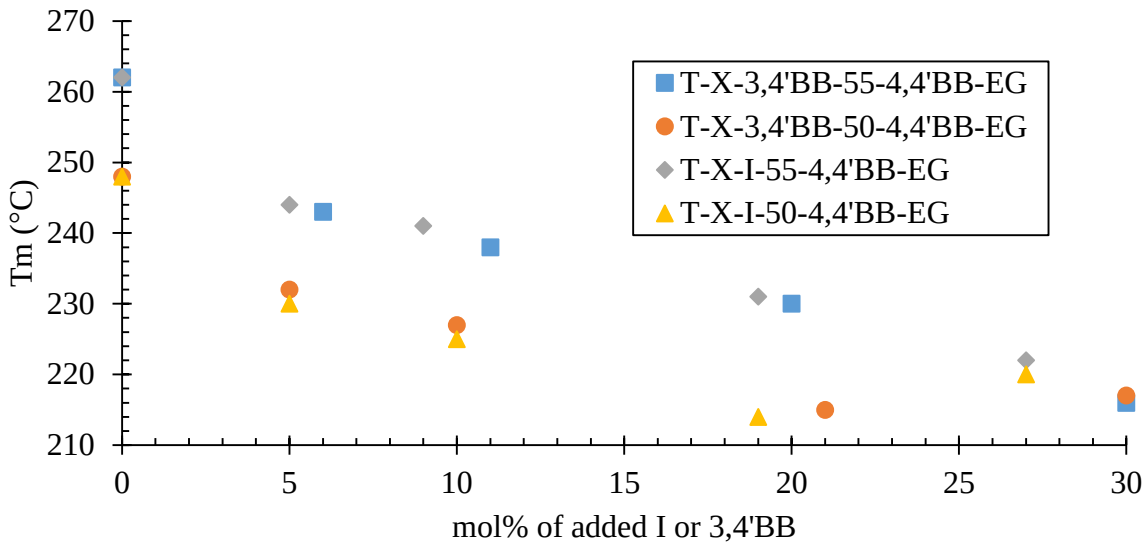

Figure 2-7. Plot of Tm vs mol% of T-X-I-55-4,4′BB-EG, T-X-I-50-4,4′BB-EG, T-X-3,4′BB-55-4,4′BB-EG and T-X-3,4′BB-50-4,4′BB-EG copolyesters.

DMA measurements were obtained on copolyester films between -150 °C and 300 °C. Low temperatures were used to study sub-T_g transitions (**Figure 2-8**). The rapid increase in modulus after the T_g is indicative of cold crystallization, which shifts to a higher temperature with increasing

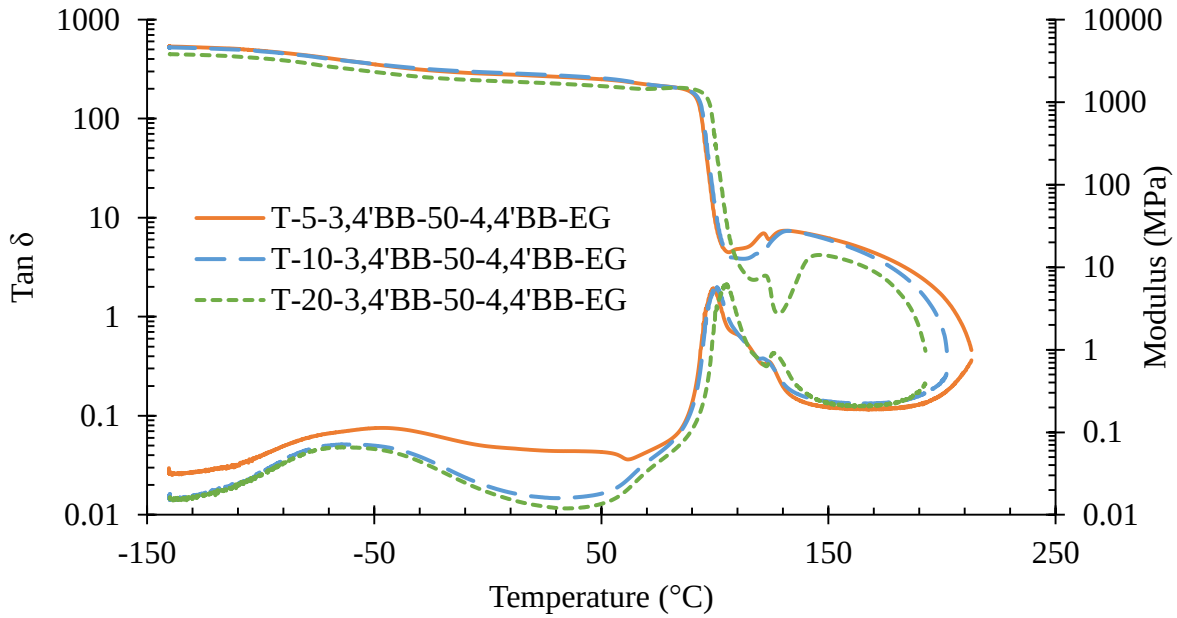

Figure 2-8. Dynamic mechanical analysis of T-X-3,4′BB-50-4,4′BB-EG copolyesters at 1 Hz and a temperature ramp of 3 °C/min.

3,4′BB content, thus demonstrating the ability of 3,4′BB to slow crystallization. The decrease in peak intensity around -65 °C, which is indicative of aromatic ring flips[5, 8, 10, 44], coincides with increasing 3,4′BB content, and indicates inhibited ring rotation caused by the meta linkage in 3,4′BB.

2.5.3 Mechanical Properties

T-X-4,4′BB-EG and T-X-3,4′BB-EG copolyesters. Measured crosshead displacement was used to estimate the Young's modulus of injection molded T-X-4,4′BB-EG and T-X-3,4′BB-EG copolyesters; however, slippage may result in a higher measured strain and lower modulus. An extensometer was used in the initial part of the test to more accurately measure strain and determine tensile modulus in accordance with ASTM D638. **Table 2-4** reports calculated values for yield stress, strain at break and modulus. Semicrystalline samples containing higher

Table 2-4. Mechanical properties of injection molded T-X-4,4′BB-EG and T-X-3,4′BB-EG copolyester dogbones.

*Semicrystalline compositions

Copolyester Composition	Yield stress (MPa)	Stress at break (MPa)	Strain at break (%)	Modulus Without Extensometer (MPa)	Modulus With Extensometer (MPa)
T-10-4,4′ BB-EG*	55.0 ± 0.3	54 ± 4	290 ± 20	1610 ± 20	2130 ± 50
T-35-4,4′ BB-EG	52.9 ± 0.3	n/a	90 ± 10	1580 ± 70	2100 ± 50
T-40-4,4′ BB-EG*	n/a	n/a	n.d.	2660 ± 50	4800
T-55-4,4′ BB-EG*	n/a	n/a	n.d.	3580 ± 350	7500
T-10-3,4′ BB-EG*	59.5 ± 0.5	56 ± 2	330 ± 20	1660 ± 30	2200 ± 100
T-40-3,4′ BB-EG	65.0 ± 0.9	51 ± 6	260 ± 40	1760 ± 70	2400 ± 100
3,4′BB-EG	74.4 ± 0.3	n/a	160 ± 40	n/a	2700 ± 300
PET Lab*	56 ± 3	52.7 ± 0.4	316 ± 4	1580 ± 40	2200 ± 200

concentrations of 4,4′BB (T-40-4,4′BB-EG and T-55-4,4′BB-EG) reported much higher moduli than completely amorphous compositions (T-35-4,4′ BB-EG and T-40-3,4′ BB-EG) and quickly broke in sections of the bar that were crystalline, indicated by a more opaque appearance. In examples where there is little or no crystallinity contributed by 4,4′BB (T-35-4,4′ BB-EG vs T-40-3,4′ BB-EG and T-10-4,4′ BB-EG and T-10-3,4′ BB-EG), 3,4′BB modified copolyesters exhibit higher moduli, indicating that 3,4′BB can enhance the modulus of amorphous polyesters. Overall, PET copolyesters modified with either 3,4′BB and 4,4′BB maintained high moduli and strength.

T-X-I-55-4,4′BB-EG, T-X-I-50-4,4′BB-EG, T-X-3,4′BB-55-4,4′BB-EG and T-X-3,4′BB-50-4,4′BB-EG copolyesters. **Table 2-5** shows tensile properties of select T-X-I-55-4,4′BB-EG, T-X-I-50-4,4′BB-EG, T-X-3,4′BB-55-4,4′BB-EG and T-X-3,4′BB-50-4,4′BB-EG copolyesters. Both 3,4′BB and isophthalate moieties have a similar effect on the tensile properties in the narrow composition window tested (5–30 % substituted for terephthalate). Increasing yield stress correlates with increasing content of both 3,4′BB and isophthalate, each affecting properties with a similar response. The modulus increases between 5 to 20 mol% incorporated isophthalate or

Table 2-5. Tensile properties of select T-X-I-55-4,4′BB-EG, T-X-I-50-4,4′BB-EG, T-X-3,4′BB-55-4,4′BB-EG and T-X-3,4′BB-50-4,4′BB-EG copolyesters. Tensile analysis followed ASTM testing method D638. Dogbones where punched from 0.55 mm compression molded films using a D638-V punch.

Composition	Yield Stress (MPa)	Break Stress (MPa)	Strain at Break (%)	Young's Modulus (MPa)
T-5-3,4′BB-51-4,4′BB-EG	44.5 ± 0.2	58 ± 6	220 ± 30	1900 ± 100
T-21-3,4′BB-50-4,4′BB-EG	47.5 ± 0.3	65 ± 7	240 ± 30	2000 ± 70
T-6-3,4′BB-56-4,4′BB-EG	48 ± 1	61 ± 6	200 ± 20	1840 ± 80
T-20-3,4′BB-56-4,4′BB-EG	50.5 ± 0.8	62 ± 6	220 ± 30	2090 ± 50
T-30-3,4′BB-55-4,4′BB-EG	50.0 ± 0.4	59 ± 3	210 ± 20	1960 ± 20
T-2-I-52-4,4′BB-EG	47.2 ± 0.8	62 ± 6	230 ± 30	1950 ± 60
T-19-I-51-4,4′BB-EG	52.3 ± 0.7	61 ± 7	230 ± 40	2170 ± 50
T-6-I-56-4,4′BB-EG	47 ± 2	58 ± 4	220 ± 30	1990 ± 70
T-19-I-56-4,4′BB-EG	51 ± 1	66 ± 4	270 ± 20	2030 ± 50
T-27-I-58-4,4′BB-EG	52.7 ± 0.3	57 ± 6	210 ± 40	2010 ± 30

3,4′BB monomer, and then decreases when going from 20 to 30 mol%. Once again, this effect appears to be relatively the same for both monomers. This tensile data contrasts with previous studies on terephthalate/ isophthalate copolyesters, wherein PET initially shows a rapid decrease in modulus and yield stress with added isophthalate up to 20–30 mol% followed by a slight increase.[15] As such, further study of mechanical properties past 30 mol% incorporation of 3,4′BB is needed in the future to probe the effect of kinked monomers on mechanical properties. The values in **Table 2-5** were obtained from completely amorphous samples. When compared to unmodified 4,4′BB compositions with higher crystallinity, modulus values were lower. These compositions, however, display higher/comparable modulus values to semicrystalline PET samples.

2.5.4 Oxygen Permeability

T-X-I-55-4,4′BB-EG, T-X-I-50-4,4′BB-EG, T-X-3,4′BB-55-4,4′BB-EG and T-X-3,4′BB-50-4,4′BB-EG copolyesters. Table 2-6 shows that the oxygen permeability values for unoriented, compression molded films are similar to the literature values[8]. Adding kinked 3,4′BB monomers to PET results in a slight decrease in permeability relative to commercial PET #418, whereas incorporation of the linear 4,4′BB monomer results in a slight increase in permeability. Only PET #418, lab synthesized PET, T-10-3,4′BB-EG, T-10-4,4′BB-EG and PEN were successfully

Table 2-6. Permeability levels of unoriented films containing 4,4′BB and 3,4′BB

Polymer	Permeability ($cc.cm/m^2/atm/day$)	Literature[8] ($cc.cm/m^2/atm/day$)	Permeability relative to PET #418
PET #418	0.500 ± 0.010	n.a.	1.00
Lab synthesized PET	0.461 ± 0.001	0.469 ± 0.002	0.920
T-10-4,4′BB-EG	0.515 ± 0.004	0.512 ± 0.004	1.03
T-10-3,4′BB-EG	0.467 ± 0.009	0.449 ± 0.008	0.932
3,4′BB-EG	0.350 ± 0.030	0.390 ± 0.004	0.691
PEN	0.155 ± 0.005	0.157 ± 0.001	0.309

biaxially oriented **(Table 2-7)**. All polymers containing bibenzoate moieties exhibit a decrease in permeability upon biaxial orientation, with PEN having a much lower permeability than either PET or T-10-3,4′BB-EG. Also, while T-10-4,4′BB-EG initially has a much higher permeability than T-10-3,4′BB-EG before orientation, T-10-4,4′BB-EG has a sharper decrease in permeability after orientation. Previous work examining the effect of uniaxial orientation on films made from PET modified with 4,4′BB and isophthalate also observed a decrease in permeability with higher degrees of biaxial orientation[30]. It was proposed in this work that orientation produces a decrease in excess-hole free volume and strains glycol linkages into more trans conformations. The hypothesis that lower permeability upon orientation depends on a polymer chain's ability to extend and tightly pack amorphous chains into dense formations (thereby decreasing gas solubility) would explain how4,4′BB copolyester, with more easily oriented para linkages, experience a more significant drop in permeability than 3,4′BB copolyester, which has a kinked meta linkage that disrupts packing.

Table 2-7. Permeability levels of biaxially oriented films containing 4,4′BB and 3,4′BB

Polymer	Permeability (cc·cm/m2/atm/day)	Permeability Relative to PET #418	Biax Permeability Relative to Biax PET #418
PET #418	0.500 ± 0.010	0.651	1.00
PET #418 (Biax)	0.330 ± 0.020		
T-10-3,4′BB-EG	0.467 ± 0.009	0.630	0.902
T-10-3,4′BB-EG (Biax)	0.290 ± 0.030		
T-10-4,4′BB-EG	0.515 ± 0.004	0.600	0.948
T-10-4,4′BB-EG (Biax)	0.309		
PEN	0.155 ± 0.005	0.323	0.153
PEN (Biax)	0.050 ± 0.001		

T-X-I-55-4,4′BB-EG, T-X-I-50-4,4′BB-EG, T-X-3,4′BB-55-4,4′BB-EG and T-X-3,4′BB-50-4,4′BB-EG copolyesters. To thoroughly study how 4,4′BB behaves when oriented, T-50-4,4′BB-EG and T-55-4,4′BB-EG compositions were modified with isophthalate and 3,4′BB to slow crystallization for biaxial orientation. **Table 2-8** shows the permeability of amorphous

Table 2-8. Permeability of amorphous quenched films made from T-X-I-55-4,4′BB-EG, T-X-I-50-4,4′BB-EG, T-X-3,4′BB-55-4,4′BB-EG and T-X-3,4′BB-50-4,4′BB-EG copolyesters

Composition	Permeability ($cc \cdot cm \cdot m^{-2} \cdot day^{-1} \cdot atm^{-1}$)	Permeability Relative to PET
PET 9921	0.395	1.000
T-2.5-3,4′BB-50-4,4′-EG	0.545	1.379
T-5-3,4′BB-50-4,4′-EG	0.541	1.369
T-7.5-3,4′BB-50-4,4′-EG	0.458	1.159
T-10-3,4′BB-50-4,4′-EG	0.461	1.165
T-2.5-I-50-4,4′-EG	0.670	1.695
T-5-I-50-4,4′-EG	0.549	1.388
T-10-I-50-4,4′-EG	0.490	1.240
T-7.5-3,4′BB-55-4,4′-EG	0.488	1.234
T-7.5-3,4′BB-55-4,4′-EG	0.515	1.303
T-10-3,4′BB-55-4,4′-EG	0.556	1.405
T-20-3,4′BB-55-4,4′-EG	0.515	1.302
T-7.5-I-55-4,4′-EG	0.488	1.236
T-10-I-55-4,4′-EG	0.488	1.236
T-15-I-55-4,4′-EG	0.440	1.112
T-20-I-55-4,4′-EG	0.396	1.002

quenched films produced by adding either 3,4′BB or isophthalate to disrupt crystallinity. Increasing 3,4′BB and isophthalate content was shown to decrease the permeability of unoriented quenched films, consistent with what past observations wherein PET was modified with 3,4′BB and isophthalate[8]. Recent research has indicated that the lowered permeability of non-oriented isophthalate and 3,4’BB copolyesters could stem from their nonlinear axis of rotation hindering ring flipping motions, producing lower diffusivity[44]. Any ring flipping would have to overcome a high energy barrier and would likely involve cooperative movement of nearby units[45]. Indeed,

DMA analysis (**Figure 2-8**) of tan δ peaks in the region commonly associated with ring flips shows a decrease β relaxation intensity with increasing 3,4′BB content. This decrease in the β relaxation has been observed in polymers containing isophthalate and furanoate[5, 8-10]. Future studies will focus on the effect biaxial orientation has on these films.

2.6 Conclusions

Melt polycondensation produced copolyesters of PET modified with 3,4′BB or 4,4′BB. These novel, melt processable copolyesters possessed enhanced T_gs relative to PET, while maintaining low enough T_ms that afford easy melt processing. Thermal analysis revealed thermal stabilities above 350 °C, T_gs in the range of 95–113 °C and T_ms in the range of 213–262 °C. DMA demonstrated a decrease in the β-relaxation peak intensity at −65 °C with increased isophthalate and 3,4′BB content, which may indicate a reduction in phenyl ring flipping from hindered monomer geometry. Tensile analysis demonstrated an increase in modulus, yield stress and elongation to break with increasing incorporation of isophthalate and 3,4′BB units into T-55-4,4′BB-EG or T-50-4,4′BB-EG. Permeability analysis of PET containing 10 mol% 3,4′BB or 4,4′BB showed that while 3,4′BB may decrease permeability in unoriented films, 4,4′BB incorporation produced a greater decrease upon orientation. To test the ability of 4,4′BB to decrease permeability at much higher concentrations, 3,4′BB and isophthalate were added to T-55-4,4′BB-EG or T-50-4,4′BB-EG copolyesters to make films easier to orient biaxially. Preliminary permeability analysis of unoriented amorphous quenched films shows a decrease in permeability with increasing comonomer content.

2.7 Acknowledgements

This work is supported by the Department of Chemistry and the Macromolecules Innovation Institute (MII) at Virginia Tech. The authors acknowledge Charles S. Carfagna Jr. of the Macromolecular Materials Discovery Center (MMDC) at Virginia Tech for help with thermal analysis. The authors thank Professor Timothy E. Long's research group at Virginia Tech for help with thermal and mechanical analysis and Professor Eric Baer's group at Case Western Reserve University for help with biaxial orientation.

2.8 References

1. Gallucci, R. R.; Patel, B. R., Poly(butylene terephthalate). In *Modern Polyesters: Chemistry and Technology of Polyesters and Copolyesters*, Scheirs, J.; Long, T., Eds. John Wiley & Sons: West Sussex, England, 2003; pp 293–321.

2. Callander, D. D., Properties and applications of poly(ethylene 2,6-naphthalate), its copolyesters and blends. In *Modern Polyesters: Chemistry and Technology of Polyesters and Copolyesters*, Schiers, J.; Long, T., Eds. John Wiley & Sons: West Sussex, England, 2003; pp 323–333.

3. Schiraldi, D. A., New poly(ethylene terephthalate) copolymers. In *Modern Polyesters: Chemistry and Technology of Polyesters and Copolyesters*, Scheirs, J.; Long, T., Eds. John Wiley & Sons: West Sussex, England, 2003; pp 245–262.

4. Turner, S. R.; Seymour, R. W.; Dombroski, J. R., Amorphous and crystalline polyesters based in 1,4-cyclohexanedimethanol. In *Modern Polyesters: Chemistry and Technology of Polyesters and Copolyesters*, Scheirs, J.; Long, T., Eds. John Wiley & Sons: West Sussex, England, 2003; pp 267–292.

5. Light, R. R.; Seymour, R. W., Effect of sub-Tg relaxations on the gas transport properties of polyesters. *Polym. Eng. Sci.* **1982,** *22* (14), 857–864.

6. Aitken, C. L.; Koros, W. J.; Paul, D. R., Effect of structural symmetry on gas transport properties of polysulfones. *Macromolecules* **1992,** *25* (13), 3424–3434.

7. Polyakova, A.; Liu, R. Y. F.; Schiraldi, D. A.; Hiltner, A.; Baer, E., Oxygen-barrier properties of copolymers based on ethylene terephthalate. *Journal of Polymer Science Part B: Polymer Physics* **2001,** *39* (16), 1889-1899.

8. Polyakova, A.; Liu, R. Y. F.; Schiraldi, D. A.; Hiltner, A.; Baer, E., Oxygen-barrier properties of copolymers based on ethylene terephthalate. *J. Polym. Sci., Part B Polym. Phys.* **2001,** *39* (16), 1889–1899.

9. Liu, R. Y. F.; Hu, Y. S.; Hibbs, M. R.; Collard, D. M.; Schiraldi, D. A.; Hiltner, A.; Baer, E., Improving oxygen barrier properties of poly(ethylene terephthalate) by incorporating isophthalate. I. Effect of orientation. *J. Appl. Polym. Sci.* **2005,** *98* (4), 1615–1628.

10. Burgess, S. K.; Leisen, J. E.; Kraftschik, B. E.; Mubarak, C. R.; Kriegel, R. M.; Koros, W. J., Chain mobility, thermal, and mechanical properties of poly(ethylene furanoate) compared to poly(ethylene terephthalate). *Macromolecules* **2014,** *47* (4), 1383–1391.

11. Vrentas, J. S.; Duda, J. L., A free-volume interpretation of the influence of the glass transition on diffusion in amorphous polymers. *J. Appl. Polym. Sci.* **1978,** *22* (8), 2325–2339.

12. Polyakova, A.; Connor, D. M.; Collard, D. M.; Schiraldi, D. A.; Hiltner, A.; Baer, E., Oxygen-barrier properties of polyethylene terephthalate modified with a small amount of aromatic comonomer. *J. Polym. Sci. Part B Polym. Phys* **2001,** *39* (16), 1900–1910.

13. Li, B.; Yu, J.; Lee, S.; Ree, M., Poly(ethylene terephthalate co ethylene isophthalate)—relationship between physical properties and chemical structures. *Eur. Polym. J.* **1999,** *35* (9), 1607–1610.

14. Schulken, R. M.; Boy, R. E.; Cox, R. H., Differential thermal analysis of linear polyesters. *J. Polym. Sci., C* **1964,** *6* (1), 17–25.

15. Karayannidis, G. P.; Sideridou, I. D.; Zamboulis, D. N.; Bikiaris, D. N.; Sakalis, A. J., Thermal behavior and tensile properties of poly(ethylene terephthalate-co-ethylene isophthalate). *J. Appl. Polym. Sci.* **2000,** *78* (1), 200–207.

16. Izard, E. F., Effect of chemical structure on physical properties of isomeric polyesters. *J. Polym. Sci.* **1952,** *9* (1), 35–39.

17. Mang, M. N.; Brewbaker, J. L. Thermoplastic polyesters containing biphenylene linkages. (The Dow Chemical Company). U.S. Patent 5,138,022, 1992.

18. Asrar, J.; Weinkauff, D. J.; Bhombal, A. H. Hydroxy ethyl bibenzoate. (Monsanto Company). U.S. Patent 5,374,707, 1994.

19. Ma, H.; Hibbs, M.; Collard, D. M.; Kumar, S.; Schiraldi, D. A., Fiber spinning, structure, and properties of poly(ethylene terephthalate-co-4,4‘-bibenzoate) copolyesters. *Macromolecules* **2002,** *35* (13), 5123–5130.

20. Meurisse, P.; Noel, C.; Monnerie, L.; Fayolle, B., Polymers with mesogenic elements and flexible spacers in the main chain: Aromatic-aliphatic polyesters. *Br. Polym. J.* **1981,** *13* (2), 55–63.

21. Gore, A. C.; Chappell, V. A.; Fenton, S. E.; Flaws, J. A.; Nadal, A.; Prins, G. S.; Toppari, J.; Zoeller, R. T., Executive summary to EDC-2: the endocrine society's second scientific statement on endocrine-disrupting chemicals. *Endocr. Rev.* **2015,** *36* (6), 593–602.

22. Nelson, A. M.; Long, T. E., A perspective on emerging polymer technologies for bisphenol-A replacement. *Polym. Int.* **2012,** *61* (10), 1485–1491.

23. Scott, C. E.; Morris, J. C.; Bradley, J. R. Clear polycarbonate and polyester blends. (Eastman Chemical Company). U.S. Patent 6,043,322, 2000.

24. Scott, C. E.; Morris, J. C.; Bradley, J. R. Clear blends of polycarbonates and polyesters. (Eastman Chemical Company). U.S. Patent 6,037,424, 2000.

25. Crawford, E. D.; Pecorini, T. J.; Mcwilliams, D. S.; Porter, D. S.; Connell, G. W.; Germroth, T. C.; Barton, B. F.; Shackelford, D. B. Polyester compositions containing cyclobutanediol having a certain combination of inherent viscosity and moderate glass transition temperature and articles made therefrom. (Eastman Chemical Company). WO 2007053549, 2007.

26. Barton, B. F.; Shackelford, D. B. Process for the preparation of copolyesters based on 2,2,4,4-tetramethyl-1,3-cyclobutanediol and 1,4-cyclohexanedimethanol. (Eastman Chemical Company). WO 2008140705, 2008.

27. Crawford, E. D.; Porter, D. S.; Connell, G. W. Polyester compositions wich comprise cyclobutanediol having certain cis/trans ratios. (Eastman Chemical Company). Eur. Pat. 2156934 2011.

28. Asrar, J., Synthesis and properties of 4,4′-biphenyldicarboxylic acid and 2,6-naphthalenedicarboxylic acid. *J. Polym. Sci., Part A: Polym. Chem.* **1999,** *37* (16), 3139–3146.

29. Hu, Y. S.; Liu, R. Y. F.; Rogunova, M.; Schiraldi, D. A.; Nazarenko, S.; Hiltner, A.; Baer, E., Oxygen-barrier properties of cold-crystallized and melt-crystallized poly(ethylene terephthalate-co-4,4′-bibenzoate). *Journal of Polymer Science Part B: Polymer Physics* **2002,** *40* (22), 2489–2503.

30. Liu, R. Y. F.; Schiraldi, D. A.; Hiltner, A.; Baer, E., Oxygen-barrier properties of cold-drawn polyesters. *J. Polym. Sci., Part B: Polym. Phys.* **2002,** *40* (9), 862–877.

31. Liu, R. Y. F.; Hu, Y. S.; Hibbs, M. R.; Collard, D. M.; Schiraldi, D. A.; Hiltner, A.; Baer, E., Comparison of statistical and blocky copolymers of ethylene terephthalate and ethylene 4,4′-bibenzoate based on thermal behavior and oxygen transport properties. *J. Polym. Sci., Part B: Polym. Phys.* **2003,** *41* (3), 289–307.

32. Hu, Y. S.; Liu, R. Y. F.; Schiraldi, D. A.; Hiltner, A.; Baer, E., Oxygen barrier properties of copolyesters containing a mesogenic monomer. *Macromolecules* **2004,** *37* (6), 2136–2143.

33. Bai, C.; Dakka, J. M.; DeCaul, L. C. Methyl-substituted biphenyl compounds, their production and their use in the manufacture of plasticizers. (Exxonmobil Chemical Patents Inc.). U.S. Patent 9,328,053, 2016.

34. Dakka, J. M.; Bai, C.; Tanke, J. J.; De Martin, G. J.; Van Nostrand, M. T.; Salciccioli, M.; Kheir, A. A.; Sangar, N. Methyl-substituted biphenyl compounds, their production and their use in the manufacture of plasticizers. (Exxonmobil Chemical Patents Inc.). U.S. Patent 20,140,275,607 2014.

35. Dakka, J. M.; DeCaul, L. C.; Tang, W. (Methylcyclohexyl)toluene isomer mixtures,their production and their use in the manufacture of plasticizers. (Exxonmobil Chemical Patents Inc.). WO 2014159100, 2014.

36. Asrar, J.; Berger, P. A.; Weinkauff, D. J., Synthesis and characterization of oligoethylene bibenzoate with hydroxyethyl end groups. *J. Appl. Polym. Sci.* **1996,** *59* (6), 1001–1008.

37. Notte, P. P. B.; Poncelet, G. M. J. L.; Remy, M. J. H.; Lardinois, P. F. M. G.; Van Hoecke, M. J. M. Catalytic process for selective alkylation of aromatic hydrocarbons. (Monsanto Company). U.S. Patent 5,233,111, 1993.

38. Periana, R. A.; Schaefer, G. F. Oxidation of tertiary-alkyl substituted aromatics. (Monsanto Company). U.S. Patent 5,068,407, 1991.

39. Sherman, S. C.; Iretskii, A. V.; White, M. G.; Gumienny, C.; Tolbert, L. M.; Schiraldi, D. A., Isomerization of substituted biphenyls by superacid. A remarkable confluence of experiment and theory. *J. Org. Chem.* **2002,** *67* (7), 2034–2041.

40. Schiraldi, D. A.; Iretski, A. V.; Sherman, S. C.; Tolbert, L. M.; White, M. G. Acid catalyzed isomerization of substituted diaryls. (Arteva North America S.A.R.L.). U.S. Patent 6,433,236, 2002.

41. Schiraldi, D. A.; Sherman, S. C.; Sood, D. S.; White, M. G. Catalytic system and method for coupling of aromatic compounds. (Arteva North America S.A.R.L.). U.S. Patent 6,103,919, 2000.

42. Mondschein, R. J.; Dennis, J. M.; Liu, H.; Ramakrishnan, R. K.; Nazarenko, S.; Turner, S. R.; Long, T. E., Synthesis and characterization of amorphous bibenzoate (co)polyesters: permeability and rheological performance. *Macromolecules* **2017,** *50* (19), 7603–7610.

43. Sekelik, D. J.; Stepanov, E. V.; Nazarenko, S.; Schiraldi, D.; Hiltner, A.; Baer, E., Oxygen barrier properties of crystallized and talc-filled poly(ethylene terephthalate). *J. Polym. Sci., Part B: Polym. Phys.* **1999,** *37* (8), 847–857.

44. Burgess, S. K.; Kriegel, R. M.; Koros, W. J., Carbon dioxide sorption and transport in amorphous poly(ethylene furanoate). *Macromolecules* **2015,** *48* (7), 2184–2193.

45. Abis, L.; Floridi, G.; Merlo, E.; Pò, R.; Zannoni, C., Investigation on the dynamics of aromatic polyesters by means of high resolution solid state CPMAS 13C NMR. *J. Polym. Sci. Part B Polym. Phys* **1998,** *36* (9), 1557–1566.

2.9 Chapter 2 Supplemental Material

2.9.1 Effect of Catalyst Concentration on T-X-4,4'BB-EG Polymerization

Previous polymerizations containing 100 ppm of titanium-based catalyst had discoloration, especially the amorphous T-20-4,4' BB-EG and T-40-4,4' BB-EG copolyesters, which showed enhanced yellowing. Here we systematically studied the effect of catalyst concentration on T-40-4,4' BB-EG copolyester. The degree of yellowing of T-40-4,4' BB-EG is proportional to the catalyst concentration (**Figure 2-9S**). Chemical composition confirmation by ^{1}H NMR suggested that the ester balance was well maintained during the polymerization process, independent of catalyst concentration. Some inconsistencies took place when the catalyst amount was only 20 ppm, the resulting polymer was relative brittle (rest of copolyesters are very tough) and the inherent viscosity measurement confirmed it was a low-molecular-weight polymer. Applying 40–100 ppm of Ti catalyst yielded tough material, the resulting inherent viscosities were all higher than literature values (0.6 dL/g)[1] and increased with the increase in catalyst concentration, summarized in **Table 2-9S**.

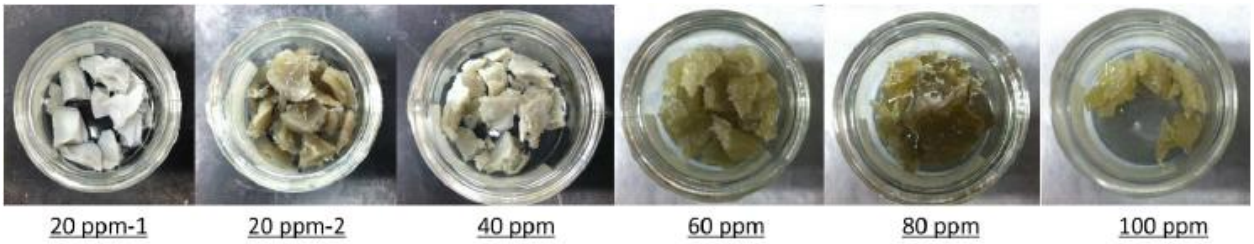

Figure 2-9S. Representations of T-40-4,4' BB-EGs synthesized under 20-100 ppm Ti catalyst concentration (Polymerizations with 20 ppm Ti catalyst were performed twice. The first sample (20 ppm-1) is relatively brittle)

Table 2-9S. Effect of $Ti(OBu)_4$ catalyst concentration on polymerization

Ti amount (ppm)	Chemical composition (T: 4,4' BB)	Inherent viscosity (dL/g)	DEG content (mol%)
20*	n.d.	0.51	n.d.
20	59.5 : 40.5	0.74	2.40
40	58.8 : 41.2	0.86	2.42
60	59.8 : 40.2	0.93	3.15
80	59.3 : 40.7	0.97	3.17
100	59.3 : 40.7	1.04	3.20

*Polymerizations with 20 ppm Ti were performed twice. The first sample was relatively brittle with lower inherent viscosity (lower molecular weight).
n.d. not determined.

The use of 40 ppm of $Ti(OBu)_4$ catalyst showed less discoloration and produced consistent polyesters with high molecular weight and low DEG incorporation (less than 3 mol%), therefore, 40 ppm of Ti catalyst will be consistently applied for the following polymerizations.

2.9.2 ^{1}H NMR Analysis of Copolyesters

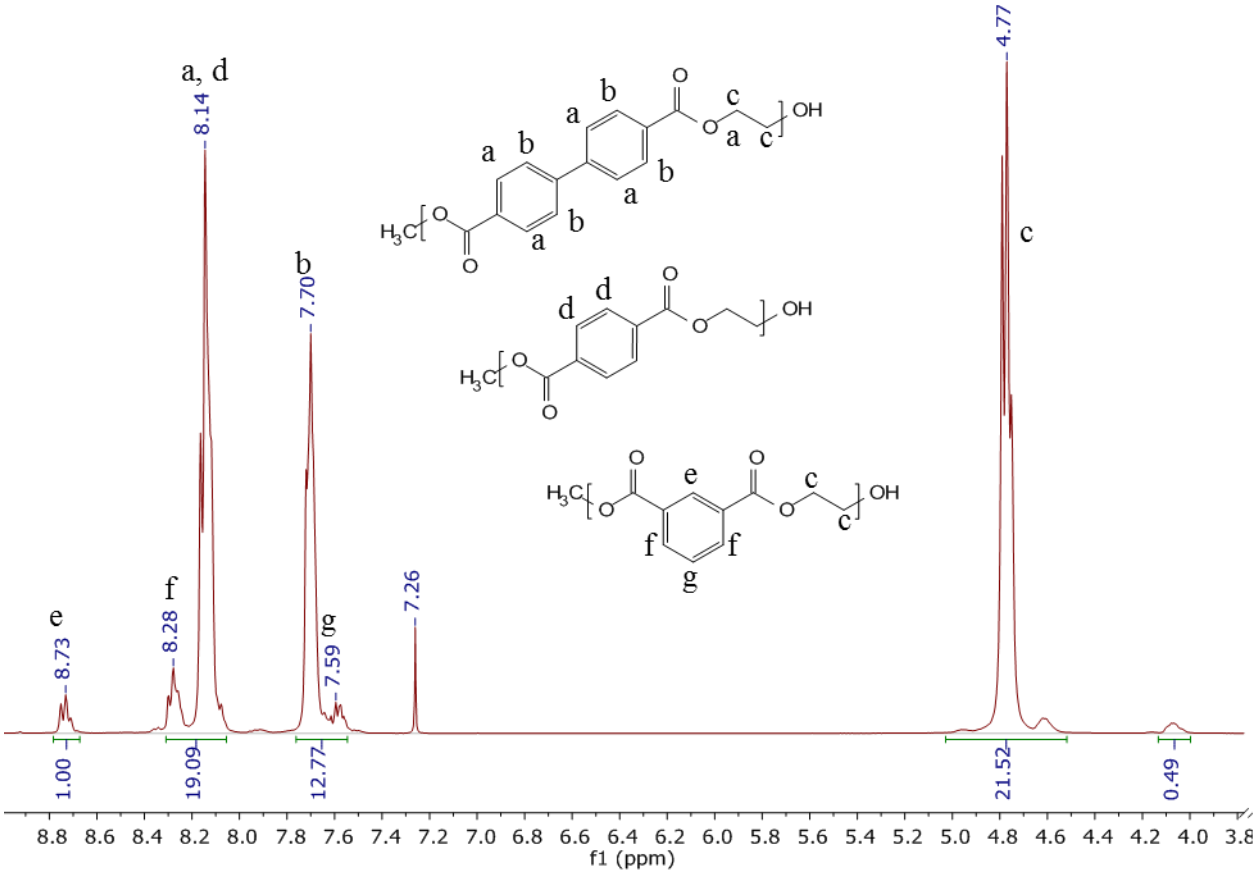

Figure 2-10S. ^{1}H NMR spectrum of T-19-I-55-4,4'BB-EG in 95:5 CDCl3:TFA-*d*. The equations below were used to determine the approximate molar ration of each monomer.

$$T_{proton} = \frac{\int(8.05 - 8.31)ppm - \int(7.55 - 7.76)ppm - \int(8.67 - 8.78)ppm}{4}$$

$$I_{proton} = \int(8.67 - 8.78)ppm$$

$$4{,}4'BB_{proton} = \int(7.55 - 7.76)ppm - \int(8.67 - 8.78)ppm$$

$$Mol\%\ T = \frac{T_{proton}}{I_{proton} + 4{,}4'BB_{proton} + T_{proton}} \times 100$$

$$Mol\%I = \frac{I_{proton}}{I_{proton} + 4{,}4'BB_{proton} + T_{proton}} \times 100$$

$$Mol\%\ 4{,}4'BB = \frac{4{,}4'BB_{proton}}{I_{proton} + 4{,}4'BB_{proton} + T_{proton}} \times 100$$

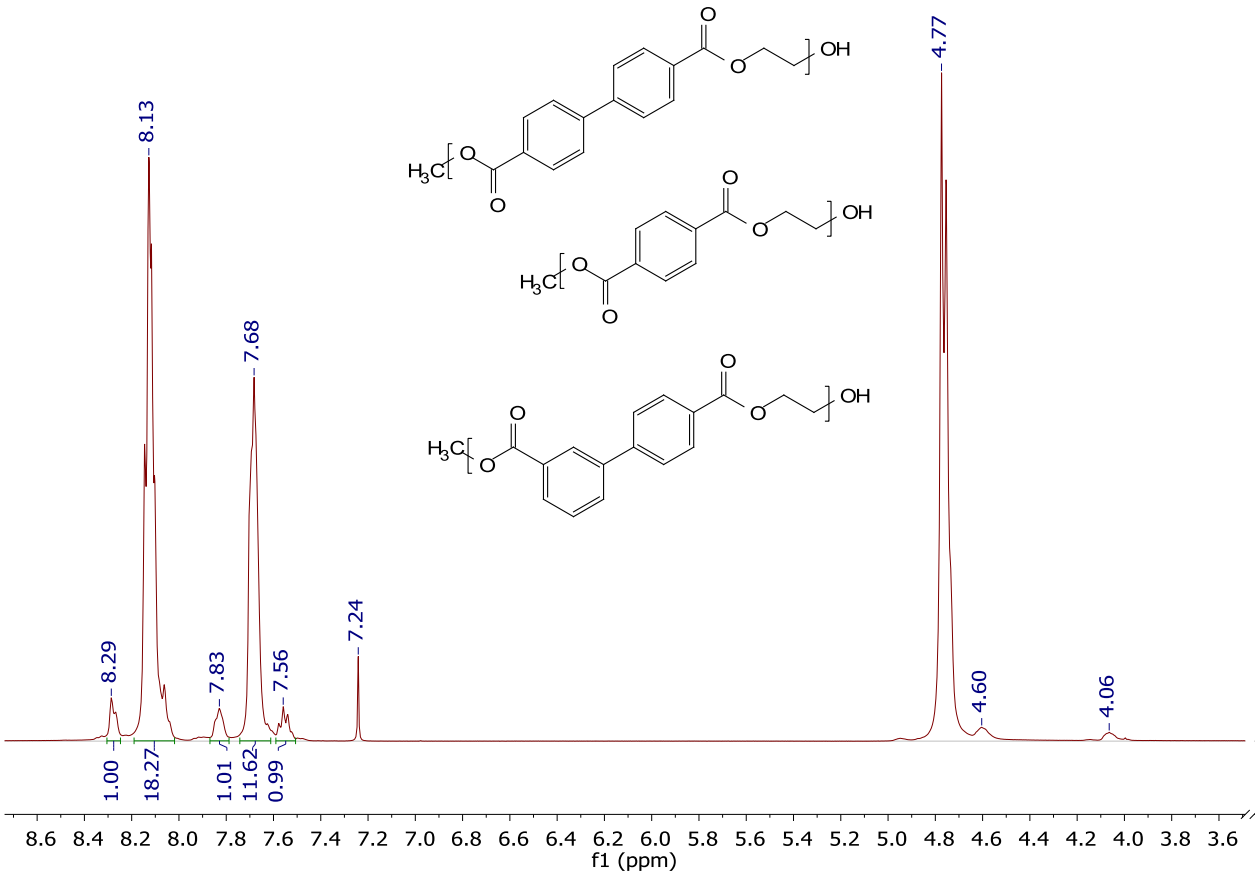

Figure 2-11S. [1]H NMR spectrum of T-21-3,4'BB-50-4,4'BB-EG in 95:5 CDCl3:TFA-*d*. The equations below were used to determine the approximate molar ration of each monomer.

$$T_{proton} = \frac{\int(8.02 - 8.19)ppm - \int(7.61 - 7.74)ppm - \int(8.25 - 8.31)ppm}{4}$$

$$3{,}4'BB_{proton} = \int(8.25 - 8.31)ppm$$

$$4{,}4'BB_{proton} = \int(7.61 - 7.74)ppm - 2 \times \int(8.25 - 8.31)ppm$$

$$Mol\%\ T = \frac{T_{proton}}{3{,}4'BB_{proton} + 4{,}4'BB_{proton} + T_{proton}} \times 100$$

$$Mol\%\ 3{,}4'BB = \frac{3{,}4'BB_{proton}}{3{,}4'BB_{proton} + 4{,}4'BB_{proton} + T_{proton}} \times 100$$

$$Mol\%\ 4{,}4'BB = \frac{4{,}4'BB_{proton}}{3{,}4'BB_{proton} + 4{,}4'BB_{proton} + T_{proton}} \times 100$$

2.9.3 Sequence Distribution of Copolyesters After Melt-phase Polymerization

Quantitative ^{13}C NMR was used to determine the randomness of the sequence of the terephthalate and bibenzoate structural units. Sample concentration was 50–60 mg/mL in a mixture of trifluoroacetic acid-*d* and $CDCl_3$ (approx. 5:95 v/v). The spectra were acquired on a Bruker Avance 500 MHz instrument operating at 125.70 MHz. The spectral width was 247 ppm, the relaxation delay was 2 s and the inverse gated decoupling was used to eliminate the nOe effect with 1024 scans.

The studies of poly(ethylene terephthalate-co-isophthalate)[2] and poly(ethylene-co-trimethylene terephthalate)[3] showed that the ipso (quaternary) carbons are more sensitive to sequence effects than any other aromatic carbons in the aryl diesters. The relative amounts of dyad and triad sequences can be then determined. Schiraldi et al. also described the sequence distribution of PETBB but without detailed randomness calculation.[4]

From the achieved spectrum (**Figure 2-12S**), carbonyl carbon peaks of terephthalate and 4,4' BB are separated at 166.7 and 167.8 ppm, respectively, from which the chemical composition can also be calculated. For sequence analysis, the spectrum optimization had to be performed, and then a clear splitting into 4 (133.4–133.6 ppm) and two peaks (128.5–128.6 ppm) was observed for the quaternary carbon of the terephthalate and 4,4' BB units. In **Figure 2-13S**, two peaks at 128.52 and 128.58 ppm can be assigned to BT and BB dyads. Meanwhile in **Figure 2-14S**, ispo carbons in terephthalate units give rise to four overlapping peaks, and the triads assignments were made in this figure.

To address peak overlapping, deconvolution of the peaks was conducted in Mnova and integration of peak areas allow for the determination of polymer randomness. The calculations were based on Bernoullian statistical model For example, if the relative possibilities of T-based

dyads (TB and TT) are made as $P_{TB} = X$ and $P_{TT} = 1-X$. Then the ratios of T-centered triads (TTT, BTB and TTB or BTT) can be derived as:

$P_{TTT} = (1-X)^2$; $P_{BTB} = X^2$ and $P_{TTB} = 2X(1-X)$

The combination of these equations was used to solve X based on the experimental integrations. PIT and PII of the bibenzoate-centered dyads were determined from the integration as well. The degree of randomness is then calculated as:

$R = P_{TB} + P_{BT}$

For random copolymer, R = 1; for block copolymer, R = 0 and for alternating copolymer R = 2. In **Table 2-10S**, the experimental values showed good agreement with the theoretical values as predicted by Bernoullian statistics. Therefore, our data suggested that the copolyesters we synthesized through melt-phase polymerization are completely random.

Table 2-10S. Experimental and theoretical (in parenthesis) sequence distribution in PET4,4'BB copolyesters

Polyester	Composition[a]		Triads (mol%)[b]			Dyads (mol%)[c]		Randomness
	T	B	TTT	BTT + TTB	BTB	BT	BB	
T-40-4,4'BB-EG	59.7	40.3	35.1 (35.6)	47.0 (48.1)	17.9 (16.2)	61.2 (59.7)	38.8 (40.3)	1.02 (1.00)

a. Calculated from the carbonyl carbon resonances
b. Triad content relative to the quaternary carbon centered at the terephthalate (T) unit
c. Dyad content relative to the quaternary carbon centered at the 4,4' BB (B) unit

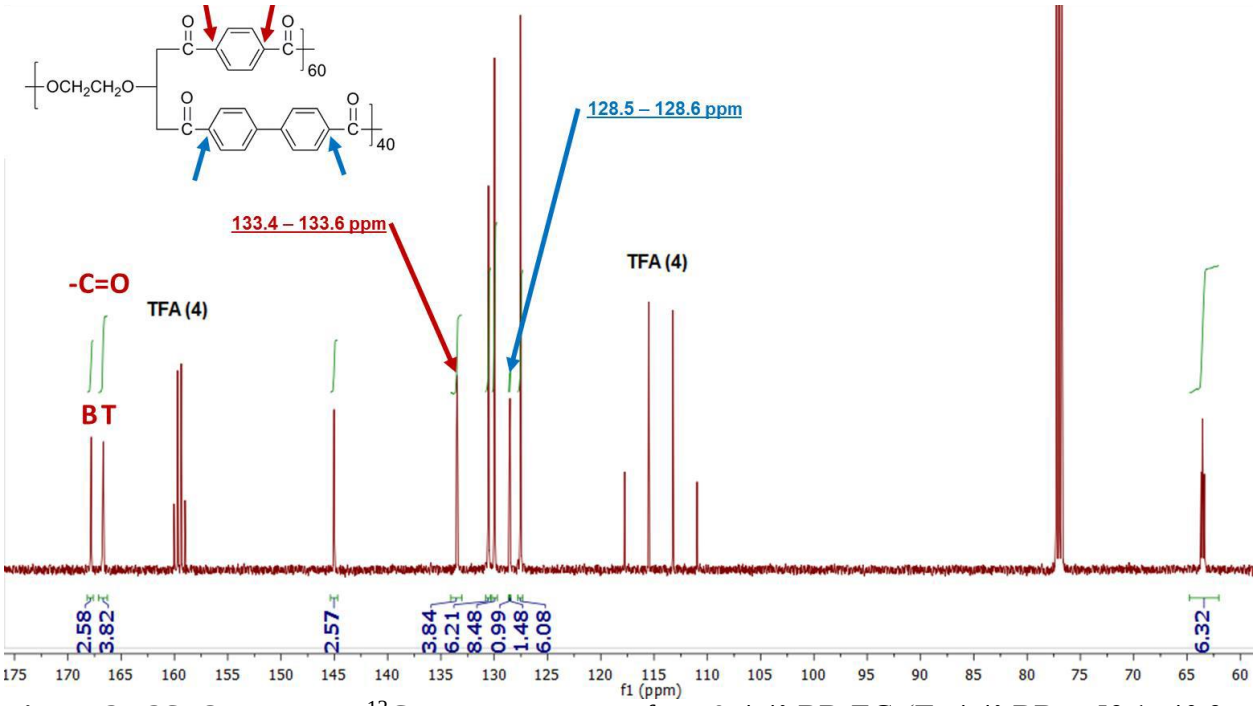

Figure 2-12S. Quantitative ^{13}C NMR spectrum of T-40-4,4' BB-EG (T: 4,4' BB = 59.1: 40.9 from ^{1}H NMR)

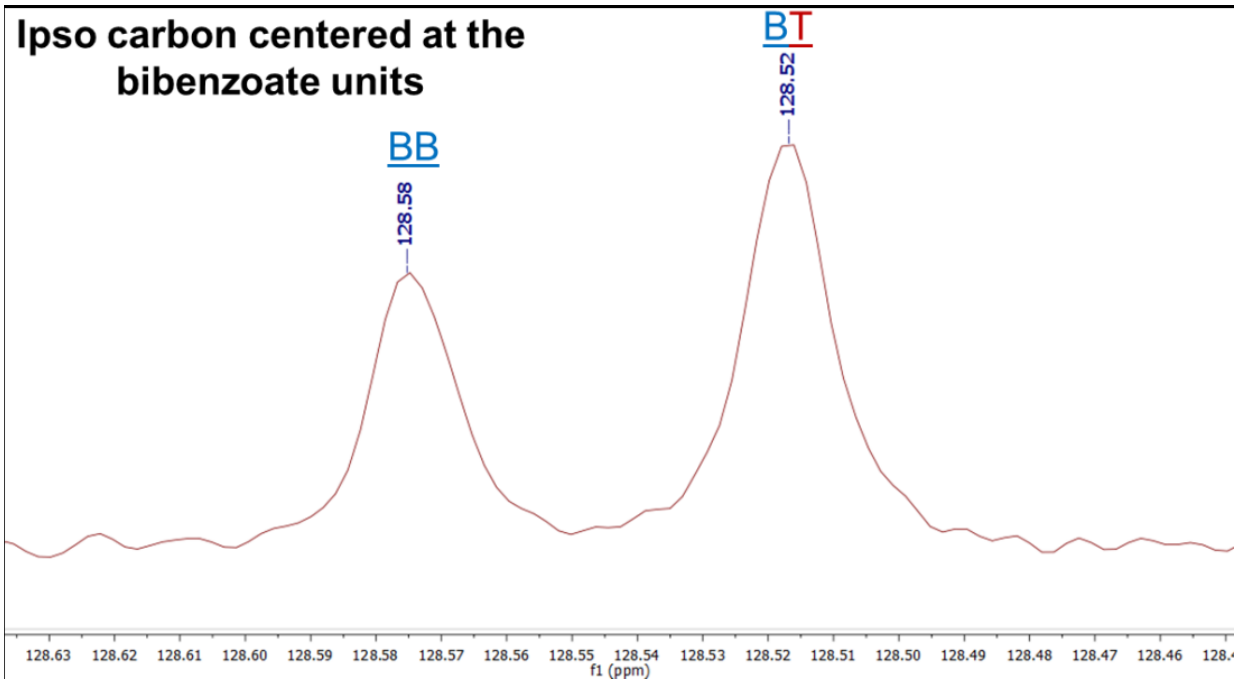

Figure 2-13S. Ipso carbon centered at 4,4' BB structural units to BB and BT dyads

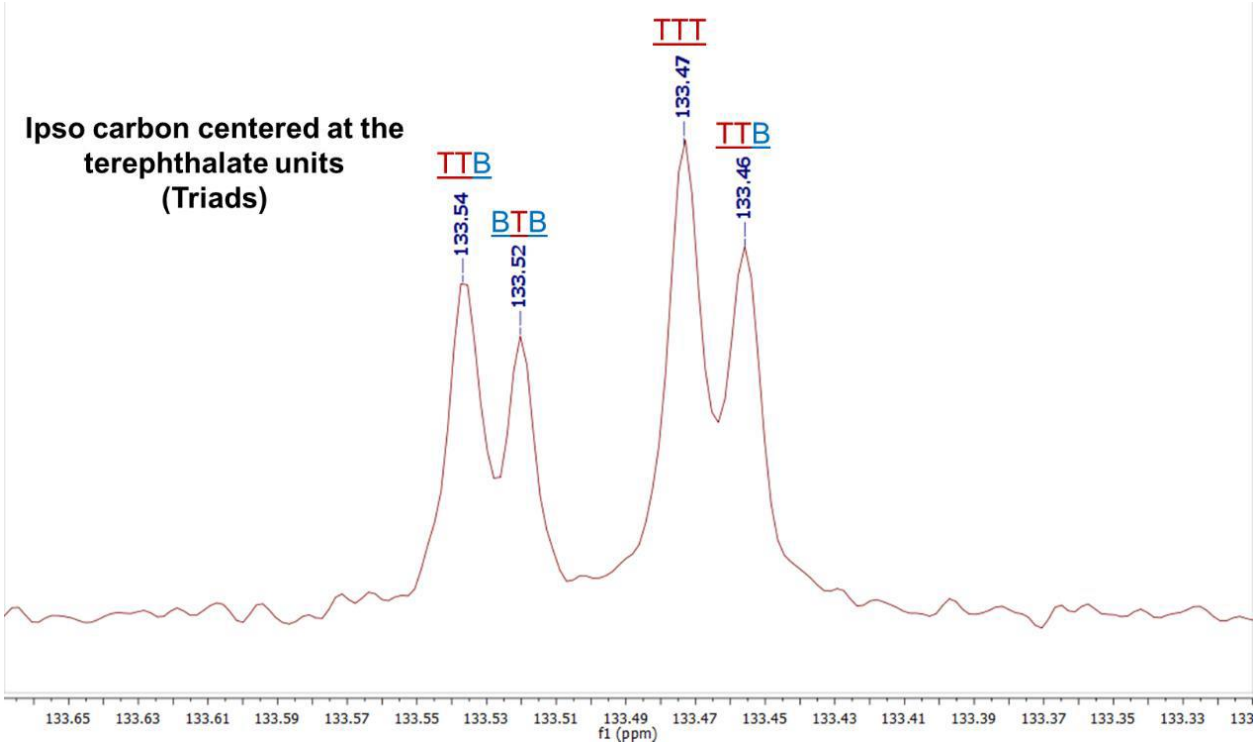

Figure 2-14S. Ipso carbon centered at terephthalate structural units to TTB, BTB and TTT dyads

2.9.4 Increasing Degradation Temperatures with Higher 3,4'BB Levels

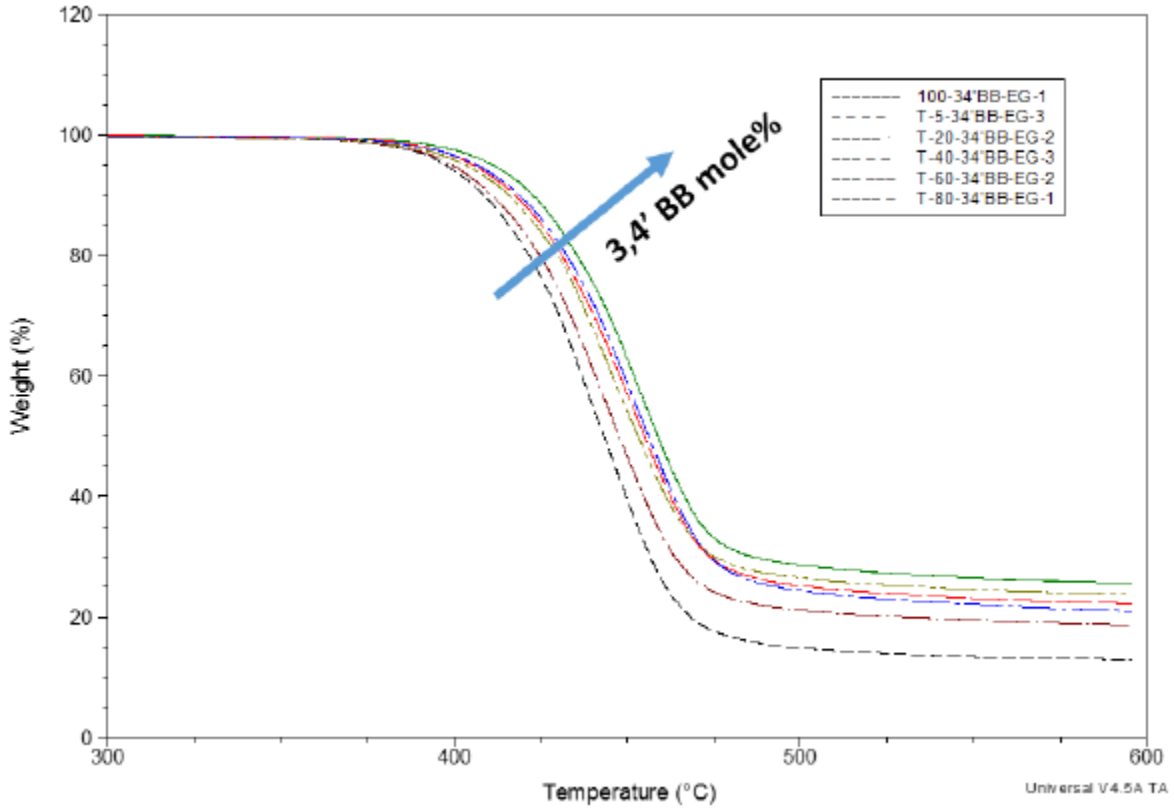

Figure 2-15S. TGA thermograms of T-X-3,4'BB-EG copolyester

2.10 Chapter 2 Supplemental References

1. Schiraldi, D. A.; Lee, J. J.; Gould, S. A. C.; Occelli, M. L., Mechanical properties and atomic force microscopic cross sectional analysis of injection molded poly(ethylene terephthalate-co-4,4'-bibenzoate). *J. Ind. Eng. Chem.* **2001,** *7* (2), 67-71.

2. Martínez de Ilarduya, A.; Kint, D. P. R.; Muñoz-Guerra, S., Sequence analysis of poly(ethylene terephthalate-co-isophthalate) copolymers by ^{13}C NMR. *Macromolecules* **2000,** *33* (12), 4596-4598.

3. Shyr, T.-W.; Lo, C.-M.; Sheng-RongYe, Sequence distribution and crystal structure of poly(ethylene/trimethylene terephthalate) copolyesters. *Polymer* **2005,** *46* (14), 5284-5298.

4. Ma, H.; Hibbs, M.; Collard, D. M.; Kumar, S.; Schiraldi, D. A., Fiber spinning, structure, and properties of poly(ethylene terephthalate-co-4,4‘-bibenzoate) copolyesters. *Macromolecules* **2002,** *35* (13), 5123-5130.

Chapter 3. Amorphous Copolyesters Based on Bibenzoic Acids and Neopentyl Glycol

3.1 Authors

*H. Eliot Edling, Ryan J. Mondschein, Timothy E. Long and S. Richard Turner**

[1]Macromolecules Innovation Institute, Department of Chemistry, Virginia Tech, Blacksburg, Virginia 24061, USA

3.2 Abstract

Novel copolyester thermoplastics containing 4,4'-bibenzoate (4,4'BB) and 3,4'-bibenzoate (3,4'BB) moieties were synthesized via melt polycondensation. Crystallization was suppressed through the addition of ethylene glycol (EG), 1,4-cyclohexane dimethanol (CHDM) and neopentyl glycol (NPG) comonomers into the copolyester backbone. Diol ratios were determined by ^{1}H NMR spectroscopy and molecular weights were assessed with inherent viscosity (η_{inh}). Thermogravimetric analysis (TGA) showed single-step weight losses in the range of 395–419 °C. Differential scanning calorimetry (DSC) was used to determine melting points and glass transition temperatures over a wide range of copolyester compositions and identified amorphous compositions. Dynamic mechanical analysis (DMA) confirmed T_gs and was used to study β-relaxations below the T_g. Rheological analysis revealed the effect of NPG structures on shear thinning and thermal stability. The impact properties of amorphous, high T_g copolyesters containing both NPG and CHDM diols were tested with Notched Izod.

3.3 Introduction

Copolyester compositions containing 3,4'BB and 4,4'BB (**Figure 3-1**) moieties have been known in the literature for quite some time.[1] In the 1990s, DOW Chemical Company claimed several copolyesters containing both 3,4'BB and 4,4'BB diesters combined with a range of linear aliphatic diols containing 2–12 carbons.[2] Copolyesters compositions containing 50 mol%

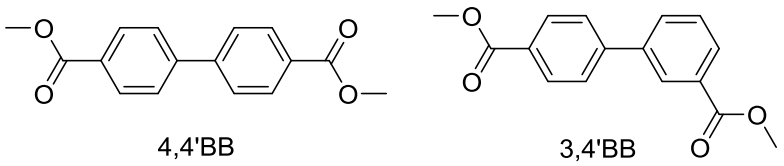

Figure 3-1. Chemical structure of 3,4'BB and 4,4'BB dimethyl esters

or more 3,4'BB were tough, amorphous and exhibited T_gs ranging from 104–111 °C, and their rheological and gas barrier properties were recently reported by Mondschein et al.[3] Compositions containing more than 50 mol% 4,4'BB exhibited high crystallinity, with melting temperatures above 300 °C and T_gs above 122 °C.[2-3] The meta substitution of the 3,4'BB moiety produces a 'kink' in the polymer backbone that disrupts crystallization and decreases the T_g relative to 4,4'BB based polyesters. This is apparent in the 3,4'BB-EG homopolyester, which is completely amorphous and has improved tensile strength and modulus relative to corresponding amorphous 4,4'BB based copolyesters.[2-4]

Early patents by Monsanto claimed copolyester compositions where PET was modified with 4,4'BB comonomer, however, very little property analysis was reported on these compositions. Over the years, both 3,4'BB and 4,4'BB were investigated for their potential to enhance gas barrier,[3-11] and recent work modified PET with 4,4'BB, 3,4'BB and isophthalate moieties in an effort to improve its thermal, mechanical and barrier properties.[4] PET copolyesters containing 15–40 mol% 4,4'BB were amorphous with T_gs ranging from 89–98 °C.

Until recently, the need for tough, amorphous, high temperature materials was satisfied by bisphenol-A polycarbonate (BPA PC) until it fell out of favor food safe applications over concerns that BPA, which has endocrine disrupting activity, may leach into food and beverages.[12-15] With polycarbonate no longer used for many high temperature food applications, such as hot filling baby food, juice and pasteurized beer, there is a strong need for food safe alternatives. Eastman's

Tritan™ (an amorphous copolyester made with terephthalate and 2,2,4,4-tetramethyl-1,3-cyclobutane diol (TMCDB)) exhibits sufficiently high heat resistance for many of these applications, but there is still a strong desire for other alternatives.[13, 16-18] Other amorphous copolyesters such as PCTG (PET modified with more than 50 mol% CHDM) do not have T_gs above 100 °C.[19]

Amorphous copolyesters containing NPG and CHDM have been claimed as an alternative to PETG (PET modified with more than 50 mol% EG) and PCTG (PET modified with more than 50 mol% CHDM) copolyesters to produce transparent, tough copolyesters with T_gs of 78–88 °C and greater shear thinning.[20] NPG is known to have high thermooxidative and UV stability[21] and is marketed by BASF and Eastman Chemical Company as an intermediate for powder coatings used in outdoor applications with high weatherability. The stability of NPG is attributed to the two methyl groups at the β position relative to the alcohols (**Figure 3-2)**. The presence of these two

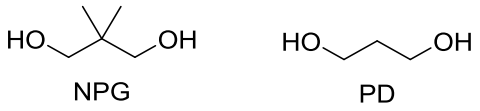

Figure 3-2. Molecular structure of NPG and PD

methyl groups is believed to inhibit Norrish II scission, which significantly contributes to the degradation of aliphatic diols.[21-22] When comparing poly(neopentyl terephthalate) (PNT) to poly(1,3-propylene terephthalate) (PPT) it becomes apparent that the additional methyl groups in NPG disrupt crystallization relative to the similarly sized 1,3-propanediol (PD) (**Figure 3-2)**, as PPT has a T_m of 228 °C and NPG only exhibits a T_m 144 °C when annealed.[23] The methyl groups of NPG also restrict the mobility and conformational freedom of the polyester chain, producing a higher T_g in PNT (77 °C) relative to PPT (47 °C).

The impact properties of a (co)polyester depend upon the T_g, level of crystallization and polymer backbone structure. The impact properties of materials typically improve at temperatures closer to the T_g, making it difficult to produce high-T_g materials with good impact.[17, 24] BPA PC (T_g = 145°C), however, is well known for having excellent impact properties and has been the subject of many studies.[14-15, 17-18, 24-25] Relaxations below the T_g (often referred to as β-relaxations) have come to be associated with good impact properties as an indication of short-range molecular motions (e.g. phenyl ring flips and crankshaft motions) increasing free volume capable of absorbing energy during impact.[26-28] CHDM is well known for enhancing the impact properties of (co)polyesters.[19] Improved impact properties of polyesters based on CHDM have been associated with increased sub-T_g transition intensity in the vicinity if -60 °C.[28] Comparison of crystalline and quenched amorphous samples of the same polyester have shown crystallinity to suppress β-relaxation intensity and shift it to higher temperatures due to restricted mobility.[29] We describe herein the polymerization and characterization of rigid copolyesters based on 3,4'BB or 4,4'BB that are modified with NPG, EG or CHDM to produce amorphous materials having high glass transition temperatures, and good mechanical properties relative to current amorphous copolyesters. Large, rigid bibenzoate diesters and NPG were utilized for their known ability to enhance mechanical and thermal properties relative to available amorphous copolyester (**Table 3-1)**. Melt polymerization was performed in glass reactors immersed into a temperature-controlled molten metal bath. Polyesters were investigated with solution viscometry, ^{1}H NMR (nuclear magnetic resonance), TGA (thermogravimetric analysis), DSC (differential scanning calorimetry), dynamic mechanical analysis (DMA), tensile testing and rheology.

Table 3-1. Mechanical property comparison of bibenzoate and NPG containing polyesters to commercial amorphous materials.

Amorphous Copolyester	Yield strength (MPa)	Young's Modulus (MPa)	Strain at break (%)
3,4'BB-EG[3]	74	2690	160
52-4,4'BB-48-3,4'BB-EG[3]	60	2340	110
65-T-35-4,4'BB-EG[3]	53	2101	90
T-51-NPG-49-CHDM[20]	44	-	180
Lexan 9440*	62	2379	110
PETG 6763**	52	1900	400
Tritan TX1001**	43	1550	210

* Sabic Product Data Sheet
** Eastman Product-Technical Data Sheet

The incorporation of bibenzoate moieties into terephthalate based copolyesters is well known to enhance the T_g of the copolyesters. However, little research is published that focuses on exploration of 4,4'BB as a T_g enhancer in amorphous copolyesters due to the propensity of 4,4'BB to impart crystallinity into the compositions—especially with the commonly used diols EG and CHDM resulting in a narrow compositional range for achieving practical amorphous compositions. NPG is reported to be an effective comonomer for reducing crystallinity in composition with terephthalate and CHDM.[20] It is hypothesized that the incorporation of NPG into 4,4'BB based copolyester compositions will lead to a broader amorphous window and enable higher 4,4'BB incorporation levels, which can lead to higher T_gs compared to known EG, CHDM amorphous copolyester compositions. This chapter reports comparative studies of various amorphous copolyesters containing 4,4'BB and combinations of NPG, CHDM and EG diols used to suppress crystallization.

3.4 Experimental

3.4.1 Materials

Dimethyl terephthalate (DMT, ≥99%) and neopentyl glycol (NPG, 99%) were purchased from Sigma Aldrich. Dimethyl 4,4'-biphenyldicarboxylate (4,4'BB) and dimethyl 3,4'-biphenyldicarboxylate (3,4'BB) were supplied by ExxonMobil Chemical company. All diesters and NPG were dried in a vacuum oven overnight at 35 °C and stored in a dry box before using. Ethylene glycol (EG, ≥99%) and 1,4-cyclohexanedimethanol (CHDM, 30:70 cis/trans, ≥99%) were obtained from Sigma Aldrich and used as received. Dichloroacetic acid (≥99%) was obtained from Alpha Aesar and used as received. Titanium (IV) butoxide (97%) was purchased from Sigma Aldrich. 1-Butanol (99.9%) was purchased from Fisher Scientific and dried over magnesium sulfate. A titanium catalyst solution (ca. 0.02 g/mL) was prepared by placing 0.2 g titanium (IV) butoxide into 10 mL volumetric flask and diluting to the calibration line with 1-butanol. The titanium solution was then transferred to a sealed container and purged with nitrogen for 10 min. Trifluoroacetic acid-*d* (TFA-*d*, 99.5 atom % D) was obtained from Sigma Aldrich. Chloroform-*d* ($CDCl_3$, 99.8% atom D +0.05% V/V TMS) was obtained from Cambridge Isotope Laboratories, Inc.

3.4.2 Characterization Methods

^{1}H NMR analysis was performed by using a Varian Unity 400 MHz spectrometer with at least 32 scans at 23 °C on polymer samples (ca. 50 mg) dissolved in a binary mixture of TFA-*d*:CDCl3 (5/95). Inherent viscosity (η_{inh}) was measured following a procedure adapted from ASTM method D4603 by using a Cannon Type B glass capillary viscometer. Thermogravimetric analysis (TGA) was performed by using a TA Instruments Q500 starting at 25 °C and proceeding to 600 °C with a 10 °C/min heating rate under nitrogen. Differential scanning calorimetry (DSC) was performed on 5–8 mg polymer samples by using a TA Instruments Q2000 under nitrogen with

10 °C/min heating and cooling rates. Glass transitions temperatures (T_gs) were determined from the midpoint of the transition inflection point on the second heating ramp. Dynamic mechanical analysis (DMA) was used to monitor modulus with increasing temperature by using a TA Instruments Q800 Dynamic Mechanical Analyzer on oscillatory tension mode at 1 Hz, 15 μm amplitude and a temperature ramp of 3 °C/min. DMA test samples were cut from compression molded ~0.55 mm thick films as 5 mm wide strips. Tensile analysis of copolyesters was performed on dogbones cut from 0.55 mm thick compression molded films with a D638-V dogbone punch, with dimensions specified in the ASTM D638 procedure. An Instron 5500R tested punched dogbone samples at a crosshead motion rate of 10mm/min and an initial grip separation of 25.4 ± 2.0 mm. Additional tensile analysis of 4,4'BB-X-NPG-Y-CHDM copolyesters was performed on 2 mm thick, injection molded D638-V dogbones, with dimensions specified in the ASTM D638 procedure. An AutoX 750 extensometer obtained tensile modulus data of injected molded dogbones on Instron 5965 at a crosshead motion rate of 50.8 mm/min. Notched Izod analysis was performed on a Ceast/Instron ResilImpactor 6958 with 2.03 and 4.06 ft-lb hammers. Dogbones and Izod specimens were injection molded by Exxon Mobil with a Boy XS injection-molding machine at 290 and 280 °C respectively. Injection pressures of 17700–18800 psi and holding pressures of 13600–17700 psi were used with an injection velocity of 50 mm/sec and a mold temperature of 40 °C. Before injection molding, multiple batches of 4,4'BB-X-NPG-Y-CHDM copolyesters were blended in the melt with a ThermoScientific Process 11 corotating twin screw extruder equipped with 11 mm screws operating at 280 °C and 125 RPM**.** Before blending, copolyester samples were ground up with a Cumberland 6508 Beside The Press Granulator equipped with a 4.76 mm screen. Rheological analysis was performed with a TA instruments Discovery Hybrid Rheometer-2 with disposable 8 mm diameter aluminum parallel plates. A strain

sweep was performed at 0.01–10 % oscillatory strain and 1 Hz to determine the linear viscoelastic region. Time sweeps were performed under air at 1 Hz and 1.25 % oscillatory strain to observe changes in viscosity over time. Amorphous copolyester compositions containing NPG were run at 280 °C and the semicrystalline 4,4'BB-50-EG-50-CHDM was tested 285 °C to prevent crystallization. Frequency sweeps of 1–100 rad/s were performed between 150 and 280 °C at 10 °C intervals and 1 % oscillatory strain. Samples were dried in a vacuum oven overnight the day before at 140 °C and then kept in a sealed jar. Time temperature superposition (TTS) master curves were generated with TA Instruments TRIOS software to observe viscosity response over a wide frequency range.

3.4.3 Polymerization

Polymerization of 4,4′BB-X-EG-Y-CHDM (20 g scale). All compositions were synthesized in a similar manner. Reactions were performed a dry round bottom flask equipped with distillation arm, nitrogen inlet and an overhead stirrer. To synthesize the composition 4,4′BB-60-EG-40-CHDM, EG (3.84 g, 0.06 mol), CHDM (4.03 g, 0.03 mol) and 4,4'BB (17.99 g, 0.07 mol) was charged into a 100 mL round bottom flask along with enough titanium catalyst solution to make up 40 ppm Ti by mass to the theoretical yield. Oxygen and moisture were removed from the flask by treating with vacuum and purging with nitrogen three times. For the transesterification step, stirring rate was set to 200 rpm and the flask was submerged into a 200 °C metal bath for 1 h, the temperature was then increased to 210 °C for 1 h, then 220 °C for 2 h and finally increased to 280 °C for 1 h. The temperature was then ramped to 310 °C while slowly applying vacuum over 15 min. The polycondensation step was then carried out with a 30–40 rpm stirring rate under decreased pressure (≤ 0.3 mmHg) for 30 min. The flask was then removed from the metal bath and allowed to cool to room temperature. All polyesters were isolated by first breaking the flask and

then removing the polyester from the stir rod by using a hammer, chisel and end nippers. Isolated polymers were rinsed with DI water and dried overnight in a vacuum oven at 10–20 °C above the glass transition of the polymer.

Polymerization of 4,4′BB-X-NPG-Y-CHDM (20 g scale). Equipment and drying procedure was performed in a similar fashion to that used for 4,4'BB-X-EG-Y-CHDM composition above. To synthesize the composition 4,4'BB-50-NPG-50-CHDM, NPG (6.30 g, 0.60 mol), CHDM (4.50 g, 0.03 mol) and 4,4'BB (16.36 g, 0.06 mol) were charged into a 100 mL round bottom flask along with catalyst solution (40 ppm Ti by mass to the theoretical yield). Transesterification was carried out at 200 °C for 1 h, 210 °C for 1 h, 220 °C for 2 h, 280 °C for 1 h. Polycondensation was performed at 280 °C and ≤ 0.3 mmHg for 1 h.

Polymerization of 4,4′BB-X-EG-Y-NPG (12 g scale). Equipment and drying procedure was performed in a similar fashion to that used for 4,4′BB-X-EG-Y-CHDM composition above. To synthesize the composition 4,4′BB-20-EG-80-NPG, NPG (3.73 g, 0.04 mol), EG (1.73 g, 0.04 mol) and 4,4'BB (10.74 g, 0.04 mol) were charged into a 100 mL round bottom flask along with catalyst solution (40 ppm Ti by mass to the theoretical yield). Transesterification was carried out at 230 °C for 2 h and 280 °C for 2 h. Polycondensation was performed at 280 °C and ≤ 0.3 mmHg for 1 h.

Polymerization of 3,4′BB-X-EG-Y-NPG. All compositions were synthesized with the same procedure. Molar ratios and conditions as followed for 4,4′BB-X-EG-Y-NPG compositions.

Polymerization of 3,4′BB-X-NPG-Y-CHDM. All compositions were synthesized with the same procedure. Molar ratios were the same as those used for 4,4′BB-X-NPG-Y-CHDM compositions. Reaction conditions followed those used for 4,4′BB-X-EG-Y-NPG compositions.

3.4.4 Compression Molding Copolyesters

Polymers pieces and or particles were melt pressed into films by using a PHI Q-230H hydraulic press heated to 280 °C. Samples (4–5 g) were sandwiched between two aluminum plates, each with a layer of Kapton® film coated with Rexco Partall® Powder Glossy Liquid mold release agent to prevent sticking. Aluminum shims inserted between the aluminum plates controlled thickness. To press films, samples were placed inside the press on top of a Kapton® layered aluminum plate until the sample started to melt (1–3 min), at which point a shim and the second layer of Kapton® and aluminum were added. The plates were then moved to the center of the press, which was lightly closed until complete melting of sample (ca. 2 min). Three press-release cycles (30 s each) were completed at 5 tons of force, followed by pressing once at 10 tons of force. After pressing, samples were immediately transferred to an ice water bath to quench the samples. Films were subsequently removed from the Kapton® and dried in a 40 °C vacuum oven overnight. Samples for DMA and tensile analysis were compression molded by using a 0.60 mm shim, which produced 0.55 mm films.

3.5 Results and Discussion

3.5.1 Polymerization and Structural Characterization

A range of copolyesters were synthesized containing either 4,4’BB or 3,4’BB comonomers incorporated into the backbone along with NPG and either CHDM or EG by using melt transesterification (**Scheme 3-1**). Transesterification was facilitated by the use of titanium (IV) butoxide and excess diol. Stirring the reaction at temperatures of 210–230 °C for several hours under nitrogen produced a clear melt and allowed the removal of methanol condensate via distillation, which was monitored to gauge reaction progress. Increasing the temperature to ~280

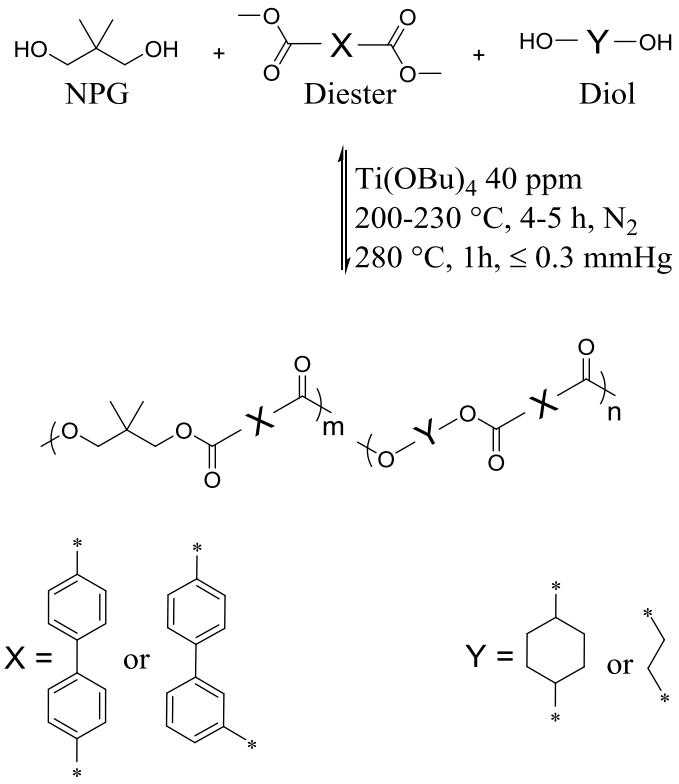

Scheme 3-1. Polymerization of amorphous copolyesters containing bibenzoate and NPG moieties

°C and stirring for another hour under nitrogen was done to ensure that transesterification was complete as low reactivity of NPG is well known.[30] Polycondensation was carried out over 1 h with a slow stirring rate so as to prevent excess wrapping of the polymer around the stir rod at higher viscosities. Reduced pressure removed nearly all excess diol to produce high molecular weight polyesters, which was indicated by an increase in melt viscosity sufficient to wrap the polymer melt around the stirring rod and preventing stirring. Most copolyester compositions were amorphous and optically transparent, with colors ranging from pale green/yellow to completely colorless. Semicrystalline composition were white or off-white. The copolyester in **Scheme 3-1** follows the naming scheme 4,4′BB-X-NPG-Y-CHDM, 4,4′BB-X-EG-Y-NPG, 3,4′BB-X-NPG-Y-CHDM, 3,4′BB-X-EG-Y-NPG, where X represents the molar ratio of NPG contained in the

copolyester and Y represents the molar ratio of either EG or CHDM contained within the copolyester. ^{1}H NMR analysis confirmed molar ratios from proton shifts unique to each comonomer (**Figure 3-12S and 3-13S**). An example is shown in **Figure 3-3** where protons from NPG overlap with CHDM. The number of protons each monomer contributes to each peak is known allowing the use of the equation in **Figure 3-3** to determine the diol molar ratio. Targeting specific molar ratios was difficult until several baseline compositions were synthesized to gauge the ratio at which each combination of diols integrated into the final polymer. Due to the different

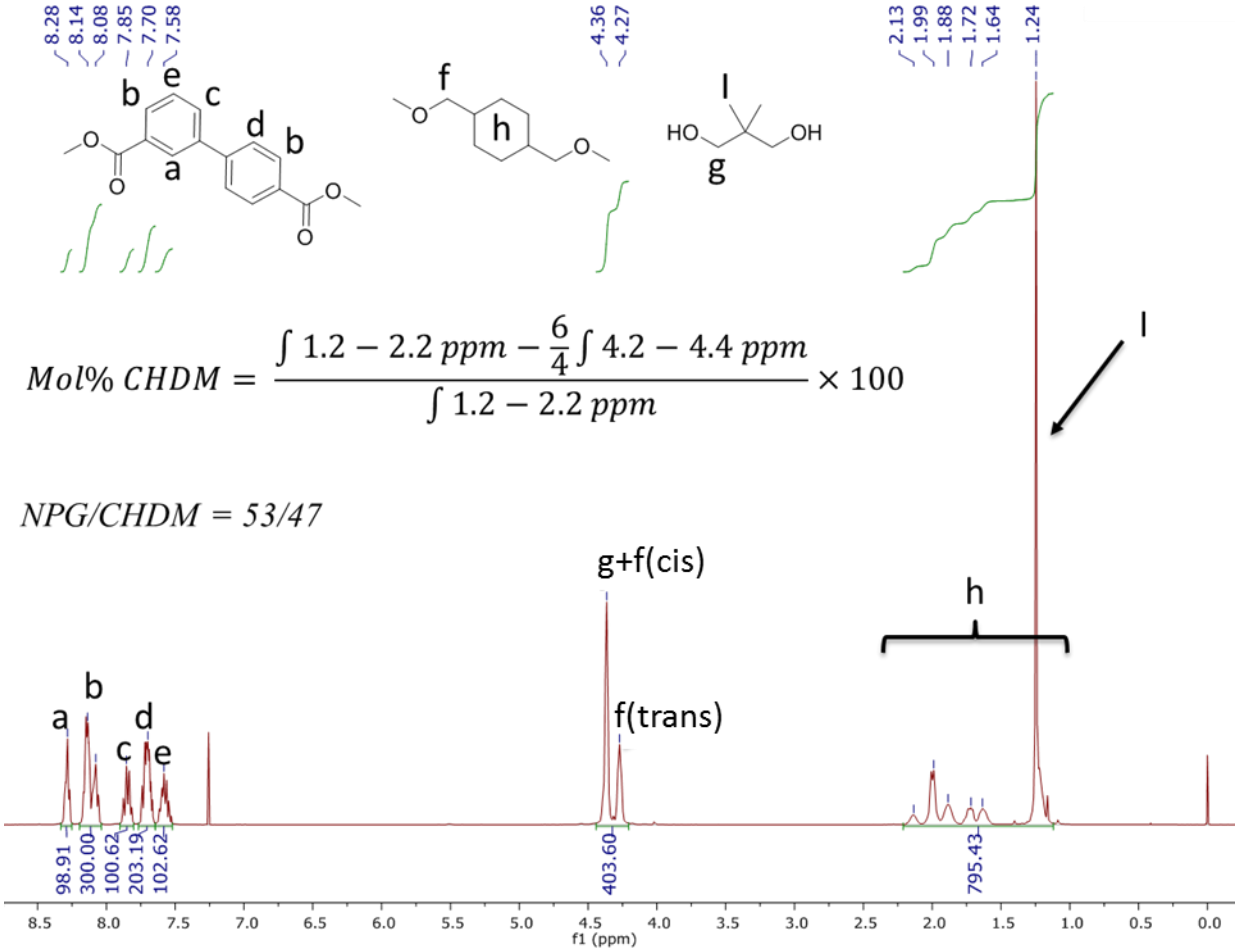

Figure 3-3. ^{1}H NMR of 3,4′BB-50-NPG-50-CHDM copolyester. Relative diacid incorporation ratios were calculated by using peaks g, f, h and l.

volatilities of each monomer, the polycondensation step removes each diol at a different rate causing the monomer ratio to shift towards the less volatile monomer. **Table 3-2** shows the molar ratios used in the feed and the actual composition that resulted in the polymer as confirmed by ^{1}H NMR analysis. Nearly all polymer samples achieved (η_{inh}) of ~0.7 dL/g or higher. **Figure 3-4** and **Figure 3-5** show a linear relationship between the molar ratio of diols in the feed and the monomer molar ratio obtained in the copolyester compositions tested. This linear relationship held true under for duplicate runs, varying polymerization conditions and, for 4,4′BB-X-NPG-X-CHDM compositions, when the scale of the reaction was increased from 12 g to 125 g reaction yields. The slope of the line is determined by how much of each monomer is incorporated into the final polyester before all excess diol is removed. A less volatile diol is expected to incorporate more

Table 3-2. Confirmed compositions, feed ratio, and inherent viscosity values (η_{inh}) of each copolyester. Y = CHDM or EG diol.

Confirmed Composition (^{1}H NMR)	**Diol Molar Ratio In Feed (Y/NPG)**	η_{inh} **(dL/g)**
4,4'BB-37-NPG-63-CHDM	1.0665	0.83
4,4'BB-54-NPG-46-CHDM	0.5150	0.97
4,4'BB-76-NPG-24-CHDM	0.1312	0.88
3,4'BB-34-NPG-66-CHDM	1.0761	1.37
3,4'BB-53-NPG-47-CHDM	0.5005	0.74
3,4'BB-74-NPG-26-CHDM	0.1325	0.74
4,4'BB-33-NPG-67-EG	2.7207	1.12
4,4'BB-41-NPG-59-EG	2.0004	0.73
4,4'BB-69-NPG-31-EG	0.7778	0.80
3,4'BB-34-NPG-66-EG	2.7207	0.86
3,4'BB-44-NPG-56-EG	1.6191	1.05
3,4'BB-67-NPG-33-EG	0.7778	0.81
4,4'BB-40-EG-60-CHDM	-	0.61
4,4'BB-50-EG-50-CHDM	-	0.99
4,4'BB-60-EG-40-CHDM	-	0.66
4,4’BB-NPG	-	0.89
3,4’BB-NPG	-	0.79
T-NPG	-	0.93

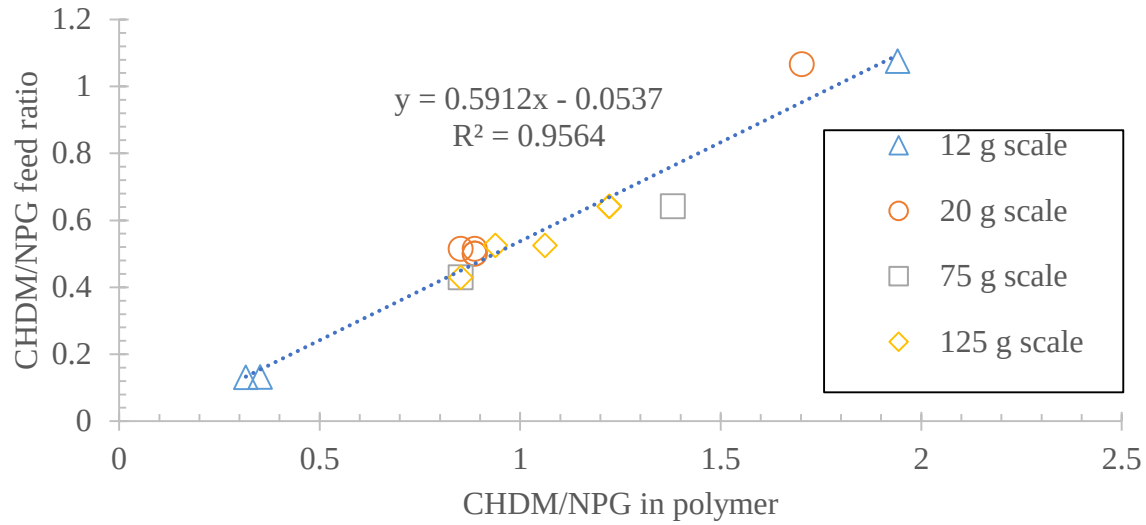

Figure 3-4. Molar ratio of CHDM and NPG monomer in the feed vs molar ratio obtained in the final copolyester

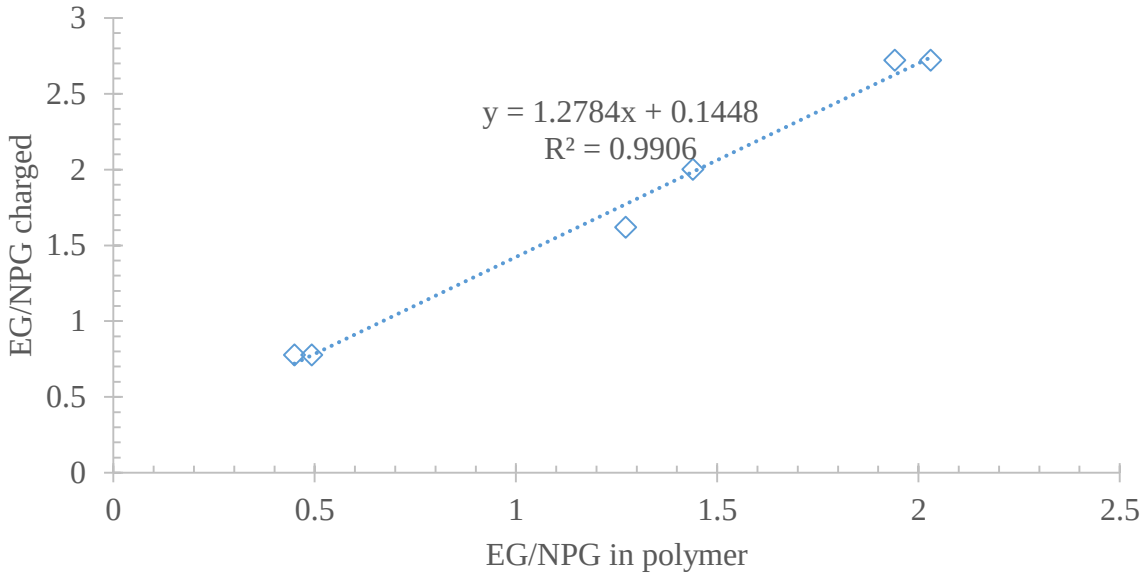

Figure 3-5. Molar ratio of EG and NPG monomer in the feed vs molar ratio obtained in the final copolyester (20 g scale).

completely into the copolyester because less is removed during polycondensation. A slope less than one in **Figure 3-4** shows that more NPG was removed during the polycondensation step than

CHDM. Conversely, a slope greater than one in **Figure 3-5** indicates that more EG was removed during the polycondensation step than NPG. The rate at which excess NPG is removed during polycondensation lies between that of CHDM and EG. As a result, copolymerizations that contain both NPG and CHDM require a large excess of NPG to achieve the targeted molar ratio. Alternatively, in copolymerizations containing both NPG and EG, a large excess of EG is required.

3.5.2 Thermal Properties

Table 3-3 summarizes the DSC results for representative copolyester compositions. All copolyester compositions displayed excellent thermal stability, exhibiting single step weight loss (**Figure 3-14S**) under TGA with degradation temperatures mostly above 400 °C and even as high 415 °C. This compares favorably to PET which typically has a $T_{d,\,5\%}$ temperatures around 385 °C. The strong tendency of 4,4'BB containing copolyesters to crystallize is demonstrated by the 4,4'BB-X-EG-Y-CHDM compositions, all of which exhibit T_ms above those expected for PET.

Table 3-3. Summary of DSC and TGA results of copolyesters. Amorphous compositions (A) did not exhibit melting transitions under DSC conditions

Composition (^{1}H NMR)	T_g (°C)	T_m (°C)	$T_{d,\,5\%}$ (°C)
4,4'BB-37-NPG-63-CHDM	131	252	403
4,4'BB-54-NPG-46-CHDM	129	A	413
4,4'BB-76-NPG-24-CHDM	120	A	410
3,4'BB-34-NPG-66-CHDM	113	A	395
3,4'BB-53-NPG-47-CHDM	109	A	415
3,4'BB-74-NPG-26-CHDM	106	A	407
4,4'BB-33-NPG-67-EG	123	256	408
4,4'BB-41-NPG-59-EG	118	230	412
4,4'BB-69-NPG-31-EG	118	A	403
3,4'BB-34-NPG-66-EG	101	A	405
3,4'BB-44-NPG-56-EG	103	A	412
3,4'BB-67-NPG-33-EG	103	A	414
4,4'BB-40-EG-60-CHDM	103	271	397
4,4'BB-50-EG-50-CHDM	99	272	407
4,4'BB-60-EG-40-CHDM	94	278	399
4,4'BB-NPG	116	A	419
3,4'BB-NPG	104	A	422
T-NPG	77	A	401

Similar copolyester compositions made with DMT instead of 4,4'BB (known as PCTG and PETG) crystallize slow enough to be considered amorphous in the range of 20–40 mol% CHDM,[19] however, the 4,4'BB compositions remain crystalline and white, even when quenched cooled from the melt in an ice bath. Homopolyesters containing NPG and either 4,4'BB or DMT appeared completely amorphous and exhibited no endotherms with DSC analysis. This is a drastic departure from the homopolyesters produced with EG or 1,3-propanediol, both of which of which produce rapidly crystallizing materials (the 4,4BB-EG homopolyester has a high T_m of 314 °C).[31] NPG disrupts crystallization so drastically that above 37 mol% NPG substituted for CHDM in 4,4'BB-X-NPG-X-CHDM copolyesters is sufficient to produce a copolyester with no melting endotherm exhibited in DSC. 4,4'BB-X-NPG-X-EG copolyesters containing 69 mol% or more NPG are also amorphous. The homopolyester of 3,4'BB and NPG appeared clouded and translucent, but no endotherm was observed under DSC. This disruption in crystallinity is believed to stem from the two methyl groups on NPG at the β-position, which limits the mobility of the aliphatic chain, increasing rigidity but also resulting in a structure that is difficult to arrange in an ordered, crystalline structure.[23] The presence of 3,4'BB in the copolyester structure also strongly disrupts crystallinity due to the meta substitution producing in the polyester backbone that does not readily fit into crystalline domains. Much like with NPG, incorporation of 3,4'BB produces an amorphous polyester when substituted into PET for more than 10 mol% DMT or when substituted for 4,4'BB in 4,4'BB-EG by more than 45 mol%.[3-4]

Substitution of NPG for CHDM in copolyesters (**Figure 3-6)** produces a decrease in the glass transition temperature, which is consistent with what has been observed in the literature.[20] Substitution of NPG for EG has little to no effect on T_g while simultaneously disrupting crystallization much more effectively, allowing the production of high T_g amorphous materials.

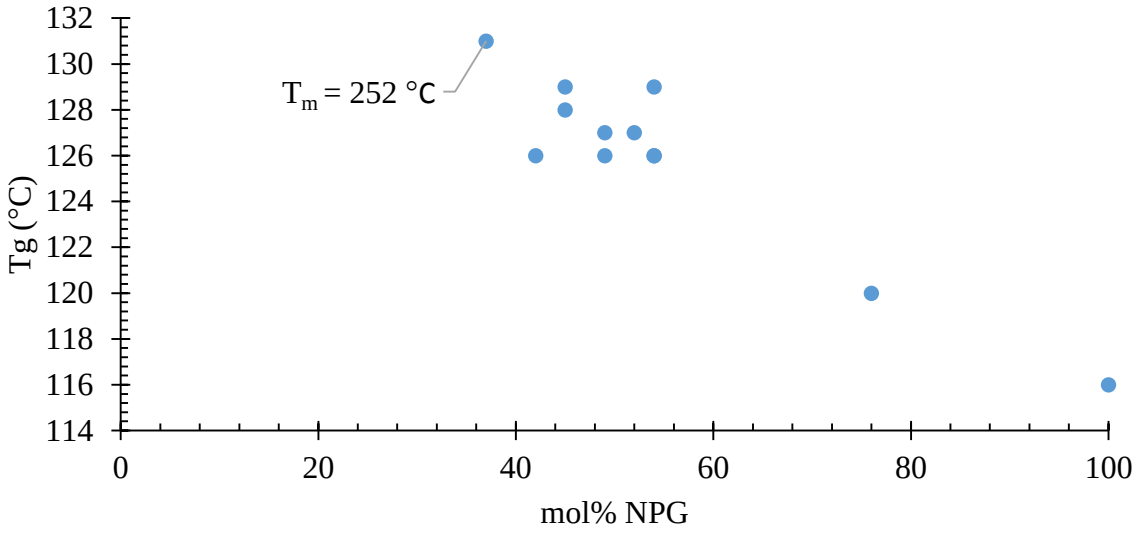

Figure 3-6. Plot of glass transition temperature vs mol% NPG in 4,4'BB-X-NPG-Y-CHDM copolyesters

The copolyesters containing both EG and CHDM exhibited unusually low T_gs given that the 4,4'BB-EG homopolyester is estimated to have a T_g as high as 124 °C and CHDM traditionally enhances the T_g above EG. Copolyester composition 4,4'BB-50-NPG-50-CHDM produced an amorphous copolyester with the highest T_g in the series. Because this composition exhibited a T_g close to that of BPA-PC, it became the subject of further investigation as a high performance amorphous copolyester. **Figure 3-6** plots T_g vs level of NPG incorporation in 4,4'BB-X-NPG-Y-CHDM copolyester. Compositions are amorphous by DSC until NPG concentration decreases to 37 mol%. Samples were annealed in a vacuum oven at 150 °C for 145 h to induce any crystallization that may be too slow to observe in the short time frames used for DSC. Melting endotherms were not observed in the DSC for 4,4'BB-55-NPG-45-CHDM and 4,4'BB-50-NPG-50-CHDM copolyesters, however, a small endotherm was observed for 4,4'BB-45-NPG-55-CHDM composition around 212 °C (**Figure 3-17S**). After annealing in the vacuum oven, 4,4'BB-

55-NPG-45-CHDM remained clear, whereas 4,4'BB-50-NPG-50-CHDM exhibited slight hazing and 4,4'BB-45-NPG-55-CHDM became translucent (**Figure 3-18S**).

DMA was used to probe the thermomechanical response of select polyesters. Samples were analyzed starting at low temperatures (-130 °C) and the temperature was increased until the sample failed. Low temperatures allowed the study of β-transitions below the T_g (**Figure 3-7**). All polyesters exhibited mostly constant moduli below the T_g (**Figure 3-19S)**. T_gs were determined from the α relaxation peaks in the tan δ curve at temperatures 6–7 °C below those determined by using DSC except for 4,4'BB-50-EG-50-CHDM. (**Table 3-4**). Despite being optically clear and not exhibiting a melting endotherm in DSC, DMA was able to detect a small degree of crystallization in the 4,4'BB-NPG homopolyester, indicated by a slight increase in modulus around 127 °C. The semicrystalline 4,4'BB-50-EG-50-CHDM composition also exhibited signs of recrystallization around 129 °C. Copolyester compositions containing CHDM exhibit higher T_gs than the NPG homopolyesters and have higher moduli in the rubbery plateau that extend to higher temperatures than the NPG homopolyester. All compositions exhibited β-relaxations around −70 °C. In polyesters containing aromatic rings, relaxations in this range are typically associated with ring flips, however relaxations form cyclohexane moieties from CHDM are also known to appear in this area.[28] Compositions made with 3,4'BB have lower intensity β-relaxations than those exhibited by 4,4'BB. This is believed to be caused by an inhibited ability to rotate due to non-symmetrical ring substitution in the 3,4'BB moiety.[32-33] Recent research indicates a correlation between restricted molecular mobility in the 3,4'BB moiety and lower gas diffusivity.[3-4] Similarly, we observe an increase in sub-T_g transition intensity with higher CHDM content. When NPG is replaced with EG in semicrystalline 4,4'BB-50-EG-50-CHDM, β-relaxation intensity increases

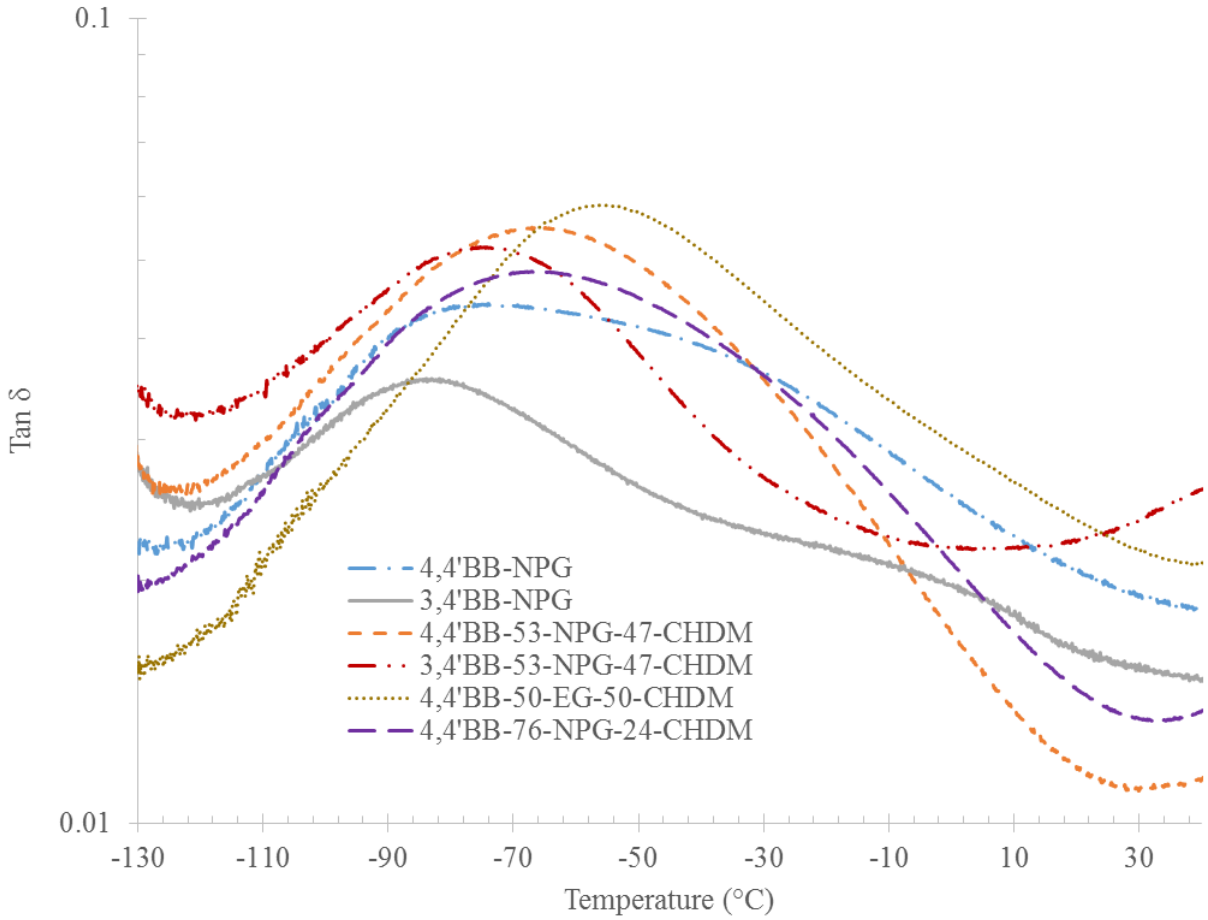

Figure 3-7. β-relaxations of samples probed by using DMA at 1 Hz with an oscillatory amplitude of 15 μm and 0.01 N static force.

Table 3-4. Summary of thermomechanical analysis results

Composition	**T_β (°C)**	**$T_{g,\ tan\ \delta}$ (°C)**	**$T_{g,\ DSC}$ (°C)**
4,4'BB-54-NPG-46-CHDM	–67	122	129
4,4'BB-76-NPG-24-CHDM	–67	113	120
3,4'BB-53-NPG-47-CHDM	–75	103	109
4,4'BB-50-EG-50-CHDM	–55	106	99
4,4'BB-NPG	–77	108	116
3,4'BB-NPG	–84	97	104

and shifts to a higher temperature. The shift to higher temperatures is consistent with the restricted mobility of semicrystalline compositions, however, the higher intensity of the β-relaxation in 4,4'BB-50-EG-50-CHDM indicates that NPG suppresses β-relaxations. CHDM is known to significantly increase the intensity of sub T_g-relaxations, which is commonly associated with the improvement in impact properties observed when EG is substituted with CHDM in PET.[19, 28]

Like other polymers, polyesters are non-Newtonian fluids that exhibit decreased viscosity with increasing shear rates. This shear thinning is an important property that affects processing techniques such as extrusion and injection blow molding.[34-35] Oscillation measurements provides a means to observe how a given composition responds over a range of different frequencies or shear rates. TTS is a powerful technique that allows the probing of frequencies over a large window of processing shear rates (1–10^5 1/s).[36] Master curves obtained with TTS (**Figure 3-8**) for several polyester compositions show complex viscosity η*, over a wide frequency range with a reference temperature of 280 °C. The temperature chosen was later used for melting blending and injection molding of multiple 4,4'BB-X-NPG-Y-CHDM batches containing 45–55 mol% NPG. Samples exhibited an increase in zero shear viscosity consistent with measured inherent viscosities. A significantly higher molecular weight made it not possible to view zero shear viscosity for 4,4'BB-53-NPG-47-CHDM. All polymer samples exhibited nearly identical shear thinning behavior past the Newtonian region, with CHDM and EG having no clearly discernable impact in shear thinning. This result contrasts with previously reported research comparing T-56-NPG-44-CHDM and PETG (31 mol% CHDM), where the NPG based copolyester exhibited greater shear thinning,[20] suggesting that shear thinning may be dominated by the large and rigid 4,4'BB unit.

Rheology was also used to probe the thermal stability of NPG based copolyesters relative to EG (**Figure 3-9).** Copolyesters containing NPG exhibited shallows drops in viscosity over a one hour period, contrasting significantly with 4,4'BB-50-EG-50-CHDM, which shows a much more rapid decline in viscosity. This demonstrates a marked difference in the thermal stability of NPG relative to EG.

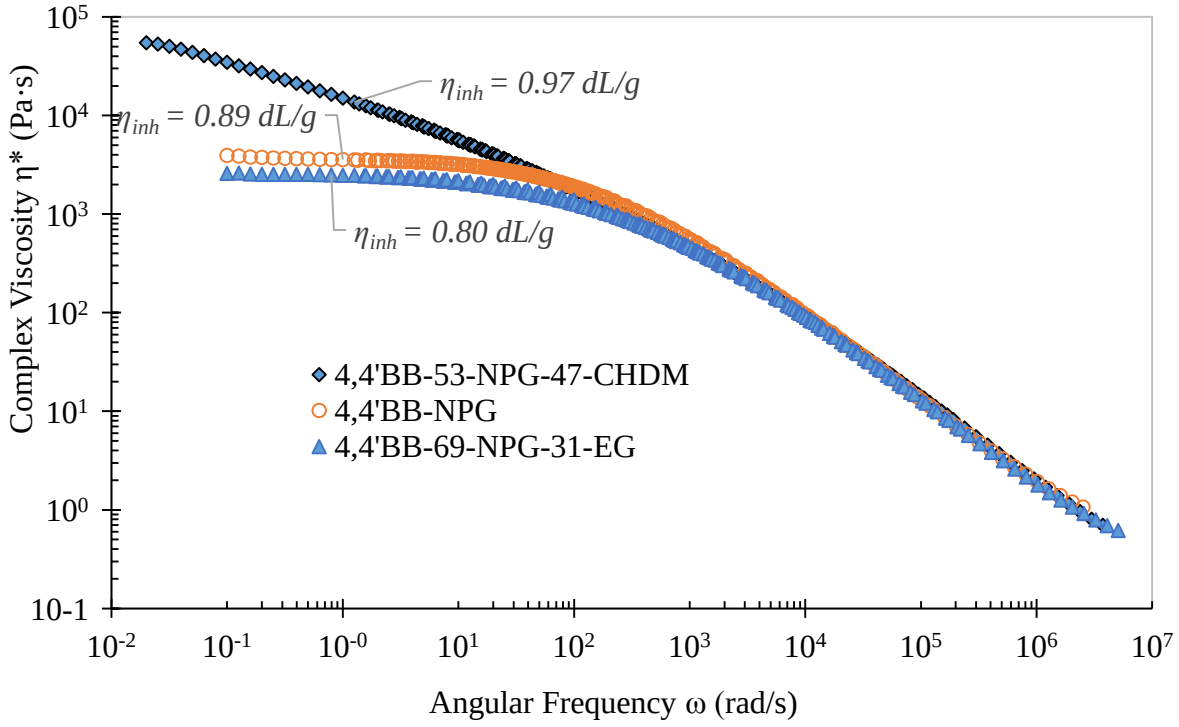

Figure 3-8. Time temperature superposition master curves of amorphous compositions at a reference temperature of 280 °C

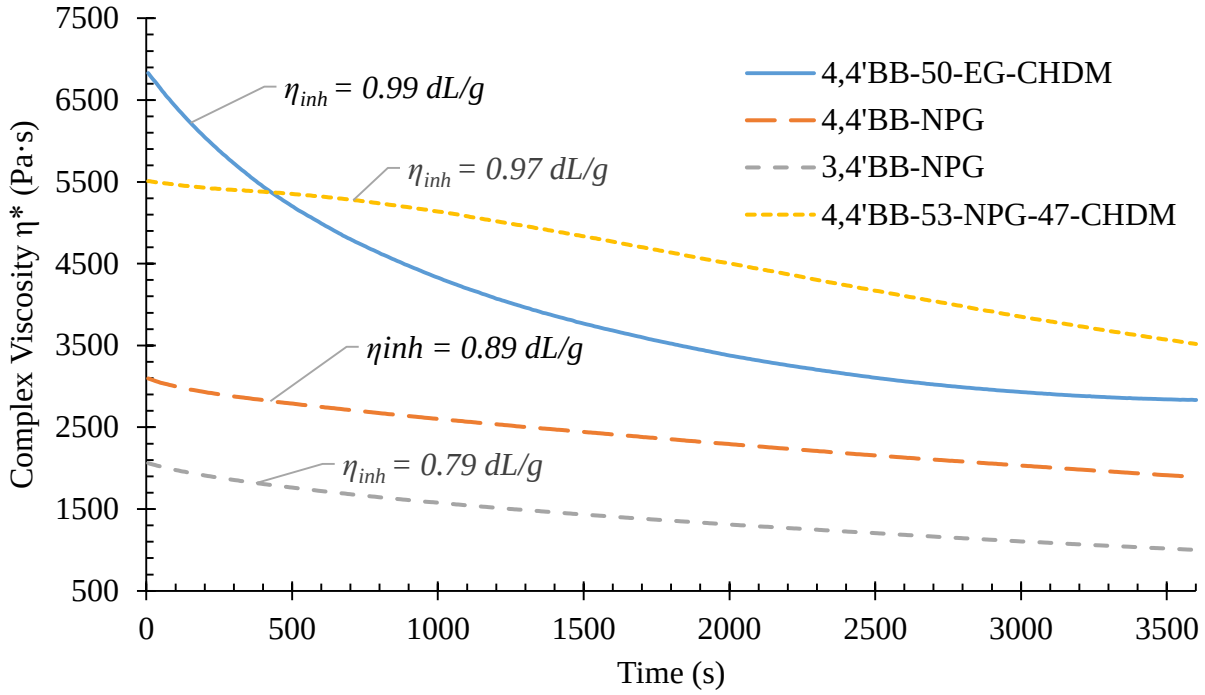

Figure 3-9. Time sweeps of copolyester compositions at 1 Hz and 280–290 °C

3.5.3 Melt Blending

Multiple batches of amorphous 4,4'BB-X-NPG-Y-CHDM samples were chosen and blended in the melt to produce a sufficient amount of material for the injection molding of dogbones for tensile analysis and impact bars for notched Izod impact testing (**Table 3-5**). The blending of batches was done so as to target compositions containing 45, 50 and 55 mol% NPG. This allowed the tracking of properties over small (5 mol%) incremental changes in composition. Batches were intentionally not dried before blending to observe how sensitive compositions were to moisture during melting. The batch containing the highest level of NPG (55 mol%) experienced the least degradation, having only lost 0.07 dL/g during blending, and the batch with the least amount of NPG experienced the most degradation, dropping by 0.16 dL/g below the weighted average of the combined batches.

Table 3-5. Compositions of batches combined in melt blending and the final composition of each blend

Batch	**mol% NPG**	η_{inh} **(dL/g)**	T_g **(°C)**
103	45	1.04	128
85	45	0.87	129
55	42	0.72	126
Weighted average	44	0.91	128
Blending results	45	0.75	

Batch	**mol% NPG**	η_{inh} **(dL/g)**	T_g **(°C)**
105 g	49	0.93	127
85 g	49	0.81	126
107 g	52	0.94	127
Weighted average	50	0.90	127
Blending results	50	0.75	

Batch	**mol% NPG**	η_{inh} **(dL/g)**	T_g **(°C)**
54	54	0.74	126
90	54	0.93	126
Weighted average	54	0.86	126
Blending results	55	0.79	

3.5.4 Mechanical Properties

Measuring crosshead displacement was used to estimate the Young's modulus in samples punched from quenched, compression molded films (**Table 3-6**). All compositions were amorphous except for 4,4'BB-50-EG-50-CHDM, which was crystalline/white, despite being quenched in an ice bath immediately after removing from the melt press. Crystalline polyesters typically have higher yield stress, modulus and stress at break when compared to amorphous polymers of the same composition. Crystallinity also typically decreases elongation to break and impact strength. Polyesters with 3,4'BB exhibited higher yield stresses and moduli relative to the 4,4'BB compositions. This trend has been observed before in the literature.[3-4] Copolyester compositions exhibit higher yield stress and Young's modulus than amorphous PET and similar stress at break. When compared to PETG amorphous copolyester, 4,4'BB-54-NPG-46-CHDM has

Table 3-6. Tensile properties of select copolyesters. Tensile analysis followed ASTM testing method D638. Dogbones where punched from 0.55 mm compression molded films by using a D638-V punch.

Sample	Yield Stress (Mpa)	Tensile Stress at Break (MPa)	Elongation to Break (%)	Young's Modulus (MPa)
4,4'BB-NPG	46.7 ± 0.3	49.0 ± 3.4	139.4 ± 21.5	1617.2 ± 56.4
3,4'BB-NPG	63.2 ± 0.9	53.4 ± 4.0	131.2 ± 23.5	2141.0 ± 62.9
4,4'BB-54-NPG-46-CHDM	59.6 ± 0.6	64.5 ± 4.4	142.1 ± 16.8	1782.5 ± 43.8
3,4'BB-53-NPG-47-CHDM	62.5 ± 0.4	56.8 ± 1.1	114.3 ± 5.6	1887.2 ± 66.1
PET 418 (tensile bars) (HL)	53.4 ± 1.7	61.2 ± 1.4	387 ±23	1600 ± 93
3,4'BB-CHDM (RM)	46.5 ± 1.7		120 ± 21	2040 ± 78
3,4'BB-EG (RM)	74.4 ± 0.25		163	2690 ± 280
PETG (31 % CHDM)*	52	59	400	1900
T-52-NPG-48-CHDM[20]	65	60	180	1919

*Eastar Copolyester 6763 Product-Technical Data Sheet

higher yield stress and break stress, but has lower elongation and Young's modulus. A comparison of the 3,4'BB homopolyester containing EG, CHDM and NPG shows NPG to consistently have mechanical properties between those of CHDM and EG. A small flexible monomer such as EG might be expected to pack more efficiently than either NPG, which has two methyl units that disrupt crystallinity, or CHDM, which is observed to have significant β-relaxations below the T_g. This correlates with CHDM producing a less dense material than PET.[19]

Producing sufficient amounts of material on a laboratory scale for injection molding is often time consuming and can requires the combination of several batches to achieve the quantities needed. As such, only the highest T_g composition was chosen for more in depth analysis. Injection molded tensile bars typically produce more consistent results over those produce from dogbones punched from compression molded films, since larger quantities of material are less subject to the influences of material defects. The tensile results (**Table 3-7**) showed trends opposite to those observed from compression molded films, with elongation to break increasing with NPG content

Table 3-7. Tensile properties of injection molded dogbones produced from melt blended copolyester compositions.

mol% NPG	Yield Strength (MPa)	Elongation to Break	Young's Modulus (MPa)
55	54.93	40	1950
50	56.17	35	1996
45	61.72	17	2173

and yield strength along with Young's modulus decreasing with higher ratios of NPG. It is possible that these unexpected results are due to a small level of crystallization present within the injection molded samples. DSC analysis of cross sections cut from the center of dogbones revealed no sign of melting on the first scan and no recrystallization was observed for the composition analyzed under DMA. Transparent sections were cut from notched Izod test bars and placed within a vacuum oven at 140 °C (10–15 °C) for 48 hours, however, no visible signs of crystallization was detected. Izod impact testing was originally performed by using a 2.03 ft-lb hammer resulting in a no break. Partial breaks (**Figure 3-24S**) were obtained by using a 4.06 ft-lb hammer**.** These mechanical properties compare favorably to similar terephthalate copolyesters, with T-52-NPG-48-CHDM copolyester[20] testing no break at >16 ft-lb/in and Lexan 9440 (12–16 ft-lb/in). It is important to note that the impact strength in **Figure 3-10** increases with higher mol% NPG in the backbone. This is unexpected as CHDM is traditionally known to improve impact properties of polymeric materials and produces larger β-relaxations relative NPG. Izod impact bars of compositions containing 50, and 55 mol% NPG are bars with 55 mol% CHDM indicating that a small amount of crystallization may be influencing impact test results. The tendency of NPG to disrupt crystallization far outweighs that of CHDM, which may be producing a higher impact material by ensuring no crystallization occurs during completely clear to visual inspection, however, a small degree of hazing is visible in test injection molding.

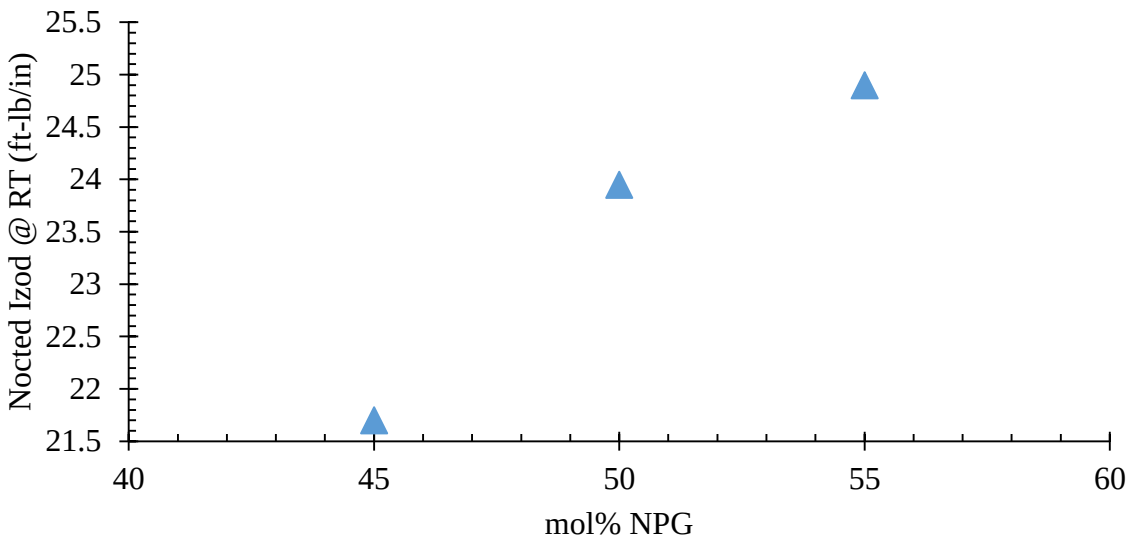

Figure 3-10. Notched Izod impact results for 4,4'BB-X-NPG-X-CHDM copolyesters

3.6 Conclusions

Melt polycondensation produced novel amorphous 3,4′BB and 4,4′BB polyesters modified with NPG, CHDM, EG. An amorphous copolyester composition was synthesized with a T_g as high as 129 °C and thermal stability above 395 °C. DMA showed decreases in the β-relaxation peak intensity at −70 °C with NPG and 3,4′BB content, indicating decreased short range molecular mobility. Rheological analysis showed improved thermal stability in NPG based copolyesters relative to EG. Melting blending of undried NPG copolyesters was performed with minimal decrease in inherent viscosity. Notched Izod impact analysis showed partial break and no break behavior.

3.7 Acknowledgements

This work is supported by the Department of Chemistry and the Macromolecules Innovation Institute (MII) at Virginia Tech. The authors acknowledge Charles S. Carfagna Jr. of the Macromolecular Materials Discovery Center (MMDC) at Virginia Tech for help with thermal

analysis. The authors thank Professor Timothy E. Long's research group at Virginia Tech for help with thermal and mechanical analysis

3.8 References

1. Izard, E. F., Effect of chemical structure on physical properties of isomeric polyesters. *J. Polym. Sci., Part A: Polym. Chem.* **1952,** *9* (1), 35–39.

2. Mang, M. N.; Brewbaker, J. L. Thermoplastic polyesters containing biphenylene linkages. (The Dow Chemical Company). U.S. Patent 5,138,022, 1992.

3. Mondschein, R. J.; Dennis, J. M.; Liu, H.; Ramakrishnan, R. K.; Nazarenko, S.; Turner, S. R.; Long, T. E., Synthesis and characterization of amorphous bibenzoate (co)polyesters: permeability and rheological performance. *Macromolecules* **2017,** *50* (19), 7603–7610.

4. Edling, H. E.; Liu, H.; Sun, H.; Mondschein, R. J.; Schiraldi, D. A.; Long, T. E.; Turner, S. R., Copolyesters based on bibenzoic acids. *Polymer* **2018,** *135*, 120–130.

5. Liu, R. Y. F.; Hu, Y. S.; Hibbs, M. R.; Collard, D. M.; Schiraldi, D. A.; Hiltner, A.; Baer, E., Improving oxygen barrier properties of poly(ethylene terephthalate) by incorporating isophthalate. I. Effect of orientation. *J. Appl. Polym. Sci.* **2005,** *98* (4), 1615–1628.

6. Hu, Y. S.; Liu, R. Y. F.; Schiraldi, D. A.; Hiltner, A.; Baer, E., Oxygen barrier properties of copolyesters containing a mesogenic monomer. *Macromolecules* **2004,** *37* (6), 2136–2143.

7. Liu, R. Y. F.; Hu, Y. S.; Hibbs, M. R.; Collard, D. M.; Schiraldi, D. A.; Hiltner, A.; Baer, E., Comparison of statistical and blocky copolymers of ethylene terephthalate and ethylene 4,4′-bibenzoate based on thermal behavior and oxygen transport properties. *J. Polym. Sci. Part B: Polm. Phys.* **2003,** *41* (3), 289–307.

8. Ma, H.; Hibbs, M.; Collard, D. M.; Kumar, S.; Schiraldi, D. A., Fiber spinning, structure, and properties of poly(ethylene terephthalate-co-4,4‘-bibenzoate) copolyesters. *Macromolecules* **2002,** *35* (13), 5123–5130.

9. Hu, Y. S.; Liu, R. Y. F.; Rogunova, M.; Schiraldi, D. A.; Nazarenko, S.; Hiltner, A.; Baer, E., Oxygen-barrier properties of cold-crystallized and melt-crystallized poly(ethylene terephthalate-co-4,4′-bibenzoate). *J. Polym. Sci. Part B: Polm. Phys.* **2002,** *40* (22), 2489–2503.

10. Polyakova, A.; Liu, R. Y. F.; Schiraldi, D. A.; Hiltner, A.; Baer, E., Oxygen-barrier properties of copolymers based on ethylene terephthalate. *J. Polym. Sci., Part B Polym. Phys.* **2001,** *39* (16), 1889–1899.

11. Polyakova, A.; Connor, D. M.; Collard, D. M.; Schiraldi, D. A.; Hiltner, A.; Baer, E., Oxygen-barrier properties of polyethylene terephthalate modified with a small amount of aromatic comonomer. *J. Polym. Sci. Part B Polym. Phys* **2001,** *39* (16), 1900–1910.

12. Gore, A. C.; Chappell, V. A.; Fenton, S. E.; Flaws, J. A.; Nadal, A.; Prins, G. S.; Toppari, J.; Zoeller, R. T., Executive summary to EDC-2: the endocrine society's second scientific statement on endocrine-disrupting chemicals. *Endocr. Rev.* **2015,** *36* (6), 593–602.

13. Nelson, A. M.; Long, T. E., A perspective on emerging polymer technologies for bisphenol-A replacement. *Polym. Int.* **2012,** *61* (10), 1485–1491.

14. Scott, C. E.; Morris, J. C.; Bradley, J. R. Clear blends of polycarbonates and polyesters. (Eastman Chemical Company). U.S. Patent 6,037,424, 2000.

15. Scott, C. E.; Morris, J. C.; Bradley, J. R. Clear polycarbonate and polyester blends. (Eastman Chemical Company). U.S. Patent 6,043,322, 2000.

16. Crawford, E. D.; Porter, D. S.; Connell, G. W. Polyester compositions wich comprise cyclobutanediol having certain cis/trans ratios. (Eastman Chemical Company). Eur. Pat. 2156934 2011.

17. Barton, B. F.; Shackelford, D. B. Process for the preparation of copolyesters based on 2,2,4,4-tetramethyl-1,3-cyclobutanediol and 1,4-cyclohexanedimethanol. (Eastman Chemical Company). WO 2008140705, 2008.

18. Crawford, E. D.; Pecorini, T. J.; Mcwilliams, D. S.; Porter, D. S.; Connell, G. W.; Germroth, T. C.; Barton, B. F.; Shackelford, D. B. Polyester compositions containing cyclobutanediol having a certain combination of inherent viscosity and moderate glass transition temperature and articles made therefrom. (Eastman Chemical Company). WO 2007053549, 2007.

19. Turner, S. R.; Seymour, R. W.; Dombroski, J. R., Amorphous and crystalline polyesters based in 1,4-cyclohexanedimethanol. In *Modern Polyesters: Chemistry and Technology of Polyesters and Copolyesters*, Scheirs, J.; Long, T., Eds. John Wiley & Sons: West Sussex, England, 2003; pp 267–292.

20. Turner, S. R.; Milburn, J. T.; Seymour, R. W.; Kab Sik Seo Amorphous copolyesters. (Eastman Chemical Company). U.S. Patent 7,026,027, 2006.

21. Maetens, D., Weathering degradation mechanism in polyester powder coatings. *Prog. Org. Coat.* **2007,** *58* (2), 172–179.

22. Plage, B.; Schulten, H. R., Thermal degradation and mass-spectrometric fragmentation processes of polyesters studied by time/temperature-resolved pyrolysis-field ionization mass spectrometry. *Macromolecules* **1990,** *23* (10), 2642–2648.

23. Soccio, M.; Lotti, N.; Finelli, L.; Gazzano, M.; Munari, A., Neopenthyl glycol containing poly(propylene terephthalate)s: structure–properties relationships. *J. Polym. Sci. Part B: Polym. Phys.* **2008,** *46* (2), 170–181.

24. Kelsey, D. R.; Scardino, B. M.; Grebowicz, J. S.; Chuah, H. H., High impact, amorphous terephthalate copolyesters of rigid 2,2,4,4-tetramethyl-1,3-cyclobutanediol with flexible diols. *Macromolecules* **2000,** *33* (16), 5810–5818.

25. Booth, C. J.; Kindinger, M.; McKenzie, H. R.; Handcock, J.; Bray, A. V.; Beall, G. W., Copolyterephthalates containing tetramethylcyclobutane with impact and ballistic properties greater than bisphenol A polycarbonate. *Polymer* **2006,** *47* (18), 6398–6405.

26. Dennis, J. M.; Fazekas, N. A.; Mondschein, R. J.; Ramakrishnan, R.; Nazarenko, S.; Long, T. E., Influence of cyclobutane segments in cycloaliphatic decahydronaphthalene-containing copolyesters. *High Perform. Polym.* **2017,** *29* (6), 750–756.

27. Dennis, J. M.; Enokida, J. S.; Long, T. E., Synthesis and characterization of decahydronaphthalene-containing polyesters. *Macromolecules* **2015,** *48* (24), 8733–8737.

28. Lee, S.-S.; Yee, A. F., Temperature-dependent transition of deformation mode in poly(1,4-cyclohexylenedimethylene terephthalate)/poly(ethylene terephthalate) copolymers. *Macromolecules* **2003,** *36* (18), 6791–6796.

29. Wyzgoski, M. G.; Yeh, G. S. Y., Origin of impact strength in polycarbonate: I. Effect of crystallization and residual solvent. *Int. J. of Polym. Mater.* **1974,** *3* (2), 133–148.

30. Moad, G.; Groth, A.; O'Shea, M. S.; Rosalie, J.; Tozer, R. D.; Peeters, G., Controlled synthesis of block polyesters by reactive extrusion. *Macromol. Symp.* **2003,** *202* (1), 37–46.

31. Meurisse, P.; Noel, C.; Monnerie, L.; Fayolle, B., Polymers with mesogenic elements and flexible spacers in the main chain: Aromatic-aliphatic polyesters. *Br. Polym. J.* **1981,** *13* (2), 55–63.

32. Burgess, S. K.; Kriegel, R. M.; Koros, W. J., Carbon dioxide sorption and transport in amorphous poly(ethylene furanoate). *Macromolecules* **2015,** *48* (7), 2184–2193.

33. Burgess, S. K.; Leisen, J. E.; Kraftschik, B. E.; Mubarak, C. R.; Kriegel, R. M.; Koros, W. J., Chain mobility, thermal, and mechanical properties of poly(ethylene furanoate) compared to poly(ethylene terephthalate). *Macromolecules* **2014,** *47* (4), 1383–1391.

34. Pang, K.; Kotek, R.; Tonelli, A., Review of conventional and novel polymerization processes for polyesters. *Prog. Polym. Sci.* **2006,** *31* (11), 1009–1037.

35. Callander, D. D., *Modern Polyesters: Chemistry and Technology of Polyesters and Copolyesters*. John Wiley and Sons: West Sussex, Endland, 2003.

36. Franck, A., Understanding rheology of thermoplastic polymers. TA Instruments.

3.9 Chapter 3 Supplemental Material

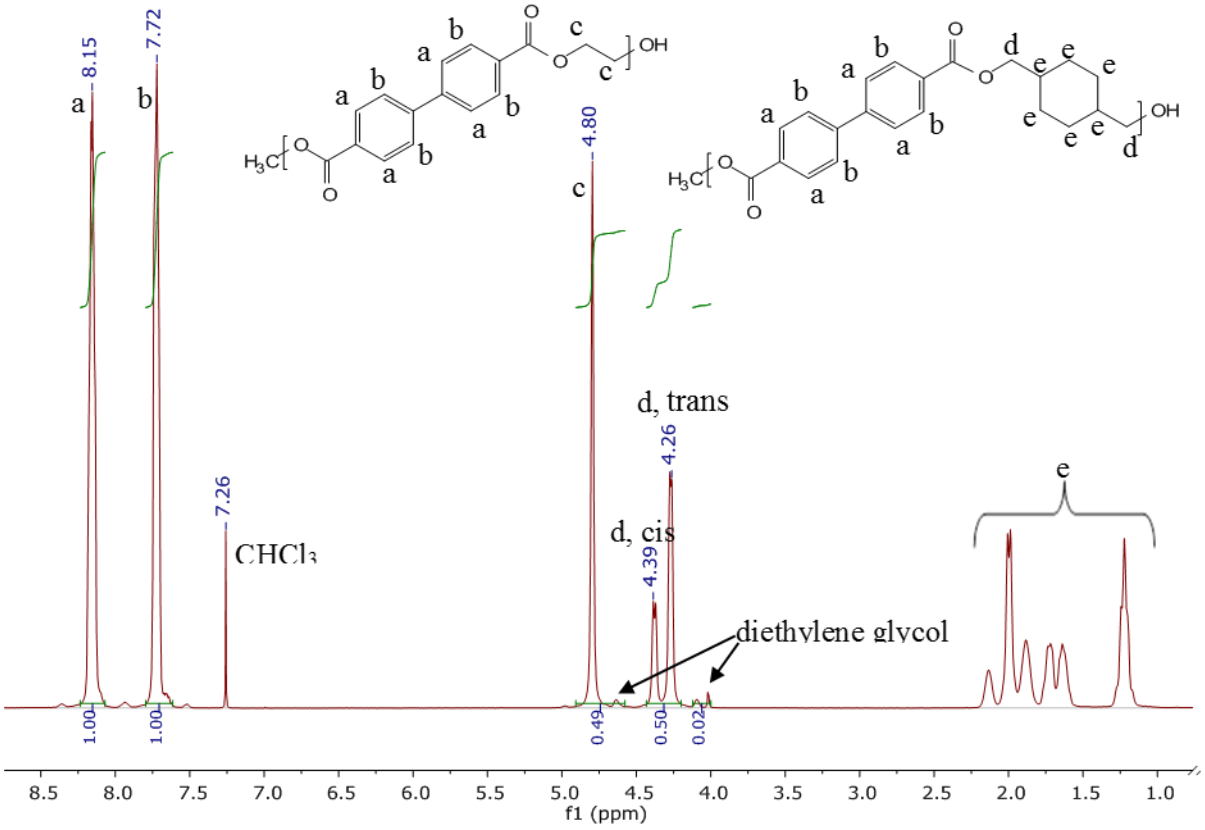

Figure 3-11S. ^{1}H NMR spectrum of 4,4'BB-50-EG-50-CHDM in 95:5 CDCl3:TFA-*d*

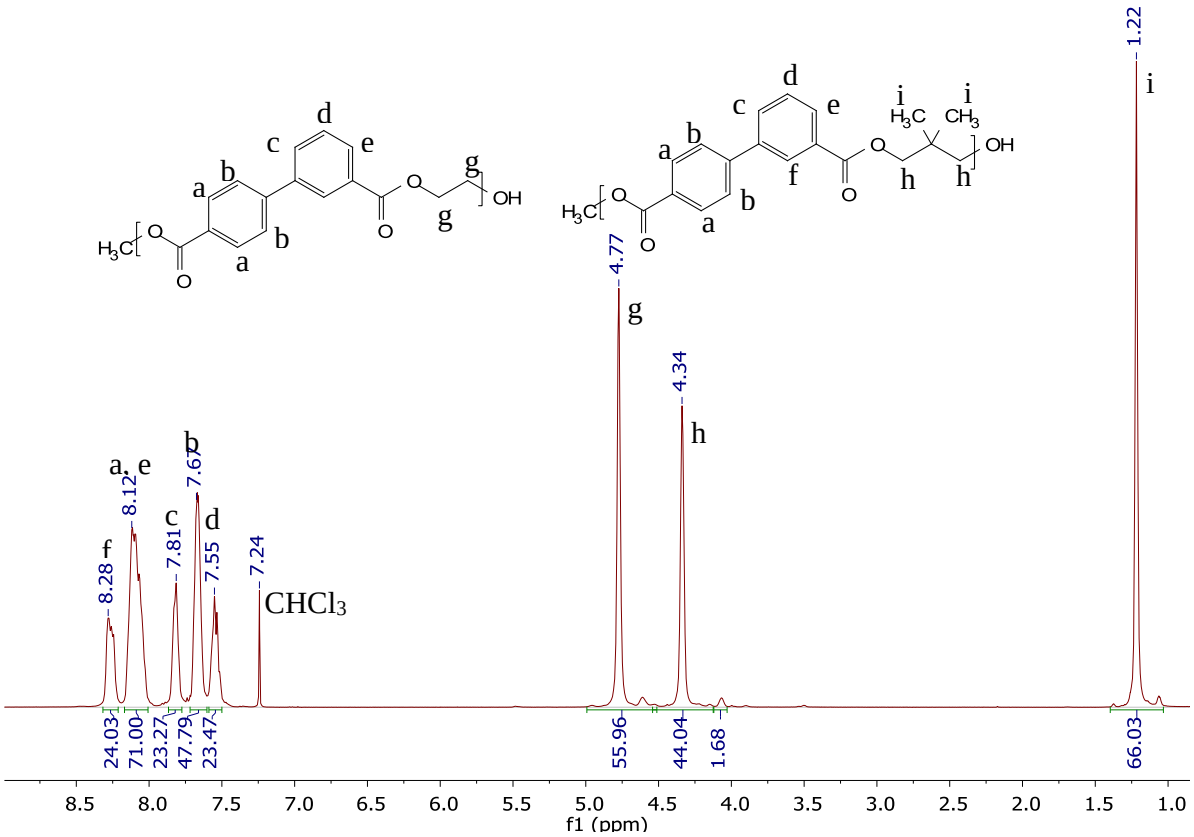

Figure 3-12S. ^{1}H NMR spectrum of 3,4'BB-44-NPG-56-CHDM in 95:5 CDCl3:TFA-*d*

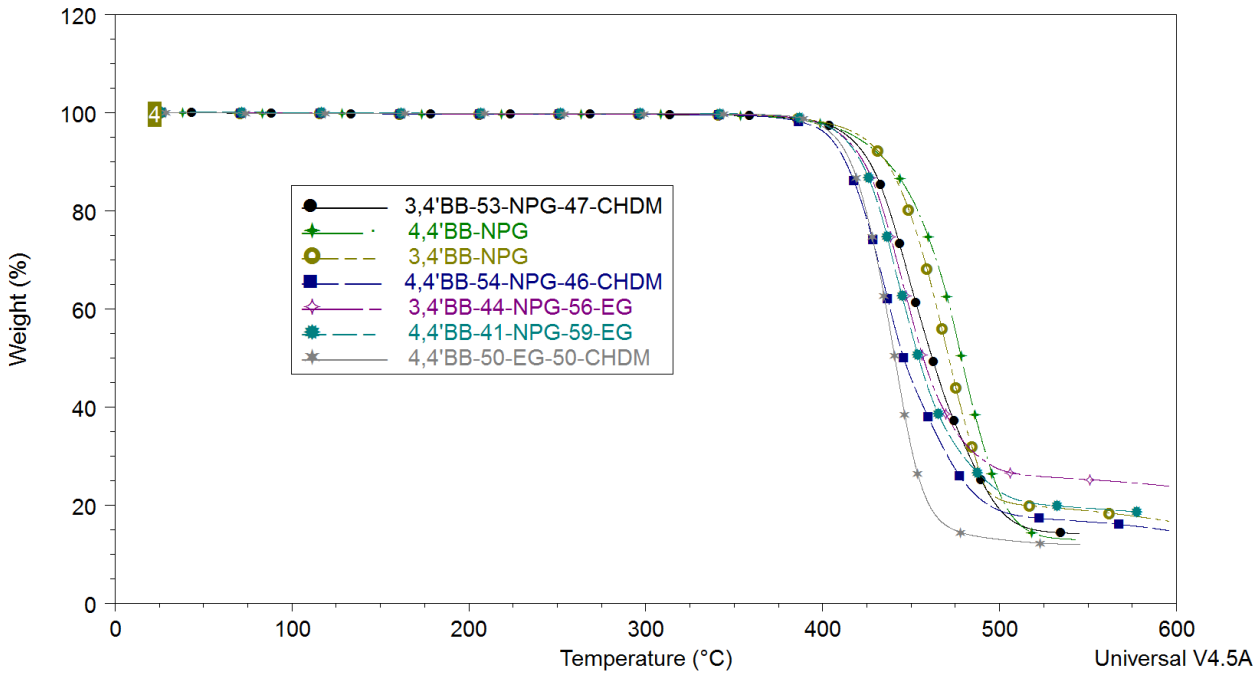

Figure 3-13S. Single step decomposition of copolyesters observed with TGA under nitrogen and 10 °C/min heating rate

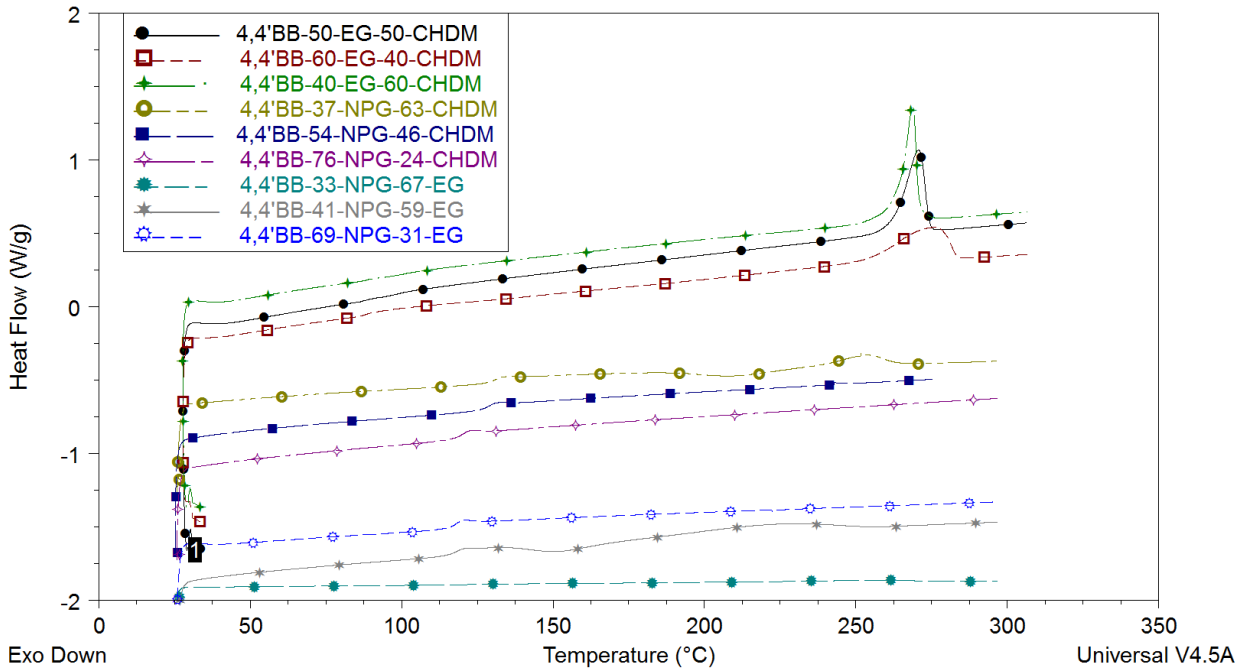

Figure 3-14S. DSC traces of 4,4'BB based copolyesters. Taken of the second heating ramp under nitrogen with 10 °C/min heating and cooling rates.

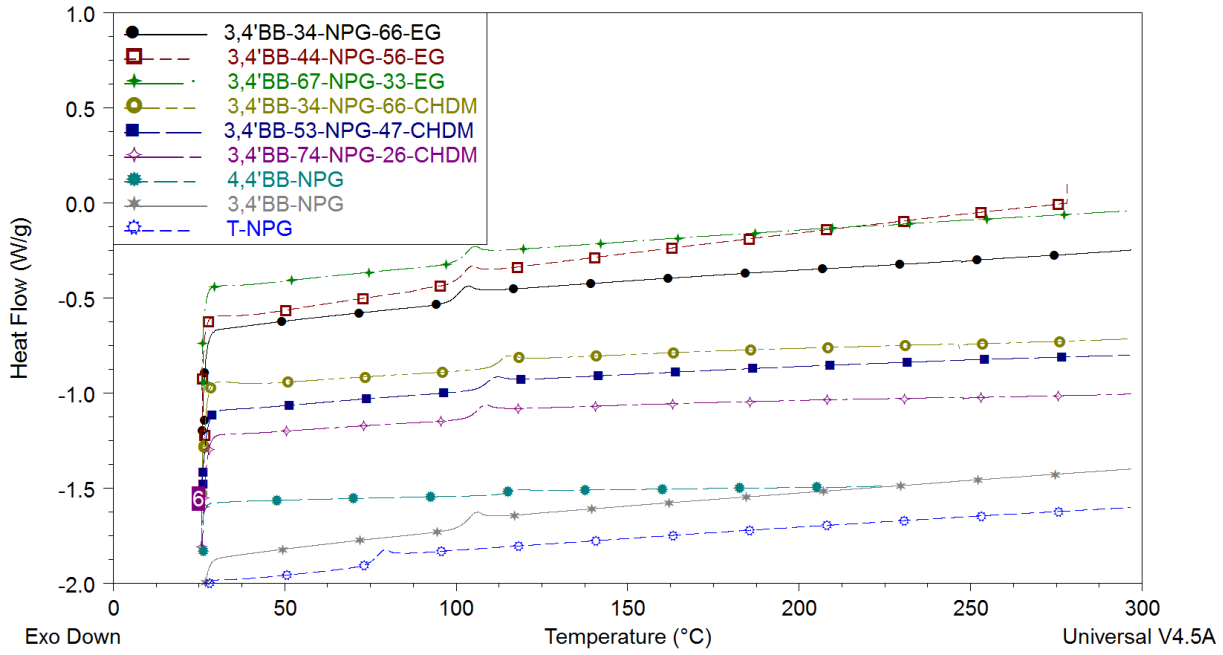

Figure 3-15S. DSC traces of 3,4'BB based copolyesters and NPG based homopolyesters. Taken of the second heating ramp under nitrogen with 10 °C/min heating and cooling rates.

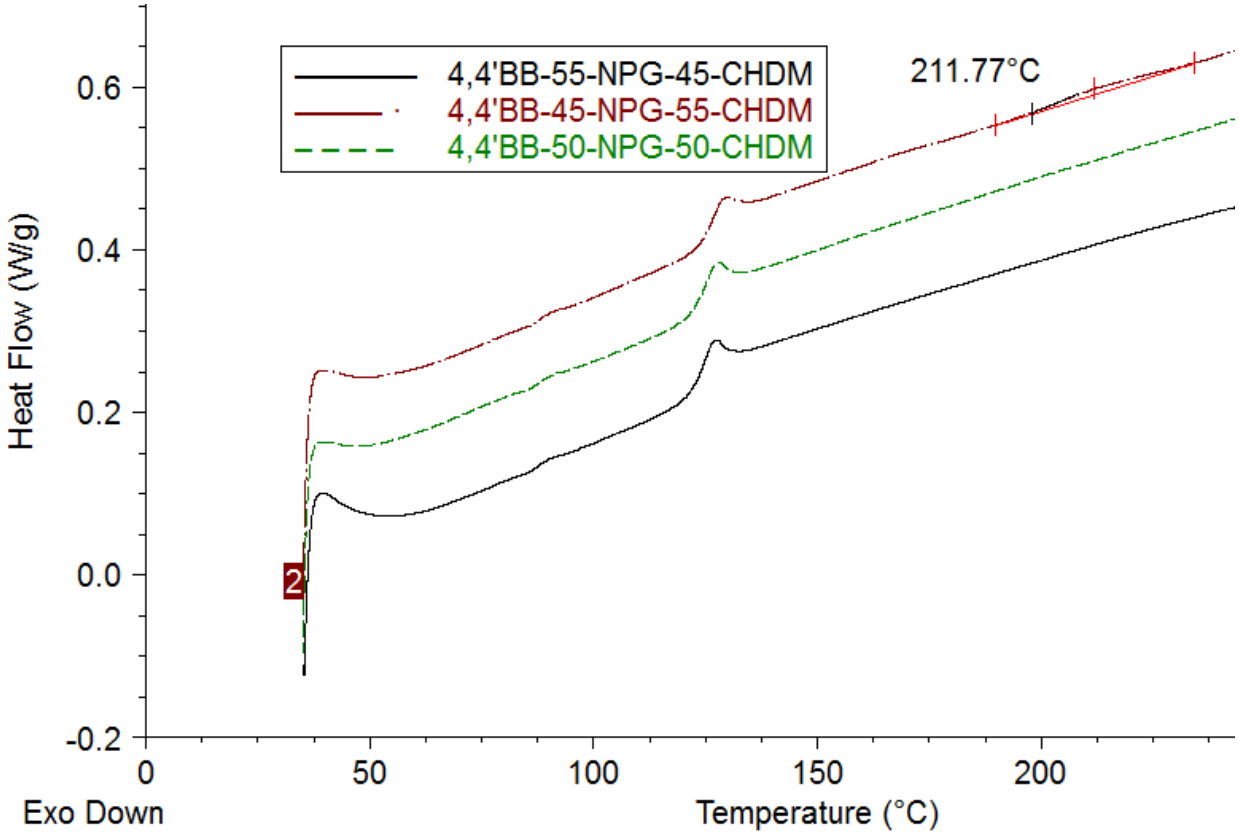

Figure 3-16S. First scan (10 °C/min) DSC traces of 4,4'BB-45-NPG-55-CHDM, 4,4'BB-50-NPG-05-CHDM and 4,4'BB-55-NPG-45-CHDM copolyesters after annealing in a vacuum oven at 150 °C for 145 h.

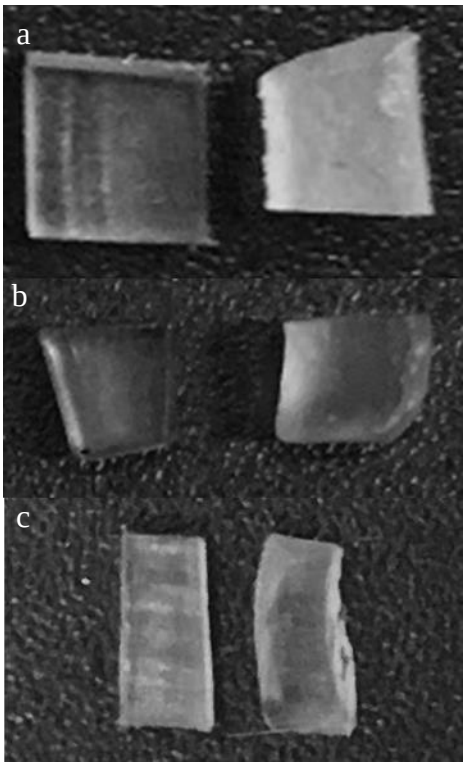

Figure 3-17S. Images of 4,4'BB-45-NPG-55-CHDM (a), 4,4'BB-50-NPG-50-CHDM (b) and 4,4'BB-55-NPG-45-CHDM (c) copolyesters before (left) and after (right) annealing in a vacuum oven at 150 °C for 145 h.

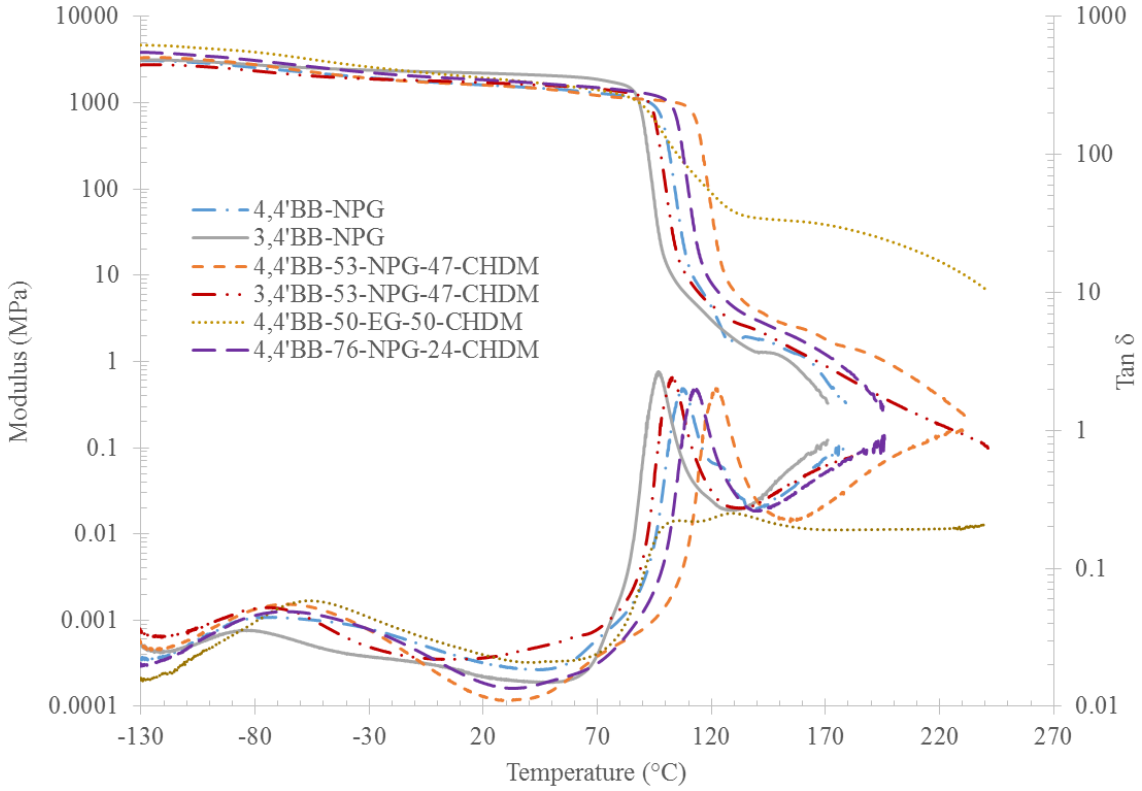

Figure 3-18S. DMA traces of polyester modulus and tan δ

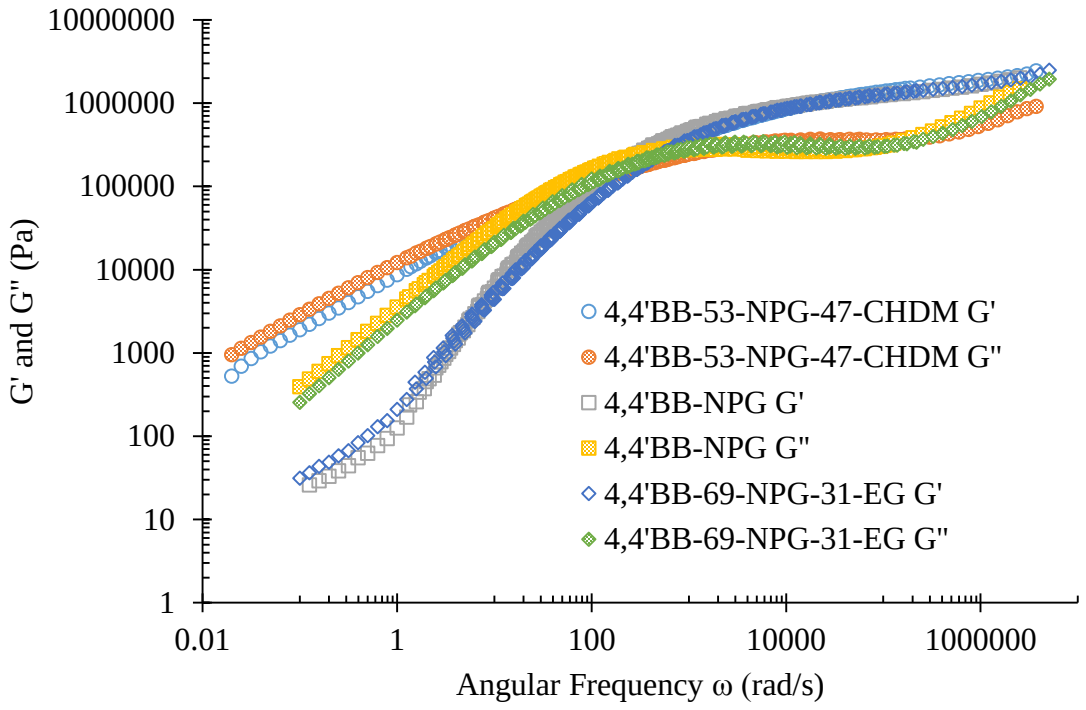

Figure 3-19S. Storage (G') and Loss (G") modulus master curves of (co) polyesters over a wide frequency range.

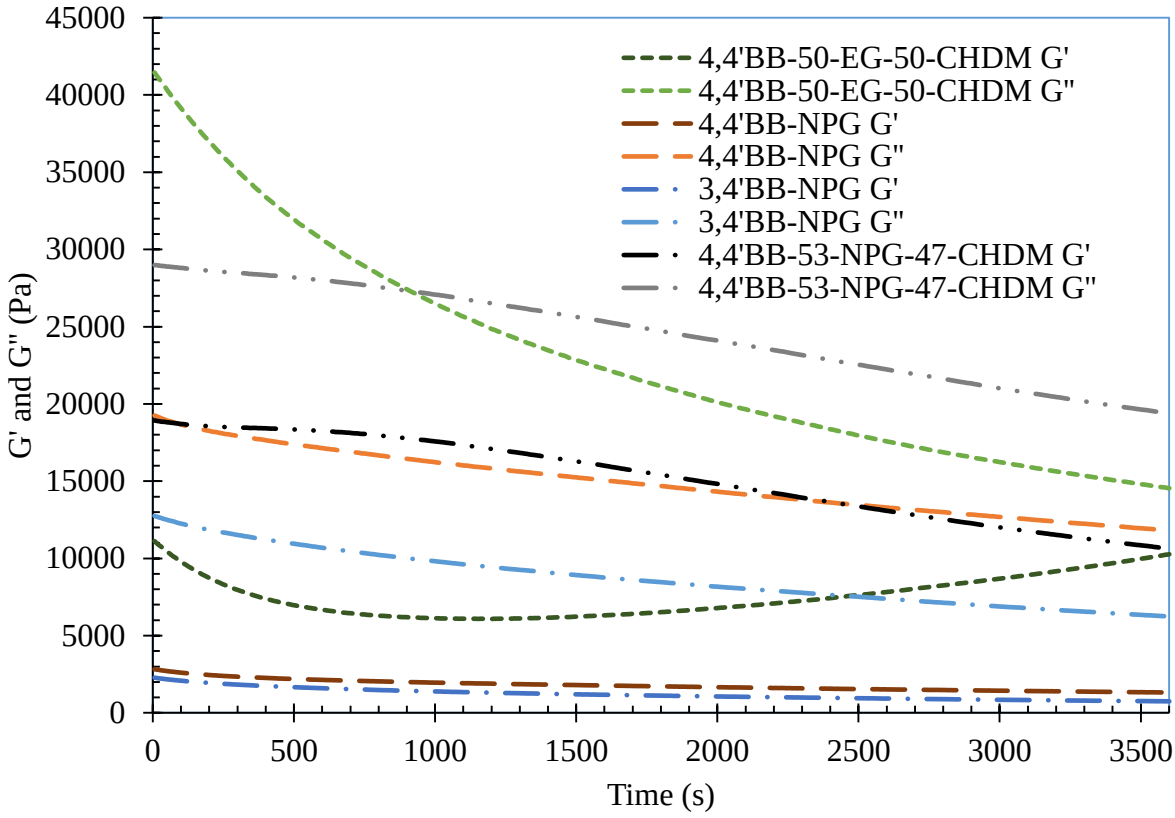

Figure 3-20S. Storage (G') and loss (G'') modulus over time at 280 °C

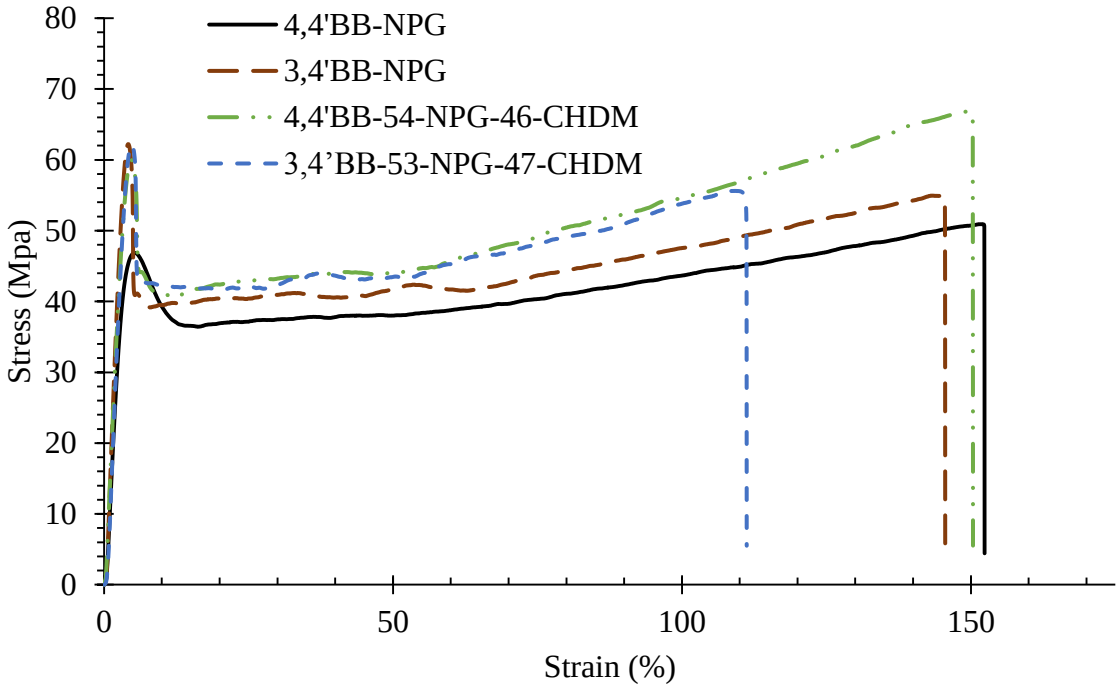

Figure 3-21S. Stress vs. strain curves. Tensile analysis followed ASTM testing method D638. Dogbones where punched from 0.55 mm compression molded films by using a D638-V punch.

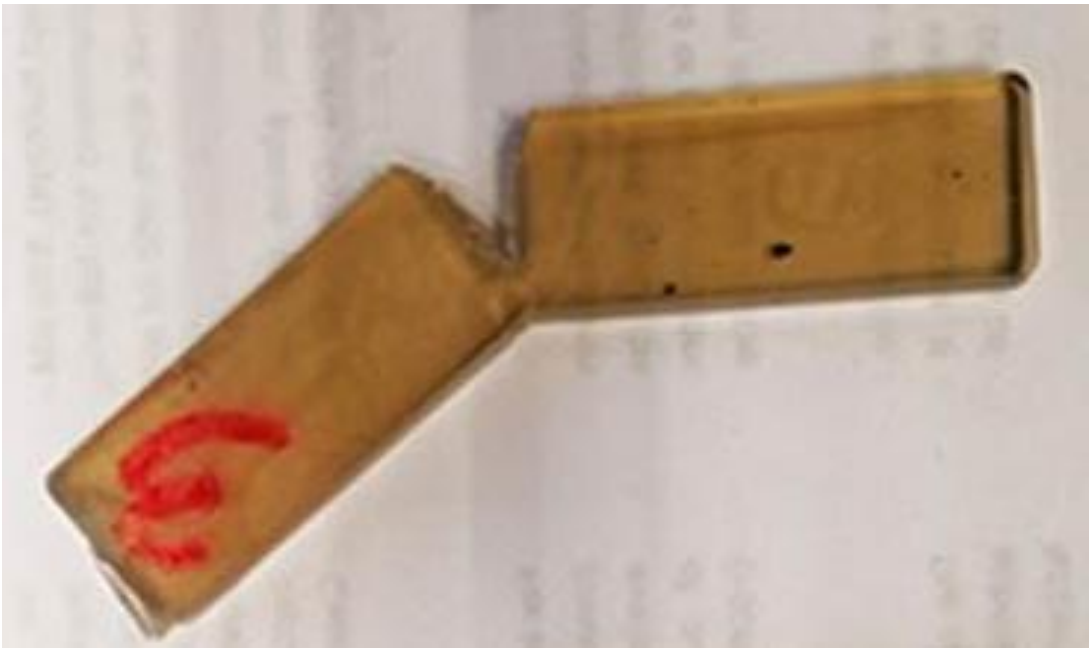

Figure 3-22S. Partial break notched Izod test samples after 4.06 ft-lb hammer test of 4,4'BB-50-NPG-50-CHDM copolyester.

Chapter 4. Synthesis and Crystallization Behavior of Rigid Copolyesters With Biphenyl-4,4'-dicarboxylate and 2,6-Naphthalenedicarboxylate in the Main Chain

(To be submitted to J. Polym. Sci., Part B: Polym. Phys.)

4.1 Authors

H. Eliot Edling, Matthew R. Vincent, Hervé Marand, Kevin Barr, S. Richard Turner

Department of Chemistry, Macromolecules and Interfaces Institute, Virginia Tech, Blacksburg, Virginia 24061-0212 Correspondence to: S. R. Turner (srturner@vt.edu)

4.2 Abstract

Structurally rigid copolyester thermoplastics were synthesized containing the diol 1,4-cyclohexanedimethanol (CHDM) and the diesters dimethyl biphenyl-4,4'-dicarboxylate (4,4′BB) and dimethyl 2,6-naphthalenedicarboxylate (DMN) via conventional melt transesterification. Both DMN and 4,4′BB produce high melting temperature (>300 ˚C) homopolymers that, when copolymerized with another monomer, allow the tuning of polymer thermal properties, such as glass transition and melting temperatures, and degree of crystallinity, simply by adjusting the composition.^{1}H NMR spectroscopy verified the copolymer composition and conventional differential scanning calorimetry (CDSC) showed all compositions to exhibit multiple endotherms upon heating. Dynamic mechanical analysis (DMA) enabled the observation of α, β and γ relaxations and confirmed the occurrence of cold crystallization observed by calorimetry. A single composition with 60/40 DMN/4,4′BB molar ratio was chosen for further thermal analysis using conventional DSC (CDSC) and fast DSC (FDSC) to investigate the origin of the multiple endotherm behavior. While three endotherms are observed for low heating rates, the upper two endotherms appear to merge at heating rates ca. 1 to 5 °C/s and a single endotherm remains above

heating rates ca. 10 to 50 °C/s. While the behavior of the upper two endotherms is consistent with the mechanism of melting-recrystallization-remelting, the low endotherm is likely to be associated with the melting of constrained secondary crystals.

4.3 Introduction

Polyesters have weak intermolecular interactions when compared to polymer materials synthesized with monomers containing more polar interactions or containing hydrogen bonding such as in polyamides and polyurethanes. As a result, polyester properties are more sensitive to variations in structure, symmetry and conformational features, leading to many efforts to quantify the structure–property relationships of polyesters.[1-9] Considerable research shows that rigid monomers with high aromatic content increase the rigidity of the polymer backbone to a greater degree than aliphatic moieties, and can yield thermoplastics with high melting temperatures (>300 ˚C).[4, 7] High melting temperature polyesters have excellent potential as high performance materials and, in cases where the melting temperature of a homopolyester is too high to process without significant degradation or less crystallinity is desired, comonomers can be added to reduce the melting temperature while maintaining many of the other desirable properties of the polymer (e.g. high T_g).[10]

Multiple melting endotherms are commonly observed in DSC heating traces of polyesters and copolyesters,[7, 11] and of many other polymers including isotactic polystyrene,[12-14] polyether ether ketones,[15-16]polycarbonate,[17-19] and syndiotactic polypropylene.[20] Multiple melting behavior can be associated with either the melting of distinct populations of crystals exhibiting different thermal stabilities or with the process of melting-recrystallization-remelting (MRR).[11, 15, 17-18, 21] The MRR phenomenon can be observed when the heating rate is sufficiently low that

recrystallization can take place during heating in the DSC subsequent to melting of the initial crystal population. Since recrystallization occurs at a higher temperature than the initial crystallization, melting of this new crystal population or remelting is observed at a higher temperature than the initial melting.[14] Depending on the heating rate and the initial crystallization temperature, the phenomenon can produce a broadened melting endotherm or more commonly two separate endotherms, with the low temperature endotherm associated with the melting of crystals originally present within the material and a higher temperature endotherm associated with the melting of crystals formed during the heating scan.[11-12, 14, 17] Higher heating rates lead to less time for recrystallization, hence, resulting in a relatively smaller endotherm observed at relatively lower temperature.

The observation of multiple endothermic transitions in the heating scan of a semicrystalline polymer can also be associated with the melting of separate populations of crystals belonging to the same or different phases. The lower temperature endotherm, when observed 10–40 ˚C above the isothermal crystallization temperature, has often been associated with the melting of less stable, secondary crystals constrained by primary crystals.[13, 15, 17] When multiple melting endotherms result from separate populations of crystals, the relative size of the endotherms does not change with heating rate in the same way as for MRR. A number of homopolymers and copolymers actually display three endotherms during heating in a conventional DSC,[11, 15, 17] where heating rates are generally less than 180 ˚C/min.[22] In this case, the lowest endothermic peak, often called the annealing peak, is observed some 10-40 ˚C above the crystallization temperature while the upper two endotherms are located at much higher temperature. An increase in heating rate typically leads to a shift of the lowest endotherm to higher temperature and a change in the relative locations and areas of the upper endotherms. Until recently such behavior was thought to be associated with

the melting of two populations of crystals: secondary crystals at the lowest endotherm and primary crystals at the intermediate endotherm. The upper endotherm was assigned to the melting of crystals formed by recrystallization during the heating scan. However, this explanation seemed to be contradicted by results of experiments carried out on it-PS and PET with fast calorimetry. Recent developments in FDSC instrumentation with thin film calorimetry have allowed for heating rates as high as 10^6 °C/s.[23] The Mettler-Toledo Flash^{TM} DSC 1, used in this study, is capable of heating rates as high as 2×10^4 °C/s and cooling rates as high as 4×10^3 °C/s. A detailed review of fast calorimetry and its applications was given by Toda et al.[23] One of the main benefits of fast calorimetry is that heating at higher rates enables the investigation of thermal transitions and metastable states without allowing sufficient time for annealing, reorganization and recrystallization effects to occur during heating. Conventional as well as fast DSC experiments were carried out with isotactic polystyrene with heating rates up to 500 °C/s.[17] Results of these experiments showed the merging of the upper two endotherms at heating rates of 10 °C/s for it and apparent total disappearance of the multiple melting behavior, that is converging of all three melting endotherms into a single endotherm at higher heating rates (between ca. 10 and 100 °C/s. The same authors reported a similar behavior for PET[18] except that disappearance of the MRR behavior was observed at heating rates in excess of 2700 °C/s. The authors interpreted these observations as a proof that the lowest endotherm is associated with the melting of the initial population of crystals and the upper two endotherms result from the melting of crystals formed by recrystallization during the heating scan. More recent work by some of these authors,[16, 19] led to a revision of their earlier hypotheses. These authors now suggest that the lowest endotherm indeed corresponds to the melting of secondary, constrained crystals, while the upper endotherms are

associated with the MRR process for primary crystals. Recent modeling of the melting-recrystallization-remelting process supports this point of view

Previous polyester research performed by the Turner group and others have focused on elucidating the general structure–property relationships of copolyesters containing cycloaliphatic rings, triptycene and bibenzoate moieties,[24-27] with the more recent research focused on how the incorporation of rigid, aromatic monomers affects crystallinity, T_g, mechanical properties and permeability.[26-27] The physical and mechanical properties of semicrystalline materials makes them desirable for high performance applications. In order to better tailor these materials to specific applications, it is necessary to develop accurate theoretical models that can predict (co)polyester properties from monomer structure.

Copolymerization of two semicrystalline homopolyesters has been shown in the literature to suppress melting temperatures, resulting in a eutectic point. This behavior was used to 'tune' the melting temperature of novel semicrystalline compositions to achieve processable, high T_m copolyesters from homopolyesters with prohibitively high T_ms. An unusual double melting temperature behavior was observed with these compositions. The origin of this was hypothesized to be either from melting-recrystallization-remelting or secondary crystals .In-depth investigation of thermal properties using CDSC and FDSC was used to identify the origin of multiple melting endotherms observed during initial thermal analysis.

4.4 Experimental

4.4.1 Materials

CHDM (99%, 30/70 cis/trans mixture), 4,4′BB (99%) and dichloroacetic acid were obtained from Sigma-Aldrich and used without further purification. DMN (>99.0%) was obtained

from TCI and used without further purification. Titanium(IV) butoxide (97 %) was purchased from Sigma-Aldrich, and a 0.08 g/mL titanium solution was prepared with 1-butanol (99.9%) obtained from Fisher.

4.4.2 Characterization Methods

^{1}H NMR spectroscopy was conducted in a mixture of trifluoroacetic acid-d/$CDCl_3$ (5/95 v/v) at 23 ˚C with a Bruker 500 MHz Avance II to provide compositional analysis of 60-DMN-40-4,4′BB-CHDM). A TA instruments Q500 determined the onset of thermal degradation when measured under a nitrogen purge with a heat ramp rate of 10 ˚C/min. CDSC was performed with a TA Instruments Q2000 DSC under a nitrogen purge of 50 mL/min. Indium was used for a single-point temperature calibration. FDSC was performed using a Mettler-Toledo Flash^{TM} DSC 1 equipped with the UFS1 sensor (XENA15 36057) using a nitrogen purge of 15 mL/min. A Leica EM UC6 Cryo-Ultramicrotome was used to prepare a 1 μm-thick film for the FDSC experiment; the 1 μm-thick film was cut down to a diameter of approximately 50 μm with a scalpel under a stereo optical microscope and then placed on the chip sensor. Dynamic mechanical analysis (DMA) was carried out with a TA instruments Q800 at a frequency of 1 Hz from -130–300 ˚C at a heating rate of 2 ˚C/min or until storage modulus dropped below 0.01 MPa. The transition temperatures were determined from the α peaks on the tan δ curve. Inherent viscosity measurements were performed in a 1B viscometer with 0.49–0.51 g/dL solutions prepared in dichloroacetic acid at 25 ˚C. The procedure for measuring inherent viscosity followed the standard test method for determining inherent viscosity (ASTM D4603).

4.4.3 Transesterification Polymerization of Poly(1,4-cyclohexylenedimethylene 2,6 naphthalate-*co*-4,4’-bibenzoate) Copolyesters

All polymer samples were synthesized in a similar fashion, an example of which is shown below. For a copolyester containing 60 mol% DMN and 40 mol% 4,4′BB diester (abbreviated 60-DMN-40-4,4′BB-100CHDM), 4,4′BB (8.65 g, 32 mmol), DMN (11.72 g, 48 mmol), CHDM (17.31 g, 120 mmol) and Titanium(IV) butoxide (100 ppm) were added to a dry 100 mL round-bottom flask. The flask was equipped with an overhead stirrer, a distillation head, a condenser, and a nitrogen inlet and the reaction vessel was degassed under vacuum and purged with nitrogen three times. While under continual nitrogen purge, the flask was submerged in a 240 ˚C molten metal bath, and the temperature was slowly increased to 280 ˚C over 25 min. The reaction mixture was then stirred at 280 ˚C for an additional 2 h. The temperature was then increased to 330 ˚C and the reaction was stirred for an additional 30 min under high vacuum (≤ 0.6 torr), after which the polymer was allowed to cool for at least 15 min while under nitrogen. The polyester, still attached to the metal stirring rod, was separated from the inside of the glass flask by again submerging the flask into the metal bath until the part of the polymer still in direct contact with the inside of the flask had melted. The stir rod was pulled to separate the part of the polymer still attached to the stir rod from the inside of the flask. The polyester was cooled to room temperature under nitrogen and the glass flask was smashed to retrieve the stirring rod and polymer. Polymer was separated from the stirring rod by first submerging it in liquid nitrogen and then removing it with a hammer and end nippers.

4.4.4 Film Preparation

Polymer samples were dried overnight under reduced pressure at 80 ˚C. Transparent polymer films were prepared with a Carver melt press. Polymer samples were pressed to a thickness of 0.29 mm between two sheets of Kapton® film by using an applied pressure of 1 metric

ton at 10 ˚C above melting for 5 min. Films were quenched between two room temperature steel plates.

4.5 Results and Discussion

The copolyester poly(1,4-cyclohexylenedimethylene 2,6-naphthalate-*co*-4,4'-bibenzoate) was synthesized with varying molar ratios of dimethyl biphenyl-4,4'-dicarboxylate and dimethyl 2,6-naphthalenedicarboxylate (**Scheme 4-1**). The diesters DMN and 4,4′BB were chosen for their rigid, aromatic structures, which have been shown to produce polymers with high melting points when synthesized with ethylene glycol, or a similar flexible diol.[7, 28] For this article, we were exploring the thermal properties of polyesters produced with the rigid diesters DMN and 4,4′BB in combination with the rigid CHDM diol.

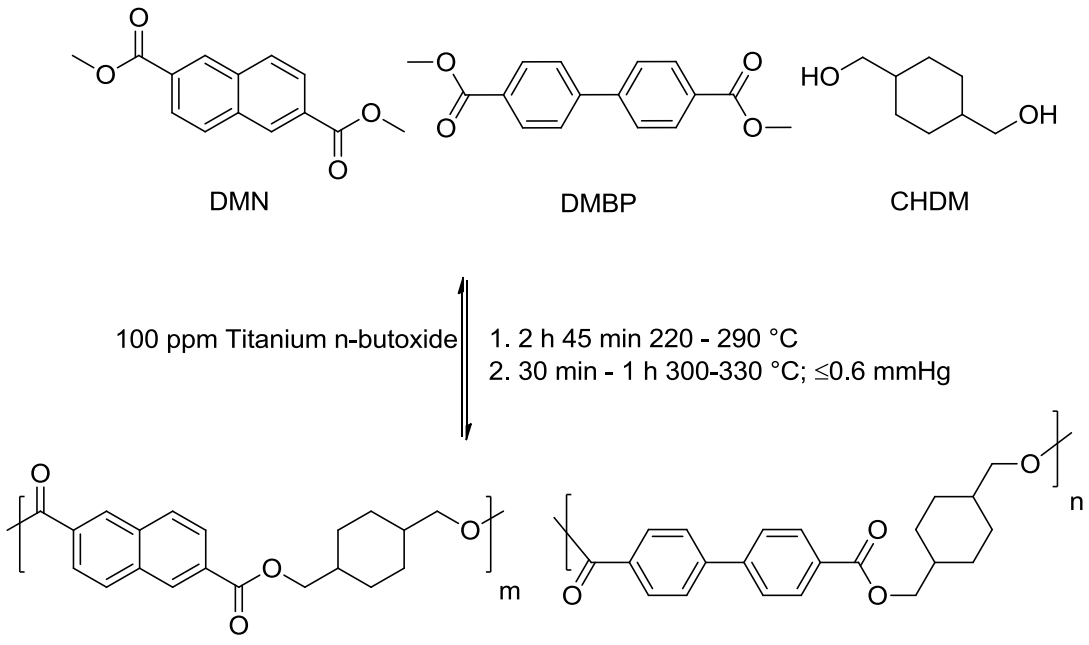

Scheme 4-1. Synthesis of copolyester poly(1,4-cyclohexylenedimethylene 2,6-naphthalate-co-4,4'-bibenzoate)

Copolyester 60-DMN-40-4,4′BB-CHDM (inherent viscosity = 0.59) was chosen for more extensive thermal analysis because it produced durable films and could be melted at temperatures

low enough to minimize thermal degradation during synthesis. Compositions with 80 mol% or more of 4,4'BB or DMN exhibited high melting temperatures (above 300 ˚C) and produced opaque/brittle films. These compositions could not undergo polycondensation for more than ~30–45 min before undergoing significant discoloration and losing viscosity due to thermal degradation.

Synthesis of 60-DMN-40-4,4′BB-CHDM copolyester produced a white polymer which could be quench cooled after melt pressing into creaseable transparent films. Polyester compositions were verified with ^{1}H NMR spectroscopy. The confirmed DMN and 4,4′BB molar ratios for all compositions were within 2 mol% of the targeted molar ratios. The characteristic peaks 'e' and 'd' from **Figure 4-1** were used to confirm molar ratios. The cis/trans ratio of the

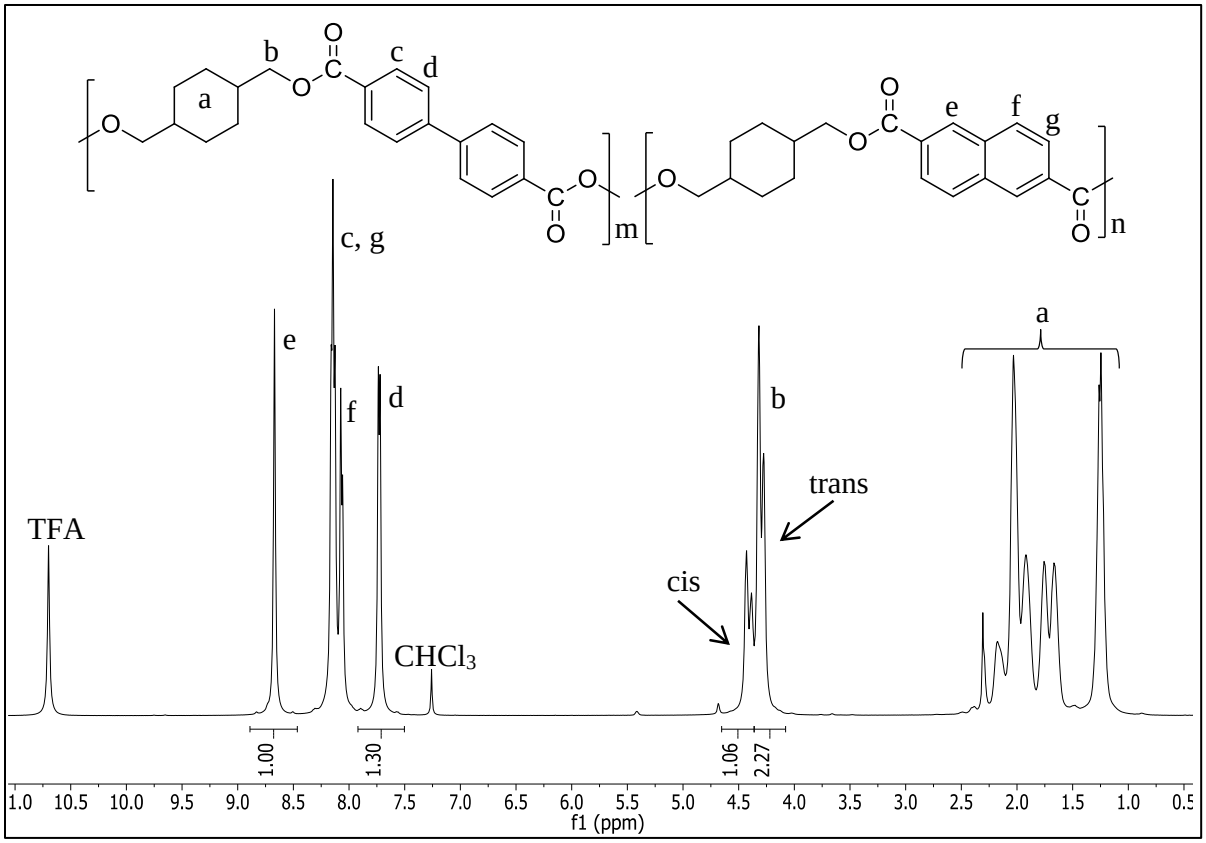

Figure 4-1. ^{1}H NMR spectrum of copolyester 60-DMN-40-4,4′BB-CHDM

cyclohexylene units was estimated from peak 'b' and remained within 2 mol% of the unincorporated monomer ratio at 30/70 cis/trans. Initial CDSC heat/cool/heat experiments were carried out at a heating and cooling rate of 10 ˚C/min between 30 and 350 ˚C. Results were used from the second heat/cool/heat cycle so as to eliminate for the thermal history of the polymer. CDSC showed multiple melting endotherms for all compositions ranging from 100 mol% DMN diester to 100 mol% 4,4′BB diester. Thermal analysis results are summarized in **Table 4-1** and **Figure 4-2**. Each homopolyester exhibits a decrease in melting temperature with increasing comonomer content with a eutectic point observed at 50 mol% DMN.

Table 4-1. Thermal Transition Characteristics for Copolyesters Containing 4,4′BB, DMN and 4,4′BB as measured by Conventional DSC during heating at 10°C/min after cooling at the same rate.

Polymer Name	mol% DMN	IV (dL/g)	T_m (II) (˚ C)	T_m (III) (˚ C)	T_g (˚ C)	ΔH (J/g)
4,4'BB-CHDM	0	0.34	320	329	ND	43.8
80-4,4′BB-20-DMN-100-CHDM	20	0.56	294	310	158	39.3
60-4,4′BB-40-DMN-100-CHDM	40	0.46	277	294	150	28.6
50-4,4′BB-50-DMN-100-CHDM	50	0.39	219	251	132	27.3
40-4,4′BB-60-DMN-100-CHDM	60	0.59	261	280	127	24.4
20-4,4′BB-80-DMN-100-CHDM	80	0.44	284	306	120	35.2
100-DMN-100-CHDM	100	0.22	303	324	ND	39.9

A similar eutectic point is observed for PCT and PET compositions modified with DMN where a eutectic melting point was observed around 40 mol% DMN.[6, 29] In most cases, the melting temperature of copolyesters decreases with increasing content of the minor comonomer component until the incompatibility results in a completely amorphous material, such as in the case of PET–PCT copolyesters.[10] The continual presence of melting endotherms across all compositions

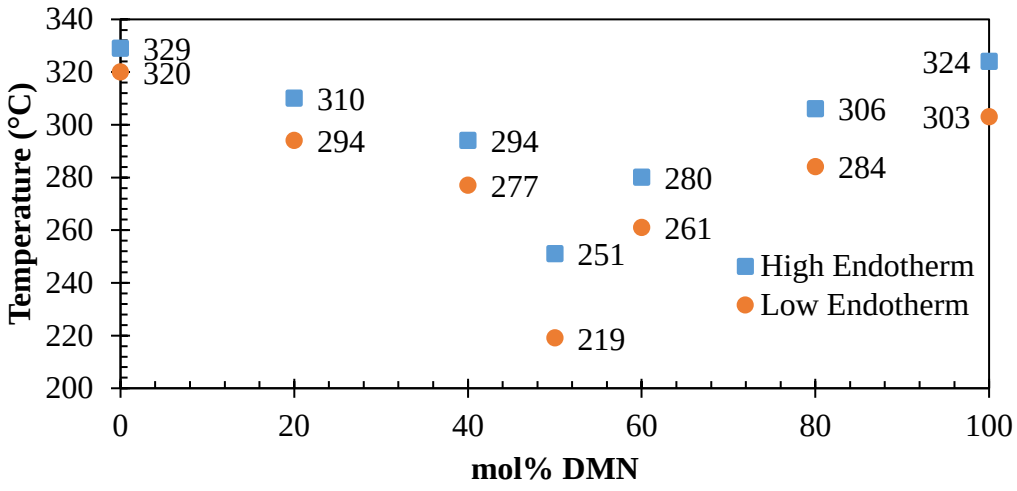

Figure 4-2. Peak temperature of the two melting endotherms plotted against diester composition

indicates that there is some degree of comonomer compatibility within the crystalline lattice.[6] Multiple melting endotherms can be seen in the DSC trace for all compositions (**Figure 4-3**), in the case of 60-DMN-40-4,4′BB-CHDM, a large melting peak appears at 280 ˚C and smaller peaks appears at 261 ˚C

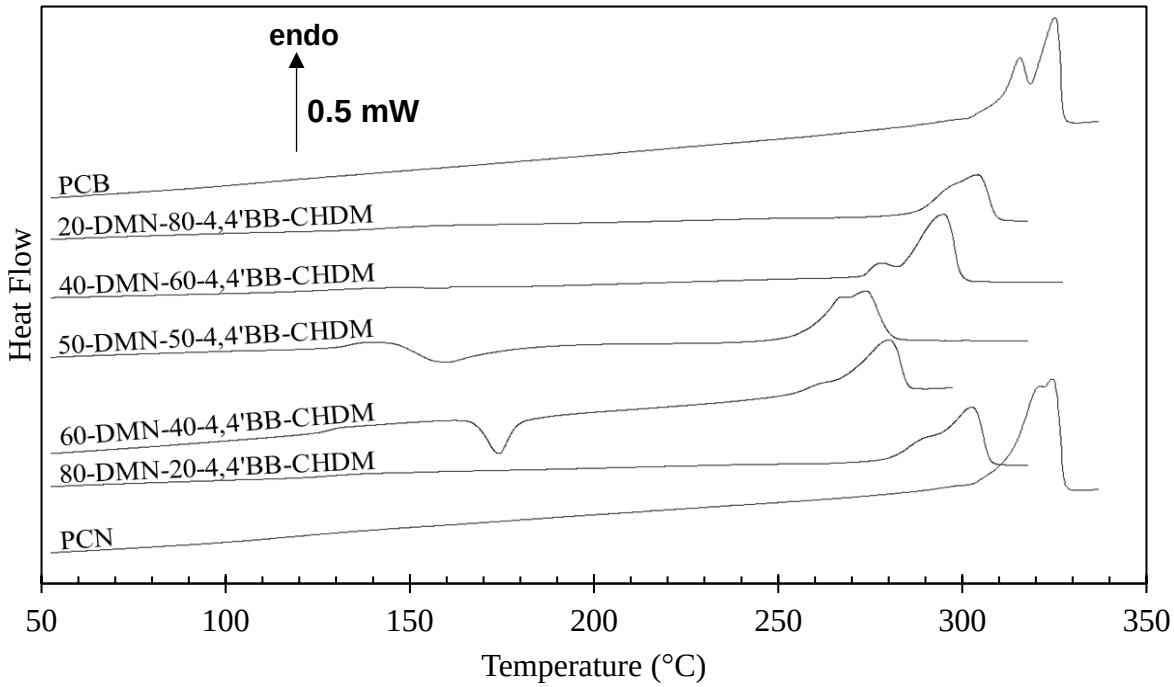

Figure 4-3. DSC traces of all copolyester compositions. Second heating at 10 °C/min after cooling at 10 °C/min from the melt.

DMA analysis (**Figure 4-4**) was used to characterize the location of thermal relaxations and compare these when appropriate with those observed using a conventional DSC. The T_g observed with DMA (129 ˚C) is close to the T_g observed with DSC (125 ˚C). Cold crystallization shortly after the T_g produces a modulus increase in the rubbery plateau and a small tan δ relaxation around 155 °C. In addition to the alpha transition at 129 ˚C, two sub-T_g transitions can also be observed at 5 ˚C (β) and -67 ˚C (γ). It is difficult to say what causes the transition at 5 ˚C since it is reported in other polymers containing 4,4′BB, DMN and CHDM[30-32]. Relaxation in the area of -67 ˚C are commonly attributed to phenyl ring flips.[33-36] Extensive studies of poly(1,4-cyclohexylenedimethylene terephthalate) (PCT) by Chen et al[31] also shows that relaxations at this temperature can be significantly enhanced by the presence of cyclohexylene units within the main

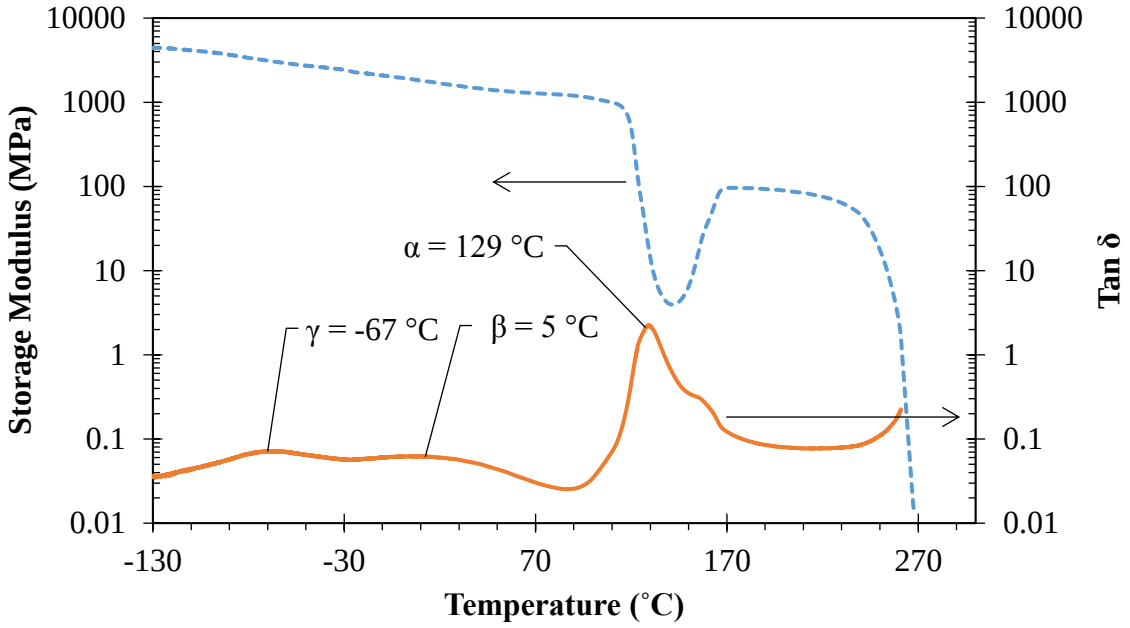

Figure 4-4. DMA spectrum of 60-DMN-40-4,4′BB-CHDM measured with a 2 °C/min heating ramp at 1 Hz

chain that increase volume fluctuations and improve the impact properties of the material due to cooperative motions of the cyclohexylene units aided by changes in ring conformation. These conclusions were based on calculated low energy conformations of the cyclohexylene rings and were supported by DMA and dipolar rotational spin-echo (DRSE) ^{13}C NMR. To test if the multiple endotherms, located at ~260 and ~280 ˚C, were due to (MRR) behavior, it was necessary to see how the magnitude of the endotherms changed with heating rate.

Three polymer samples were isothermally crystallized using CDSC at 190 ˚C for 15 min, 215 ˚C for 30 min and 315 ˚C for 60 min then melted with heating rates of 5, 10, 20 and 40 ˚C/min (**Figure 4-5)**. Isothermal crystallization above the cold crystallization temperature (T_{cc} ≈173 ˚C), immediately followed by heating, limited any crystallization that might occur during the heating scan, which might influence the shape of the melting endotherm. **Figure 4-5** shows that the endotherm at ~265 ˚C (from now on referred to as T_m(II)) increases in size relative to the higher

temperature endotherm at ~280 ˚C (from now on referred to as T_m(III)) at higher heating rates. A decrease in the peak temperature of T_m(III)) is also apparent with increasing heating rate. This behavior is indicative of the MRR behavior. Isothermal crystallization at higher temperatures leads to thicker crystalline lamellae and thus more stable crystals. Additionally, nucleation rates and crystallization rates decrease at higher temperatures, leading to a smaller extent of MRR. As a result T_m(II) and T_m(III) converge at higher isothermal crystallization temperatures, and the ratio of the third endotherm relative to the second decreases.

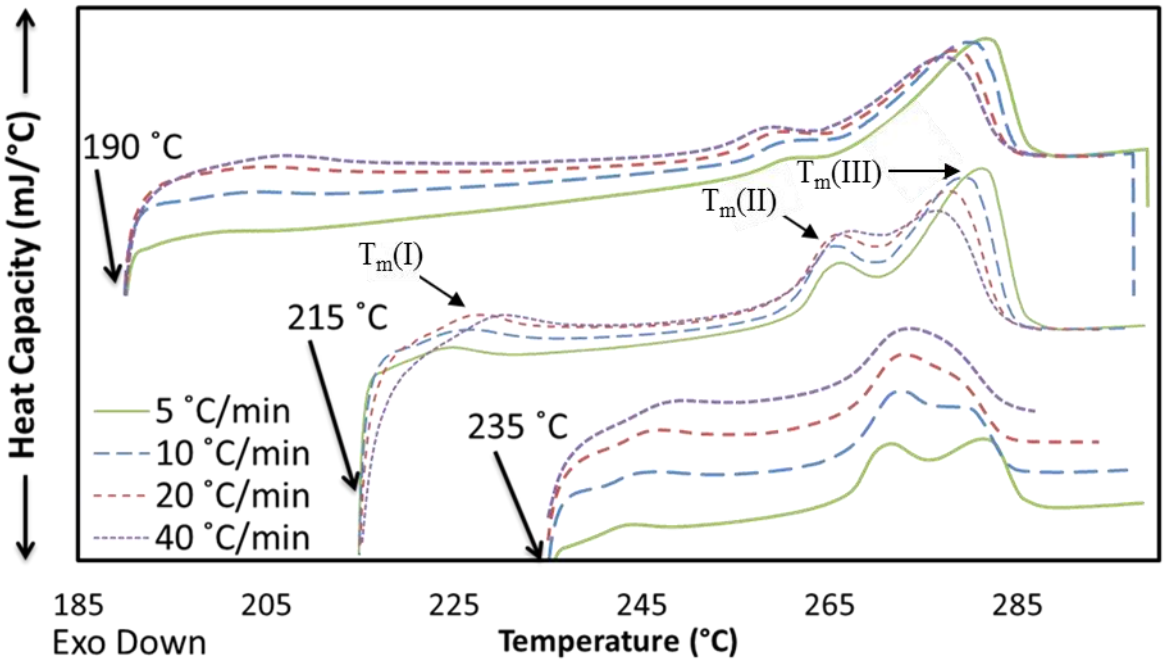

Figure 4-5. Conventional DSC scans of a 60-DMN-40-DMBP-CHDM sample isothermally crystallized at 190 ˚C for 15 min, 215 ˚C for 30 min and 315 ˚C for 60 min heated at rates of 5, 10, 20 and 40 ˚C/min.

Isothermal crystallization above T_{cc} = 173 ˚C also produced a small melting endotherm approximately ~10–20 ˚C above the isothermal crystallization temperature (from now on referred to as T_m(I)) (**Figure 4-5)**. Such behavior has been observed before for many polymers and is now attributed to the melting of constrained, secondary crystals.[15-17, 19] Unlike with MRR behavior,

where relative size of the endotherms depends on heating rate, endotherms associated with the melting of secondary crystals are not known to change significantly in magnitude with increasing heating rate, but shift to higher temperatures with higher heating rates, as observed here. The larger superheating observed for secondary crystals relative to primary crystals is consistent with the larger constraints experienced by secondary crystals.

Analysis of the CDSC data showed that the relative sizes of the second and third endotherms as well as their respective peak temperatures are independent of crystallization time, as expected for the MRR behavior (**Figure 4-6).** Note also that the first endotherm shifts to higher temperature and increases in enthalpy as the crystallization time increases, as a consequence of secondary crystallization.

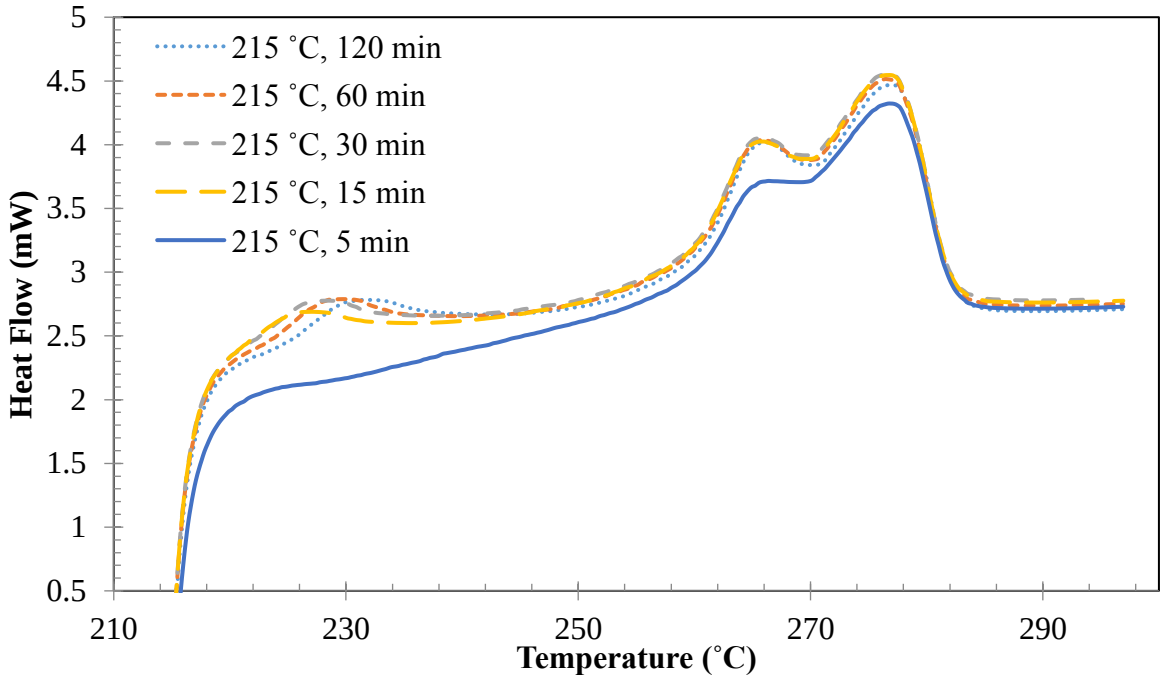

Figure 4-6. Multiple DSC scans of 60-DMN-40-DMBP-CHDM sample isothermally crystallized at 215 ˚C for 5, 15, 30, 60 and 120 minutes then heated at 20 °C/min

Isothermal crystallization at 215 °C for 30 min was further investigated using FDSC with heating rates from 5 to 10^4 °C/s (3×10^2 to 6×10^5 °C/min). FDSC data (**Figure 4-7**) showed two peaks for heating at 5 and 10 °C/s and only one peak at heating rates 50 to 10^4 °C/s. The melting temperature as a function of heating rate is shown for both CDSC and FDSC data in **Figure 4-8**. Keeping in mind that differences in calibration between the two instruments can lead to an error of ± 5 °C,[37] CDSC and FDSC data appear to be self-consistent. It should be noted that a baseline interpolation and subtraction procedure was used to obtain $T_m(I)$ for FDSC where the raw baseline is considerably sloped.

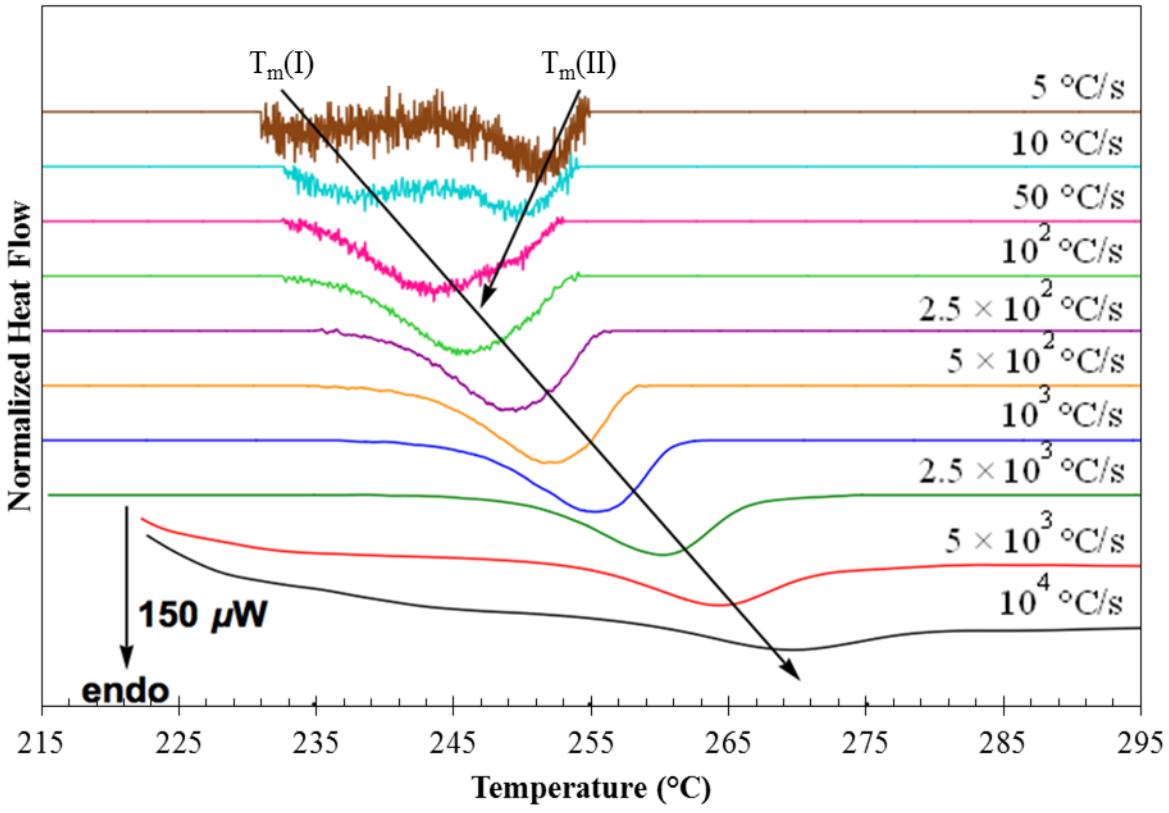

Figure 4-7. FDSC thermograms of 60-DMN-40-4,4′BB-CHDM isothermally crystallized at 215°C for 30 min and heated at 5, 10, 50, 10^2, 2.5×10^2, 5×10^2, 10^3, 2.5×10^3, 5×10^3, and 10^4 °C/s. A linear baseline was interpolated and subtracted from the raw data for 5–2.5×10^3 °C/s.

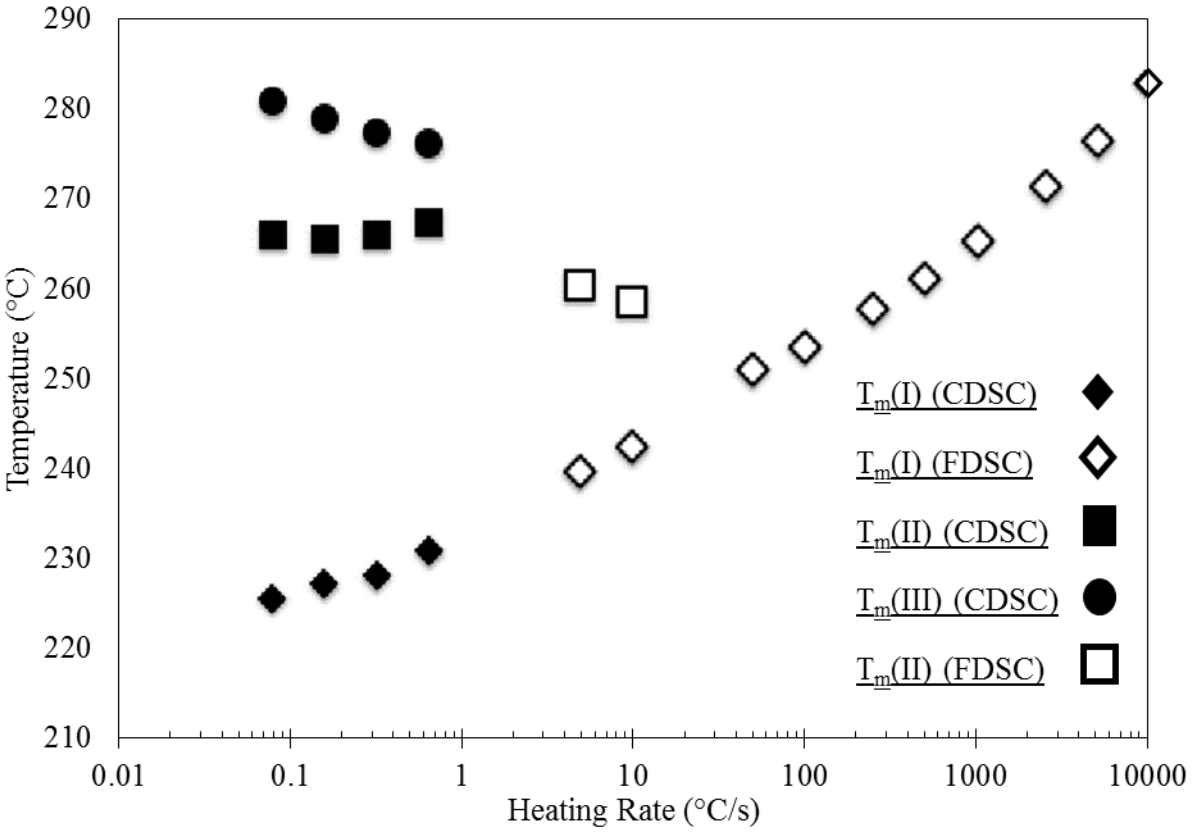

Figure 4-8. Heating rate dependence of the various melting peaks temperatures observed with CDSC (filled symbols) and FDSC (open symbols).

Figure 4-8 shows a significant amount of superheating (ca. 60 °C) for T_m(I) when the heating rate increases from 0.2 to 10^4 °C/s. Such large superheating is indeed expected for the melting of highly confined secondary crystals.[15] **Figure 4-8** also suggests the merging of the endotherms II and III at a heating rate ca. 1-5 °C/s, which is indicative of the MRR mechanism. Endotherm I is observed to merge with the upper endotherm (II + III) at a heating rate ca. 50 to 100 °C/s. The merging of these endotherms results from different superheating characteristics between primary crystals and topologically-constrained, secondary crystals. Since secondary crystals are constrained by primary crystals, they cannot melt at higher temperatures than primary

crystals. Hence above a critical heating rate only one melting transition is observed for all crystals. The observations reported here for copolyesters are in line with these discussed by Schick et al for nylon-6 and PEEK.[16, 19]

4.6 Conclusions

A series of copolyesters containing different compositions of DMN and 4,4′BB were synthesized via conventional melt transesterification polymerization with CHDM diol. Multiple melting temperatures were observed for all compositions containing both DMN and 4,4′BB as well as the homopolymers. The melting temperatures of the DMN and 4,4′BB homopolymers, 323 ˚C and 329 ˚C respectively, decreased when 4,4′BB and DMN comonomers, respectively, were added to the composition, resulting in a 251 ˚C eutectic point at the 50/50 molar ratio. This is an indication that the DMN units are not completely compatible with the crystal lattice of 4,4′BB and vice versa. The presence of multiple melting peaks suggested the existence of two populations of crystals (primary and secondary) and also pointed to the role of melting–recrystallization–remelting during heating if the heating rate was sufficiently low.

4.7 Acknowledgements

The authors thank Solvay Specialty Polymers for financial support and the supply of monomers 4,4′BB and DMN. They would also like to thank Prof. Timothy Long’s group for the use of their TGA, DSC and DMA. They would also like thank Prof. Robert Moore’s group, in particular Dr. E. Bruce Orler, for assistance with running DSC and DMA.

4.8 References

1. Daubeny, R. P.; Bunn, C. W., The crystal structure of polyethylene terephthalate. *Proc. R. Soc. London, Ser. A* **1954,** *226* (1167), 531-542.

2. Izard, E. F., Effect of chemical structure on physical properties of isomeric polyesters. *J. Polym. Sci., Part A: Polym. Chem.* **1952,** *9* (1), 35–39.

3. Izard, E. F., The effect of chemical composition on selected physical properties of linear polymers. *J. Polym. Sci., Part A: Polym. Chem.* **1952,** *8* (5), 503–518.

4. Scheirs, J.; Long, T. E., *Modern Polyesters: Chemistry and Technology of Polyesters and Copolyesters*. John Wiley & Sons Ltd: Chinchester, England, 2003.

5. Wilfong, R. E., Linear polyesters. *J. Polym. Sci., Part A: Polym. Chem.* **1961,** *54* (160), 385–410.

6. Lorenzetti, C.; Finelli, L.; Lotti, N.; Vannini, M.; Gazzano, M.; Berti, C.; Munari, A., Synthesis and characterization of poly(propylene terephthalate/2,6-naphthalate) random copolyesters. *Polymer* **2005,** *46* (12), 4041–4051.

7. Meurisse, P.; Noel, C.; Monnerie, L.; Fayolle, B., Polymers with mesogenic elements and flexible spacers in the main chain: Aromatic-aliphatic polyesters. *Br. Polym. J.* **1981,** *13* (2), 55–63.

8. Martin, E. V.; Kibler, C. J., Polyesters of 1,4-cyclohexanedimethanol. In *Man-Made Fiber Science and Technology*, Mark, H. F.; Atlas, S. M.; Cernia, E., Eds. Wiley-Interscience: New York, 1968; Vol. 3, pp 83–134.

9. Cabpenter, A. S., Recent developments in synthetic fibres. *J. Soc. Dyers Colour* **1949,** *65* (10), 469–478.

10. Turner, S. R.; Seymour, R. W.; Dombroski, J. R., Amorphous and crystalline polyesters based in 1,4-cyclohexanedimethanol. In *Modern Polyesters: Chemistry and Technology of Polyesters and Copolyesters*, Scheirs, J.; Long, T., Eds. John Wiley & Sons: West Sussex, England, 2003; pp 267–292.

11. Nichols, M. E.; Robertson, R. E., The multiple melting endotherms from poly(butylene terephthalate). *J. Polym. Sci., Part B: Polym. Phys.* **1992,** *30* (7), 755–768.

12. Lemstra, P. J.; Schouten, A. J.; Challa, G., Suppression of recrystallization of isotactic polystyrene single crystals by chemical modification. *J. Polym. Sci., Part B: Polym. Phys.* **1972,** *10* (11), 2301–2304.

13. Lemstra, P. J.; Schouten, A. J.; Challa, G., Secondary crystallization of isotactic polystyrene. *J. Polym. Sci., Part B: Polym. Phys.* **1974,** *12* (8), 1565–1574.

14. Overbergh, N.; Berghmans, H.; Smets, G., Influence of thermal history on the melting behavior of isotactic polystyrene. *J. Polym. Sci., Part C: Polym. Symp.* **1972,** *38* (1), 237–250.

15. Marand, H.; Alizadeh, A.; Farmer, R.; Desai, R.; Velikov, V., Influence of structural and topological constraints on the crystallization and melting behavior of polymers. 2. Poly(arylene ether ether ketone). *Macromolecules* **2000,** *33* (9), 3392–3403.

16. Furushima, Y.; Toda, A.; Rousseaux, V.; Bailly, C.; Zhuravlev, E.; Schick, C., Quantitative understanding of two distinct melting kinetics of an isothermally crystallized poly(ether ether ketone). *Polymer* **2016,** *99*, 97-104.

17. Sohn, S.; Alizadeh, A.; Marand, H., On the multiple melting behavior of bisphenol-A polycarbonate. *Polymer* **2000,** *41* (25), 8879–8886.

18. Minakov, A. A.; Mordvintsev, D. A.; Schick, C., Melting and reorganization of poly(ethylene terephthalate) on fast heating (1000 K/s). *Polymer* **2004,** *45* (11), 3755–3763.

19. Furushima, Y.; Nakada, M.; Ishikiriyama, K.; Toda, A.; Androsch, R.; Zhuravlev, E.; Schick, C., Two crystal populations with different melting/reorganization kinetics of isothermally crystallized polyamide 6. *J. Polym. Sci. Part B: Polym. Phys.* **2016,** *54* (20), 2126-2138.

20. Schawe, J. E. K.; Strobl, G. R., Superheating effects during the melting of crystallites of syndiotactic polypropylene analysed by temperature-modulated differential scanning calorimetry. *Polymer* **1998,** *39* (16), 3745–3751.

21. Minakov, A. A.; Mordvintsev, D. A.; Tol, R.; Schick, C., Melting and reorganization of the crystalline fraction and relaxation of the rigid amorphous fraction of isotactic polystyrene on fast heating (30,000 K/min). *Thermochim. Acta* **2006,** *442* (1–2), 25–30.

22. Toda, A., Heating rate dependence of melting peak temperature examined by DSC of heat flux type. *J. Therm. Anal. Calorim.* **2016,** *123* (3), 1795-1808.

23. Toda, A.; Androsch, R.; Schick, C., Insights into polymer crystallization and melting from fast scanning chip calorimetry. *Polymer* **2016,** *91*, 239-263.

24. Liu, Y.; Turner, S. R.; Wilkes, G., Melt-phase synthesis and properties of triptycene-containing copolyesters. *Macromolecules* **2011,** *44* (11), 4049–4056.

25. Liu, Y.; Turner, S. R., Synthesis and properties of cyclic diester based aliphatic copolyesters. *J. Polym. Sci., Part A: Polym. Chem.* **2010,** *48* (10), 2162–2169.

26. Edling, H. E.; Liu, H.; Sun, H.; Mondschein, R. J.; Schiraldi, D. A.; Long, T. E.; Turner, S. R., Copolyesters based on bibenzoic acids. *Polymer* **2018,** *135*, 120–130.

27. Mondschein, R. J.; Dennis, J. M.; Liu, H.; Ramakrishnan, R. K.; Nazarenko, S.; Turner, S. R.; Long, T. E., Synthesis and characterization of amorphous bibenzoate (co)polyesters: permeability and rheological performance. *Macromolecules* **2017,** *50* (19), 7603–7610.

28. Buchner, S.; Wiswe, D.; Zachmann, H. G., Kinetics of crystallization and melting behaviour of poly(ethylene naphthalene-2,6-dicarboxylate). *Polymer* **1989,** *30* (3), 480–488.

29. Hoffman, D. C.; Pecorini, T. J., Copolyesters of poly(1,4-cyclohexanedimethylene terephthalate) with isophthalic acid and 2,6-naphthalene dicarboxylic acid. *Am. Chem. Soc., Div. Polym. Chem., Polym. Prepr.* **1999,** *40* (1), 572–573.

30. Aoki, Y.; Li, L.; Amari, T.; Nishimura, K.; Arashiro, Y., Dynamic mechanical properties of poly(ethylene terephthalate)/poly(ethylene 2,6-naphthalate) blends. *Macromolecules* **1999,** *32* (6), 1923–1929.

31. Chen, L. P.; Yee, A. F.; Goetz, J. M.; Schaefer, J., Molecular structure effects on the secondary relaxation and impact strength of a series of polyester copolymer glasses. *Macromolecules* **1998,** *31* (16), 5371–5382.

32. Ma, H.; Collard, D. M.; Schiraldi, D. A.; Kumar, S., Structure and dynamic mechanical properties of poly(ethylene terephthalate-co-4,4′-bibenzoate) fibers. *Polymer* **2007,** *48* (6), 1651–1658.

33. Burgess, S. K.; Kriegel, R. M.; Koros, W. J., Carbon dioxide sorption and transport in amorphous poly(ethylene furanoate). *Macromolecules* **2015,** *48* (7), 2184–2193.

34. Burgess, S. K.; Leisen, J. E.; Kraftschik, B. E.; Mubarak, C. R.; Kriegel, R. M.; Koros, W. J., Chain mobility, thermal, and mechanical properties of poly(ethylene furanoate) compared to poly(ethylene terephthalate). *Macromolecules* **2014,** *47* (4), 1383–1391.

35. Polyakova, A.; Liu, R. Y. F.; Schiraldi, D. A.; Hiltner, A.; Baer, E., Oxygen-barrier properties of copolymers based on ethylene terephthalate. *J. Polym. Sci., Part B Polym. Phys.* **2001,** *39* (16), 1889–1899.

36. Light, R. R.; Seymour, R. W., Effect of sub-Tg relaxations on the gas transport properties of polyesters. *Polym. Eng. Sci.* **1982,** *22* (14), 857–864.

37. Mathot, V.; Pyda, M.; Pijpers, T.; Vanden Poel, G.; van de Kerkhof, E.; van Herwaarden, S.; van Herwaarden, F.; Leenaers, A., The Flash DSC 1, a power compensation twin-type, chip-based fast scanning calorimeter (FSC): First findings on polymers. *Thermochim. Acta* **2011,** *522* (1), 36-45.

4.9 Chapter 4 Supplemental Material

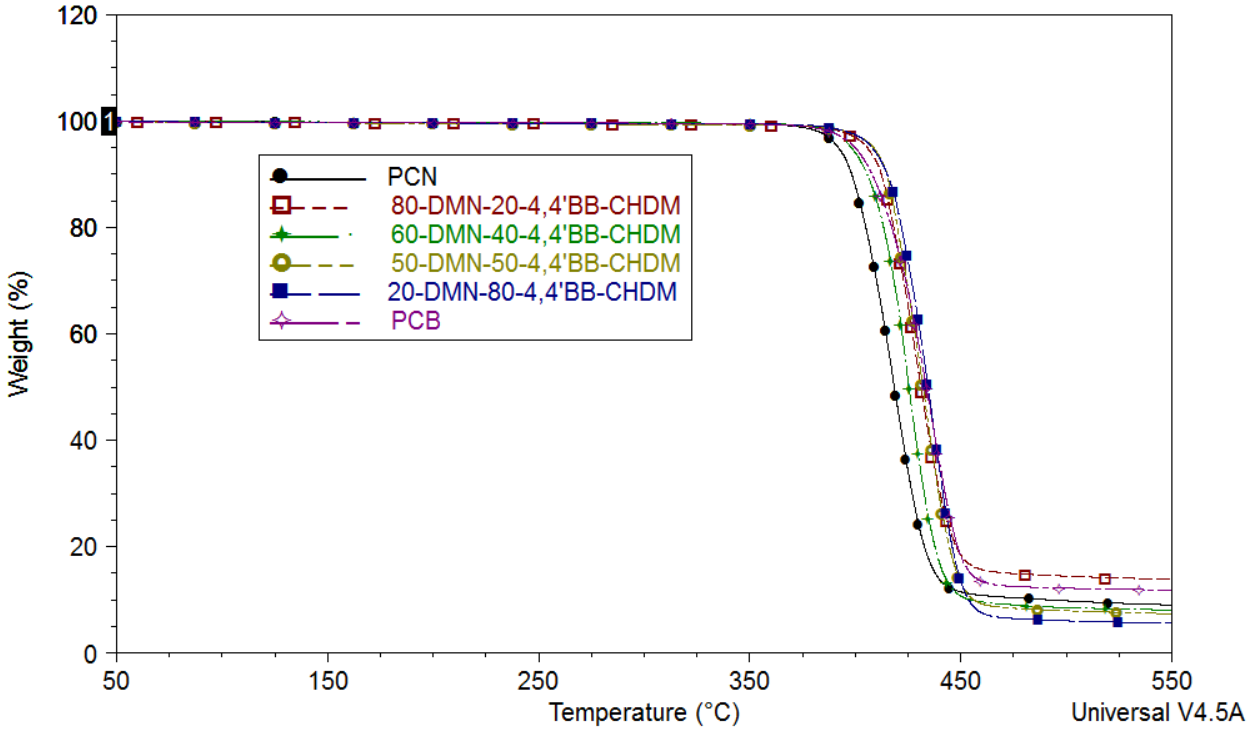

Figure 4-9S. TGA traces for copolyester compositions show degradation temperatures above 385 °C

Chapter 5. Exploration of Semicrystalline Copolyesters Modified with *p*-Terphenyl Units

5.1 Authors

H. Eliot Edling and S. Richard Turner

5.2 Abstract

Exploratory polymerizations were performed making polyesters containing 1,4-cyclohexanedimethanol (CHDM) and 2,6-naphthalate (DMN), 4,4'-bibenzoate (4,4'BB) or terephthalate (DMT) and modifying them with up to 20 mol% *p*-terphenyl-4,4''-dicarboxylate (DMTP). Dimethyl *p*-terphenyl-4,4''-dicarboxylate was synthesized in a fashion similar to that described in the literature and used directly in melt polycondensation to synthesize copolyesters. [1] Thermogravimetric analysis (TGA) showed single step weight loss for all compositions above 384 °C. DSC analysis showed decreasing melting temperatures with increasing DMTP content up to 20 mol% and increasing glass transition (T_g) temperatures with DMTP content up to 20 mol%. Preliminary rheological analysis suggests improved melt stability of copolyesters containing DMTP.

5.3 Introduction

High service temperature applications require high melting temperature (T_m) polyesters. Materials such as poly(1,4-cyclohexylenedimethylene terephthalate) (PCT), are often melt processed with additives (e.g. glass fiber) to produce molded parts at temperatures as high as 300 °C.[1] One of the most important properties of PCT is the high heat distortion temperature (250-260 °C), which results from having a high T_m (290 °C) and T_g (88 °C), giving PCT an advantage over significantly more expensive liquid crystalline polymers. [1-2] When comparted to PET, CHDM imparts more hydrophobic character to PCT, making it less susceptible to hydrolytic degradation[3] and is less susceptible to thermal degradation than ethylene glycol (EG),[4] making it attractive for

designing thermally stable polyesters. Poly(ethylene 2,6-naphthalate) (PEN) is another well studied semicrystalline polyester that has been shown to possess increased T_g (126 vs 80 °C), T_m (265 °C) and room temperature modulus (5200 vs 3900 MPa) relative to PET.[5] Substitution of PCT units with 2,6-naphthalate (DMN) units has been shown to enhance melting temperatures when the molar ratio is 40 % or higher,[6-7] making DMN an excellent candidate for high T_m applications due to its rigid structure and highly aromatic character.[8-10]

Semicrystalline (co)polyesters containing 4,4'-bibenzoate units have been studied since the 1950s,[11-20] and have exhibited great potential for engineering applications, however, interest was limited until more economical means of monomer synthesis were developed.[21-24] Poly(ethylene 4,4'-bibenzoate) (4,4'BB-EG) homopolyester has a high melting temperature (T_m= 343 °C)[17, 25] that makes melt polycondensation impractical, however, copolymerization has been successfully used to suppress melting temperatures to produce melt processable materials.[11-12, 16-17, 20] Even though 4,4'BB has received little attention relative to other highly rigid aromatic moieties such as 2,6-naphthalate, the high rigidity and melting temperatures of 4,4'BB indicate good potential for high performance engineering copolyesters.

The *p*-terphenyl-4,4''-dicarboxylate (DMTP) moiety has a longer, more aromatic structure than either 4,4'BB or DMN monomers (**Figure 5-1**). The high rigidity of DMTP, produces highly crystalline materials with high melting temperatures, often with liquid crystalline behavior.[26-27] The highly rigid character of DMTP offers great potential for enhancing the properties of copolyester thermoplastics, however, DMTP has yet to be thoroughly explored for non-LCP applications. Synthesis of dimethyl *p*-terphenyl-4,4''-dicarboxylate involves the dicarboxylation of *p*-terphenyl,[28] and allows for direct incorporation of DMTP into melt processable polyesters. In addition to increasing the rigidity and T_g of high temperature thermoplastics, the extended

chromophore of DMTP has potential to improve the UV stability of copolyesters by acting as an ultraviolet absorber[29] unlike more common diacids containing only one or two aromatic rings.

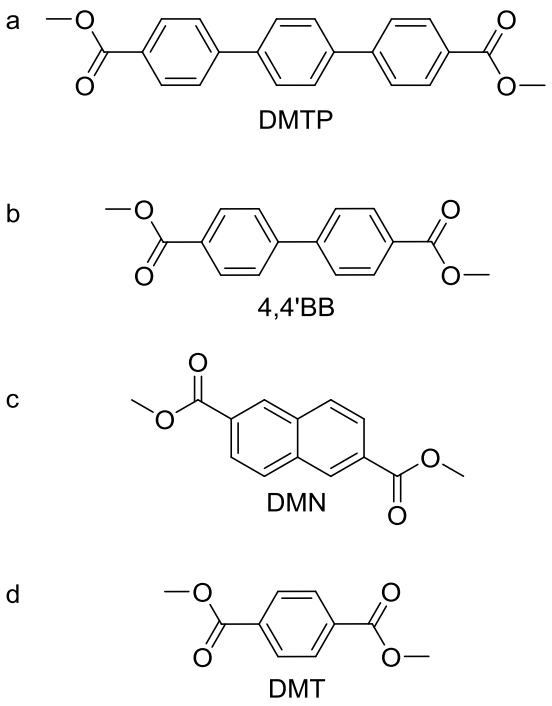

Figure 5-1. Dimethyl esters of *p*-terphenyl-4,4"-dicarboxylate (a), 4,4'-bibenzoate (b), 2,6-naphthalate (c) and terephthalate (d)

Depending on the level of comonomer compatibility within a crystal lattice, addition of comonomer may suppress the T_m[7, 30-31] or can completely suppress crystallization of a copolyester and produce an amorphous window.[2, 32-33] If a copolyester is made by combining two semicrystalline homopolyesters, it is possible to observe suppressed melting temperatures across the entire composition range. As the concentration of the minor comonomeric units increases, the melting temperature decreases until a minimum melting temperature is reached (called a eutectic point), at which point the minor comonomeric unit then becomes the major component within the

crystal lattice and the melting temperature begins to increase again. This phenomenon is referred to as isodimorphism and continues to be well studied.[34-38] Only in very rare cases are the homopolyester crystal lattices similar enough to produce no observed suppression of melting temperature.[31]

The large rigid structure of DMTP makes it a prime candidate for producing novel and rigid copolyester thermoplastics with high T_ms and T_gs ideal for high temperature applications typically reserved for LCPs. By copolymerizing DMTP with other rigid semicrystalline polyesters, it is possible to significantly increase the application temperatures of these materials, while simultaneously decreasing the melting temperature sufficiently to render thermally processable. In addition, the extended chromophore of DMTP relative other diacids structures also shows promise as a UV absorber, which has potential to increase the optical stability of the copolyesters.

5.4 Experimental

5.4.1 Materials

Dimethyl terephthalate (DMT, ≥99%) and dimethyl 4,4'-biphenyldicarboxylate (4,4'BB, 99%) were purchased from Sigma Aldrich. Dimethyl 2,6-naphthalene dicarboxylate (DMN, >99.0%) was purchased from TCI. Dimethyl *p*-terphenyl-4,4''-dicarboxylate (DMTP) synthesized according to known procedures with purity tested by using ^{1}H NMR and melting point analysis. All diesters were dried in a vacuum oven overnight at 35 °C and stored in a dry box before using. Ethylene glycol (EG, ≥99%) and 1,4-cyclohexanedimethanol (CHDM, 70:30 tans/cis, 99%) was obtained from Sigma Aldrich and used as received. Dichloroacetic acid (≥99%) was obtained from Alpha Aesar and used as received. Titanium (IV) butoxide (97%) was purchased from Sigma Aldrich. 1-Butanol (99.9%) was purchased from Fisher Scientific and dried over magnesium sulfate. A titanium catalyst solution (ca. 0.08 g/mL) was prepared by placing 0.8 g titanium (IV)

butoxide into 10 mL volumetric flask and diluting to the calibration line with 1-butanol. The titanium solution was then transferred to a sealed container and purged with nitrogen for 10 min. Trifluoroacetic acid-*d* (TFA-*d*, 99.5 atom % D) was obtained from Sigma Aldrich. Chloroform-*d* ($CDCl_3$, 99.8% atom D +0.05% V/V TMS) was obtained from Cambridge Isotope Laboratories, Inc.

5.4.2 Characterization Methods

^{1}H NMR spectroscopy was conducted in a mixture of trifluoroacetic acid-*d*/$CDCl_3$ (5:95 v/v) at 23 ˚C with a Bruker 500 MHz Avance II to provide compositional analysis of copolyester compositions. A TA instruments Q500 determined the onset of thermal degradation when measured under a nitrogen purge with a heat ramp rate of 10 ˚C/min. Dynamic scanning calorimetry (DSC) was performed with a TA Instruments Q2000 DSC under a nitrogen purge of 50 mL/min with a heating rate of 10 ˚C/min and a cooling rate of 100 ˚C/min. Glass transitions (T_g) were determined from the middle of the inflection point. Dynamic mechanical analysis (DMA) was carried out with a TA instruments Q800 at a frequency of 1 Hz from -130 to 300 ˚C at a heating rate of 2 ˚C/min or until storage modulus dropped below 0.01 MPa. The glass transition temperatures were determined from the α peaks on the tan δ curve. Inherent viscosity (η_{inh}) measurements were performed in a Cannon Type B glass capillary viscometer with 0.49–0.51 g/dL solutions prepared in dichloroacetic acid at 25 ˚C. The procedure for measuring inherent viscosity followed the standard test method for determining inherent viscosity (ASTM D4603). Rheological analysis was performed on a TA instruments AR-G2 equipped with disposable 25 mm diameter aluminum parallel plates. A strain sweep from was performed at 0.01–10 % oscillatory strain and 1 Hz to determine the linear viscoelastic region. Time sweeps were performed under air at 1 Hz

and 1 % oscillatory strain to observe changes in viscosity over time. Copolyester compositions were run at 305 °C.

5.4.3 Monomer Synthesis

Synthesis of dimethyl *p*-terphenyl-4,4''-dicarboxylate involves the decarboxylation of *p*-terphenyl and was adapted from a process described in the literature[28] and produces a diester that can be directly incorporated into known homopolyesters. The following procedure (**Scheme 5-1**) was used to produce 18.74 g (55.2 mol% yield) of dimethyl *p*-terphenyl-4,4''-dicarboxylate. P-terphenyl (22.5 g, 98 mmol), oxalyl chloride (74.7 g, 589 mmol), aluminum chloride (20 g, 150 mmol) and carbon disulfide (350 mL) was added to a round bottom flask equipped with an overhead stirrer and ice bath. The mixture was stirred for 1 h, after which the ice bath was removed and another more aluminum chloride (15 g, 113 mmol) was added to the flask. The reaction was allowed to stir for another 48 hours. Additional carbon disulfide was added if the mixture became too thick to stir. Reaction mixture was thick and black. After 48 hours, ice was added to the mixture and carbon disulfide was removed with a rotary evaporator. Yellow solid was washed with 500 mL of 1.2 M HCl. The remaining yellow solid was dried completely in the oven before proceeding to the next step. The dried yellow solid was placed in a round bottom flask equipped with an oil bath and reflux condenser. Thionyl chloride (138 mL, 1.9 mol) and pyridine (20 mL) were slowly added to the flask and the reaction mixture was refluxed for 5 h. The reaction mixture was then placed under reduced pressure until thionyl chloride was removed. The remaining yellow solid was dissolved in boiling toluene, treated with carbon, and hot filtered. Toluene was removed with a rotary evaporator and then refluxed for 1 h in methanol. Methanol was removed with a rotary evaporator and the remaining yellow solid was recrystallized in hot dimethylformamide (1.3 L). Recrystallized solid was filtered and washed with cold DMF. Yellow crystals were dried overnight

in a vacuum oven at 90 °C, with a final yield of 18.74 g (55%) and mp 300.6–300.9 °C (lit.[28] mp 305-306 °C).

5.4.4 Polymerization

Polymerization of T-X-DMTP-CHDM and T-X-DMTP-50-EG-50-CHDM (11 g scale). All compositions were synthesized in a similar manner. Polymerizations were performed in a dry round bottom flask equipped with distillation arm, nitrogen inlet and an overhead stirrer. Polymerization requires monomers to be immersed into a high temperature metal bath and immediate ramping to melt polycondensation temperatures to prevent solidification of the melt. To synthesize the composition T-20-DMTP-CHDM, CHDM (6.25 g, 43 mmol), DMT (5.61 g, 29 mmol) and DMTP (2.50 g, 7 mmol) were charged into a 100 mL round bottom flask along with enough titanium catalyst solution to make up 100 ppm Ti by mass to the theoretical yield. Oxygen and moisture were removed from the flask by treating with vacuum and purging with nitrogen three times. For the transesterification step, stirring rate was set to 200 rpm and the flask was submerged into a 220 °C, which was increased to 290 °C over 30 min. The polycondensation step was then carried out with a 30–40 rpm stirring rate under decreased pressure (≤ 0.3 mmHg) for 50 min. The flask was then removed from the metal bath and allowed to cool to room temperature. All polyesters were isolated by first breaking the flask and then removing the polyester from the stir rod by using a hammer, chisel and end nippers. Isolated polymers were rinsed with DI water and dried overnight in a vacuum oven at 10–20 °C above the glass transition of the polymer.

Polymerization of DMN-X-DMTP-CHDM (11 g scale). The equipment and drying procedure used for this polymerization is similar to that used for the **T-X-DMTP-CHDM** compositions above. To synthesize the composition DMN-10-DMTP-CHDM, CHDM (6.69 g, 39 mmol), DMN (7.23 g, 30 mmol) and DMTP (1.14 g, 3 mmol) were charged into a 100 mL round

bottom flask along with enough titanium catalyst solution to make up 100 ppm Ti by mass to the theoretical yield. Transesterification was carried out during a ramp from 220 °C to 320–330 °C over 30 min. Polycondensation was performed at 320–330 °C and ≤ 0.3 mmHg for 20 min.

Polymerization of 4,4'BB-X-DMTP-CHDM (30 g scale). The equipment and drying procedure used for this polymerization is similar to that used for the **T-X-DMTP-CHDM** compositions above. To synthesize the composition 4,4'BB-5-DMTP-CHDM, CHDM (14.52 g, 101 mmol), 4,4'BB (21.55 g, 80 mmol) and DMTP (1.45 g, 4 mmol) were charged into a 100 mL round bottom flask along with enough titanium catalyst solution to make up 100 ppm Ti by mass to the theoretical yield. Transesterification was carried out during a ramp from 235 °C to 325–335 °C over 30 min. Polycondensation was performed at 325–335 °C and ≤ 0.3 mmHg for 20 min.

5.5 Results and Discussion

5.5.1 Monomer Synthesis, Polymerization and Structural Characterization

DMTP monomer was synthesized in a manner consistent with procedures in the literature (**Scheme 5-1**). [28] The monomer melting range was narrow, mp 300.6–300.9 °C (lit.[28] mp 305-306 °C), and ~4 °C below the literature value. ^{1}H NMR spectroscopy was conducted in *d*-DMSO at 90 ˚C with a Bruker 500 MHz Avance II to confirm addition to both sides of *p*-terphenyl (**Figure 5-6S**). Impurities were not detectable by ^{1}H NMR. A series of copolyesters were synthesized by modifying a several high melting temperature polyesters with DMTP (**Scheme 5-2**). Titanium (IV) butoxide was used as catalyst to facilitate transesterification and polycondensation. CHDM diol was used in excess (120 mol% of diacid) to facilitate transesterification. Polyester samples were submerged in a 220–235°C metal bath and immediately ramped to 290–335 °C, which was necessary to keep the monomer mixture in the melt and prevent crystallization. High temperatures limited transesterification time to 30–60 min to minimize thermal degradation. Compositions

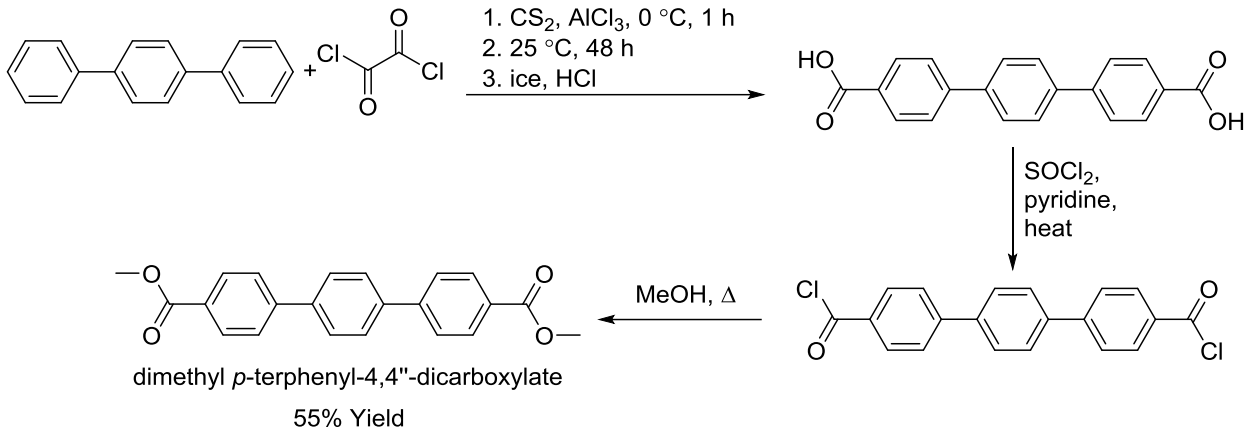

Scheme 5-1. Synthesis of dimethyl *p*-terphenyl-4,4"-dicarboxylate

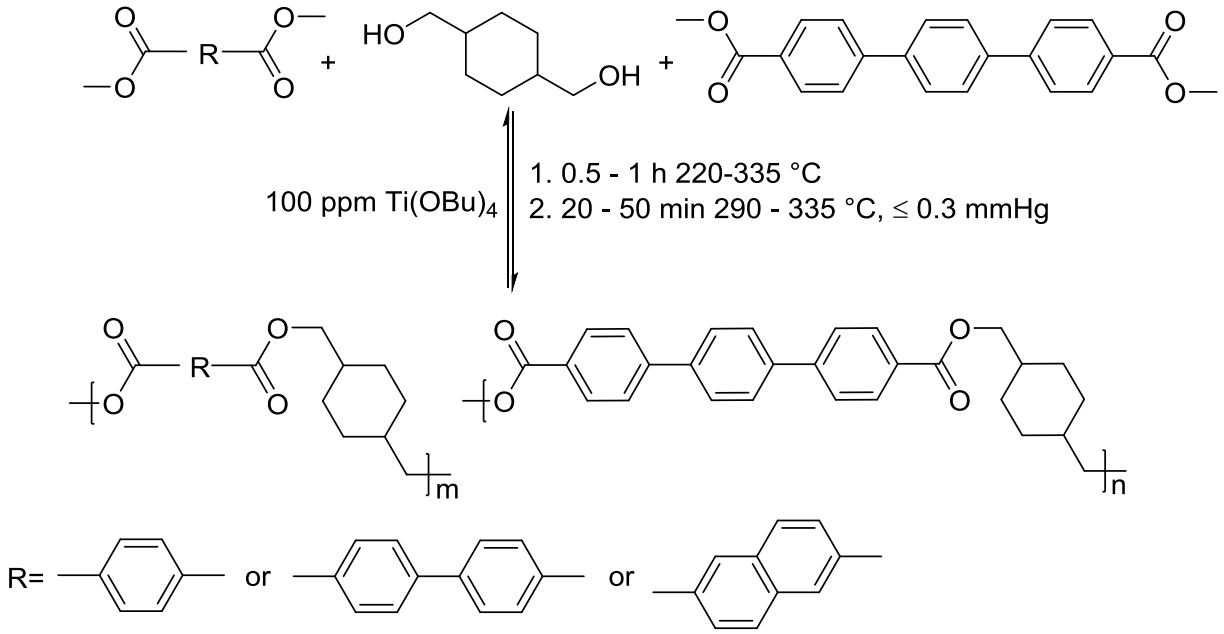

Scheme 5-2. Polymerization of semicrystalline (co)polyesters containing DMTP units

containing DMN and 4,4'BB required high temperatures (>320 °C) to prevent crystallization before and during polycondensation, as a result, polycondensation times were very short (20 min) to prevent degradation. Nearly all compositions studied were semicrystalline and were either white

or off white. ^{1}H NMR analysis confirmed molar ratios from proton shifts unique to each comonomer for all copolyesters except those containing 4,4'BB, which were insoluble to NMR solvents (**Figure 5-6S**). An example ^{1}H NMR trace (**Figure 5-2**) shows clear resolution of the characteristic peaks used to calculate comonomer ratios. All compositions achieved diacid ratios within 1 mol% of the targeted ratio. **Table 5-1** shows inherent viscosities (η_{inh}) above 0.70 dL/g or most compositions, indicating high molecular weights were achieved in most cases. High melting temperatures and short polycondensation times resulted in lower inherent viscosities. All compositions below 0.70 dL/g, were brittle.

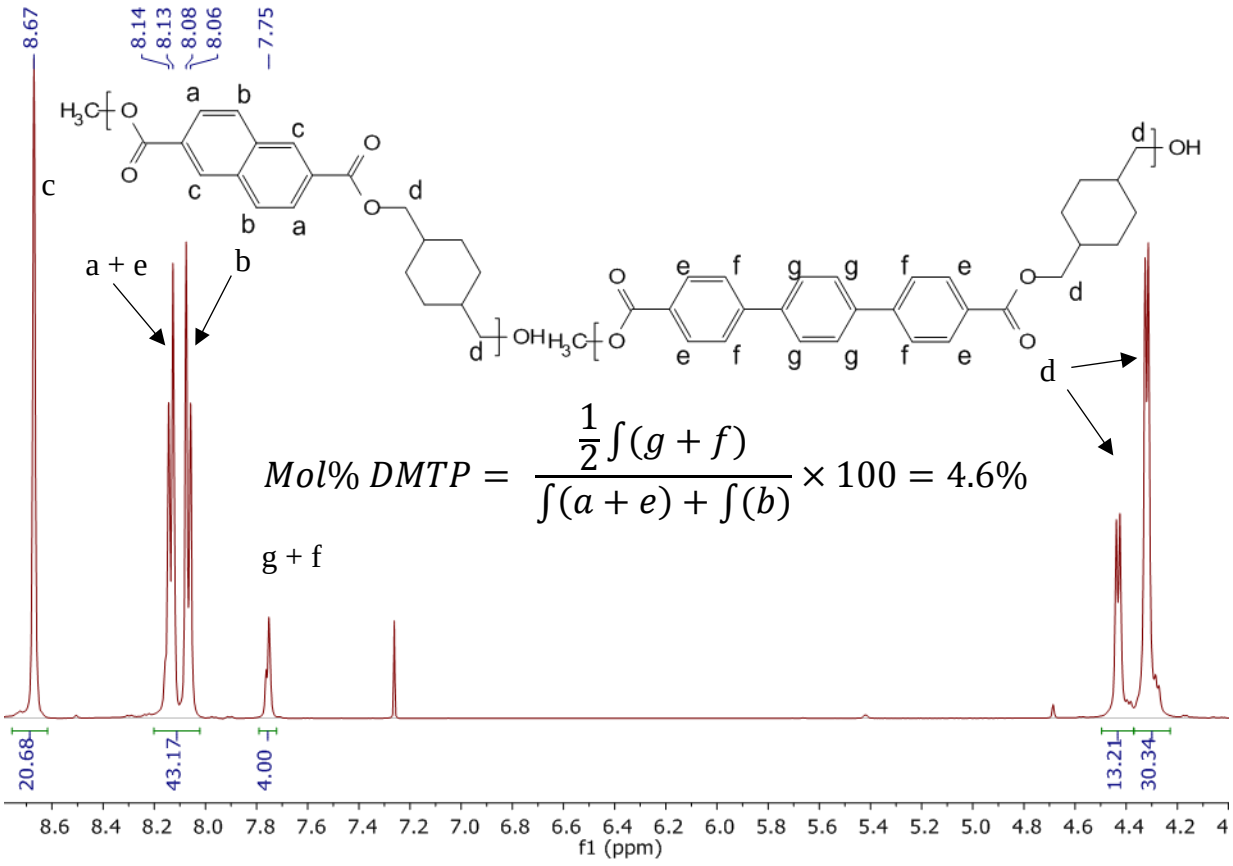

Figure 5-2. ^{1}H NMR of DMN-5-DMTP-CHDM copolyester. Relative diacid incorporation ratios were calculated from characteristic peaks

Table 5-1. Compositional and thermal analysis of terephthalate (T), 2,6-naphthalate (DMN) and 4,4'-bibenzoate (4,4'BB) based copolyesters modified with *p*-terphenyl-4,4''-dicarboxylate (DMTP)

Composition (Feed)	mol% DMTP (^{1}H NMR)	η_{inh} (dL/g)	T_g (°C)	T_m (°C)	$T_{d,5\%}$ (°C)	ΔH_f (J/g)
PCT	0	0.83	97	288	387	45
T-1-DMTP-CHDM	0.9	0.86	101	279	384	38
T-5-DMTP-CHDM	4.8	0.72	104	281	386	37
T-10-DMTP-CHDM	9.8	0.83	103	275	392	36
T-20-DMTP-CHDM	19.9	0.76	112	257	396	30
PCN	0	0.42	-	326	385	43
DMN-5-DMTP-CHDM	4.6	0.57	121	317	388	42
DMN-10-DMTP-CHDM	9.8	0.8	128	308	397	36
DMN-20-DMTP-CHDM	19.8	0.81	135	299	401	35
PCB	-	0.5	-	324	393	39
4,4'BB-5-DMTP-CHDM	-	0.7	-	324	397	30
4,4'BB-10-DMTP-CHDM	-	0.66	142	317	398	26
4,4'BB-20-DMTP-CHDM	-	0.78	150	302	396	24
T-50-EG-50-CHDM	-	0.76	86	-	392	0
T-5-DMTP-50-EG-50-CHDM	4.7	1.27	92	-	387	0
T-10-DMTP-50-EG-50-CHDM	10.2	1.17	96	-	391	0
T-20-DMTP-50-EG-50-CHDM	20.9	0.78	100	190	389	1

5.5.2 Thermal Analysis

Table 5-1 summarizes the results from DSC and TGA. TGA showed all copolyesters to exhibit single step weight loss with degradation temperatures above 385 °C at 5% weight loss. Char content was observed to increase with higher DMTP content in all cases except in copolyesters containing 4,4'BB (**Figure 5-7S** through **Figure 5-9S**). **Figure 5-3** shows a comparative plot of the melting temperatures of semicrystalline copolyesters. Compositions containing both EG and CHDM were completely amorphous until 20 mol% DMTP had been incorporated into the backbone, resulting in small, low temperature endotherm at 190 °C. DMTP incorporation decreases the melting point of PCT most significantly with a decrease of 31 °C at 20 mol% DMTP in the backbone and decreases the melting point of PCB the least with only a 22

°C decrease. Decrease in melting point is also accompanied by decreasing heat of fusion (ΔH_f), indicating that DMTP incorporation is disrupting the formation of crystalline regions. The T_g could not be identified via DSC for compositions with T_ms above 320 °C (**Figure 5-4**). DMTP was able to decrease crystallinity sufficiently to observe the glass transition. DMTP produces a steep increase in T_g due to its large, rigid structure. The T-20-DMTP-CHDM copolyester has a T_g of 112 °C, which is 15 °C higher than the PCT homopolyester.

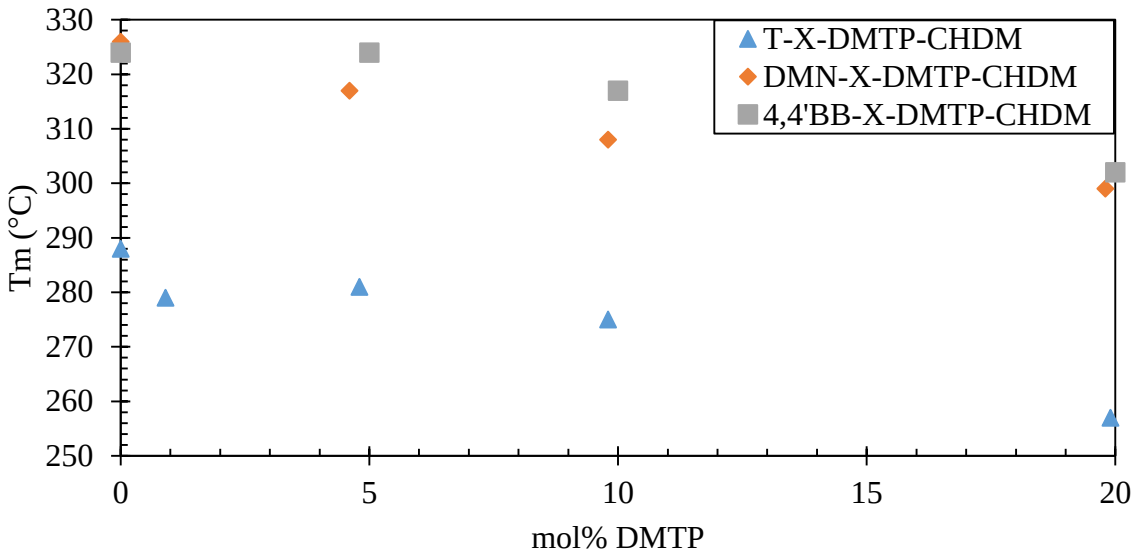

Figure 5-3. Plot of T_m vs mol% DMTP copolyester content

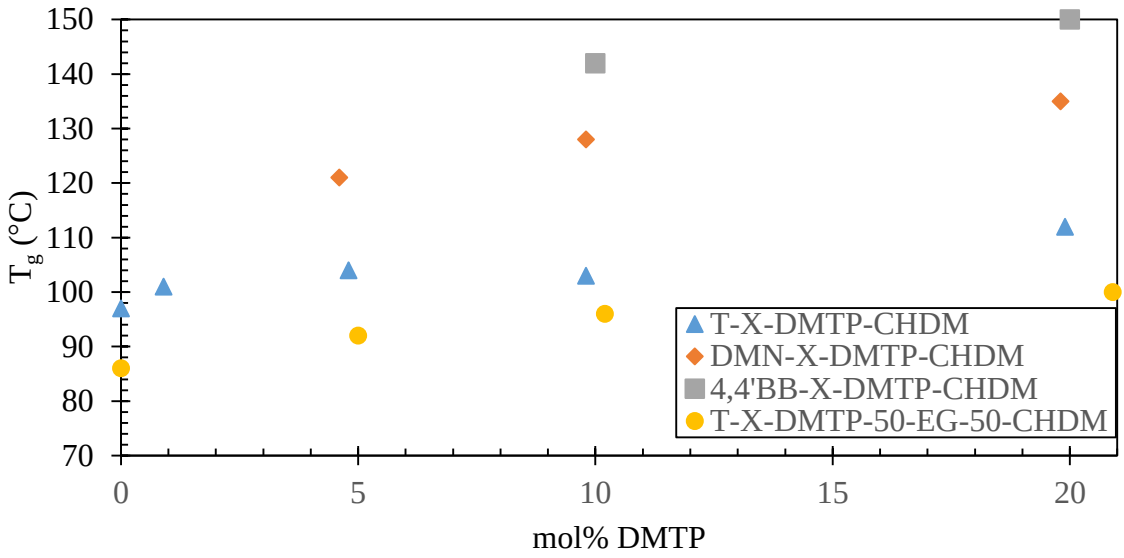

Figure 5-4. Plot of T_g vs mol% DMTP copolyester content

5.5.3 Rheology

Melt polycondensation and melt processing of polyesters with high melting temperature (≥300 °C) must be done carefully due to the higher tendency toward thermal degradation in the form of chain scission or crosslinking.[8-10, 39-40] Thermal stability of PCT and T-5-DMTP-CHDM was followed by measuring the complex viscosity at constant shear over 1 h (**Figure 5-5**). The T-5-DMTP-CHDM experiences a steeper initial drop in viscosity, indicating a loss of molecular weight. PCT begins to steeply increase in viscosity around 17 min, indicating it has an earlier onset thermal degradation relative to T-5-DMTP-CHDM, and may be undergoing crosslinking. In polyesters, the initial decrease in viscosity observed in **Figure 5-5** is commonly attributed to chain scission, which decreases molecular weight.[8-10, 39] Studies of PET degradation in the melt has also shown evidence of crosslinking through the formation of a trifunctional 2,3',5-biphenyltricarboxylate moiety[40-41], which might be responsible for the increasing viscosity of PCT after 17 min. Work by T.Grossetête et al[4] has also shown that degradation of CHDM can form pendant carboxylic acid groups, which can lead to further crosslinking.

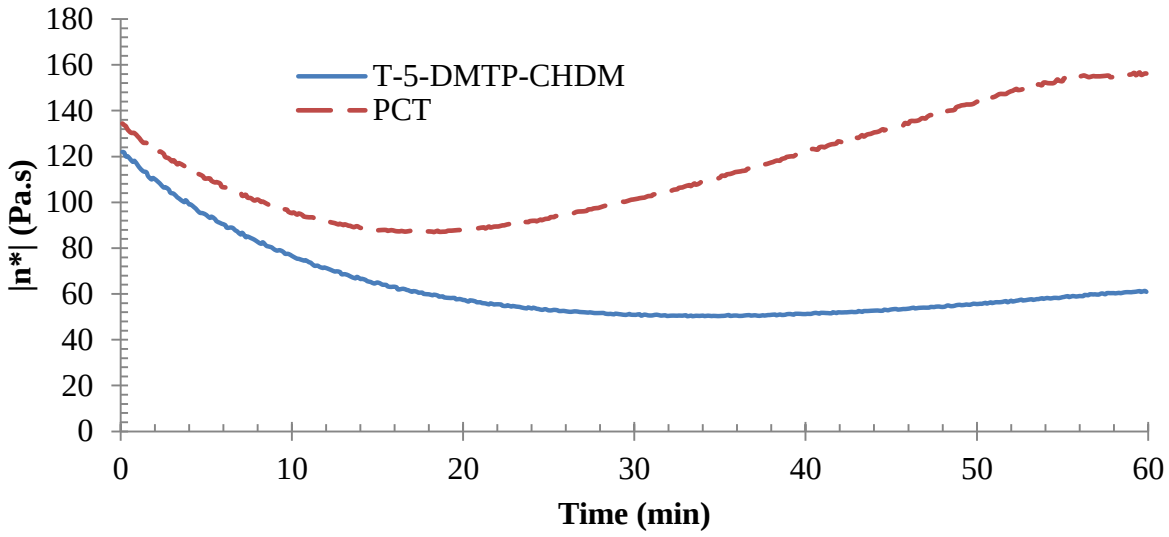

Figure 5-5. Time sweep of PCT and T-5-DMTP-CHDM under air at 305 °C and 1 Hz

5.6 Suggested Future Work

As shown in **Figure 5-3**, even though it is common for the melting temperature to be suppressed by the addition of a comonomer, it is still unknown if additional DMTP will result in an amorphous window,[2, 32-33] or a eutectic point. [7, 30-31] Studies have shown that monomer length plays an important role in the ability of comonomers to be incorporated into the crystalline phase of another comonomer.[6, 42-45] Copolyesters containing a systematic increase in the number of aromatic rings of the diacid comonomer would make a useful case study to compare to current theories that attempt to model the suppression of melting point with cocrystallization.[34-38, 42] Such research would be need to be supported by wide angle X-ray scattering to identify any crystal phases changes, as well as NMR studies to confirm random incorporation of monomers into the backbone. Further rheological analysis would be used to probe melt processability and thermal stability of copolyester compositions. Tensile analysis would show the effect of terphenyl moieties on mechanical properties and DMA would show T_g transitions that cannot be observed by using

DSC and how terphenyl affects sub-T_g transitions. Absorption and emission spectra of quenched amorphous PCT and T-5-DMTP-CHDM films (**Figure 5-16S**) shows terphenyl to influence the absorption and emission spectrum of PCT. Due to the susceptibility of polyesters to UV degradation, future studies would determine the influence of terphenyl on UV stability.

5.7 Acknowledgements

The authors thank Solvay Specialty Polymers for financial support and the supply of monomers 4,4′BB and DMN and the *p*-terphenyl starting material. They would also like to thank Prof. Timothy Long's group for the use of their TGA, DSC and DMA. They would also like thank Prof. Charles Frazier's group for assistance with running rheology.

5.8 References

1. East, A. J., Polyesters, Thermoplastic. In *Kirk-Othmer Encyclopedia of Chemical Technology*, John Wiley & Sons, Inc.: 2000.

2. Turner, S. R., Development of amorphous copolyesters based on 1,4-cyclohexanedimethanol. *J. Polym. Sci: Part A: Polym. Chem.* **2004,** *42* (23), 5847–5852.

3. Auerbach, A. B.; Sell, J. W., Evaluation of poly(1,4-cyclohexylene dimethylene terephthalate) blends for improved processability. *Poly. Eng. Sci.* **1990,** *30* (17), 1041–1050.

4. Grossetête, T.; Rivaton, A.; Gardette, J. L.; Hoyle, C. E.; Ziemer, M.; Fagerburg, D. R.; Clauberg, H., Photochemical degradation of poly(ethylene terephthalate)-modified copolymer. *Polymer* **2000,** *41* (10), 3541-3554.

5. Callander, D. D., *Modern Polyesters: Chemistry and Technology of Polyesters and Copolyesters*. John Wiley and Sons: West Sussex, Endland, 2003.

6. Jeong, Y. G.; Jo, W. H.; Lee, S. C., Synthesis and isodimorphic cocrystallization behavior of poly(1,4-cyclohexylenedimethylene terephthalate-co-1,4-cyclohexylenedimethylene 2,6-naphthalate) copolymers. *j. Polym. Sci. Part B: Polym. Phys.* **2004,** *42* (1), 177–187.

7. Hoffman, D. C.; Pecorini, T. J., Copolyesters of poly(1,4-cyclohexanedimethylene terephthalate) with isophthalic acid and 2,6-naphthalene dicarboxylic acid. *Am. Chem. Soc., Div. Polym. Chem., Polym. Prepr.* **1999,** *40* (1), 572–573.

8. Amari, T.; Nishimura, K.; Minou, K.; Kawabata, A.; Ozaki, Y., End-group characterization of homo- and copolyesters of cyclohexane-1,4-dimethanol. *J. Polym. Sci. Part A: Polym. Chem.* **2001,** *39* (5), 665–674.

9. Laubriet, C.; LeCorre, B.; Choi, K. Y., Two-phase model for continuous final stage melt polycondensation of poly(ethylene terephthalate). 1. Steady-state analysis. *Ind. Eng. Chem. Res.* **1991,** *30* (1), 2–12.

10. Ravindkanath, K.; Mashelkar, R. A., Modeling of polyethylene terephthalate reactors: 7. MWD considerations. *Polym. Eng. Sci.* **1984,** *24* (1), 30–41.

11. Edling, H. E.; Liu, H.; Sun, H.; Mondschein, R. J.; Schiraldi, D. A.; Long, T. E.; Turner, S. R., Copolyesters based on bibenzoic acids. *Polymer* **2018,** *135*, 120–130.

12. Mondschein, R. J.; Dennis, J. M.; Liu, H.; Ramakrishnan, R. K.; Nazarenko, S.; Turner, S. R.; Long, T. E., Synthesis and characterization of amorphous bibenzoate (co)polyesters: permeability and rheological performance. *Macromolecules* **2017,** *50* (19), 7603–7610.

13. Liu, R. Y. F.; Schiraldi, D. A.; Hiltner, A.; Baer, E., Oxygen-barrier properties of cold-drawn polyesters. *J. Polym. Sci., Part B: Polym. Phys.* **2002,** *40* (9), 862–877.

14. Polyakova, A.; Liu, R. Y. F.; Schiraldi, D. A.; Hiltner, A.; Baer, E., Oxygen-barrier properties of copolymers based on ethylene terephthalate. *J. Polym. Sci., Part B Polym. Phys.* **2001,** *39* (16), 1889–1899.

15. Asrar, J., Synthesis and properties of 4,4′-biphenyldicarboxylic acid and 2,6-naphthalenedicarboxylic acid. *J. Polym. Sci., Part A: Polym. Chem.* **1999,** *37* (16), 3139–3146.

16. Asrar, J.; Weinkauff, D. J.; Bhombal, A. H. Hydroxy ethyl bibenzoate. (Monsanto Company). U.S. Patent 5,374,707, 1994.

17. Mang, M. N.; Brewbaker, J. L. Thermoplastic polyesters containing biphenylene linkages. (The Dow Chemical Company). U.S. Patent 5,138,022, 1992.

18. Aitken, C. L.; Koros, W. J.; Paul, D. R., Effect of structural symmetry on gas transport properties of polysulfones. *Macromolecules* **1992,** *25* (13), 3424–3434.

19. Light, R. R.; Seymour, R. W., Effect of sub-Tg relaxations on the gas transport properties of polyesters. *Polym. Eng. Sci.* **1982,** *22* (14), 857–864.

20. Izard, E. F., Effect of chemical structure on physical properties of isomeric polyesters. *J. Polym. Sci., Part A: Polym. Chem.* **1952,** *9* (1), 35–39.

21. Dakka, J. M.; Bai, C.; Tanke, J. J.; De Martin, G. J.; Van Nostrand, M. T.; Salciccioli, M.; Kheir, A. A.; Sangar, N. Methyl-substituted biphenyl compounds, their production and their use in the manufacture of plasticizers. (Exxonmobil Chemical Patents Inc.). U.S. Patent 20,140,275,607 2014.

22. Sherman, S. C.; Iretskii, A. V.; White, M. G.; Gumienny, C.; Tolbert, L. M.; Schiraldi, D. A., Isomerization of substituted biphenyls by superacid. A remarkable confluence of experiment and theory. *J. Org. Chem.* **2002,** *67* (7), 2034–2041.

23. Schiraldi, D. A.; Iretski, A. V.; Sherman, S. C.; Tolbert, L. M.; White, M. G. Acid catalyzed isomerization of substituted diaryls. (Arteva North America S.A.R.L.). U.S. Patent 6,433,236, 2002.

24. Schiraldi, D. A.; Sherman, S. C.; Sood, D. S.; White, M. G. Catalytic system and method for coupling of aromatic compounds. (Arteva North America S.A.R.L.). U.S. Patent 6,103,919, 2000.

25. Watanabe, J.; Hayashi, M., Thermotropic liquid crystals of polyesters having a mesogenic p,p'-bibenzoate unit. 1. Smectic A mesophase properties of polyesters composed of p,p'-bibenzoic acid and alkylene glycols. *Macromolecules* **1988,** *21* (1), 278–280.

26. Noel, C.; Friedrich, C.; Bosio, L.; Strazielle, C., Thermotropic liquid crystalline polyesters with terphenyl moieties and flexible 'ether' spacers in the main chain. *Polymer* **1984,** *25* (9), 1281–1290.

27. Meurisse, P.; Noel, C.; Monnerie, L.; Fayolle, B., Polymers with mesogenic elements and flexible spacers in the main chain: Aromatic-aliphatic polyesters. *Br. Polym. J.* **1981,** *13* (2), 55–63.

28. Campbell, T. W., Dicarboxylation of terphenyl. *J. Am. Chem. Soc.* **1960,** *82* (12), 3126–3128.

29. David R. Fagerburg; Donelson, M. E. Blends of ultraviolet absorbers and polyesters. (Eastman Chemical Company). US Patent 5,480,926, 1995.

30. Lorenzetti, C.; Finelli, L.; Lotti, N.; Vannini, M.; Gazzano, M.; Berti, C.; Munari, A., Synthesis and characterization of poly(propylene terephthalate/2,6-naphthalate) random copolyesters. *Polymer* **2005,** *46* (12), 4041–4051.

31. Jeong, Y. G.; Jo, W. H.; Lee, S. C., Synthesis and crystallization behavior of poly(m-methylene 2,6-naphthalate-co-1,4-cyclohexylenedimethylene 2,6-naphthalate) copolymers. *Macromolecules* **2003,** *36* (11), 4051–4059.

32. Turner, S. R.; Seymour, R. W.; Dombroski, J. R., Amorphous and crystalline polyesters based in 1,4-cyclohexanedimethanol. In *Modern Polyesters: Chemistry and Technology of Polyesters and Copolyesters*, Scheirs, J.; Long, T., Eds. John Wiley & Sons: West Sussex, England, 2003; pp 267–292.

33. Schiraldi, D. A., New poly(ethylene terephthalate) copolymers. In *Modern Polyesters: Chemistry and Technology of Polyesters and Copolyesters*, Scheirs, J.; Long, T., Eds. John Wiley & Sons: West Sussex, England, 2003; pp 245–262.

34. Wendling, J.; Suter, U. W., A new model describing the cocrystallization behavior of random copolymers. *Macromolecules* **1998,** *31* (8), 2516–2520.

35. Sanchez, I. C.; Eby, R. K., Thermodynamics and crystallization of random copolymers. *Macromolecules* **1975,** *8* (5), 638–641.

36. Helfand, E.; Lauritzen, J. I., Theory of copolymer crystallization. *Macromolecules* **1973,** *6* (4), 631–638.

37. Baur, V. H., Einfluß der sequenzlängenverteilung auf das schmelz-ende von copolymeren. *Makromol. Chem.* **1966,** *98* (1), 297–301.

38. Flory, P. J., Theory of crystallization in copolymers. *Trans. Faraday Soc.* **1955,** *51* (0), 848–857.

39. Bhatia, A.; Gupta, R. K.; Bhattacharya, S. N.; Choi, H. J., An investigation of melt rheology and thermal stability of poly(lactic acid)/ poly(butylene succinate) nanocomposites. *J. Appl. Polym. Sci.* **2009,** *114* (5), 2837–2847.

40. Nealy, D. L.; Jane Adams, L., Oxidative crosslinking in poly(ethylene terephthalate) at elevated temperatures. *J. Polym. Sci. Part A: Polym. Chem.* **1971,** *9* (7), 2063–2070.

41. Franck, A., Understanding rheology of thermoplastic polymers. TA Instruments.

42. Yu, Y.; Wei, Z.; Zhou, C.; Zheng, L.; Leng, X.; Li, Y., Miscibility and competition of cocrystallization behavior of poly(hexamethylene dicarboxylate)s aliphatic copolyesters: Effect of chain length of aliphatic diacids. *Eur. Polym. J.* **2017,** *92* (Supplement C), 71–85.

43. Konstantopoulou, M.; Terzopoulou, Z.; Nerantzaki, M.; Tsagkalias, J.; Achilias, D. S.; Bikiaris, D. N.; Exarhopoulos, S.; Papageorgiou, D. G.; Papageorgiou, G. Z., Poly(ethylene furanoate-co-ethylene terephthalate) biobased copolymers: Synthesis, thermal properties and cocrystallization behavior. *Eur. Polym. J.* **2017,** *89* (Supplement C), 349–366.

44. Hong, M.; Tang, X.; Newell, B. S.; Chen, E. Y. X., "Nonstrained" γ-butyrolactone-based copolyesters: copolymerization characteristics and composition-dependent (thermal, eutectic, cocrystallization, and degradation) properties. *Macromolecules* **2017,** *50* (21), 8469–8479.

45. Jeong, Y. G.; Lee, J. H.; Lee, S. C., Structures and cocrystallization behavior of copolyesters based on poly(octamethylene terephthalate) and poly(octamethylene 2,6-naphthalate). *Polymer* **2009,** *50* (6), 1559–1565.

5.9 Chapter 5 Supplemental Material

5.9.1 Structural Analysis

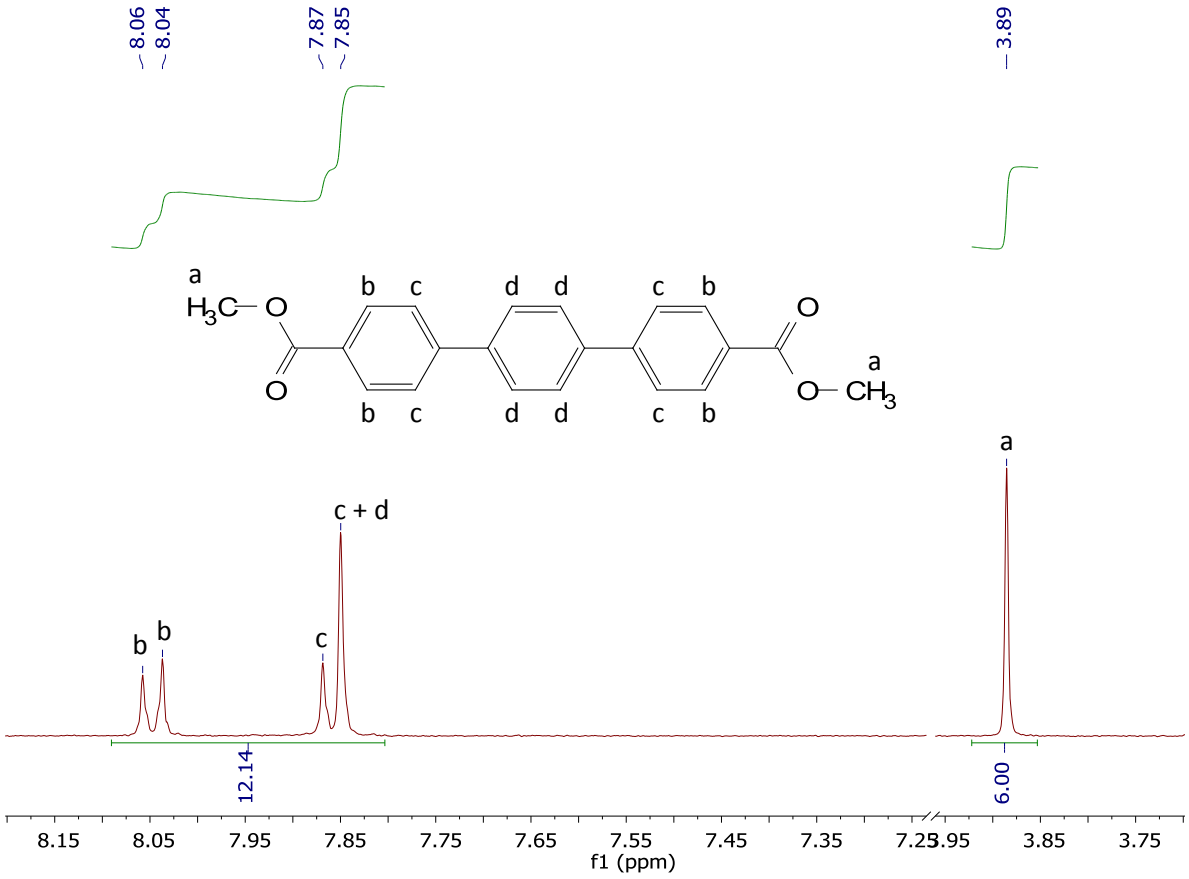

Figure 5-6S. [1]H NMR spectrum of dimethyl *p*-terphenyl-4,4''-dicarboxylate in d-DMSO at 90 °C

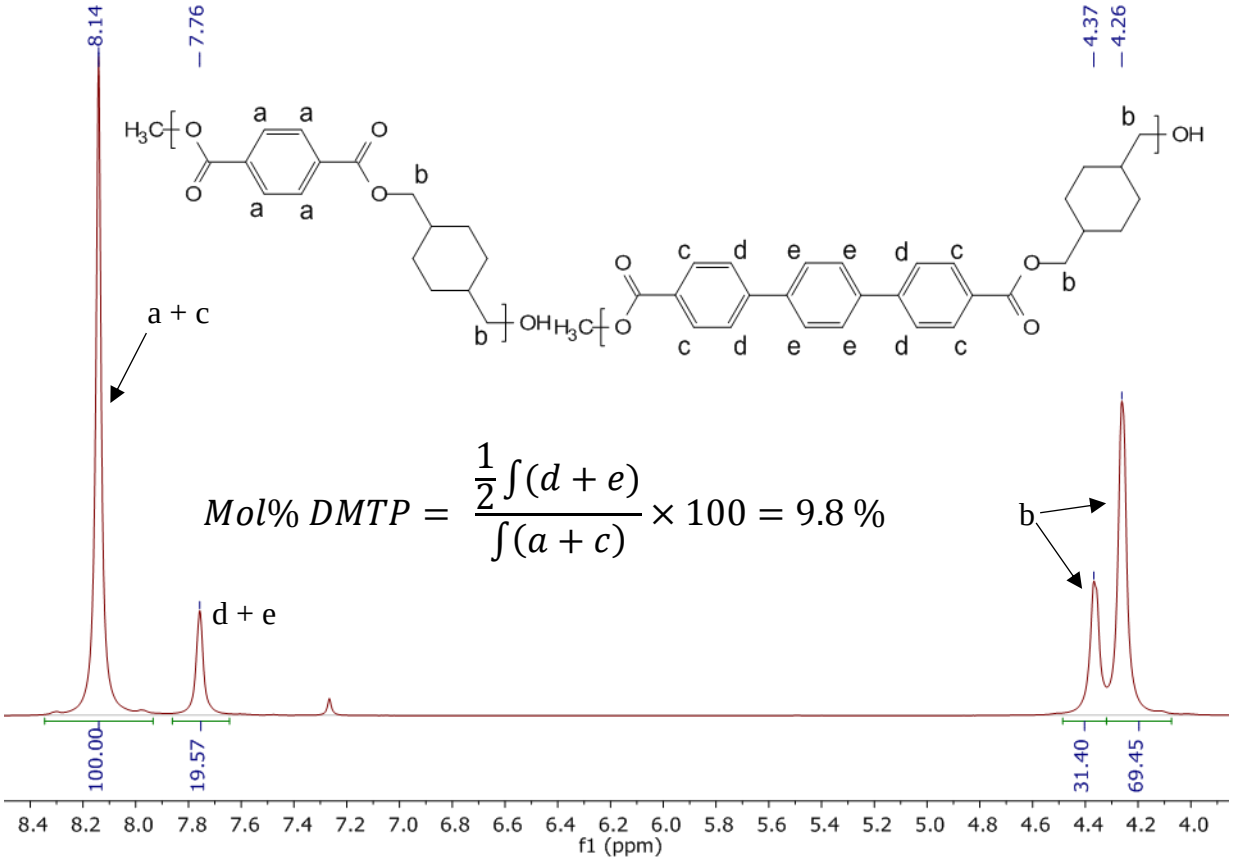

Figure 5-7S. [1]H NMR of T-10-DMTP-CHDM copolyester. Relative diacid incorporation ratios were calculated by using characteristic peaks

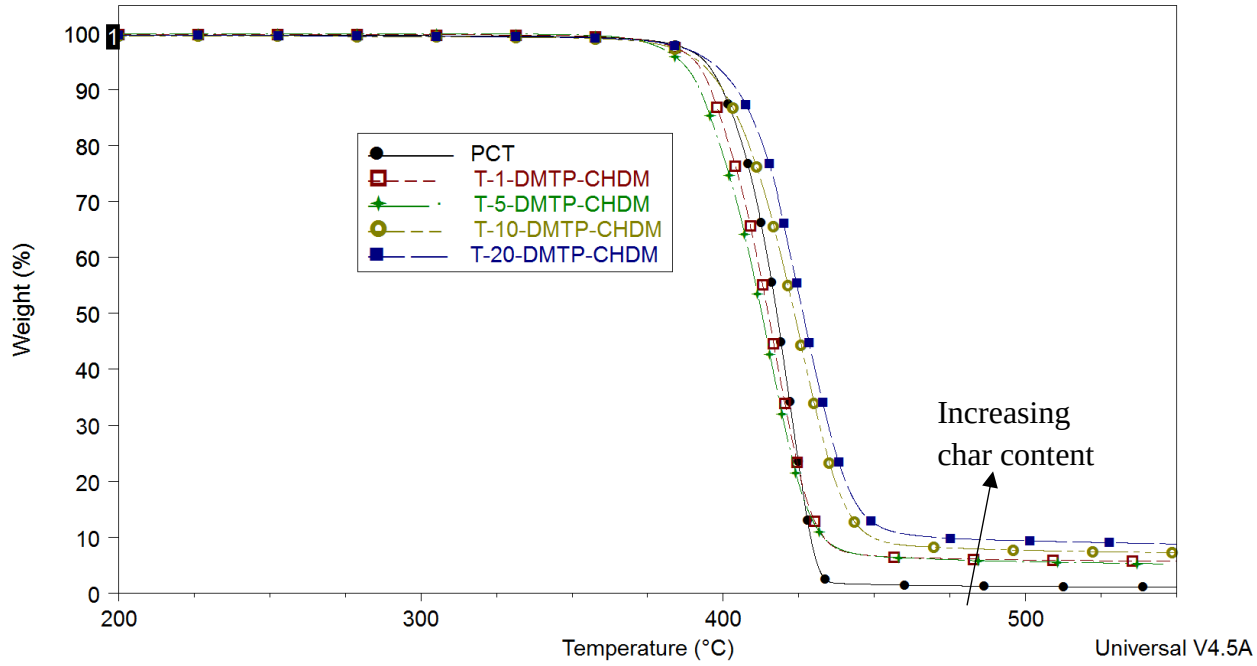

Figure 5-8S. Thermal degradation of PCT copolyesters modified with DMTP

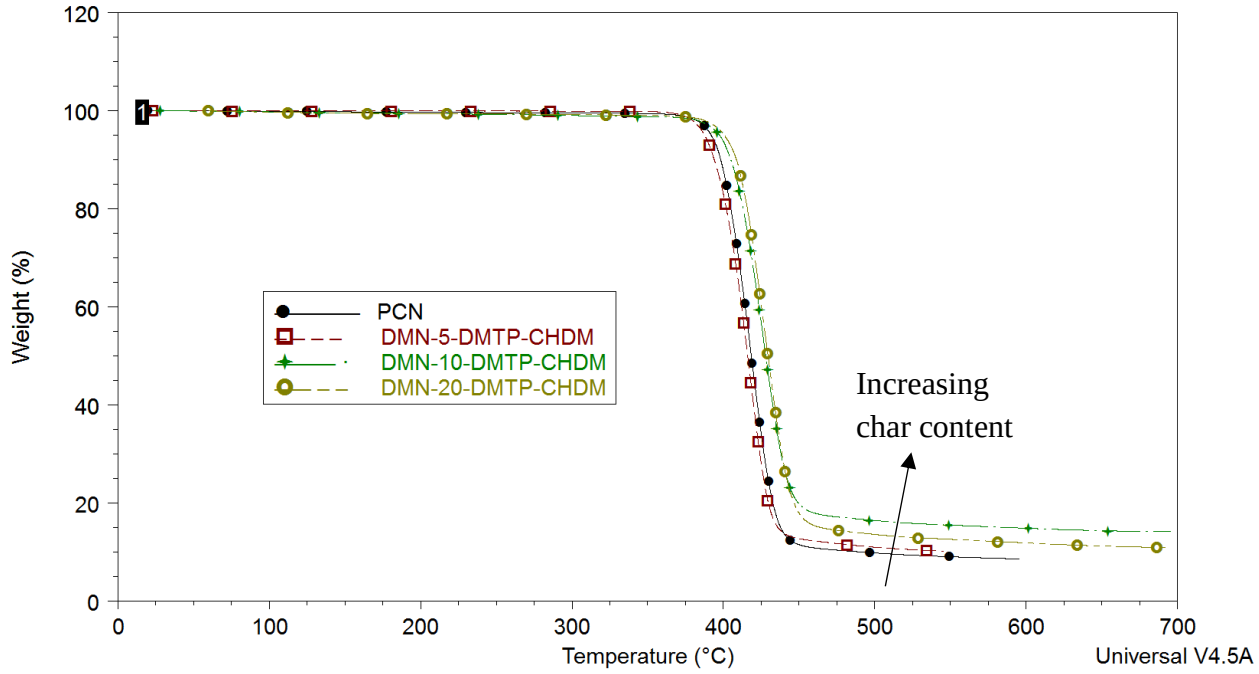

Figure 5-9S. Thermal degradation of PCN copolyesters modified with DMTP

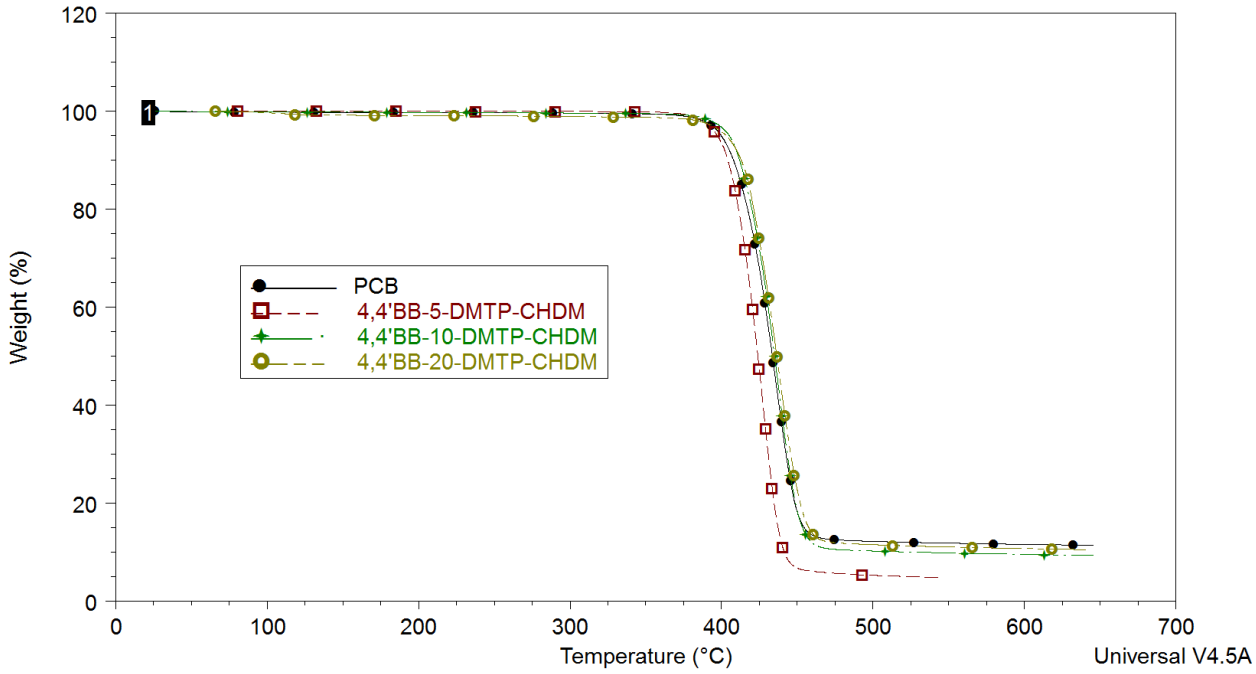

Figure 5-10S. Thermal degradation of PCB copolyesters modified with DMTP

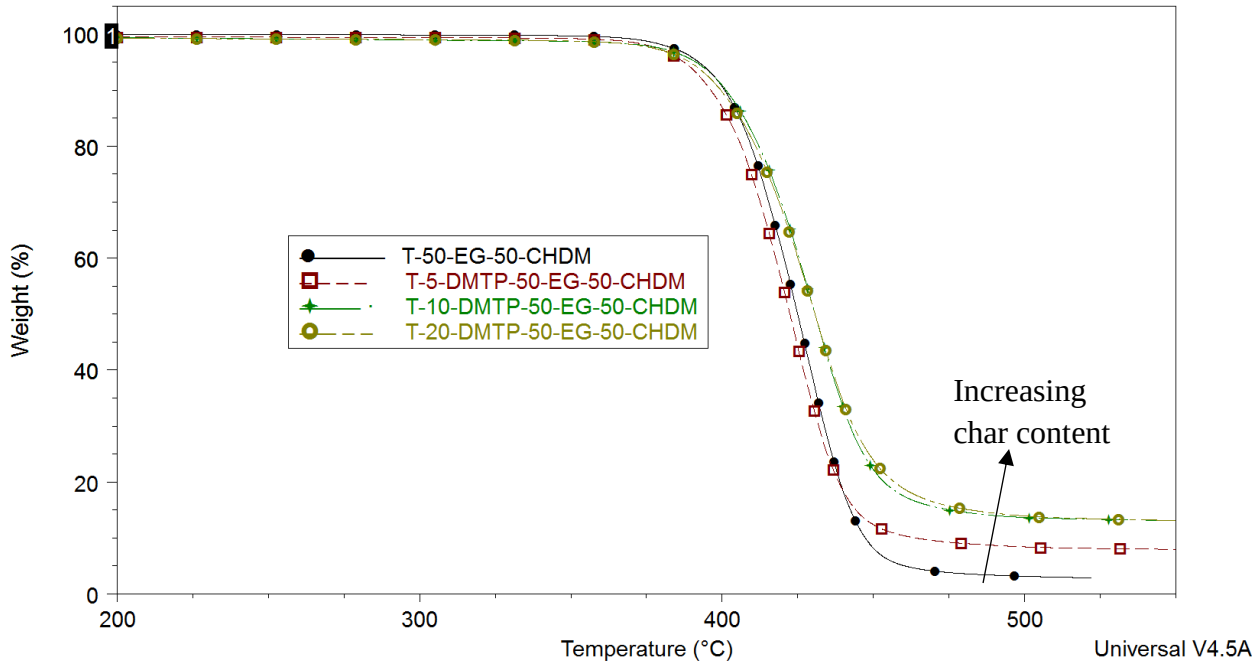

Figure 5-11S. Thermal degradation of T-50-EG-50-CHDM copolyesters modified with DMTP

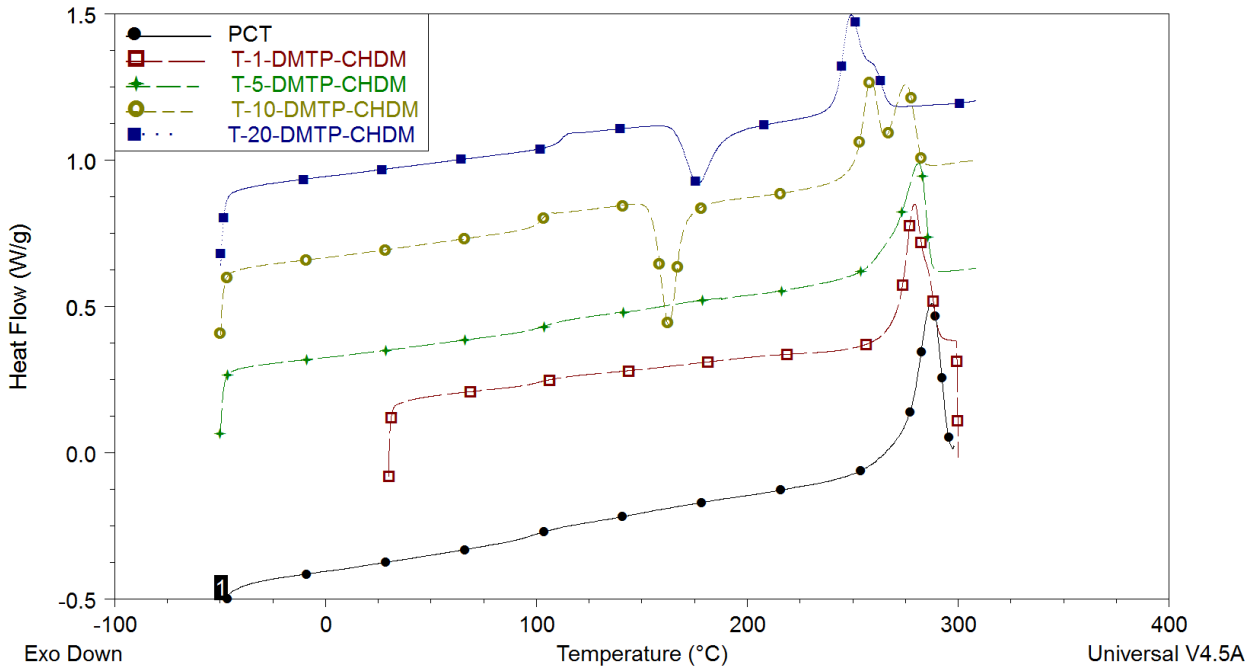

Figure 5-12S. DSC of PCT copolyesters modified with DMTP at 10 °C/min on second scan after quench cooling

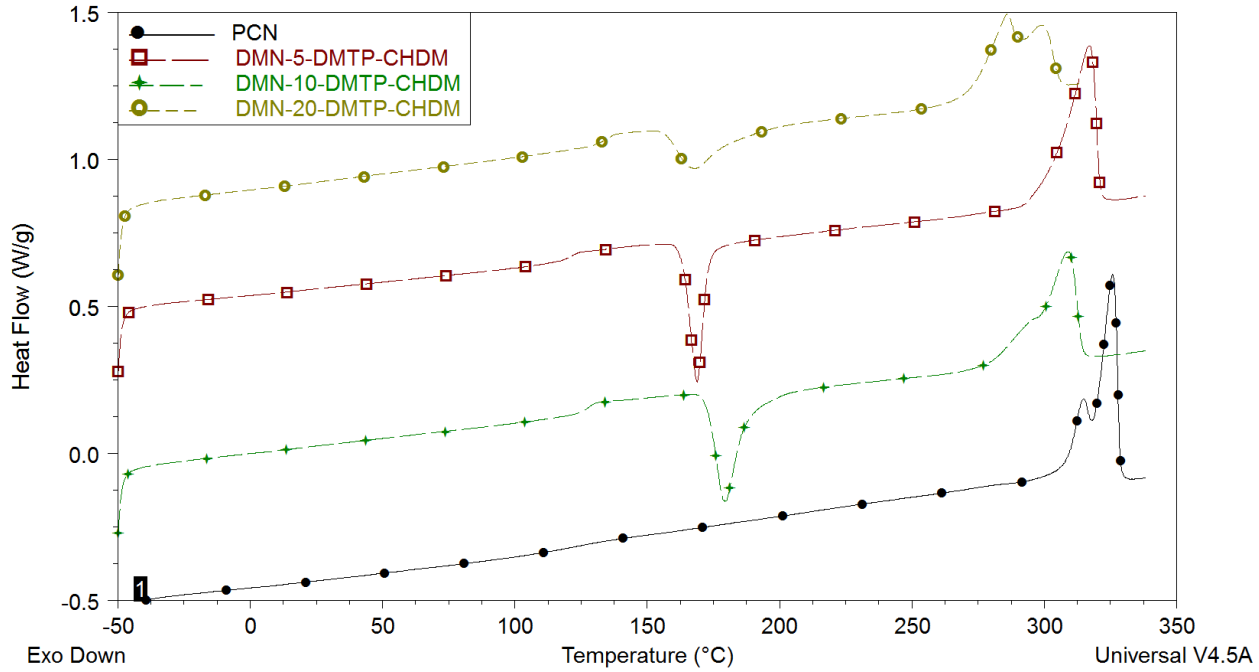

Figure 5-13S. DSC of PCN copolyesters modified with DMTP at 10 °C/min on second scan after quench cooling

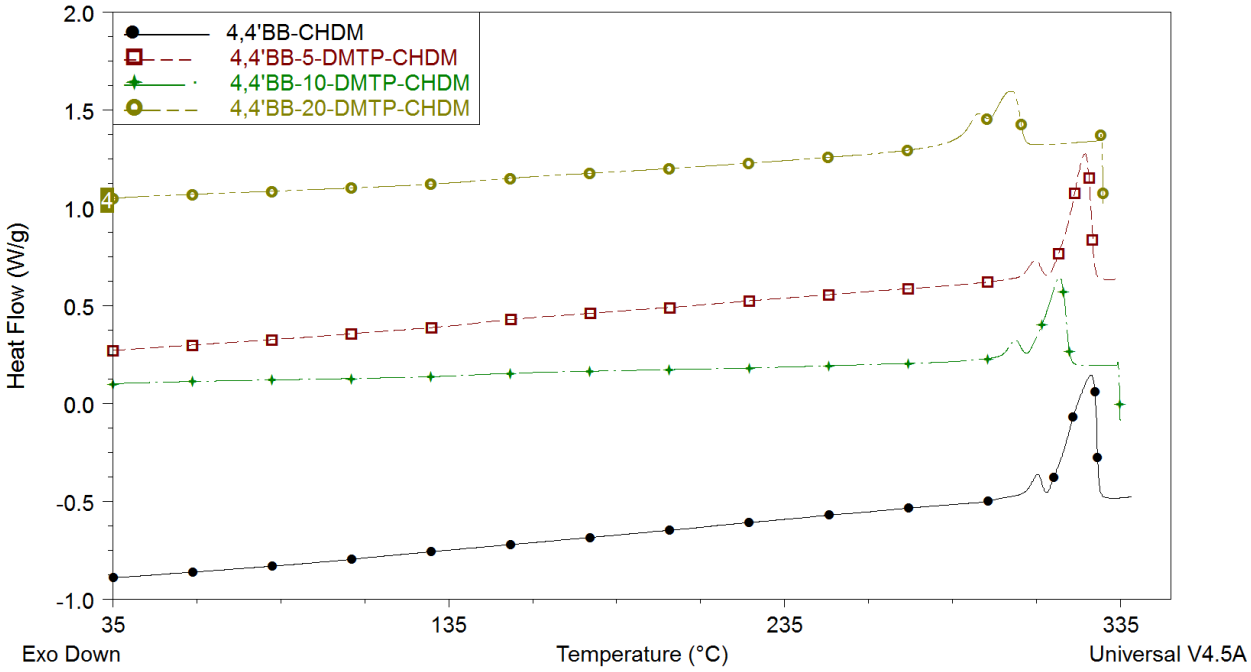

Figure 5-14S. DSC of PCB copolyesters modified with DMTP at 10 °C/min on second scan after quench cooling

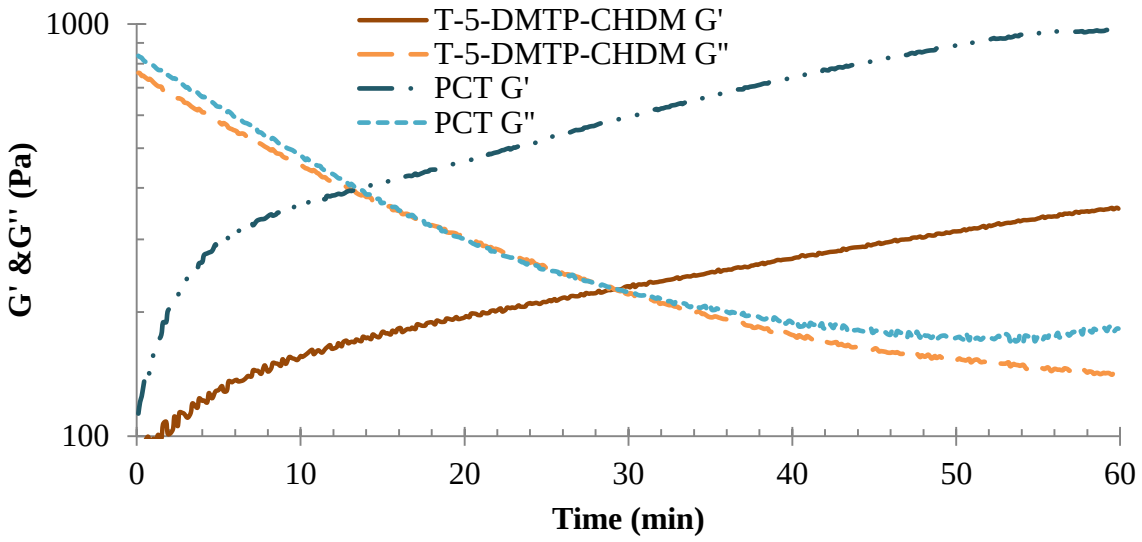

Figure 5-15S. Storage and loss modulus over 1 h at 305 °C

5.9.3 Absorption and Emission of Polyester Films

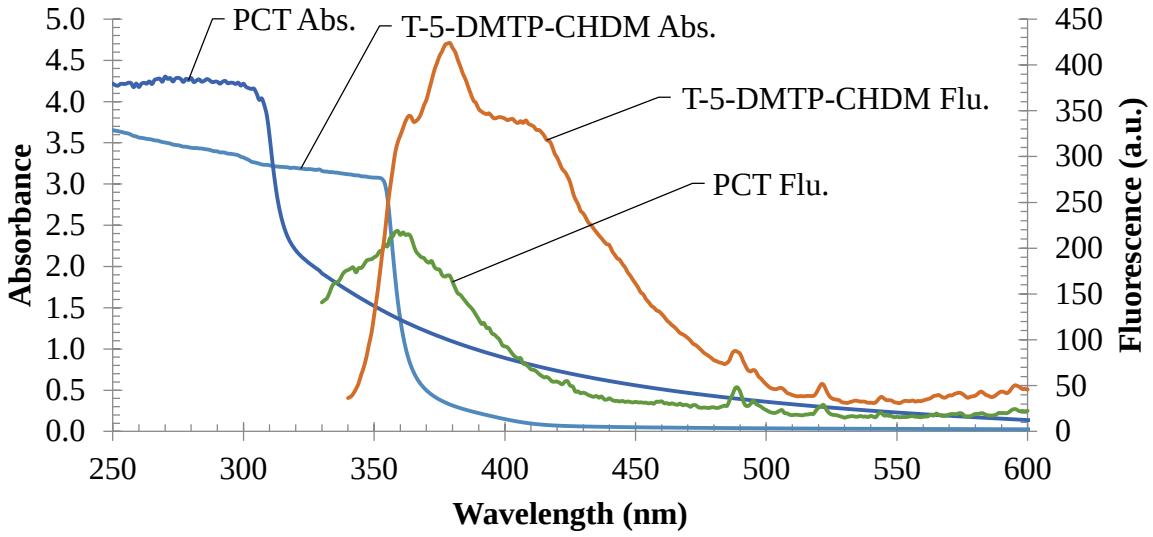

Figure 5-16S. Absorption and fluorescence spectrum of quenched amorphous PCT (0.16 mm) and T-5-DMTP-CHDM (0.17 mm) films. Data was collected using Agilent's Cary 5000 UV-Vis-NIR.